



Host DNA damage responses to the typhoid toxin of *Salmonella enterica*

Daniel Stark

**Department of Biosciences
Faculty of Science
University of Sheffield**

A thesis submitted in partial fulfilment of the requirements for the degree of
Doctor of Philosophy

July 2022

Declaration

I, Daniel Stark, confirm that this thesis is my own work. I am aware of the University's Guidance on the Use of Unfair Means (www.sheffield.ac.uk/ssid/unfair-means). This work has not previously been presented for an award at this, or any other, university.

Daniel Stark, July 2022

Acknowledgements

I would like to thank Dan Humphreys for being a fantastic supervisor during my PhD. I owe him a huge amount for all of his support and guidance and could not have hoped for a better mentor! I would also like to thank all past and present members of the Humphreys lab. Mohamed ElGhazaly has been a kind and patient mentor and friend. Angela Ibler always had ideas for new experiments, even when she was 8 months pregnant! Zhou Zhu is brilliantly helpful and always has an answer to every question. Thank you to Nadia Baseer for putting up with me as a mentor for her master's lab project where we learnt how to do qRT-PCR together. I would also like to thank Salma Srour, Kate Naylor, Weronika Buczek, Nataya Deans and Michelle King for making the lab such a friendly environment to work in.

Outside of the lab, I would like to thank my advisors, David Strutt and Steve Brown, for their advice and support. I would like to thank my friends and colleagues in the department, including Keivan, James Vines, Katie, Ruth, Ash, Anna, Chris, Juliana, Laura and James McManus, for helping make my PhD such an enjoyable experience.

Thank you to my mum Kate and grandparents Jarda and Sheelagh. I am incredibly lucky to have such a kind and supportive family. Finally, thank you Wendy for all of your incredible support. You have kept me going during a global pandemic and whilst writing up, and I am enormously grateful for you and everything you do.

I would like to dedicate this thesis to my dad Jaroslav and my grandmother Olga. I owe both of you so much for where I am today.

Abstract

The typhoid toxin is a virulence factor of the bacterial pathogen *Salmonella enterica*, which causes typhoid fever. The toxin has been shown to cause a DNA damage response in intoxicated human cells and to promote infection (Ibler *et al.*, 2019). DNA damage responses have been shown to activate innate immune pathways via leakage of self-DNA into the cytosol and activation of the cGAS-STING pathway (Wolf *et al.*, 2016). This thesis shows that purified typhoid toxin upregulates a type-I interferon-like response, including the antiviral ubiquitin-like interferon-stimulated gene 15 (ISG15), in a STING-dependent manner. ISG15 was upregulated in response to toxigenic *Salmonella* infection and overexpression of ISG15 reduced *Salmonella* burden, suggesting a role in host defence. Chronic *Salmonella* infection has been linked to gallbladder cancer (Di Domenico *et al.*, 2017), and ISG15 has been implicated as a regulator of P53 and thus tumour suppression in response to DNA damage (Park *et al.*, 2016). The toxin induces cell death in wild-type MEFs, whereas ISG15 KO MEFs survive and proliferate despite hallmarks of genomic instability such as micronuclei. This suggests that ISG15 may protect the host from pathogen-induced genomic instability. Taken together, this thesis provides new insights into host responses to the typhoid toxin, and the findings may be applicable to other bacterial genotoxins.

Contents

List of Figures	13
List of Tables.....	15
List of Abbreviations.....	16
Part 1: Literature Review	21
1 <i>Salmonella</i> infection.....	21
1.1 Introduction.....	21
1.2 Disease outcomes of <i>Salmonella</i> infection	22
1.3 Diagnostics and Treatment.....	25
1.3.1 Diagnosis of <i>Salmonella</i> infection	25
1.3.2 Antibiotic Resistance.....	26
1.3.3 Vaccination.....	26
1.4 Pathogenesis of <i>S. Typhi</i>	27
1.4.1 <i>Salmonella</i> entry into host cells.....	27
1.4.2 SPI-1.....	29
1.4.3 SPI-2.....	30
1.4.4 <i>S. Typhi</i> specialisation.....	31
1.4.5 Gallbladder cancer	33
1.5 The typhoid toxin	34
1.5.1 Cytotoxic distending toxins.....	34
1.5.2 Secretion and delivery of the typhoid toxin.....	36
1.5.3 <i>In vivo</i> effects of the typhoid toxin	38
2 DNA Damage Response.....	41
2.1 Causes of DNA Damage	41
2.1.1 Exogenous causes	41
2.1.2 Endogenous causes.....	42
2.2 Replication stress.....	42
2.3 Apical Kinases.....	43
2.3.1 Double-strand break response.....	44
2.3.2 Single-strand break response	46

2.4	Cell cycle regulation	47
2.4.1	P53	48
2.4.2	Apoptosis	49
2.4.3	Senescence.....	50
2.5	The DNA damage response to the typhoid toxin.....	50
3	Innate Immune Responses to DNA damage	53
3.1	Introduction.....	53
3.2	Interferons	55
3.3	IFN induction by pattern recognition receptors	56
3.3.1	TLRs, RLRs and NLRs.....	56
3.3.2	Cytoplasmic DNA sensors	57
3.4	IFN signalling.....	59
3.5	IFN signalling and host-pathogen interactions	61
3.5.1	IFN signalling and viruses	61
3.5.2	IFN signalling and bacteria.....	61
3.5.3	IFN signalling and <i>Salmonella</i>	62
3.6	Host responses to the typhoid toxin.....	63
3.7	Aims and Hypothesis	64
	Part 2: Results	65
4	Host responses to the typhoid toxin.....	65
4.1	Introduction.....	65
4.2	Results	65
4.2.1	Purification of recombinant typhoid toxin	65
4.2.2	The toxin causes both ATR- and ATM-dependent DNA damage responses.....	69
4.2.3	The toxin activates a type-I IFN response.....	72
4.2.4	The IFN response is not S/G2 dependent.....	74
4.2.5	Validation of the toxin-induced IFN response	76
4.2.6	Determining the role of IFNs in the toxin ISG response	82
4.3	Discussion.....	83
5	Regulation of the toxin ISG response	86

5.1	Introduction.....	86
5.2	Results	86
5.2.1	The toxin induces single strand breaks, micronuclei and cytosolic DNA leakage	86
5.2.2	The role of ssDNA-binding proteins in regulation of the toxin ISG response	89
5.2.3	Toxin induced ISG15 is dependent on STING	96
5.3	Discussion.....	100
6	The role of ISG15 in the host response to the typhoid toxin	103
6.1	Introduction.....	103
6.1.1	The ISGylation pathway	104
6.1.2	Free ISG15	106
6.1.3	Antiviral Functions of ISG15.....	106
6.1.4	Role of ISG15 in non-viral infections.....	107
6.1.5	ISG15 in the DDR	108
6.2	Results	109
6.2.1	ISG15 is upregulated by <i>Salmonella</i> Javiana infection	110
6.2.2	ISG15 overexpression reduces <i>Salmonella</i> CFUs.....	114
6.2.3	ISG15 knockout promotes oncogenic phenotypes	117
6.3	Discussion.....	122
	Part 3: Discussion	124
7	Discussion.....	124
7.1	The effect of the toxin ISG response on <i>Salmonella</i> infection	124
7.2	What regulates the toxin ISG response?	125
7.3	Is toxin induced ISG15 in free or conjugated form?	126
7.4	The role of ISG15 in <i>Salmonella</i> infection	128
7.5	The role of ISG15 in cancer	129
7.6	Conclusion	130
	Part 4: Materials & Methods.....	131
8	Biochemical assays.....	131

8.1	Bacterial transformation.....	131
8.1.1	Creation of chemically competent cells	131
8.1.2	Transformation in chemically competent cells.....	131
8.1.3	Purification of plasmid DNA by midiprep	131
8.2	Purification of recombinant typhoid toxin	132
8.3	Cell fractionation	132
8.4	Protein gels	133
8.4.1	Cell lysate preparation.....	133
8.4.2	SDS-PAGE protein gel preparation.....	133
8.4.3	Coomassie staining.....	134
8.4.4	Immunoblotting	134
8.5	Flow cytometry.....	136
8.6	Microarray	136
8.7	qRT-PCR.....	137
9	Cell biology.....	139
9.1	Mammalian cell culture	139
9.2	Mammalian cell treatment.....	139
9.2.1	Standard intoxication assay	139
9.2.2	Cell cycle arrest by serum-starvation.....	140
9.2.3	Drug and recombinant protein treatment.....	140
9.2.4	Transfection of mammalian cells.....	141
9.3	Clonogenic Assay	142
9.4	Cell staining.....	143
9.4.1	Immunofluorescence.....	143
9.4.2	EdU staining	145
9.4.3	<i>In vitro</i> polymerase assay.....	145
9.5	Infection assay	145
9.5.1	Preparation of cells and bacterial culture.....	145
9.5.2	CFU assay	146
9.6	Microscopy	146
9.7	Statistical analysis.....	147
	Bibliography.....	148

List of Figures

Fig. 1.1 Pathogenesis of invasive and non-invasive <i>Salmonella</i>	23
Fig. 1.2 Typhoid toxin structure and delivery	36
Fig. 2.1 DNA damage responses to single- and double-strand DNA breaks	44
Fig. 3.1 Pattern recognition receptors detect DNA damage and initiate an innate immune response.....	55
Fig. 4.1 Purification of recombinant typhoid toxin	66
Fig. 4.2 The typhoid toxin causes a DNA damage response and cell cycle arrest...68	
Fig. 4.3 The typhoid toxin causes distinct DNA damage responses in G0/G1 and G2/S phase	71
Fig. 4.4 The typhoid toxin induces a type-1 IFN signalling response	73
Fig. 4.5 The toxin-dependent type-I IFN-like response occurs in G0/G1	75
Fig. 4.6 Validation of the toxin-dependent type-I IFN-like response by qRT-PCR ...77	
Fig. 4.7 ISG15 and IFIT1 are upregulated in response to typhoid toxin	79
Fig. 4.8 Immunofluorescence analysis of ISG15.....	81
Fig. 4.9 Examining the role of IFN in the toxin ISG response.....	83
Fig. 5.1 Toxin activity results in ssDNA formation and DNA leakage into the cytosol	87
Fig. 5.2 Regulation of ssDNA-binding proteins in response to the toxin	90
Fig. 5.3 Regulation of HMGB2 and the SOSS complex in response to the toxin	91
Fig. 5.4 NABP1 is upregulated in response to the toxin	93
Fig. 5.5 NABP1 knockdown enhances the toxin dependent ISG15 response.....	95
Fig. 5.6 The toxin does not directly regulate expression of cytosolic DNA sensors..97	
Fig. 5.7 The toxin dependent ISG15 response is dependent on STING and TBK1 ..99	
Fig. 6.1 ISG15 is a ubiquitin-like modifier that ISGylates other proteins	104
Fig. 6.2 <i>Salmonella</i> Javiana infection causes cell cycle arrest.....	111
Fig. 6.3 <i>Salmonella</i> Javiana infection induces a DNA damage response and upregulates ISG15	113
Fig. 6.4 IFN pre-treatment reduces <i>Salmonella</i> burden 24 h post-infection.....	115
Fig. 6.5 ISG15 over-expression reduces <i>Salmonella</i> burden 24 h post-infection...116	
Fig. 6.6 Validation of MEF ^{ISG15^{-/-}} and MEF ^{USP18^{C61A}} cell lines	118

Fig. 6.7 ISG15 knockout promotes tumorigenic phenotypes in response to the toxin120

Fig. 6.8 ISG15 knockout permits greater MEF colony formation in the presence of the toxin121

Fig. 7.1 Proposed model for the role of ISG15 in response to the toxin.....129

List of Tables

Table 8-1 Primary antibodies used for immunoblotting	136
Table 8-2 Primers used for qRT-PCR	138
Table 9-1 Drugs and recombinant proteins used to treat mammalian cells	141
Table 9-2 siRNAs used for transfection of mammalian cells	142
Table 9-3 Primary antibodies used for immunofluorescence	144

List of Abbreviations

53BP1 p53-binding protein 1

AMR antimicrobial resistant

APH aphidicolin

APS ammonium persulfate

ATM Ataxia Telangiectasia Mutated

ATR Ataxia telangiectasia and Rad3 related

ATRIP ATR interacting protein

BSA bovine serum albumin

CDK cyclin-dependent kinase

CDT cytolethal distending toxin

CFU colony forming unit

cGAS cyclic GMP-AMP synthase

CldU 5-chloro-2'-deoxyuridine

DAMP damage-associated molecular pattern

DDR DNA damage response

DMEM Dulbecco's modified Eagle medium

DNA-PKc DNA-dependent protein kinase, catalytic subunit

DSB double-strand break

dsDNA double-stranded DNA

DTT Dithiothreitol

EdU 5-Ethynyl-2-deoxyuridine

ER endoplasmic reticulum

ERAD ER-associated degradation

ETP etoposide

FBS Foetal Bovine Serum

FISH fluorescence in situ hybridisation

FT flow through

GST glutathione S-transferase

HA human influenza hemagglutinin

HDR homology directed repair

His histidine

HMGB High mobility group box protein

HQ toxin catalytically inactive toxin with CdtB-H160Q mutation

IFIH1 interferon induced with helicase C domain 1 (also known as MDA5)

IFIT interferon induced protein with tetratricopeptide repeat

IFN interferon

IKK I κ B kinase

IL interleukin

INT3 integrator complex subunit 3

iNTS invasive non-typhoidal *Salmonella*

IPTG Isopropyl β - d-1-thiogalactopyranoside

IR infrared radiation

IRAK interleukin 1 receptor associated kinase

IRF interferon regulatory factor

ISG interferon stimulated gene

ISG15 interferon stimulated gene 15

ISGF3 interferon stimulated gene factor 3

ISRE interferon-sensitive response element

JAK Janus kinase

LB Lysogeny broth

LPS Lipopolysaccharide

MDR multidrug-resistant

MEF mouse embryonic fibroblast

MES 2-(N-morpholino) ethanesulfonic acid

MHC major histocompatibility complex

MLN mesenteric lymph nodes

MOI multiplicity of infection

MQ Milli-Q water

MRN Mre11-Rad50-Nbs1 complex

NABP Nucleic Acid Binding Protein

Neu5Ac N-Acetylneuraminic acid

Neu5Gc N-Glycolylneuraminic acid

NF κ B Nuclear Factor kappa-light-chain-enhancer of activated B cells

NHEJ non-homologous end joining

NiNTA nickel-nitrilotriacetic acid

NK natural killer

ns non-significant

NT non-targeting

NTS non-typhoidal *Salmonella*

OAS 2'-5'-oligoadenylate synthetase

OD optical density

PAMP pathogen-associated molecular pattern

PBS phospho-buffered saline

pcDNA plasmid cloning DNA

PCR polymerase chain reaction

PFA paraformaldehyde

PLT pertussis-like toxin

PVDF polyvinylidene difluoride

qRT-PCR Real-Time Quantitative Reverse Transcription PCR

RING response induced by a genotoxin

ROS reactive oxygen species

RPA replication protein A

rpm revolutions per minute

SASP senescence associated secretory phenotype

SBP ssDNA-binding protein

SCV *Salmonella* containing vacuole

SDS sodium dodecyl sulphate

SDS-PAGE SDS–polyacrylamide gel electrophoresis

Sif *Salmonella* induced filaments

siRNA small interfering RNA

SOC super optimal broth

SOSS sensor of single-stranded DNA

SPI *Salmonella* pathogenicity island

SSB single-strand break

ssDNA single-stranded DNA

ST *Salmonella* Typhimurium

STAT signal transducer and activator of transcription

STING Stimulator of interferon genes

T3SS type 3 secretion system

TBK tank-binding kinase

TBS tris-buffered saline

TEMED tetramethylethylenediamine

Tris trisaminomethane

TLR toll-like receptor

TLS translesion DNA synthesis

TYK tyrosine kinase

UBE1L Ubiquitin-like modifier-activating enzyme 7

USP18 Ubiquitin Specific Peptidase 18

UV ultraviolet

WHO World Health Organisation

WT wild type

XDR extensively drug resistant

γ H2AX phosphorylated H2A histone family member X

Part 1: Literature Review

1 *Salmonella* infection

1.1 Introduction

The typhoidal serovars of *Salmonella enterica*, including Typhi and Paratyphi (henceforth *S. Typhi* and *S. Paratyphi*) are intracellular Gram-negative bacteria that cause typhoid fever and paratyphoid fever respectively, collectively known as enteric fever. Enteric fever is a life-threatening infectious disease transmitted to humans by contaminated food and water and threatens human populations in regions lacking access to clean water and good sanitation (Parry *et al.*, 2002; Crump and Mintz, 2010; Galán, 2016). Typhoid fever is the best characterised and will be discussed henceforth.

Typhoid fever is a human-specific disease that has threatened humanity since the earliest recorded plagues, with evidence that it was cause of the plague of Athens in 430 BC (Papagrigrorakis *et al.*, 2006). In modern history, typhoid fever was a major cause of illness in the USA and Europe during the 19th Century, but has been largely eradicated in high-income countries over the preceding century following improvements in sanitation (Parry *et al.*, 2002). Today, typhoid fever affects low- to middle-income countries, predominantly in sub-Saharan Africa, South Asia, South East Asia and Oceania (World Health Organization, 2018). Although the overall global burden of typhoid fever appears to have reduced since the 1990s, global morbidity and mortality remains high (Als *et al.*, 2018). As of 2018 there were between 11 to 21 million cases worldwide, and of these cases, 128,000 to 161,000 people die every year (World Health Organization, 2018). There are gaps in the data available and inconsistencies in data acquisition between regions, making the true extent of the global burden of typhoid fever uncertain (Als *et al.*, 2018).

Besides typhoid fever itself, *S. Typhi* infection is associated with other global health issues (Gunn *et al.*, 2014). Chronic carriage of *S. Typhi* can be asymptomatic, which increases infection spread and complicates diagnosis and treatment. Furthermore,

chronic infection has been linked to increased incidence of gallbladder cancer. In this chapter I will describe how typhoidal *Salmonella* causes infection and how this can lead to typhoid fever, chronic carriage, and cancer.

1.2 Disease outcomes of *Salmonella* infection

There are more than 2600 known serovars of *Salmonella enterica* which differ in host specificity and disease outcome (Brenner *et al.*, 2000; Gal-Mor, Boyle and Grassl, 2014). In terms of those that affect humans, these serovars can be divided into typhoidal and non-typhoidal *Salmonella*, referring to whether infection can lead to typhoid fever. They can also be categorised as invasive or non-invasive, based on whether they establish systemic or localised infection (**Fig. 1.1**).

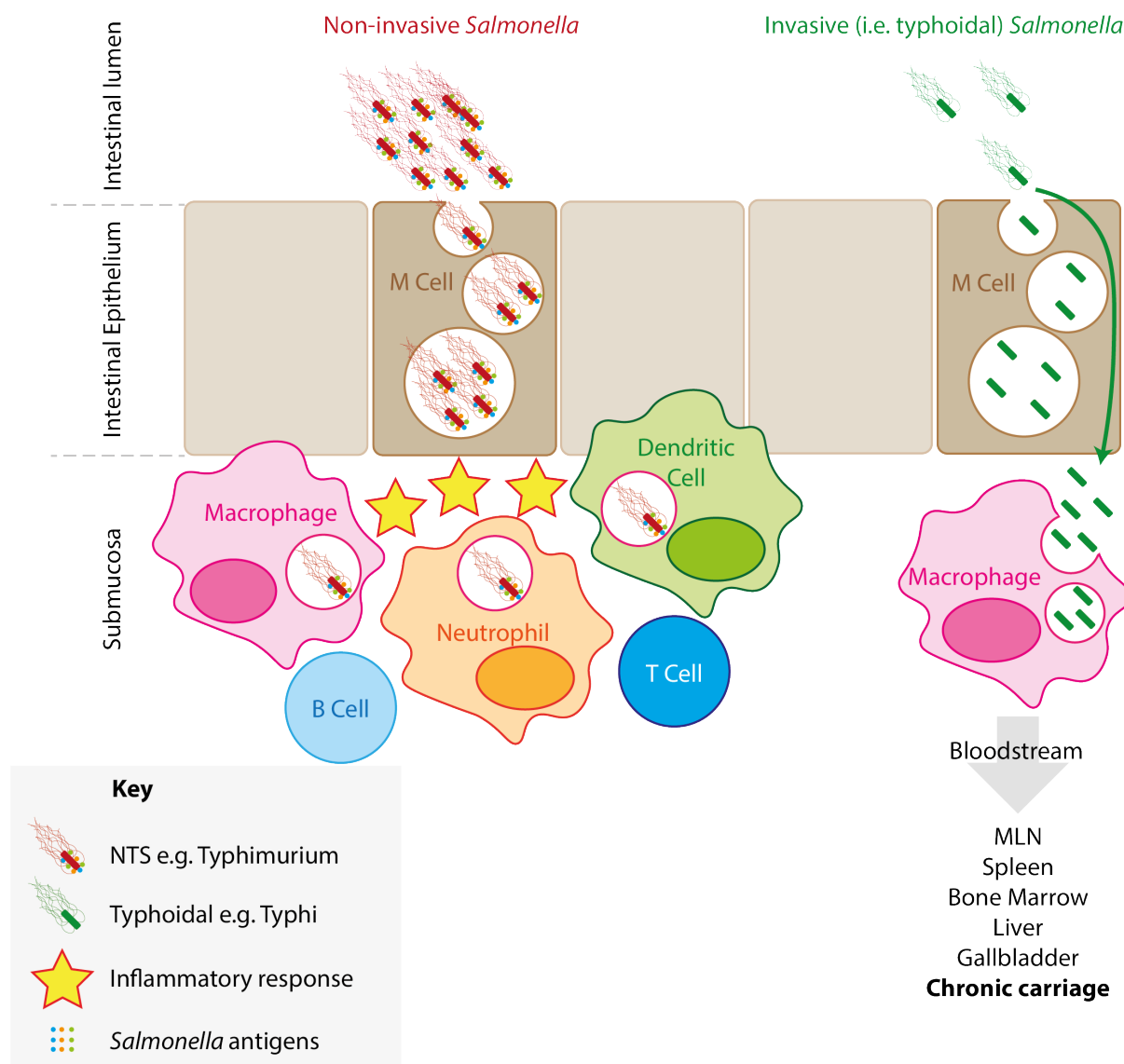


Fig. 1.1 **Pathogenesis of invasive and non-invasive *Salmonella***

Non-invasive *Salmonella* triggers a localised inflammatory response and recruitment of immune cells that limits dissemination. Invasive *Salmonella*, including typhoidal serovars, breaches the gut epithelium and spreads via the bloodstream and immune cells to systemic sites, which can result in chronic carriage.

Non-invasive, non-typhoidal *Salmonella* (NTS) typically causes rapid onset of gastroenteritis 6 – 72 h after infection. Infection is generally self-limiting and lasts an average of 10 days in immunocompetent individuals. Symptoms include vomiting and diarrhoea. Infection can still be lethal in immunocompromised individuals, and NTS infection still causes approximately 150,000 deaths per year. The most common NTS serovar affecting humans is *S. Typhimurium* sequence type 19 (ST19) (Gal-Mor, Boyle and Grassl, 2014).

Invasive non-typhoidal *Salmonella* (iNTS) is associated with a reduced host inflammatory response and the ability to replicate within macrophages (Ramachandran *et al.*, 2015). iNTS can cause systemic infection, symptoms similar to typhoid fever, and higher fatality rates than other NTS serovars, particularly in immunocompromised individuals (Crump *et al.*, 2015; Stanaway *et al.*, 2019). iNTS serovars include *Salmonella enterica* Javiana (R. A. Miller and Wiedmann, 2016), the multidrug resistant *S. Typhimurium* sequence type 313 (ST313) and *Salmonella* Enteritidis ST11 (Ramachandran *et al.*, 2015; Kantei *et al.*, 2021).

Typhoidal *Salmonella* includes serovars Typhi, Paratyphi A, B and C, and Sendai (Gal-Mor, Boyle and Grassl, 2014). Unlike NTS infection, *S. Typhi* incubation ranges from 3 to 60 days and causes minimal gastrointestinal inflammation. Typhoidal *Salmonella* establishes a systemic infection, colonising the intestine, mesenteric lymph nodes, liver, spleen, and bone marrow (Parry *et al.*, 2002; Raffatellu *et al.*, 2008). Symptoms of infection include a fever of $>38^{\circ}\text{C}$, lethargy and other influenza-like symptoms, which last for an average of 3 weeks. Up to 10% of patients infected with *S. Typhi* shed the bacteria in their faeces for up to three months following infection. 1-4% become chronic carriers, shedding the bacteria for more than a year (Parry *et al.*, 2002; Gal-Mor, Boyle and Grassl, 2014; Gal-Mor, 2019). Of these long-term carriers, most carry the infection asymptotically, and 25% have no history of acute typhoid symptoms, suggesting that the initial infection was asymptomatic or misdiagnosed (Parry *et al.*, 2002). These chronic carriers retain the pathogen in the population and can transmit the infection to others via their faeces, which can then present as typhoid fever. A famous example of an asymptomatic chronic carrier is Mary Mallon, also known as 'Typhoid Mary', an Irish cook in New York in the early 1900s who inadvertently killed over 50 people by serving them contaminated food, whilst never suffering symptoms of typhoid fever herself (Gal-Mor, Boyle and Grassl, 2014; Galán, 2016).

1.3 Diagnostics and Treatment

1.3.1 Diagnosis of *Salmonella* infection

Accurate diagnosis of typhoid fever is complicated by the lack of distinct symptoms, which leads to cases being confused with malaria, dengue and other febrile disease (Parry *et al.*, 2002). Asymptomatic chronic carriage also complicates clinical diagnosis of *Salmonella* infection, to the extent that the WHO has made development of new tools to identify and treat chronic carriers a research priority (World Health Organization, 2018).

S. Typhi can be cultured from patient samples including faeces, blood, and bone marrow (Gilman *et al.*, 1975). In each case, test accuracy is dependent on the amount of sample cultured but can still correctly diagnose typhoid even after antibiotic courses have started. Bone marrow samples are the most sensitive, positive in 80 – 95% of typhoid patients, followed by blood samples, positive in 60 – 80% of typhoid patients, and stool samples, which are positive in 30% of typhoid patients (Hussein Gasem *et al.*, 1995; Wain *et al.*, 2001; Parry *et al.*, 2002).

In addition to culture tests, there are several antibody tests available. The most common is Widal's Test, which measures levels of antibody against O and H antigens of *S. Typhi* (Andrews and Ryan, 2015). However, levels of these antibodies do not directly correlate to the extent of infection and vary between populations and individuals. Furthermore, the O and H antigens of *S. Typhi* are common to other serovars of *Salmonella*. A test that measures antibody levels against the Typhi-specific Vi polysaccharide antigen has been shown to be 70 – 80% sensitive and 80 – 95% specific. Overall, antibody tests are useful diagnostic tools when corrected for differences in population and when used in conjunction with other tests (Parry *et al.*, 2002, 2011).

A recent study was able to identify distinct metabolite signatures between acute and chronic typhoid cases, and were able to narrow their findings to five metabolic markers (Näsström *et al.*, 2018). Machine learning techniques on patient gene expression profiles have also discovered a diagnostic signature that can differentiate typhoid fever from other febrile illnesses, even in cases where

Salmonella could not be cultured from samples. PCR-based diagnostics are a promising diagnostic tool (Blohmke *et al.*, 2019).

1.3.2 Antibiotic Resistance

Salmonella infection is ordinarily treated with antibiotics (Gal-Mor, Boyle and Grassl, 2014). However, multidrug resistant (MDR) strains of *S. Typhi* have increased over the past decades, resistant to first line antibiotics such as ampicillin, trimethoprim-sulfamethoxazole and chloramphenicol (World Health Organization, 2018; Yang, Chong and Song, 2018). For example, MDR *S. Typhi* caused treatment failures in Nepal (Thanh *et al.*, 2016) and the incidence of MDR *S. Typhi* in Malawi increased from 7% to 97% between 2010 and 2014 (Feasey *et al.*, 2015). The resultant switch to the use of second- and third-line antibiotics for treatment has seen the emergence of extensively drug resistant (XDR) strains in Pakistan, with resistance to fluoroquinolones and third generation cephalosporins as well as first line antibiotics (Klemm *et al.*, 2018). There are few treatment options for XDR *S. Typhi* infection, prompting the World Health Organisation to make research into new treatment measures a research priority (World Health Organization, 2018).

1.3.3 Vaccination

In addition to antibiotic treatment, there are three vaccines for typhoid fever currently licensed for use by the WHO. These include a typhoid conjugate vaccine (TCV), unconjugated Vi polysaccharide (ViPS) and a live vaccine (Ty21A) (World Health Organization, 2018).

TCV consists of, and stimulates an immune response against, the Vi polysaccharide antigen of *S. Typhi* and tetanus toxin protein. TCV was shown to be 54.6% effective at preventing all possible typhoid fever symptoms in adults in randomised controlled trials, with an efficacy of 87.1% in preventing the field definition of typhoid fever: $>38^{\circ}\text{C}$ fever and bacteraemia (Jin *et al.*, 2017). There is currently insufficient data to validate the efficacy of TCV in the field following natural exposure to typhoid fever (Milligan *et al.*, 2018). However, its introduction is still

recommended by the WHO in countries with a severe typhoid burden due to its superior immunological properties compared to the other vaccine options (World Health Organization, 2018).

ViPS, consisting of the Vi polysaccharide antigen alone, displays differences in vaccine efficacy dependent on the population tested. For instance, 52% of healthy typhoid-naïve adults taking part in a randomised control trial were protected, compared to 64%-72% of patients in Nepal, China and South Africa where typhoid is endemic and interaction with *S. Typhi* more likely (Jin *et al.*, 2017; World Health Organization, 2018). Furthermore, age affects the efficacy of the vaccine: field studies in India revealed 56% protection in children aged 5-14 years and 80% protection in children aged 2-4 years (World Health Organization, 2018). Overall, a meta-analysis of typhoid vaccine studies concluded that ViPS has an efficacy of 45% to 69% two years after vaccination, with a three year cumulative efficacy suggested to be 55% (Milligan *et al.*, 2018).

Ty21A is an attenuated strain of *S. Typhi* lacking virulence genes including the Vi capsule and stimulates an immune response against O, H, and other surface antigens of *S. Typhi*. Field trials in Chile and Egypt indicate it prevented typhoid fever in 62% to 96% of cases up to 7 years after vaccination (World Health Organization, 2018).

Mathematical modelling has predicted that vaccination alone is not sufficient to eradicate typhoid (Pitzer *et al.*, 2014). Therefore, improvements in diagnostics and alternative treatments are an international research focus. To achieve this, a better understanding of the pathogenesis of *S. Typhi* is needed.

1.4 Pathogenesis of *S. Typhi*

1.4.1 *Salmonella* entry into host cells

Salmonella infections are caused by ingestion of contaminated food or water. *Salmonella* enters the gastrointestinal (GI) system and survives due to a high tolerance for the acidic conditions in the stomach (Ohl and Miller, 2001). Bacteria progress through the GI tract into the small intestine, where they adhere to intestinal epithelial cells, favouring specialised cells known as M cells (**Fig. 1.1**) (Fàbrega and

Vila, 2013; Dougan and Baker, 2014). These cells are found within Peyer's patches, which are the key interface between the lymph system and the intestine. M cells transport antigens from the intestinal lumen to immune cells in the lymph nodes, providing *S. Typhi* with a route to disseminate further into the body via phagosomes in the lymph system (Dougan and Baker, 2014).

NTS invasion of host cells stimulates an inflammatory response, such as secretion of pro-inflammatory cytokines, pyroptosis of infected epithelial and macrophage cells, and recruitment of neutrophils (Knodler *et al.*, 2014). However, *S. Typhi* invasion elicits a weaker and subclinical inflammatory response, allowing it to disseminate to other organ systems and establish systemic infection (Dougan and Baker, 2014; Winter *et al.*, 2015).

As *S. Typhi* is host restricted to humans there have been efforts to find effective animal models to model *S. Typhi* infection. Much of the work on *Salmonella* pathogenesis has been done using *S. Typhimurium* in mouse or *in vitro* models (Dougan and Baker, 2014). However, it is important to note differences between *S. Typhimurium* and *S. Typhi* invasion, virulence and immune evasion mechanisms.

Roughly 90% of the *S. Typhi* genome consists of genes homologous to *S. Typhimurium* serovars, showing that there is a conserved *Salmonella* core genome (Chan *et al.*, 2003). *Salmonella* pathogenicity is controlled by genomic segments known as *Salmonella* pathogenicity islands (SPIs), which encode genes with roles in cell attachment and invasion, immune evasion, and bacterial effector secretion (Dougan and Baker, 2014). *Salmonella* invasion of host cells is mediated by SPI-1 and SPI-2, which together facilitate cell entry by bacterial-mediated macropinocytosis, and formation of an intracellular niche within a *Salmonella*-containing vacuole (SCV). Work on SPI-1 and SPI-2 has predominantly been done in *S. Typhimurium*, and whereas *Typhi* does encode a functional SPI-1 and SPI-2, there are differences in effectors and the virulence strategies that *S. Typhimurium* and *S. Typhi* employ.

1.4.2 SPI-1

SPI-1 encodes a type-III secretion system (T3SS), a needle-like appendage found in certain species of Gram-negative bacteria that acts to sense eukaryotic host cells and translocate effector proteins into them. In *S. Typhimurium*, SPI-1 effector proteins include SipA (McGhie, Hayward and Koronakis, 2001, 2004) and SopE (Hardt *et al.*, 1998; Humphreys *et al.*, 2012), which subvert host cell signalling pathways responsible for rearrangement of the actin cytoskeleton. This results in the formation of membrane ruffles, forming large vesicles that engulf the adherent *Salmonellae* and draw them into the cell (McGhie *et al.*, 2009; Lorkowski *et al.*, 2014). The SPI-1 effector SopB is a phosphoinositide phosphatase that interrupts progression of the SCV through the normal endosomal maturation pathway, causing it to become enlarged and thus creating a spacious environment for *Salmonella* growth and replication (Hernandez *et al.*, 2004).

SPI-1 effectors also modulate immune responses to *Salmonella* infection, which differ between *S. Typhimurium* and *S. Typhi*. Inflammatory responses are triggered by SPI-1 effectors such as SopA (Wood *et al.*, 2000; Zhang *et al.*, 2006) and are favoured by *S. Typhimurium*, as neutrophil recruitment reduces the intestinal microbiota to give *Salmonella* a competitive advantage (Sekirov *et al.*, 2010). However, SopA is a pseudogene in *S. Typhi* (Dougan and Baker, 2014) which correlates with the fact that inflammation is not a characteristic of *S. Typhi* infection. Furthermore, *S. Typhi* has mutations in genes such as *ttrS* that would otherwise enable NTS to capitalise on the high levels of reactive oxygen species generated by neutrophils (Dougan and Baker, 2014).

S. Typhimurium has also evolved SPI-1 dependent mechanisms to evade recognition and host defence responses. SPI-1 deletion *S. Typhimurium* mutants invaded primary porcine alveolar macrophages less efficiently than wild type, and SPI-1 effectors suppressed pro-inflammatory cytokine production and promoted macrophage death (Pavlova *et al.*, 2011). *Salmonella* effector SopB can prevent infection-induced apoptosis by maintaining levels of the pro-survival kinase Akt (Knodler, Finlay and Steele-Mortimer, 2005). Other *S. Typhimurium* SPI-1 effectors with anti-inflammatory effects including *avrA*, which inhibits NF-KB signalling and

contributes to intracellular bacterial survival *in vivo* (Collier-Hyams *et al.*, 2002; Wu, Jones and Neish, 2012), and *sptP*, which reduces membrane ruffling following bacterial entry and downregulates proinflammatory cytokine release (Lin, Le and Cowen, 2003; Johnson *et al.*, 2017). Although *sptP* is also expressed in *S. Typhi* with a 94% sequence identity, it is not translocated into the host, indicating that *S. Typhi* and NTS employ different virulence strategies (Johnson *et al.*, 2017).

1.4.3 SPI-2

Once *Salmonella* is internalised within the SCV, SPI-2 encodes effectors that are released across the phagosomal membrane into the host cell cytosol. These act to interrupt the normal progression of vesicle trafficking and maturation, allowing the SCV to escape from lysosomal degradation and instead act as an intracellular niche for *Salmonella* to replicate in (McGhie *et al.*, 2009; Fàbrega and Vila, 2013; Liss *et al.*, 2017). For example, a key SPI-2 effector is SopD2, which targets both Rab7 and Rab32 and inhibits normal endosomal trafficking (D'Costa *et al.*, 2015; Spanò *et al.*, 2016). SopD2 deletion in *S. Typhimurium* attenuates virulence in mice, although interestingly SopD2 is a pseudogene in *S. Typhi*, suggesting that *S. Typhi* employs a different evasion mechanism (Parkhill *et al.*, 2001; Spanò *et al.*, 2016). Indeed, a study in human macrophages suggested that SPI-2 was not essential for *S. Typhi* survival, whereas SPI-2 deficient *S. Typhimurium* is highly attenuated in mice (Hensel *et al.*, 1998; Forest *et al.*, 2010).

Other SPI-2 effectors in *S. Typhimurium* include SpiC, which inactivates the host protein Hook3, a key component of endosomes responsible for endosomal fusion with organelles (Uchiya *et al.*, 1999; Shotland, Krämer and Groisman, 2003). *S. Typhimurium* can also recruit host proteins to the autophagosome, such as focal adhesion kinase (FAK) which inhibits autophagy (Owen, Anderson and Casanova, 2016).

Studies in *S. Typhimurium* have shown that SCVs traffic to the perinuclear region of the host cell, adjacent to the Golgi apparatus, where the replicative niche is reinforced by the formation of tubulovesicular *Salmonella*-induced filaments (SIFs) through the action of the SPI-2 effector SifA (Stein *et al.*, 1996). SIFs form a network

that extends outwards into the host cell, using the host microtubular network, which serves to provide nutrients to the SCV (Rajashekar *et al.*, 2008; Knuff and Finlay, 2017; Liss *et al.*, 2017).

As well as modulating endosomal trafficking, multiple SPI-2 effectors also inhibit innate immune signalling in *S. Typhimurium* (Jennings, Thurston and Holden, 2017). For example, SpyC dephosphorylates ERK, p38 and MAPKs, thus inhibiting proinflammatory cytokine transcription (Mazurkiewicz *et al.*, 2008). GtgA suppresses inflammation by cleavage of the DNA binding loop in p65 and RelB (Sun *et al.*, 2016). SseK2 and SseK3 inhibit TNF α -stimulated NF- κ B signalling (Yang *et al.*, 2015; Günster *et al.*, 2017). GogB mutants exhibit severe caecal inflammation in mice (Pilar *et al.*, 2012). Finally, SpvD binds Exportin-2 and thus interrupts the import and export of KPNA1, thus inhibiting nuclear import of p65 (Rolhion *et al.*, 2016).

1.4.4 *S. Typhi* specialisation

A comparative genomic analysis divided *S. enterica* into two subpopulations, referred to as clade A and clade B (den Bakker *et al.*, 2011). *S. Typhi* and *S. Paratyphi A* were found in a subclade of clade A and shared SPIs including SPI-18, which has roles in invasion, and a cytolethal distending toxin (CDT) islet, which will be covered in greater detail in the following section. These islets were unique to the *Typhi* subclade and were not found in the other clade A serovars studied, which included NTS such as *S. Typhimurium*. Of the 98 species of *S. enterica* studied approximately 20% were in clade B, which were found to also contain SPI-18 and the CDT islet, as well as β -glucuronidase and S-fimbrial operons (den Bakker *et al.*, 2011; Rodriguez-Rivera *et al.*, 2015). These clade B serovars included *S. Javiana* and *S. Montevideo*, which are examples of disease-causing iNTS (den Bakker *et al.*, 2011; R. A. Miller and Wiedmann, 2016).

Although *S. Typhi* and *S. Typhimurium* have a common core genome, *S. Typhi* shows specialised methods of immune evasion and dissemination within the host. *S. Typhi* has reduced approximately 10% of the NTS genome into pseudogenes, including genes that contribute to virulence and host interactions in *S. Typhimurium*

(Parkhill *et al.*, 2001). Furthermore, the *S. Typhi* genome contains 300-400 Typhi-specific genes in unique SPIs, including SPI-7, -15, -17 and -18 (Chan *et al.*, 2003; Dougan and Baker, 2014).

SPI-7 encodes genes implicated in attachment to human cells, including a specialised type IVB pilus that binds to the host epithelial cystic fibrosis transmembrane conductance regulator (CFTR) and enables host adhesion (Tsui *et al.*, 2003). This differs from NTS such as *S. Typhimurium*, which adhere to intestinal epithelial cells via specialised fimbriae (Bäumler, Tsolis and Heffron, 1996). The genetic sequences for these fimbriae were found to be compromised in *S. Typhi* and other serovars capable of causing systemic infection (Townsend *et al.*, 2001; Bishop *et al.*, 2008; Kisiela *et al.*, 2012; Dougan and Baker, 2014).

SPI-7 also encodes the Vi capsule, an $\alpha(1\rightarrow4)$ -D-GalpANAc homopolymer that encapsulates the *S. Typhi* bacterium and shields surface antigens from host innate immune recognition and response (Pickard *et al.*, 2003; Dougan and Baker, 2014). The Vi capsule was shown to prevent TLR4-dependent recognition of *S. Typhi* and thus prevent macrophage production of pro-inflammatory IL-6 (Wilson *et al.*, 2008). Furthermore, neutrophils did not extend chemotactic pseudopodia towards Vi-positive *S. Typhi*, but did towards *S. Typhimurium* and *E.coli* (Wangdi *et al.*, 2014). This allows *S. Typhi* to evade an acute host inflammatory response and establish persistent and systemic infection. Indeed, *S. Typhimurium* engineered to express the Vi capsule was shown to persist in mice when compared to infection with the wild-type (Jansen *et al.*, 2011).

S. Typhi is able to downregulate production of pattern-associated molecular patterns (PAMPs) to reduce host inflammatory responses. For example, *S. Typhi* encodes the transcriptional regulator TviA, which allows it to repress expression of flagellin which otherwise stimulates host production of proinflammatory IL-8 and pyroptosis (Winter *et al.*, 2008, 2015).

S. Typhi infects dendritic cells or CD18⁺ phagocytes in the gut-associated lymph tissue (Watson and Holden, 2010). Rather than be degraded within the lysosome, *S. Typhi* can survive and replicate, and can use infected phagocytes to be disseminated throughout the body. Invasion of the lymph system allows *S. Typhi* to

access the liver, spleen and, via bile, the gallbladder, where it has been shown to establish replicative niches (Watson and Holden, 2010).

1.4.5 Gallbladder cancer

S. Typhi and *S. Typhimurium* encodes environmental sensor kinases PhoQ and PhoP, which induce activation of genes providing resistance to the hostile environment of the gallbladder (van Velkinburgh and Gunn, 1999). This resistance enables *S. Typhi* to form biofilms on gallstones and to establish a chronic and asymptomatic infection within the gallbladder (Prouty, Schwesinger and Gunn, 2002; Crawford *et al.*, 2010).

Chronic *S. Typhi* carriage within the gallbladder has been linked with gallbladder cancer, a cancer with poor prognosis (Di Domenico *et al.*, 2017). Gallbladder cancer is rare in the western world but relatively common in India and Pakistan where 85% of worldwide typhoid cases occur (Scanu *et al.*, 2015). There is a positive correlation between the presence of gallstones and gallbladder carcinoma with presence of both *S. Typhi* Vi and flagellin (Dutta *et al.*, 2000; Nath *et al.*, 2008). For example, 44% of gallbladder cancer patients were positive for *S. Typhi* in Chile, where typhoid is endemic (Koshiol *et al.*, 2016). Between 1922 and 1975 in New York, chronic typhoid carriers were 6 times more likely to die of cancer than controls (Welton, Marr and Friedman, 1979).

S. Typhi infection was shown to transform susceptible mice, gallbladder organoids and mouse embryonic fibroblasts (MEFs) via activation of AKT and MAPK pathways (Scanu *et al.*, 2015). Susceptibility to transformation was dependent on mutations in P53 and amplification of c-Myc, suggesting that patients with mutations in these oncogenes may be predisposed to developing gallbladder cancer following *S. Typhi* infection (Scanu *et al.*, 2015).

The study did not identify which *S. Typhi* effectors were responsible for AKT and MAPK-dependent transformation. However, it is well established that a common trigger of oncogenesis and malignant transformation is DNA damage, and *S. Typhi* encodes a genotoxic virulence factor known as the typhoid toxin. Thus, the typhoid

toxin is an interesting candidate for linking *S. Typhi* infection and gallbladder cancer.

1.5 The typhoid toxin

1.5.1 Cytolethal distending toxins

The typhoid toxin was first identified in *S. Typhi* as a cytolethal distending toxin (CDT), with its name coined because of its suggested link to typhoid fever symptoms (Haghjoo and Galán, 2004). CDTs induce a DNA damage response (DDR), cellular and nuclear distension, and subsequently cell death, in eukaryotic cells. They have been identified in multiple bacterial species including *Campylobacter* spp., enteropathogenic *Escherichia coli* (Pérès *et al.*, 1997), *Shigella dysenteriae* (Okuda, Kurazono and Takeda, 1995), *Haemophilus ducreyi* (Cope *et al.*, 1997), *Actinobacillus actinomycetemcomitans* (Sugai *et al.*, 1998; Yamano *et al.*, 2003), and *Helicobacter hepaticus* (Young, Knox and Schauer, 2000). Interestingly, since the discovery of the typhoid toxin more than 40 NTS serovars have been found to encode CDT-toxins distinct from the typhoid toxin, which also cause DDRs and have been shown to influence infection (den Bakker *et al.*, 2011; Rodriguez-Rivera *et al.*, 2015; R. Miller and Wiedmann, 2016; Miller *et al.*, 2018).

CDTs in most species are tripartite oligomeric proteins that are secreted by bacteria during infection. They consist of the CdtA, CdtB and CdtC subunits. CdtA and CdtC are responsible for delivery of the DNase-I like CdtB into the host nucleus, where CdtB acts as the catalytic subunit and induces a DDR and cell cycle arrest (Lara-Tejero and Galan, 2000; Hassane *et al.*, 2001; Lara-Tejero and Galán, 2001, 2002; Li *et al.*, 2002; Hassane, Lee and Pickett, 2003; Guerra *et al.*, 2011). This damage was shown to be via induction of single strand breaks in DNA that then developed into double strand breaks during DNA replication (Fedor *et al.*, 2013). CDTs have been shown to induce apoptosis in intoxicated cells (Gelfanova, Hansen and Spinola, 1999; Cortes-Bratti *et al.*, 2001; Alaoui-El-Azher *et al.*, 2010). Chronic exposure to CDTs has been linked to increases in chromosomal instability and mutation frequency (Guidi, Guerra, *et al.*, 2013).

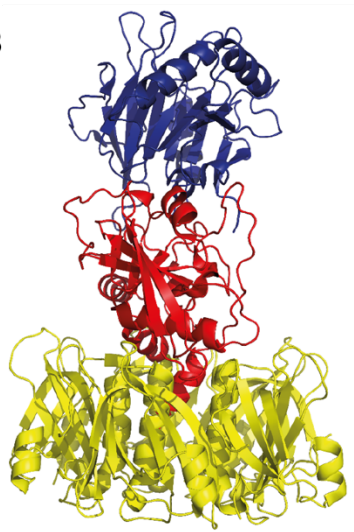
Intriguingly, CdtB has attenuated nuclease activity relative to DNase I, displaying only 0.01% efficiency compared to bovine DNase I (Elwell *et al.*, 2001). However, mutagenesis of conserved residues between DNase I and CdtB abrogates the ability of CdtB to cause cell cycle arrest (Elwell and Dreyfus, 2000). For example, two histidines (H160 and H274) were found to be critical for CdtB toxicity, and a H160Q mutation was sufficient to abolish toxicity (Nešić, Hsu and Stebbins, 2004). Furthermore, comet assays and pulsed field gel electrophoresis have shown that DNA is fragmented by CdtB (Elwell and Dreyfus, 2000; Frisan *et al.*, 2003; Fedor *et al.*, 2013; Fahrer *et al.*, 2014).

The *S. Typhi* genome was found to contain a sequence with 50% sequence similarity to the CdtB subunit of other CDTs. Interestingly, however, *S. Typhi* contains no homologues for CdtA or CdtC (Haghjoo and Galán, 2004). Instead, *S. Typhi* was found to encode two sequences homologous to the pertussis toxin of *Bordetella pertussis*: pertussis-like toxin A and B (PltA and PltB) (**Fig. 1.2**). The typhoid toxin is a hybrid toxin formed of one subunit of each of CdtB and PltA, with a PltB pentamer, together formed into a pyramid-like structure. CdtB performs the same DNase-like function as seen in other CDTs, and the ADP-ribosylating subunit PltA acts as a linker region to PltB, which binds glycoproteins on the host cell-surface membrane to mediate toxin uptake (Spanò, Ugalde and Galán, 2008; Song, Gao and Galan, 2013).

A



B



CdtB

PltA

PltB

C

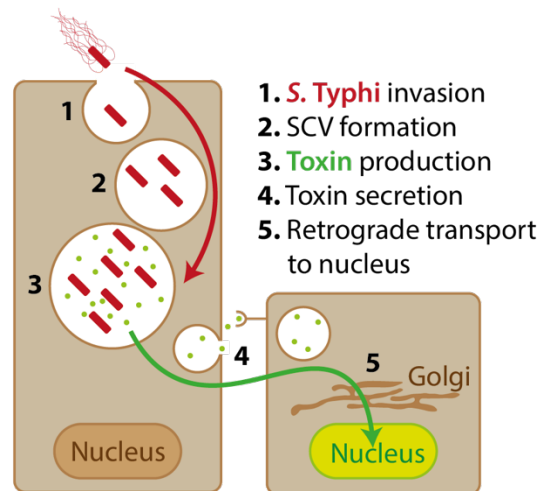


Fig. 1.2 Typhoid toxin structure and delivery

(A) The typhoid toxin encoding islet contains the three subunits of the toxin, *cdtB*, *pltA* and *pltB*, and a muramidase, *ttsA*. (B) The 3D structure of the typhoid toxin showing the CdtB (blue), PltA (red) and PltB (yellow) subunits (Song, Gao and Galan, 2013). (C) *S. Typhi* invades gut epithelial cells and is enclosed within a *Salmonella* containing vacuole (SCV), where it secretes the typhoid toxin. The typhoid toxin is exocytosed from the infected cell and binds to target host cells via PltB in an autocrine or paracrine manner. The toxin is endocytosed and trafficked to the host nucleus by retrograde transport.

Typhoid toxin orthologues are also found in iNTS serovars. Predicted peptide products of typhoid toxin orthologues across Typhi and the iNTS serovars Javiana, Montevideo, Oranienburg and Mississippi was found to have 98.1%, 96.1%, and 99.4% conserved amino acids for *pltA*, *pltB*, and *cdtB* (R. A. Miller and Wiedmann, 2016). The toxin of iNTS *S. Javiana* was found to induce DNA damage and cell cycle arrest in a similar manner to typhoid toxin, but to elicit different clinical presentations dependent on differences in the receptor binding subunit *pltB* (R. A. Miller and Wiedmann, 2016; Lee *et al.*, 2020).

1.5.2 Secretion and delivery of the typhoid toxin

The toxin is synthesised by *S. Typhi* and secreted into the SCV lumen via a holin/endolysin system (Galán, 2016). The timing of toxin secretion is dependent on the *Salmonella* PhoP-PhoQ sensing system, which induces toxin expression upon

detection of the environment conditions within the SCV (Fowler and Galán, 2018). The transcriptional regulator IgeR also prevents CdtB production when *Salmonella* is in an extracellular environment (Haghjoo and Galán, 2007).

Toxin subunits are individually exported from the bacterial cytoplasm into the periplasm, where the full toxin is assembled. The endolysin TtsA (typhoid toxin secretion A), an N-acetyl-b-D-muramidase, is encoded in the same genomic islet as the subunits of the typhoid toxin. TtsA is released into the *S. Typhi* periplasmic space via pores in the inner membrane formed by holins (Geiger *et al.*, 2018). Once delivered, TtsA catalyses localised and controlled disruption of the peptidoglycan layer of the bacterial cell wall, allowing for selected proteins, such as the typhoid toxin, to be secreted through it (Hodak and Galán, 2013). TtsA was found to not be necessary for CDT-toxin secretion in non-typhoidal *Salmonella* serovars (Miller *et al.*, 2018).

Once in the SCV lumen, the toxin is exocytosed from the host cell via outer membrane vesicle intermediates in a process dependent on SPI-2 effectors including SifA (Spanò, Ugalde and Galán, 2008; Guidi, Levi, *et al.*, 2013). The toxin can then be endocytosed in an autocrine or paracrine manner.

Plasma membrane binding on the target cell is mediated by the PltB pentamer, which recognises and binds specific N-linked surface glycans. The toxin was found to bind tri-antennary sialylated glycoproteins with the greatest binding affinity, specifically with the consensus sequence Neu5Ac2-3Gal β 1-3/ β 1-4Glc/GlcNAc (Song, Gao and Galan, 2013; Deng *et al.*, 2014; Galán, 2016). However, it could bind to a wide range of N-linked glycoproteins and even glycolipids, though with reduced affinity, allowing the toxin to bind a wide variety of cell types (Song, Gao and Galan, 2013). The presence of Neu5Ac in the consensus sequence is particularly interesting. Human sialoglycans primarily terminate with Neu5Ac, as humans do not express CMP-N-acetylneuraminic acid hydroxylase (CMAH), which converts Neu5Ac to Neu5Gc (Varki *et al.*, 2011). CMAH is expressed in most mammals, meaning that most non-human mammalian sialoglycans are terminated in Neu5Gc. Whilst the typhoid toxin binds Neu5Ac terminated glycans with high affinity, it does not recognise Neu5Gc, meaning that the toxin can recognise and

bind human cells but not cells of many other mammals. This is another example of the human specificity of *S. Typhi*, and could be reason for it only causing disease in humans (Deng *et al.*, 2014). For example, *S. Typhi* only causes mild symptoms consistent with NTS infection in chimpanzees (Edsall *et al.*, 1960; Gaines, Tully and Tigertt, 1968) which express CMAH and thus Neu5Gc. Mice, however, do still express Neu5Ac and therefore can be used as models for investigating the effects of the toxin.

In a process similar to other CDTs, the typhoid toxin has been shown to be transported in a retrograde manner from endosomes to the Golgi and endoplasmic reticulum, exploiting the endoplasmic reticulum associated degradation (ERAD) pathway to be translocated into the cytosol and then into the nucleus via nuclear pores (Guerra *et al.*, 2005, 2009; Frisan, 2016; Chang *et al.*, 2019). An N-terminal segment of *Actinobacillus actinomycetemcomitans* CdtB was found to be necessary for active nuclear localisation, although it is currently unknown exactly how the typhoid toxin enters the nucleus (Nishikubo *et al.*, 2003). Once in the nucleus, CdtB of the typhoid toxin has been shown to cause DNA damage and cell cycle arrest, which is consistent with CdtB of other CDTs (Song, Gao and Galan, 2013; Ibler *et al.*, 2019).

1.5.3 *In vivo* effects of the typhoid toxin

The typhoid toxin is currently seen as one of the principal virulence factors of *S. Typhi*. Many pathogens use genotoxic virulence effectors to exploit host DDRs as a strategy to promote infection and pathogen survival (Weitzman and Weitzman, 2014; Grasso and Frisan, 2015; Chumduri *et al.*, 2016). When the typhoid toxin was first discovered it was suggested that it had a role in causing typhoid fever symptoms (Song, Gao and Galan, 2013), but more recently studies have suggested a role in promoting chronic and systemic infection, as well as having a significant effect on bacteraemia (Del Bel Belluz *et al.*, 2016; Miller *et al.*, 2018; Gibani *et al.*, 2019). Furthermore, the toxin was shown to induce an anti-inflammatory response in healthy mice, suggesting a role in immunomodulation and possibly immune evasion (Martin *et al.*, 2021).

Peritoneal injection of the toxin into mice caused symptoms of typhoid fever, including lethargy, weight loss, and a reduction of leukocytes and neutrophils, with death in all mice occurring after 5 days (Song, Gao and Galan, 2013). The phenotype was dependent on the catalytic site of CdtB, as an H160 mutant did not have the same effect. Constitutive expression of Neu5Gc-glycosylated receptors in the mice was sufficient to provide resistance to the effects of the toxin, showing that receptor-binding of the toxin was necessary for the phenotype (Deng *et al.*, 2014).

However, in an infection model using recombinant *S. Typhimurium* engineered with the toxin islet, the presence of the toxin promoted mouse survival and significantly reduced gut inflammation in the early stages of infection (Del Bel Belluz *et al.*, 2016). Using *S. Typhimurium* strains developed to induce typhoid-fever symptoms in mice, the study showed that infection with toxin-negative *S. Typhimurium* resulted in death for 40% of the infected population after 15 days with excessive inflammation identified in the gut. However, all mice infected with toxin-expressing *S. Typhimurium* survived the full course of the experiment. Interestingly, whereas the toxin reduced the gut inflammatory response it enhanced the inflammatory response in the liver. The toxin also promoted chronic carriage, with toxigenic *S. Typhimurium* isolated from livers, caeca, and MLNs of infected mice 180 days post-infection. No *Salmonella* was recovered at the 180-day timepoint from mice infected with control non-toxigenic strains indicating toxin-dependent chronic carriage (Del Bel Belluz *et al.*, 2016). Expression of the toxin was found to promote infection of the liver in mice by the toxigenic NTS serovar *S. Javiana*, suggesting a role in immune evasion and systemic dissemination (Miller *et al.*, 2018). Furthermore, infection with toxigenic *Salmonella* was shown to cause both a DDR and senescence *in vivo*, but interestingly also a toxin-dependent anti-inflammatory environment which is characteristic of *S. Typhi* infection (Martin *et al.*, 2021).

In 2019 a human challenge study suggested that the toxin in fact had no role in the initiation of typhoid fever symptoms (Gibani *et al.*, 2019). 40 human volunteers were infected with wild-type or toxin-negative *S. Typhi* and monitored for 14 days until treatment with antibiotics. Interestingly there was no significant difference in the rate of typhoid infection or clinical manifestations between infection strains, aside

from a significantly prolonged bacteraemia in volunteers treated with the toxin-negative strain (i.e., wild-type 48h, toxin-negative 96h). Understandably, the study could not investigate differences in severe typhoid disease or bacterial carriage (Gibani *et al.*, 2019).

Based on current *in vivo* data it was hypothesised that the typhoid toxin is secreted by *S. Typhi* to facilitate infection strategies such as immune evasion, dissemination and chronic carriage. However, it is unknown how this hypothesis correlates with *in vitro* studies of the toxin, which show that it has a severe genotoxic effect on host cells. It is possible that the toxin is the transformative effector causing gallbladder cancer in cases of chronic *S. Typhi* infection. My PhD thesis aims to explore how the host responds to intoxication and counteracts dangerous phenotypes linked to DNA damage, such as cancer. To address this, I will first describe the host DDR.

2 DNA Damage Response

DNA is a fragile molecule that is prone to damage. This damage can be caused exogenously, such as by genotoxic molecules or radiation, or endogenously, such as in the process of DNA replication. Tens of thousands of DNA damage events occur in a single human cell every day, meaning that DNA metabolism and maintenance is a constantly active process (Jackson and Bartek, 2009).

Damage can be characterised by the appearance of single or double strand breaks (DSBs and SSBs respectively) in the DNA backbone, mismatches, base modifications such as alkylation or deamination or the appearance of crosslinks between stacked bases (Jackson and Bartek, 2009; Deans and West, 2011). All of these are potentially mutagenic, and all can cause the replication machinery to stall, putting the cell in a state of replication stress.

A variety of DDR pathways stabilise vulnerable sites, recognise damage, recruit repair proteins, and pause the cell cycle, allowing for the cell to initiate repair before the damage can escalate (Jackson and Bartek, 2009).

2.1 Causes of DNA Damage

2.1.1 Exogenous causes

Exogenous damage to DNA can occur through high energy radiation such as ultraviolet (UV) or ionising radiation (IR), or via numerous chemical agents, including bacterial genotoxins and chemotherapeutic drugs.

UV radiation, particularly at >280 nm wavelength, induces reactions and covalent structural rearrangements in pyrimidines leading to the formation of cytotoxic derivatives (Rastogi *et al.*, 2010). IR can ionise either DNA itself or lead to the formation of high-energy radical oxygen species that subsequently interact with DNA. This can result in both SSBs and DSBs as well as base modifications and DNA-protein crosslinks, which can proliferate by generation of further radicals (Mavragani *et al.*, 2019).

DNA damaging agents are often targeted against the components of the replication fork or associated machinery. For example, camptothecin and doxorubicin stabilise the interaction between topoisomerase and DNA or block it from binding, preventing it from relieving torsional stress in unreplicated DNA upstream of replication forks that leads to DNA breaks (Hsiang *et al.*, 1985; Wassermann *et al.*, 1990; Sørensen *et al.*, 1994). Hydroxyurea (HU) inhibits synthesis of deoxyribonucleotides, thus depleting the pool necessary for DNA replication and resulting in stalling of the replication fork (Collins and Oates, 1987). Aphidicolin is an inhibitor of DNA polymerase α (Pol- α), forming a bond with DNA close to the nucleotide binding site of polymerase that results in replication stress and DNA breaks (Baranovskiy *et al.*, 2014).

2.1.2 Endogenous causes

DNA damage can occur through errors in DNA replication, damage by reactive oxygen species and spontaneous hydrolysis at 37°C (Lindahl and Barnes, 2000). For example, DNA polymerases have an error rate of 1 in every 1000-30000 bp, leading to a high rate of incorporated mismatched bases. However proper function of the DNA repair response reduces these mismatches to 1 in 10^8 - 10^{11} (Kunkel and Loeb, 1981).

Helicases unwind the DNA double helix for replication or transcription, and in doing so inflict significant torsional stress on adjacent double stranded DNA, which if untreated would lead to DNA breakage. Topoisomerases reduce this tension upstream of helicase by introducing SSBs in double strand DNA (Wang, 1985; Pommier *et al.*, 1998). These cleavages are resealed, but in the case that they are not, for example if the replication machinery stalls and breaks down, then this also leaves untreated single strand nicks in the DNA backbone.

2.2 Replication stress

Sites of DNA damage can block the progression of DNA polymerase. During DNA replication, helicases generate two single strand templates that are then processed by DNA polymerase. If DNA polymerase stalls while helicase continues to race

ahead, long tracts of single-strand DNA (ssDNA) form, resulting in a state of replication stress. Unless stabilised, stalled forks are vulnerable to collapse. ssDNA is more fragile than double-strand DNA (dsDNA), and indeed ssDNA at the replication fork has been shown to be a precursor to chromosomal breakage (Feng *et al.*, 2011). Widespread fork breakdown is known as replication catastrophe, characterised by massive DNA breakage and disruption of the entire genome (Toledo *et al.*, 2014; Toledo, Neelsen and Lukas, 2017). DNA replication is therefore a carefully monitored process.

2.3 Apical Kinases

Cells use a variety of sensing pathways to identify mismatched bases, cross-linking, SSBs or DSBs. Mismatched bases, base modifications, and cross-linked bases can be excised and replaced by the correct base (Jalal, Earley and Turchi, 2011). However longer tracts of ssDNA or DSBs cannot be repaired in this manner and require more complex process. In these cases, three kinases are recruited to sites of damage using evolutionarily conserved motifs, where they regulate cell cycle checkpoints, prevent origin of replication firing, and trigger accumulation of specific repair factors (Shechter, Costanzo and Gautier, 2004; Falck, Coates and Jackson, 2005; Bekker-Jensen *et al.*, 2006). DNA dependent protein kinase (DNA-PK) and Ataxia Telangiectasia mutated (ATM) are recruited at DSBs (Caron *et al.*, 2015), whereas ATM and RAD3-related (ATR) is recruited to SSBs (Blackford and Jackson, 2017) (**Fig. 2.1**).

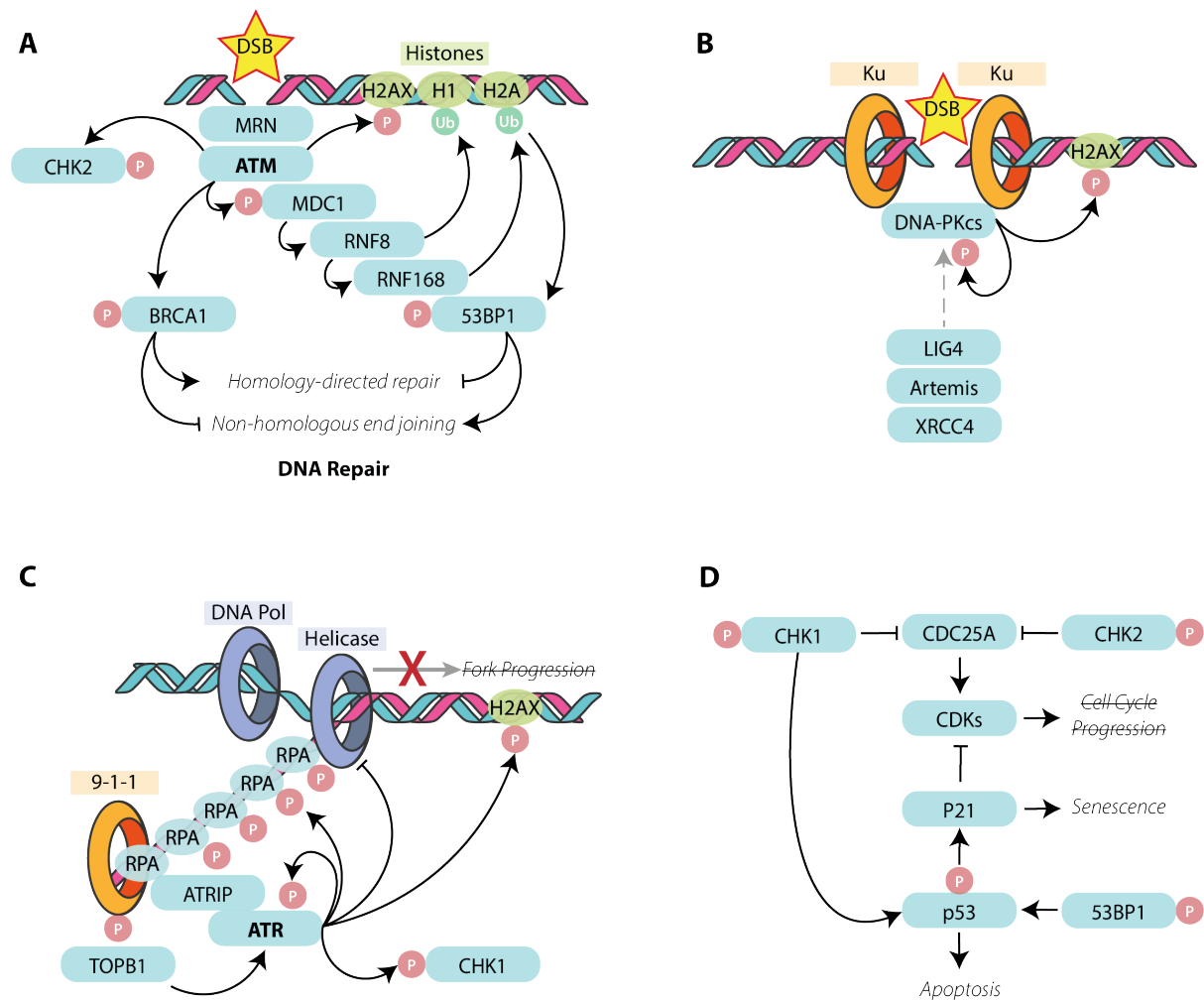


Fig. 2.1 **DNA damage responses to single- and double-strand DNA breaks**

ATM is recruited to DSBs by the MRN complex, where it phosphorylates multiple effectors including CHK2 and BRCA1, and 53BP1 via a phosphorylation and ubiquitination cascade. BRCA1 phosphorylation triggers homology directed repair, whereas 53BP1 can trigger non-homologous end joining. **(B)** Ku 70/80 cap either end of a DSB and recruit DNA-PKcs, which recruits repair factors including LIG4, Artemis and XRCC4. **(C)** Stalled DNA polymerase during replication results in lengthening tracts of fragile ssDNA. RPA stabilises ssDNA and recruits ATR via the adaptor protein ATRIP. RPA also stimulates the binding of the RAD9-RAD1-HUS1 (9-1-1) checkpoint clamp, which binds TopBP1, which subsequently activates ATR. ATR phosphorylates effector proteins such as CHK1, which reduces replication fork progression, origin firing and the G2/M transition. This reduces the burden of replication stress on the cell, prevents further damage, and allows the cell to activate DNA repair pathways. **(D)** Phosphorylated CHK1 and CHK2 inhibit CDC25A and thus cell cycle progression. CHK1 and 53BP1 also activate P53, which is a crucial transcription factor regulating cell fate decisions including entry into apoptosis or senescence via target genes including P21.

2.3.1 Double-strand break response

ATM is the master regulator of the cell response to DNA DSBs. A kinase, it phosphorylates a variety of substrates involved in DNA repair, the cell cycle and cell fate decisions. ATM is recruited to DSBs by the MRE11-RAD50-NBS1 (MRN) complex and undergoes autophosphorylation at numerous sites, resulting in ATM monomerization and activation (Bakkenist and Kastan, 2003; Kozlov *et al.*, 2011).

ATM can also be activated in an MRN-independent manner, in response to oxidative stress or certain conformational changes in chromatin (Kim *et al.*, 2009; Guo *et al.*, 2010).

Upon activation, ATM initiates a phosphorylation and ubiquitination signalling cascade. A key phosphorylation target is H2AX, one of four histone H2A variants that makes up 11-25% of H2A within the cell (West and Bonner, 1980; Kinner *et al.*, 2008). H2A phosphorylation at Ser139 is a marker of DNA damage and leads to formation of phospho-H2AX (γ H2AX). Phosphorylation occurs quickly following damage and has been seen as soon as 1 minute after exposure to IR whilst peaking 15-20 minutes after exposure (Rogakou *et al.*, 1999; Redon *et al.*, 2009). γ H2AX does not act as the initial sensor of DNA damage, but rather a platform for recruitment of further DNA repair factors, and acts to transmit signal up to 15 Mbp away from the site of damage via further H2AX phosphorylation (Rogakou *et al.*, 1999; Celeste *et al.*, 2003; Bewersdorf, Bennett and Knight, 2006; Deltaille, Kepkay and Bazett-Jones, 2009). This amplification signal both recruits DNA repair factors from further away and arrests transcription or replication in proximity to the break to prevent further damage.

As depicted in **Fig. 2.1A**, γ H2AX recruits mediator of DNA damage checkpoint 1 (MDC1), bringing it into proximity with ATM where it is phosphorylated (Stucki *et al.*, 2005). This initiates ubiquitination of H1 and H2A by ubiquitin ligases RNF8 and RNF168 (Mattioli *et al.*, 2012). The scaffold protein P53 binding protein 1 (53BP1) is then recruited to the DSB, which recruits further DNA repair proteins (Blackford and Jackson, 2017).

DNA-PKcs is recruited to DSBs by Ku70/80 (**Fig. 2.1B**), a basket-shaped heterodimer that caps each dsDNA end of the break (Walker, Corpina and Goldberg, 2001). The resulting holoenzyme, DNA-PK, binds both Ku 'caps' and thus brings the DNA ends together for ligation.

Both ATM and DNA-PK initiate repair of DSBs by non-homologous end joining (NHEJ), a cell cycle independent repair process (Riballo *et al.*, 2004; Jette and Lees-Miller, 2015). NHEJ does not use a template for repair, making it potentially error prone and mutagenic, although a low rate of errors is observed (Bétermier,

Bertrand and Lopez, 2014). DNA-PK autophosphorylation allows recruitment of NHEJ factors including Artemis, which processes both ends using 5' to 3' endonuclease activity (Ma *et al.*, 2002). Ligation of DNA ends is carried out by DNA-ligase IV and stabilising factor XRCC4 (Sibanda *et al.*, 2001).

ATM and Artemis can also promote homology directed repair (HDR) in G2 phase by phosphorylation of the tumour suppressor BRCA1 (Beucher *et al.*, 2009). HDR uses a replicated intact sister chromatid as a template for repair, and directly competes with 53BP1-dependent NHEJ activation. DNA ends are resected into ssDNA overhangs by nucleases to allow invasion of a template strand. Elongation and ligation complete the repair (Pardo, Gómez-González and Aguilera, 2009).

2.3.2 Single-strand break response

ATR is recognised as being the main responder to replication stress (**Fig. 2.1C**). Inhibition of DNA-PK (but not ATM) has been shown to cause replication stress, suggesting a role as well (Liu *et al.*, 2012). ATR is key to preventing collapse of fragile ssDNA sites into more severe DSBs. ATR deficiencies have been shown to lead to an increase in fragile sites on chromosomes, which increases the chances of replication stress or mutagenesis (Casper *et al.*, 2002). Repetitive DNA sequences are prone to forming secondary structures and are thus vulnerable to polymerase stalling and replication stress during DNA replication. ATR was found to be essential for prevention of fork collapse at these sites (Shastri *et al.*, 2018).

The ATR pathway is activated by binding of replication protein A (RPA) bound to ssDNA. RPA is a highly conserved heterotrimer formed of 70 kDa, 32 kDa and 14 kDa subunits (Wold, 1997). RPA protects ssDNA from collapse into DSB, prevents formation of fork stalling hairpins, and prevents untimely reannealing of ssDNA during homology directed DNA repair. RPA is phosphorylated upon binding to ssDNA and acts as a dynamic scaffold which regulates association and dissociation of repair factors (Fanning, Klimovich and Nager, 2006). Exhaustion of nuclear pools of RPA lead to escalation of replication stress and resultant replication catastrophe, signified by nuclear-wide chromosomal breakage which drives the cell into

senescence (Toledo *et al.*, 2014; Toledo, Neelsen and Lukas, 2017; Ibler *et al.*, 2019).

Independently, two complexes translocate to the RPA-ssDNA complex. ATR, via ATR-interacting protein (ATRIP), binds to ssDNA via RPA (Cortez *et al.*, 2001; Zou and Elledge, 2003). Meanwhile, RPA stimulates the binding of the RAD17-Rfc2-5 (RSR) complex to ssDNA, and facilitates the subsequent binding of the RAD9-RAD1-HUS1 (9-1-1) checkpoint clamp in an ATP-dependent reaction (Bermudez *et al.*, 2003; Zou, Liu and Elledge, 2003). Rad9 binds DNA topoisomerase 2-binding protein 1 (TopBP1), which subsequently activates ATR (Kumagai *et al.*, 2006; Lee, Kumagai and Dunphy, 2007). Another protein, ETAA1, also activates ATR and is brought into proximity to ATR by direct binding with RPA (Bass *et al.*, 2016; Feng *et al.*, 2016; Haahr *et al.*, 2016; Lee *et al.*, 2016). Whether TOPBP1 and ETAA1 act as redundancy measures towards each other, or whether they are necessary for ATR activation in different scenarios is unknown.

ATR activation also leads to γ H2AX foci formation, suggesting that γ H2AX has a role in surveillance of replication. γ H2AX was shown to colocalise with PCNA, BRCA1 and 53BP1 at arrested replication forks in S phase cells (Ward and Chen, 2001).

Another protein known as Schlafen-11 (SLFN11) also binds RPA in an ATR-independent manner and acts to inhibit replication fork progression, suggesting that there are redundant pathways for sensing replication stress (Murai *et al.*, 2018).

2.4 Cell cycle regulation

The cell cycle is a carefully regulated series of phases and checkpoints that control DNA replication and cell division. Diploid cells begin in G1 phase with two sets of 23 chromosomes. They undergo DNA replication in S phase, upon which they enter G2 phase. Cells then undergo mitosis (M phase) and split into two G1 daughter cells. Cells can also enter G0 phase, where they adopt quiescence and the cell cycle is temporarily paused (Vermeulen, Van Bockstaele and Berneman, 2003).

Progression through the cell cycle is controlled by cyclins, which control cyclin-dependent kinases (CDKs) and a resultant phosphorylation cascade promoting

progression of the cell cycle. A series of checkpoints monitor entry of the cell into each phase of the cell cycle and will arrest the cell cycle in certain conditions such as unrepaired DNA damage. Cell cycle arrest is controlled by CDK inhibitors such as P21, a P53 target, which prevents formation of the CDK-cyclin complex (Deshpande, Sicinski and Hinds, 2005) (**Fig. 2.1D**). P21, alongside another CDK inhibitor P16, prevents CDK-driven phosphorylation of retinoblastoma tumour suppressor protein (Rb). In its unphosphorylated state, Rb sequesters the E2F transcription factor and thus prevents transcription of genes essential for G1 to S phase transition (Ohtani *et al.*, 2004).

ATR serves as a key S/G2 phase checkpoint, preventing early S phase exit and premature entry into mitosis (Saldivar *et al.*, 2018). CHK1 is recruited by the mediator protein Claspin and phosphorylated by ATR (Kumagai and Dunphy, 2000; Liu *et al.*, 2000). Phosphorylated CHK1 (pCHK1) is a kinase that inhibits origin of replication firing, preventing accumulation of further DNA damage (Maya-Mendoza *et al.*, 2007) (**Fig. 2.1D**).

ATM recruits a similar kinase, CHK2, which also regulates a key cell cycle checkpoint. CHK1 and CHK2 phosphorylate CDC25 (cell division control protein 25), a phosphatase that activates cyclin dependent kinases CDK1 and CDK2. Phosphorylation promotes CDC25 degradation and blocks CDK-1 and -2 dependent mitotic entry (Furnari, Rhind and Russell, 1997; Peng *et al.*, 1997; Sanchez *et al.*, 1997; Matsuoka *et al.*, 2000) (**Fig. 2.1D**).

When a cell undergoes DNA damage, it can temporarily exit from the cell cycle and activate DNA repair pathways to fix the damage. If the damage is too excessive to be repaired, the cell must prevent further propagation of mutations which could lead to tumorigenesis. It can do this via controlled self-destruction (apoptosis) or permanent cell cycle arrest (senescence). A key regulator of these cell fates is P53.

2.4.1 P53

P53 is a key transcription factor that determines whether the cell activates pro-survival or apoptotic pathways (Tyner *et al.*, 2002; Dumble *et al.*, 2007; Shu, Li and Wu, 2007). It is phosphorylated and activated by CHK1 via ATR and 53BP1 via ATM

(Tibbetts *et al.*, 1999; Cuella-Martin *et al.*, 2016). ATR activation was found to induce P53-dependent cell cycle arrest and senescence, even in the absence of any DNA damage (Toledo *et al.*, 2008).

P53 is continually produced and degraded within the cell by Mdm2-dependent ubiquitination (Haupt *et al.*, 1997). P53 phosphorylation at Ser-15 and -37 inhibits ubiquitination and degradation and results in accumulation of activated P53 (Shieh *et al.*, 1997). When activated, P53 acts as a transcription factor for target genes involved in apoptosis, as well as cell cycle arrest, including CDK inhibitors. This includes P21, which inhibits cyclin B and CDC2, leading to cell cycle arrest during any phase of the cell cycle (El-Deiry *et al.*, 1993; Agarwal *et al.*, 1995, 1998; Innocente *et al.*, 1999).

2.4.2 Apoptosis

If DNA damage is extensive enough that it cannot be repaired, the cell can self-destruct in a programmed way that prevents release of immunogenic debris (Taylor, Cullen and Martin, 2008). DNA-PK phosphorylation of γ H2AX is required for apoptosis (Mukherjee *et al.*, 2006). γ H2AX foci migrate to the nuclear periphery during early apoptosis, forming an 'apoptotic ring' and localising with ATM, DNA-PK and Chk2 (Solier *et al.*, 2009; Solier and Pommier, 2014). P53 mediates inactivation of the pro-survival gene B-cell lymphoma 2 (Bcl-2) via a downstream GTPase Cdc42 (cell division control protein 42) (Thomas, Giesler and White, 2000). P53 also upregulates the homologous Bcl-2-associated X (BAX), which penetrates the outer mitochondrial membrane to release pro-apoptotic markers that trigger a caspase cascade (Toshiyuki and Reed, 1995; Gross *et al.*, 1998; Tait and Green, 2010) Caspases are proteases that cleave substrates including PARP and lamins (Lazebnik *et al.*, 1994, 1995). Morphological features of apoptotic cells include nuclear fragmentation, shrinkage, and condensation of chromatin, as the cell is carefully packaged into small blebs that can be endocytosed and degraded by immune cells (Kerr, Wyllie and Currie, 1972).

2.4.3 Senescence

Senescence is permanent cell cycle arrest, characterised by cell distension, flattening, and secretion of a senescence-associated secretory phenotype (SASP) (Hernandez-Segura, Nehme and Demaria, 2018). Common markers of senescent cells include expression of senescence-associated β -galactosidase, tumour suppressor P16 and a persistent DNA damage phenotype (Hernandez-Segura, Nehme and Demaria, 2018).

What triggers the cell to enter senescence is unclear and is likely based on context and different factors. However, the P53 target gene P21 is known to be an important regulator of entry into senescence. Persistence of DNA repair intermediates leads to accumulation of P21 and nuclear entrapment of cyclin B1, leading to permanent G2 arrest (Feringa *et al.*, 2018). The decision to enter senescence appears to be based in the relative levels of P21 and high mobility group box 1 (HMGB1). Doxorubicin-induced senescent cells showed elevated levels of P21 and HMGB1 as opposed to apoptotic cells, which displayed reduced levels of both (Lee *et al.*, 2019).

Although senescence is typically viewed as a mechanism of preventing cancer, senescence can be pro-tumorigenic. Senescence can induce a senescence-associated inflammatory response which can be pro- or anti-tumorigenic depending on P53 activity (Pribluda *et al.*, 2013). SASP can include pro-inflammatory factors including IL-6, IL-1, and IL-8, which can promote inflammation and immune cell migration. This can trigger aberrant effects in surrounding cells, including secondary senescence (Secher *et al.*, 2013; Hernandez-Segura, Nehme and Demaria, 2018; Ibler *et al.*, 2019). Chronic inflammation can cause tissue damage and lead to tumorigenesis (Coppé *et al.*, 2010).

2.5 The DDR to the typhoid toxin

Previous studies in the Humphreys lab revealed that the typhoid toxin activated both ATR and ATM, suggesting the formation of both SSBs and DSBs. The toxin induced hyperphosphorylation of RPA and replication stress in S/G2 phase, leading

to ATR activation and downstream phosphorylation of P53 and CHK1. The toxin also induced DSBs labelled by 53BP1 in G0/G1 phase (Ibler *et al.*, 2019).

Furthermore, toxin-induced replication stress was shown to induce a senescence-like phenotype. This was characterised by cell distension, permanent cell cycle arrest and a secretory phenotype that induced secondary senescence in bystander cells. Cells treated with secretomes from intoxicated cells underwent senescence and became more susceptible to *Salmonella* infection, suggesting that the toxin was creating replicative niches and facilitating infection spread (Ibler *et al.*, 2019). This correlated with *in vivo* data implicating the toxin in systemic bacterial dissemination, chronic carriage, bacteraemia and suppression of host inflammatory responses (Del Bel Belluz *et al.*, 2016; Miller *et al.*, 2018; Gibani *et al.*, 2019).

Toxin nuclease activity saturated the RPA pathway through excessive SSB production, which provided mechanistic details of how the toxin-induced replication stress caused this senescence response facilitating infection (Ibler *et al.*, 2019). Senescence caused by replication stress has been implicated in many disease states, such as progeria, which is characterised by premature ageing. Expression of a truncated form of lamin, known as progerin, results in loss of lamin function and leads to replication stress (Kreienkamp *et al.*, 2018). In this study and in others, replication stress has been shown to cause leakage of fragments of damaged DNA into the cytosol, activating an immune response that resulted in cellular senescence (Wolf *et al.*, 2016; Kreienkamp *et al.*, 2018). The DDR has been shown to directly activate immune responses in different contexts, characterised with induction of antimicrobial peptides and recruitment of immune cells (Nakad and Schumacher, 2016). Furthermore, recent studies have shown that other bacterial genotoxins such as *E. coli* CDT induce immune responses in a DNA damage-dependent manner (Pons *et al.*, 2021).

The immune response is key to host recognition of threats, including DNA damage. Innate immune pathways recognise markers of damage and regulate cell fate decisions to suppress tumorigenic effects. This includes triggering apoptosis or senescence to prevent replication of potentially cancerous cells. It was hypothesised that the toxin was triggering a replication stress-induced immune

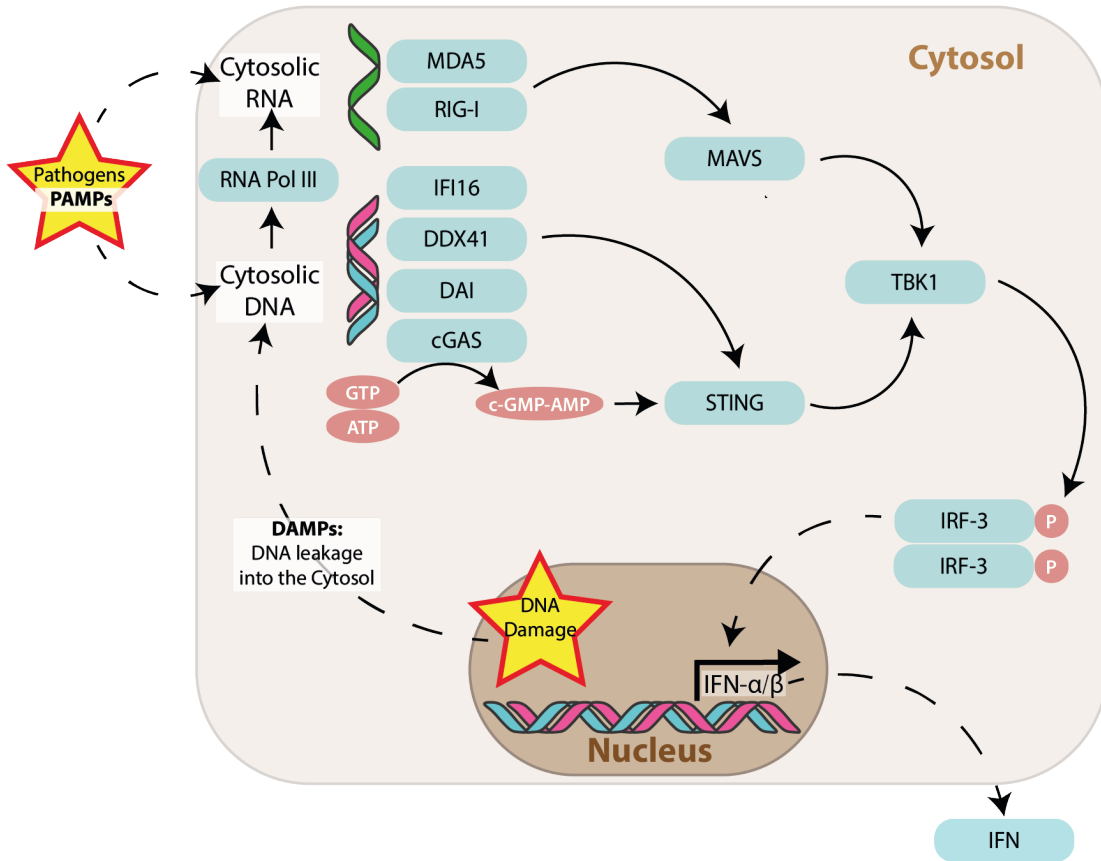
response to promote senescence and thus a *Salmonella*-permissive microenvironment. To explore this hypothesis, I will first describe the innate immune response with a focus on the downstream responses to DNA damage.

3 Innate Immune Responses to DNA damage

3.1 Introduction

Pathogen invasion is typically accompanied by release of numerous molecular motifs such as bacterial lipopolysaccharides, flagellin, and bacterial and viral nucleic acids RNAs (Akira, Uematsu and Takeuchi, 2006; Li and Wu, 2021). These motifs are known as pathogen associated molecular patterns (PAMPs). Cellular stresses, such as such as genomic instability within cancer cells, cause release of damage-associated molecular patterns (DAMPs). For example, a major DAMP is cytoplasmic DNA released from the nucleus or mitochondria (Dempsey and Bowie, 2015; Grazioli and Pugin, 2018). Replication stress leads to formation of micronuclei containing aggregates of dsDNA breaks (Xu *et al.*, 2011), which can rupture and spill free DNA into the cytoplasm (MacKenzie *et al.*, 2017; Bakhoun *et al.*, 2018). These PAMPs and DAMPs act as ligands for an array of pattern recognition receptors (PRRs), which stimulate antimicrobial or proinflammatory responses including interferon (IFN) induction in order to contain the threat (Haller, Kochs and Weber, 2007) (**Fig. 3.1**).

A PRR activation of the type 1 IFN pathway



B The Type 1 IFN pathway

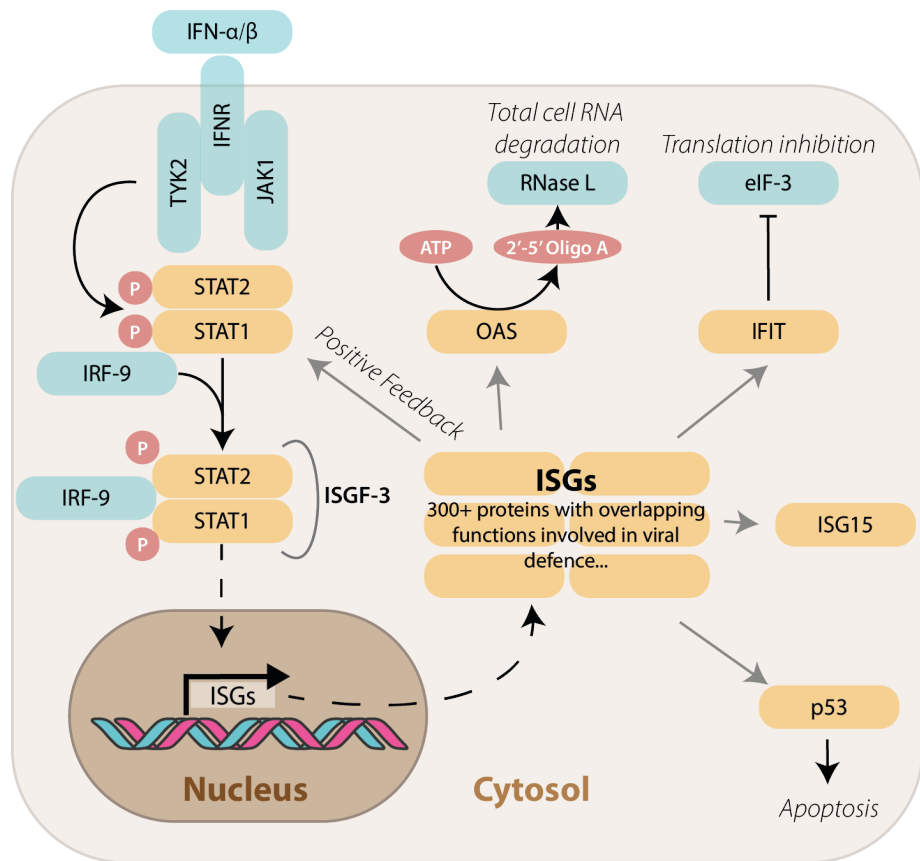


Fig. 3.1 **Pattern recognition receptors detect DNA damage and initiate an innate immune response**

(A) DNA damage or pathogen invasion introduce immunogenic nucleic acids into the cytosol. Cytosolic DNA and RNA are detected by different pattern recognition receptors such as cGAS, Ku70/DNA-PK, RIG-I and MDA5, among others. These PRRs, once activated, initiate signalling responses via STING, which phosphorylates the kinase TBK1. TBK1 in turn phosphorylates IRF3, causing it to dimerise and translocate to the nucleus and promote expression of IFNs. **(B)** Type-I IFNs bind their cognate receptor, activating a JAK-STAT system and stimulating phosphorylation of STAT1. Phosphorylated STAT1 forms the heterotrimeric transcription factor ISGF3 with IRF9. ISGF3 translocates to the nucleus and promotes expression of a wide variety of IFN stimulated genes.

3.2 Interferons

When host cells are challenged by pathogen invasion, they mount a rapid innate immune response to counteract the threat. This may take the form of direct inactivation of pathogenic virulence factors, or activation of different cell fate pathways to prevent infection spread. Conversely, some pathogens have evolved mechanisms by which they are able to manipulate these immune responses to their advantage.

DNA damage also causes induction of IFNs. For example, the DNA damage inducer etoposide was shown to initiate type I and II IFNs, IFN stimulated genes (ISGs) and IFN regulatory factors-1 and -7 in an NF- κ B dependent manner (Brzostek-Racine *et al.*, 2011). IFN induction has also been linked to replication stress (Wolf *et al.*, 2016; Kreienkamp *et al.*, 2018).

The IFN system is an important component of the innate immune response. IFNs were first discovered in 1957 as secreted factors that exerted an antiviral effect, so named because they were able to ‘interfere’ with viral replication (Isaacs and Lindenmann, 1958). They are a group of cytokines secreted by damaged or infected cells that signal to bystander cells to increase host defences. This may be via upregulation of immune pathways, activation of immune cells such as T cells, or upregulation of antigen presentation (Crouse, Kalinke and Oxenius, 2015; Boxx and Cheng, 2016). There are more than twenty IFN genes in humans, which are divided into three classes, type-I, -II and -III (Haller, Kochs and Weber, 2007; Boxx and Cheng, 2016). Mammalian type-I IFNs include 14 subtypes of IFN α , as well as IFN β , IFN ω , IFN κ , IFN ζ , IFN δ , IFN τ and IFN ϵ . In humans, IFN α and IFN β are the most abundant, IFN ω is expressed in certain contexts and the remaining isoforms are

encoded as a single IFN κ isoform. Type-II IFNs solely include IFN γ , whereas type-III IFNs comprise of 4 subtypes of IFN λ (Boxx and Cheng, 2016).

Type-I and -II IFNs are used in the defence against either viruses or bacteria in different contexts (Haller, Kochs and Weber, 2007; Boxx and Cheng, 2016). Type-III IFNs are structurally distinct from type-I IFNs but were initially thought to have redundant functions. However, more recent studies have shown that type-III IFNs have distinct roles, such as reinforcing epithelial barriers during bacterial infection (Odendall, Voak and Kagan, 2017). Furthermore, whereas type-I IFNs induced a strong acute response, type III IFNs induced a weaker but longer term response, resulting in the creation of unique antiviral environments in different cell types (Pervolaraki *et al.*, 2018).

3.3 IFN induction by pattern recognition receptors

Type-I IFN induction is driven by IFN regulatory factors (IRFs), which are phosphorylated by IRF kinases including TBK1 (TANK binding kinase 1) and the IKK (κ B kinase) family. IFN regulatory factor (IRF)-3 is constitutively expressed in the cytosol and following phosphorylation by TBK1 undergoes dimerization and nuclear translocation (**Fig. 3.1A**). Once in the nucleus, it binds to coactivators CBP and p300 and binds to the IFN promoter region to induce IFN transcription. Another regulatory factor, IRF-7, initially exists at low levels, but upon IFN-induction is upregulated and forms a heterodimer with IRF-3, acting as a amplifying transcription factor that boosts IFN production (Honda, Takaoka and Taniguchi, 2006).

3.3.1 TLRs, RLRs and NLRs

The IRF kinases are activated by a wide array of PRRs, which recognise different ligands and trigger different signalling cascades to initiate a response. One such class are the **toll-like receptors (TLRs)**, a family of 14 transmembrane receptors that monitor the cell surface and endosomal compartments for viral and bacterial PAMPs including nucleic acids (Medzhitov, 2007; Ishii *et al.*, 2008). Some TLRs, including TLR7 and TLR9, have been shown to recognise self-nucleic acids as well

which has been linked to autoimmune disorders such as systemic lupus erythematosus (Barrat *et al.*, 2005; Celhar, Magalhães and Fairhurst, 2012). A subset of TLRs induce type-I IFN expression including endosomal TLR7, TLR8, TLR9 and TLR13, which recognise pathogenic nucleic acids within endosomal compartments (Mancuso *et al.*, 2009; Eigenbrod *et al.*, 2015; Castiglia *et al.*, 2016; Martínez-Campos, Burguete-García and Madrid-Marina, 2017). For TLRs, IFN production is induced by MyD88-dependent phosphorylation of the IFN regulatory factor (IRF) kinases IRAK (interleukin-1 receptor associated kinase) and IKK α (Boxx and Cheng, 2016). TLR4 also induces type-I IFN expression but in a slightly different manner, it is located at the plasma membrane where it surveys the extracellular space for bacterial cell surface components. Upon ligation, it is endocytosed within autophagosomes and triggers type-I IFN induction in a mechanism dependent on the TRAM-TRIF adaptor and the IRF kinases TBK1 and IKK ϵ (Kagan *et al.*, 2008). TBK1 and the IKK family are key signal transducers between PRRs and IFN regulation and are conserved in several other mechanisms (Fitzgerald *et al.*, 2003; Sharma *et al.*, 2003).

Cytoplasmic PAMPs are detected by **RIG-I-like receptors (RLRs)** and nucleotide-binding and oligomerising domain (**NOD**)-like receptors (**NLRs**), both of which also act via phosphorylation of TBK1 and IKK ϵ (Boxx and Cheng, 2016). RLRs include RIG-I (retinoic acid-inducible gene 1) itself and MDA5 (melanoma-associated differentiation protein 5), which recognise viral double stranded RNAs and bind to the protein adaptor MAVS (mitochondrial antiviral-signalling protein, also known as VISA) upon ligation, which triggers IRF phosphorylation and IFN induction (Ishii *et al.*, 2008; Boxx and Cheng, 2016). NLRs, including NOD1 and NOD2, bind bacterial cell wall peptides such as the muropeptide iE-DAP (Bi *et al.*, 2017) and signal via the adaptor RIP2 (Pandey *et al.*, 2009; Watanabe *et al.*, 2010).

3.3.2 Cytoplasmic DNA sensors

Cytoplasmic DNA is a marker of either pathogen infection or genomic instability and is recognised by a variety of DNA sensors, leading to pro-inflammatory responses

and programmed cell death (Paludan and Bowie, 2013; Paludan, Reinert and Hornung, 2019).

Many DNA sensors signal through activation of the adaptor protein **STING** (stimulator for IFN genes, also known as MITA), a transmembrane protein in the endoplasmic reticulum (Ishikawa and Barber, 2008; Bhat and Fitzgerald, 2014). STING activation triggers IFN induction via recruitment of TBK1, which phosphorylates both it and IRF-3 (Zhong *et al.*, 2008; C. Zhang *et al.*, 2019). Interestingly, STING has also been shown to directly induce autophagy via translocation to ER-Golgi intermediate compartments in a process independent of TBK1 and IFNs (Gui *et al.*, 2019). Abrogation of STING function via epigenetic silencing or missense mutations in many tumours has been shown to impede IFN and production of other pro-inflammatory cytokines following DNA damage, thus allowing damaged and potentially cancerous cells to evade immune cells (Konno *et al.*, 2018).

DNA sensors acting via STING include cGAS (cyclic GMP-AMP synthase), DAI (DNA dependent activator of IRFs), Mre11, DDX41 (DexD/H box helicase) and IFI16 (gamma IFN-inducible protein 16).

cGAS binds to cytosolic DNA and catalyses the reaction of GMP and AMP into cyclic-GMP-AMP (cGAMP), which acts as a second messenger in activating STING (Sun *et al.*, 2013; Wu *et al.*, 2013; Shang *et al.*, 2019). cGAS has been shown to detect both pathogenic and self-DNA in the cytoplasm (Sun *et al.*, 2013; Wolf *et al.*, 2016). A recent study has indicated that rather than being a cytoplasmic sensor, cGAS actually localised to specific phosphoinositides on the plasma membrane, thus helping it distinguish between self- and viral-DNA (Barnett *et al.*, 2019).

Detection of self-DNA has been linked to aberrant inflammatory responses with links to metabolic and autoimmune disorders such as diabetes (Ablasser and Chen, 2019; Bai and Liu, 2019). cGAS has been described as essential to senescence, with cGAS deletion abolishing SASP and causing spontaneous immortalisation of mouse embryonic fibroblasts upon treatment with DNA damaging agents (Yang *et al.*, 2017). cGAS was found to be essential in detection of cytosolic DNA released by cells undergoing replication stress (Wolf *et al.*, 2016).

DAI has been shown to upregulate type-I IFNs via NF- κ B and IRF-3 in response to poly(dA:dT) (Takaoka *et al.*, 2007). **Mre11**, better known as a component of the MRN complex in DNA repair, has been shown to activate STING in response to cytosolic DNA (Kondo *et al.*, 2013). **DDX41** binds dsDNA, as well as the bacteria-specific metabolites cyclic-di-AMP and cyclic-di-GMP (Z. Zhang *et al.*, 2011; Parvatiyar *et al.*, 2012). **IFI16** is an AIM2-like receptor (ALR) which detects viral DNA (Unterholzner *et al.*, 2010) and which can cooperate with cGAS in response to herpes simplex infection (Orzalli *et al.*, 2015). It has been shown to activate STING in a non-canonical ATM-dependent manner following DNA damage (Dunphy *et al.*, 2018).

Beyond STING-dependent processes, there are several DNA sensors that use unique mechanisms to trigger immune responses. For example, **RNA-polymerase III** transcribes AT rich dsDNA into an RNA intermediate that is then recognised by RIG-I leading to IFN β induction (Ablasser *et al.*, 2009; Chiu, MacMillan and Chen, 2009). **LRRFIP1** (Leucine-Rich Repeat Flightless-Interacting Protein 1) was found to induce IFN β following *Listeria monocytogenes* infection or dsDNA treatment via phosphorylation of β -catenin and subsequent recruiter of the IFN coactivator p300 (Yang *et al.*, 2010). **AIM2** has been shown to detect cytoplasmic viral dsDNA and facilitate ASC recruitment and caspase-1 activation (Bürckstümmer *et al.*, 2009; Fernandes-Alnemri *et al.*, 2009; Hornung *et al.*, 2009; Roberts *et al.*, 2009).

Other DNA repair factors also perform a DNA sensing role. **Ku70** was shown to bind longer tracts of DNA (>500 bp) in the cytosol and trigger production of type-III IFNs via IRF1 and IRF-7 (X. Zhang *et al.*, 2011). **RAD50** has been shown to induce IL-1 β in response to viral DNA (Roth *et al.*, 2014).

3.4 IFN signalling

Type-I IFNs signal in an autocrine or paracrine manner through a heterodimeric IFN α/β receptor (IFNAR). Ligand binding causes crosslinking of the IFNAR1 and IFNAR2 subunits, causing the cytoplasmic tails of the heterodimer to activate Janus-kinase 1 (JAK1) and tyrosine kinase 2 (TYK2) (**Fig. 3.1B**). These kinases

phosphorylate members of the STAT family and stimulate formation of STAT dimers. In the case of type-I IFNs, this is predominantly a STAT1 and STAT2 heterodimer, which forms a heterotrimeric complex with IRF-9 known as the IFN-stimulated gene factor 3 (ISGF3) complex. ISGF3 binds to IFN-stimulated response elements (ISREs) located in the promoter regions of ISGs (Levy *et al.*, 1989). Type-I and -II IFNs can also activate STAT1 homodimers, which bind to γ -activated sequences and lead to transcription of regulatory genes such as IRF1 (Boxx and Cheng, 2016).

The IFN response is self-sustaining, as STATs and IRFs have ISREs themselves and thus are stimulated by IFN. As well as phosphorylated ISGF3, the initial pulse of IFN β also leads to formation of an unphosphorylated ISGF3 complex (uISGF3), which binds a distinct group of ISREs and results in a long-term constitutive antiviral response. Constant exposure to low levels of IFNs, seen in cancers and chronic infections, results in increased expression of uISGF3-induced proteins (Cheon *et al.*, 2013; Wang *et al.*, 2017; Michalska *et al.*, 2018).

ISG induction can occur independently of IFNs. For example, STATs can be directly phosphorylated and activated by TLR2, TLR4 and TLR9 (Luu *et al.*, 2014). IRF-3 can directly induce transcription of ISGs, including IFIT1 (Grandvaux *et al.*, 2002). Finally, some ISGs such as ISG15 have been shown to have P53-response elements (Park *et al.*, 2016).

ISGs are a large pool of more than 300 genes with various roles in innate immunity, inflammation and cell fate decisions (Cho *et al.*, 2008; Yu *et al.*, 2015). The role of ISGs in response to pathogen invasion is well established (Haller, Kochs and Weber, 2007; Boxx and Cheng, 2016; Alphonse, Dickenson and Odendall, 2021), however many ISGs are activated in response to DNA damage as well. For example, the P53 gene has an ISRE and is induced by IFN. P53 acts as an enhancer of the IFN response by promoting transcription of regulatory factors including IRF-9 (Muñoz-Fontela *et al.*, 2008). IFN-activated P53 has been shown to induce senescence in response to DNA damage (Yu *et al.*, 2015). ISGs such as STAT1, the IFIT family (IFN induced proteins with tetratricopeptide repeats), the OAS family (oligoadenylate synthase), and ISG15 were upregulated following

progerin-induced replication stress, in which context ISG upregulation was linked to senescence (Kreienkamp *et al.*, 2018).

3.5 IFN signalling and host-pathogen interactions

IFN signalling is activated in response to a wide variety of pathogens, often as a defensive mechanism. However, pathogens have evolved ways to subvert IFN signalling to promote virulence, and excessive or chronic IFN signalling in response to infection can have negative effects on the host.

3.5.1 IFN signalling and viruses

The type-I IFN response is well recognised as an antiviral response, and indeed ISGs have varying roles that interfere with viral replication and infection. For example, viperin was shown to inhibit replication, budding and egress of multiple viruses including Influenza A, HIV and Bunyamwera virus (Helbig and Beard, 2014). The OAS family synthesise 2'-5' oligoadenylates that activate rNase L, which degrades viral RNA and thus inhibits the viral life cycle (Liang, Quirk and Zhou, 2006). IFI6 is localised to the ER and has roles in inhibition of hepatitis C virus and flavivirus, and regulation of apoptosis in response to dengue virus 2 (Meyer *et al.*, 2015; Qi *et al.*, 2015; Richardson *et al.*, 2018). EGR1 is a transcription factor with a broad range of targets that has been shown to enhance signal transduction in response to viral replication, including foot and mouth disease virus (Zhu *et al.*, 2018). ISG15 has antiviral roles against influenza, herpes and Sindbis virus, among others (Lenschow *et al.*, 2005, 2007; Giannakopoulos *et al.*, 2009).

3.5.2 IFN signalling and bacteria

Bacterial infection has also been shown to induce type-I IFN responses, which can be both protective and detrimental to the host depending on context (Alphonse, Dickenson and Odendall, 2021). For example, type-I IFNs prevent hyperinflammation caused by *Streptococcus pyogenes* (Castiglia *et al.*, 2016),

prevent transmigration of *Streptococcus pneumoniae* across the lung (LeMessurier *et al.*, 2013), and promote CXCL10-dependent cell recruitment in response to *Helicobacter pylori* (Watanabe *et al.*, 2010). ISGs including OAS and ISG15 have been shown to restrict *Mycobacterium tuberculosis* (Bogunovic *et al.*, 2012; Leisching *et al.*, 2019), and viperin restricts *Shigella flexneri* replication (Helbig *et al.*, 2019). Bacteria have therefore evolved mechanisms to block IFN signalling, such as *Shigella*, which secretes OspC to block calcium signalling and thus interrupt JAK/STAT signalling (Alphonse *et al.*, 2022). Furthermore, some species of bacteria exploit IFN signalling, such as *Listeria monocytogenes* and *Francisella tularensis*. In these examples, infection leads to IFN-dependent suppression of IL-17, which is detrimental to the host and helps promote infection (Henry *et al.*, 2010).

3.5.3 IFN signalling and *Salmonella*

Salmonella induces IFN signalling in different manners depending on host cell type. For example, *S. Typhimurium* mRNA is detected by RIG-I, which induces a type-I IFN response in non-phagocytic cells (Schmolke *et al.*, 2014). In phagocytic cells, *Salmonella* LPS is recognised by TLR4, which also drives a type-I IFN response (Boxx and Cheng, 2016). However the Vi capsule prevents TLR-4 dependent recognition in *S. Typhi* (Wilson *et al.*, 2008).

IFN signalling have both beneficial and detrimental impacts on *Salmonella* infection. Type-III IFNs can protect epithelial barriers from damage induced by *S. Typhimurium* (Odendall, Voak and Kagan, 2017). However, *S. Typhimurium* can subvert the type-I IFN response to its advantage, promoting macrophage necroptosis and repressing host defensive responses such as IL-1 cytokine and neutrophil chemokine release (Robinson *et al.*, 2012; Perkins *et al.*, 2015). IFNAR1-deficient mice survive better than wild-type mice, and display a reduced *Salmonella* burden in the liver and spleen (Robinson *et al.*, 2012). The impact of IFN signalling on *S. Typhi* is less clear, although transcriptomic data has revealed the upregulation of ISGs such as the IFIT family and EGR1 in response to *S. Typhi* infection (Hannemann and Galán, 2017).

It is possible that *S. Typhi* may stimulate an IFN response via secretion of the typhoid toxin. There are examples of bacteria inducing IFN and inflammatory responses via activity of other genotoxins, such as CDTs. As discussed previously (section 2.5), genotoxic stress can lead to activation of DNA sensing pathways and IFN signalling. Indeed, the type-I IFN response was recently found to be activated by DNA damage caused by *E. coli* CDT (Pons *et al.*, 2021), and CDT of *H. ducreyi* was shown to trigger a senescence phenotype including secretion of pro-inflammatory cytokines such as IL-6 (Péré-Védrenne *et al.*, 2017). Beyond CDTs, *E. coli* also secretes a genotoxin known as colibactin, which causes interstrand DNA crosslinks. Colibactin has been shown to induce a senescence phenotype including secretion of inflammatory SASP (Secher *et al.*, 2013). Further study will be needed to examine host responses to the typhoid toxin and its wider role in *Salmonella* virulence.

3.6 Host responses to the typhoid toxin

The typhoid toxin causes ssDNA nicks that induce replication stress and senescence in host cells (Ibler *et al.*, 2019). Toxin-induced senescence responses lead to formation of microenvironments of cells that are susceptible to *Salmonella* infection, thus suggesting that *S. Typhi* secretes the toxin to promote its infection of the host (Ibler *et al.*, 2019). This correlates to *in vivo* studies showing that the toxin promotes systemic dissemination and chronic carriage (Del Bel Belluz *et al.*, 2016; Miller *et al.*, 2018; Gibani *et al.*, 2019). However, *S. Typhi* has also been implicated in gallbladder cancer, and the genotoxic effects of the toxin could induce mutagenesis and cancer (Di Domenico *et al.*, 2017). It is possible that the host cell undergoes senescence to defend itself from tumorigenesis and in doing so presents an opportunity for *Salmonella* to hijack the process and facilitate its dissemination.

In other disease states such as progeria, replication stress leads to DNA leakage into the cytosol, activation of cGAS and a type-I IFN response (Wolf *et al.*, 2016; Kreienkamp *et al.*, 2018). IFN β was shown to amplify DDRs to promote senescence while inactivation of the IFN pathway prevents progeria and extends lifespan (Yu *et al.*, 2015). *E. coli* CDT has been shown to promote an IFN response in response to

DNA damage (Pons *et al.*, 2021), although it remains to be seen whether the typhoid toxin does the same.

Some patients infected with *S. Typhi* will chronically carry the infection asymptotically and go on to develop gallbladder cancer. To understand the role of the toxin in different manifestations of *S. Typhi* infection a greater understanding of the wider host response to the toxin, particularly the innate defences counteracting bacterial genotoxins, is needed.

3.7 Aims and Hypothesis

I hypothesise that the host induces an immune response to prevent genotoxic, potentially cancerous, phenotypes induced by the toxin. Understanding this aspect of the host-pathogen interaction will illuminate interplay between the DDR, innate immunity and *Salmonella* infection.

This thesis aims to:

1. Characterise the host responses to the typhoid toxin by determining toxin-dependent differences in the host transcriptome.
2. Identify specific factors that contribute to the host response to the toxin.
3. Determine whether the toxin can induce cancerous phenotypes and how the host can protect itself against these.

This will help elucidate the functional role of the typhoid toxin, provide a mechanistic link between the genotoxic effects of the toxin and observable phenotypes of intoxication, and possibly discover relevant links between the typhoid toxin, chronic carriage, and cancer.

Part 2: Results

4 Host responses to the typhoid toxin

4.1 Introduction

The typhoid toxin of *Salmonella* Typhi causes replication stress and senescence *in vitro* (Ibler *et al.*, 2019). Both phenotypes have been linked to cancer and bacterial-associated oncogenesis (Cougnoux *et al.*, 2014). Indeed, *S. Typhi* is a significant risk factor for gallbladder cancer (Scanu *et al.*, 2015). Thus, it stands to reason that diverse host defence mechanisms operate to protect humans from the effects of genotoxic *Salmonella*, but no mechanism has been reported for typhoid toxin. With the aim of gaining a greater understanding of host responses to the toxin, GeneChip microarray analysis was exploited to investigate transcriptional changes in cultured cells treated with typhoid toxin.

4.2 Results

4.2.1 Purification of recombinant typhoid toxin

There are two possible methods to study the host responses to the typhoid toxin. One is to infect cells with toxigenic *Salmonella*, such as *S. Typhi*, the NTS serovar *S. Javiana* (Miller *et al.*, 2018), or engineered toxigenic *S. Typhimurium* (Del Bel Belluz *et al.*, 2016). However, *Salmonella* also encodes other virulence effectors that may also activate DDRs and innate host defences. To uncouple the toxin from other *Salmonella* virulence factors, recombinant toxin was purified from *E. coli* as described in Ibler *et al.* 2019. This approach has been used to study the effects of the toxin in other studies (Song, Gao and Galan, 2013; Ibler *et al.*, 2019).

The DE3 *E. coli* strain C41 Rosetta was transformed with pETDuet-1 expression vector encoding epitope-tagged toxin subunits *pltA*-Myc, *pltB*-His and *cdtB*-FLAG under the control of T7 RNA polymerase promoter. Addition of the lactose analogue IPTG (Isopropyl β -D-1-thiogalactopyranoside) activated expression of T7 RNA

polymerase in C41 that drove expression of toxin subunits, which, in the absence of any secretory mechanism, accumulate in the bacterial periplasm as a fully assembled holotoxin. NiNTA affinity chromatography was used to isolate the toxin via *pltB*-His from the C41 *E. coli* lysate (**Fig. 4.1**).

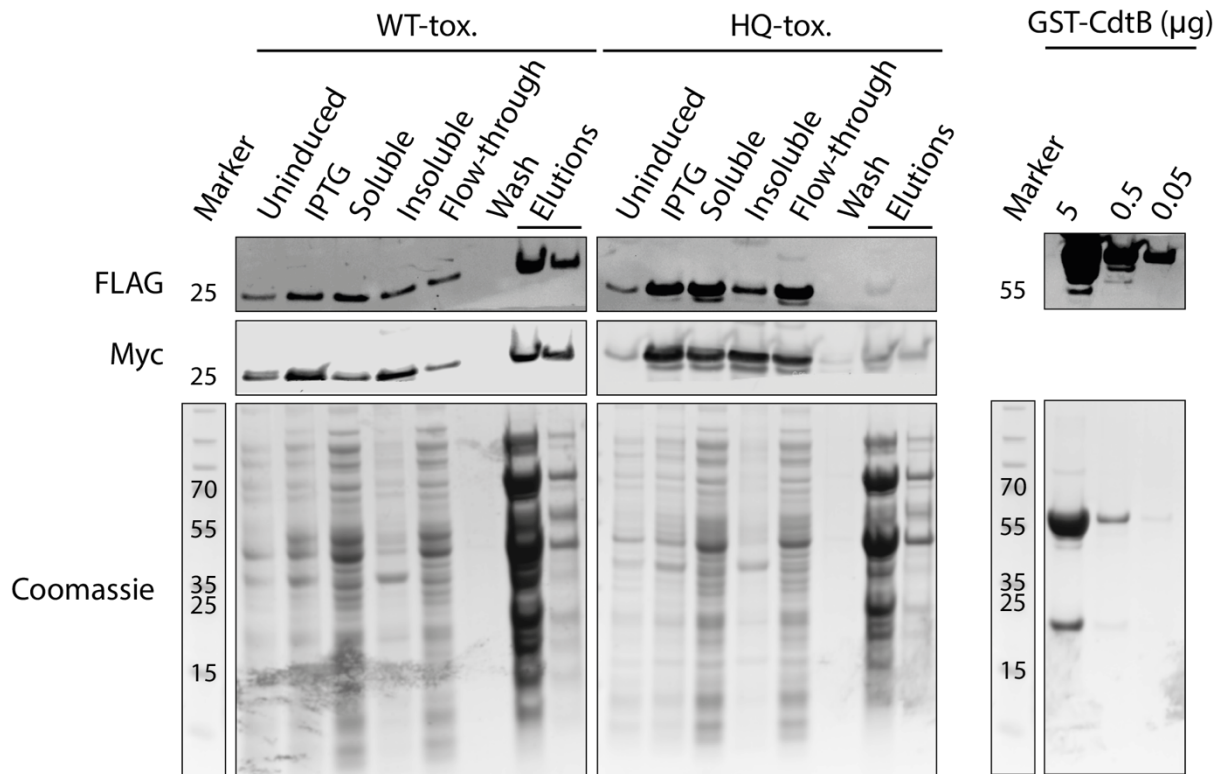


Fig. 4.1 Purification of recombinant typhoid toxin

Immunoblots of FLAG (CdtB-FLAG) and Myc (PltA-Myc), and Coomassie stains, of each fraction of the NiNTA purification of WT-toxin and HQ-toxin. The uninduced and induced fractions are *E. coli* lysate before and after IPTG treatment. The lysate is fractionated into soluble and insoluble fractions, and the soluble fraction is passed through the NiNTA column. The flow-through is the unbound fraction. The beads are then washed before the bound fraction is eluted from the beads. Purified GST-CdtB of known concentrations was used to create a standard curve to extrapolate the concentration of the eluted toxin fraction using intensities measured in Image Studio. Purification was performed together with Mohamed ElGhazaly, who took the gel images.

Simultaneous preparations were made of a wild-type typhoid toxin and a mutant *cdtB*-H160Q toxin with attenuated catalytic activity (henceforth WT-toxin and HQ-toxin) as previously described (Ibler *et al.*, 2019). Coomassie stain analysis of the protein gel of the fractions showed that the eluted fractions were a crude preparation including other *E. coli* proteins. However, use of the HQ-toxin acted as a control for the potential effects of other *E. coli* contaminants in downstream assays in cultured cells. The presence of CdtB-FLAG, PltA-Myc and PltB-His was confirmed in the eluted fraction using Western-blotting for FLAG and Myc antibodies respectively. CdtB-FLAG and PltA-Myc were detected in the HQ-toxin

elution but at 10-fold lower levels than in the WT-toxin elution. This was possibly due to low expression of the His-tag on PltB.

CdtB-FLAG densitometry was compared to that of a GST-CDTB purification. CdtB-GST was shown by Coomassie to be ~80% homogeneity and concentration was calculated by Bradford assay using GST-CDTB as a standard. This enabled extrapolation of the concentration of toxin from a standard curve of GST-CDTB preparations.

To confirm that the purified toxin was functional, an *in vitro* intoxication assay was used as described in Ibler *et al.* 2019 in human fibrosarcoma HT1080 cells (henceforth standard intoxication assay). Briefly, 20 ng/ml of WT- and HQ-toxin was added to cells for 2 h to allow for toxin endocytosis, before removal and replacement with fresh media. Cells were fixed 24 h later and prepared for immunofluorescence analysis of the DNA damage marker γ H2AX (**Fig. 4.2A**). WT-toxin treatment induced γ H2AX in 82% of DAPI-stained nuclei (outlined in **Fig. 4.2A**), which was significantly higher than 33% of HQ-toxin treated cells (**Fig. 4.2B**). Positivity was defined as a greater γ H2AX fluorescence intensity than the upper quartile of untreated γ H2AX intensity, meaning the baseline γ H2AX positivity was 25% in untreated cells. WT-toxin treatment induced a greater γ H2AX response than that of 24 h continuous treatment with DNA-polymerase inhibitor aphidicolin (68% positivity), which acted as a positive control. Immunofluorescence also revealed that cell nuclei became distended upon WT-toxin treatment, which was consistent with observations in other studies (Haghjoo and Galán, 2004; Spanò, Ugalde and Galán, 2008; Guidi, Levi, *et al.*, 2013; Ibler *et al.*, 2019).

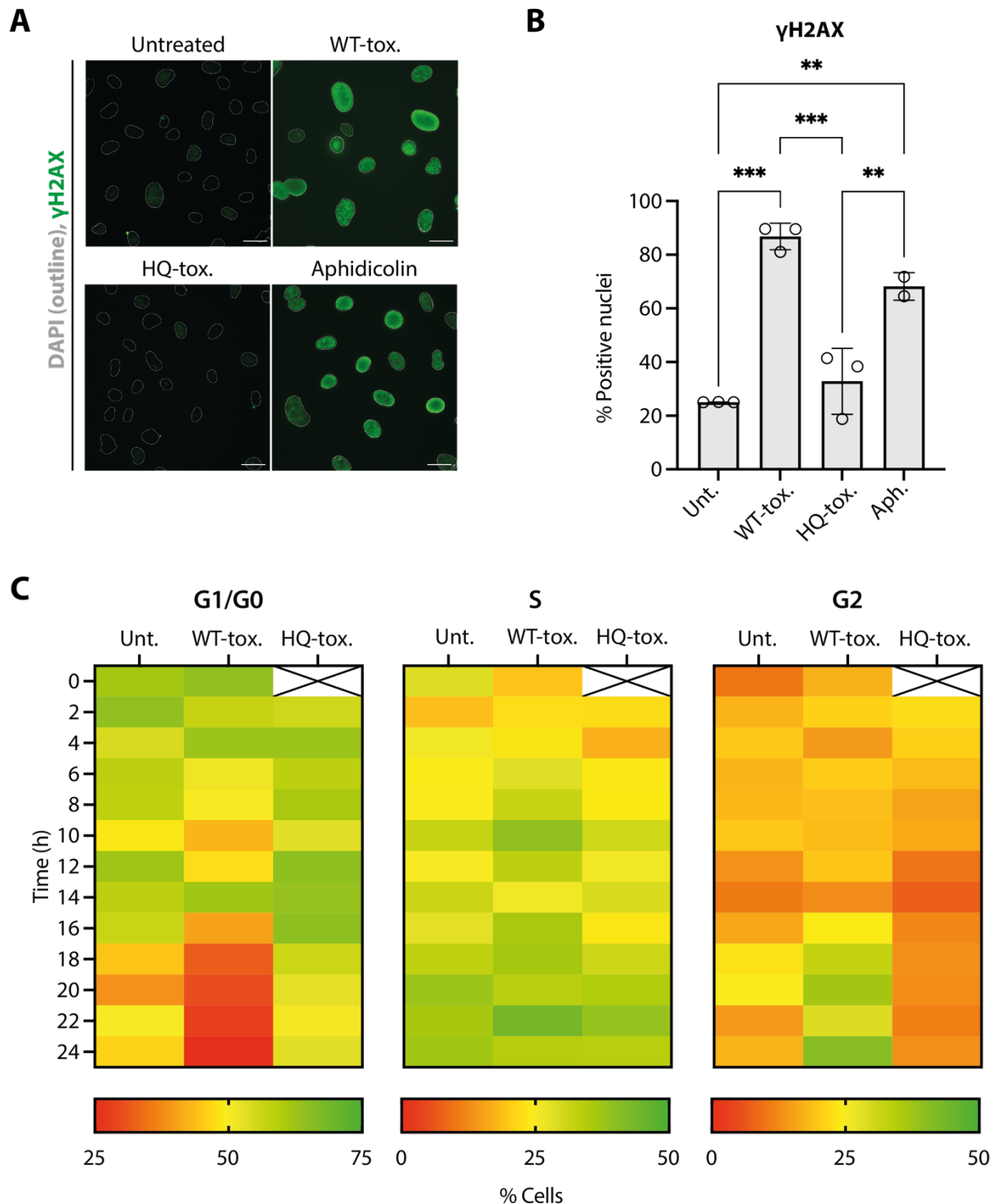


Fig. 4.2 The typhoid toxin causes a DNA damage response and cell cycle arrest

(A) The DNA damage response 24h post-intoxication by WT- and HQ-toxin preparations was assayed in HT1080 cells using immunofluorescence of γ H2AX (green). Nuclei indicated by DAPI outline (grey). Scale bars are 20 μ m. (B) Quantification of γ H2AX-positive nuclei in (A). Nuclei were counted as positive if greater than the upper quartile of untreated γ H2AX intensity. Each circle is an independent replicate each consisting of three technical replicates. One way ANOVA was used with Šidák's multiple comparison test. Asterisks indicate significance. Bars indicate mean and error bars indicate SD. (C) Heatmap shows percentages of HT1080 cells in G1, G2 and S phase at 2 hourly timepoints across 24 h following intoxication, determined by measurement of propidium iodide using flow cytometry. Experiment was performed together with Angela Ibler. One independent replicate consisting of three technical replicates.

To check whether the toxin caused cell cycle arrest, cells were synchronised by 24 h serum starvation before a standard intoxication assay was performed. Samples were prepared for flow cytometry analysis every 2h after intoxication over the 24h media chase. The overall effect of the toxin is best observed at 24h where flow cytometry analysis revealed that 40% of WT-toxin treated cells were in G2 phase compared to only 13% and 17% of cells in HQ-toxin treated and untreated cells respectively (**Fig. 4.2C**). This G2 accumulation coincided with a decrease in cells in G1 from 53% and 46% in HQ-toxin treated and untreated cells to 25% in WT-toxin treated cells. Thus, the toxin causes a G2 arrest in the cell cycle.

In addition, the time-course provided insight into the effects of the toxin. From 6h, the proportion of cells in S phase increases relative to HQ-toxin treated and untreated cells. At the 8 h timepoint through the 12 h timepoint, there were approximately 8% more WT-toxin treated cells in S phase than either HQ-toxin treated or untreated cells, suggesting that the toxin was stalling DNA replication forks in S phase, which is consistent with replication stress observed by Ibler *et al.* 2019. This delay and the accumulation of cells in G2 showed that the toxin was causing cell cycle arrest in S/G2 phase.

4.2.2 The toxin causes both ATR- and ATM-dependent DDRs

The toxin causes two distinct DDR phenotypes that lead to senescence: (i) RPA-labelled SSBs at replication forks in S/G2 phase resulting in DNA replication stress marked by phosphorylation of T21 in RPA, and (ii) 53BP1-labelled DSBs in G0/G1 (Ibler *et al.*, 2019). In order to confirm that this was the case with purified toxin, RPA32 pT21 and 53BP1 were examined in intoxicated cells by immunofluorescence (**Fig. 4.3A**). In parallel, cells were incubated with the thymidine analogue EdU for 24 h before fixation to identify cells synthesising DNA and thus progressing through the cell-cycle. Both RPA32 pT21 and 53BP1 were increased in response to the WT-toxin compared to negative controls. RPA32 pT21 foci were induced in response to the WT-toxin in 33% of cells, compared to 2% of untreated and HQ-toxin treated cells (**Fig. 4.3B**). 6% of WT-toxin treated cells were positive for 53BP1 foci

compared to 0% untreated and HQ-toxin treated cells. The toxin also caused a decrease in DNA replication. Whereas 87% and 73% of untreated and HQ-toxin treated cells were positive for EdU, showing that they were undergoing DNA replication, only 26% of WT-toxin treated cells were EdU positive.

There were no nuclei positive for both EdU and 53BP1, which was consistent with 53BP1 being recruited to DSBs in G0/G1. However, approximately 10% of nuclei were positive for both EdU and RPA32 pT21 in response to the WT-toxin, consistent with RPA phosphorylation occurring during DNA replication stress.

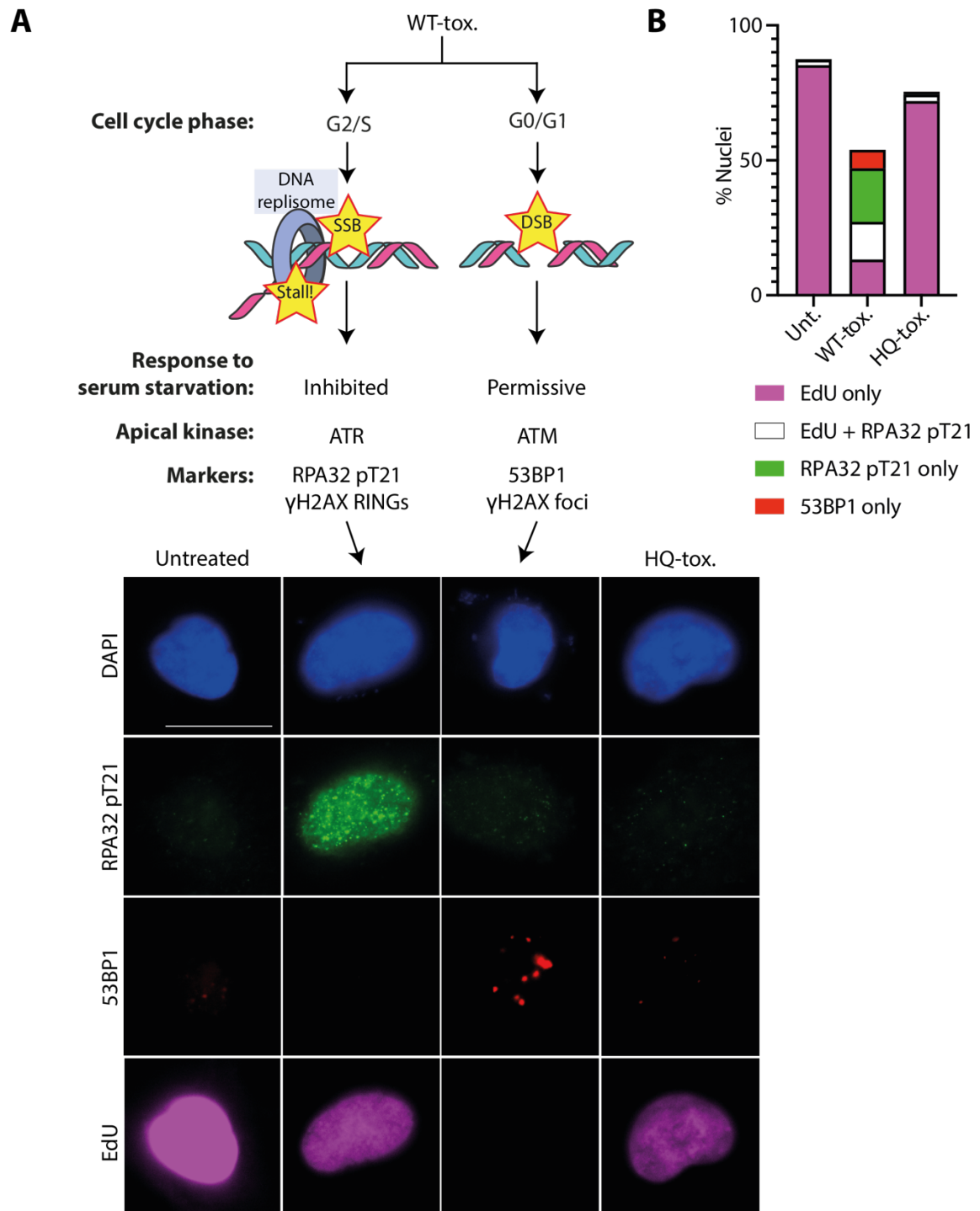


Fig. 4.3 The typhoid toxin causes distinct DNA damage responses in G0/G1 and G2/S phase

(A) The DNA damage response 24h post-intoxication by WT- and HQ-toxin preparations was assayed in HT1080 cells using immunofluorescence of phosphorylated RPA32 (RPA32 pT21, green), 53BP1 (red) and EdU (magenta). Distinct responses to the WT-toxin in G0/G1 and G2/S phase are indicated. Scale bars indicate 20 μ m. **(B)** Quantification of positive nuclei in (A). Nuclei were counted as positive if greater than the upper quartile of untreated intensity. Bars indicate total percentage across three technical replicates from one independent replicate.

4.2.3 The toxin activates a type-I IFN response

Having confirmed that purified typhoid toxin activates DDRs, host defence pathways were investigated by analysing the transcriptome of intoxicated HT1080 cells. The experiment was performed in collaboration with my colleague Angela Ibler who intoxicated HT1080 cells for 2h with either WT- or HQ-toxin before extraction of cellular RNA at 48h. The RNA was analysed using Clariom™S transcriptome profiling microarray at the Sheffield Microarray and Next Generation Sequencing Core Facility who provided data for analysis by myself (experimental pipeline indicated in **Fig. 4.4A**).

19460 genes were detected in both WT- and HQ-toxin treated samples, and of these 1885 genes were significantly differentially expressed ($p < 0.05$) with a log₂ fold change > 1 or < -1 (**Fig. 4.4B**). Analysis of these 1885 genes performed with STRING v11.0 revealed the WT-toxin dependent enrichment of a variety of biological processes. This included 11 biological processes which were upregulated, of which 6 were related to immune responses (**Fig. 4.4C**, marked in bold). Of these six processes, the most upregulated was the type-I IFN signalling pathway, characterised by upregulation of 11 genes (**Fig. 4.4D-E**) which has been previously shown to be activated by replication stress and is implicated in premature senescence (Kreienkamp *et al.*, 2018). The gene set included 2 ISG transcription factors (IRF-9 and STAT1) and 7 ISGs including IFN-induced proteins with tetratricopeptide repeats 1-3 (IFIT-1, -2 and -3), 2'-5' oligoadenylate synthase 1 and 3 (OAS-1 and -3), early-growth response gene 1 (EGR1), viperin (also known as RSAD2), IFN- α inducible protein 6 (IFI6) and IFN-stimulated gene 15 (ISG15).

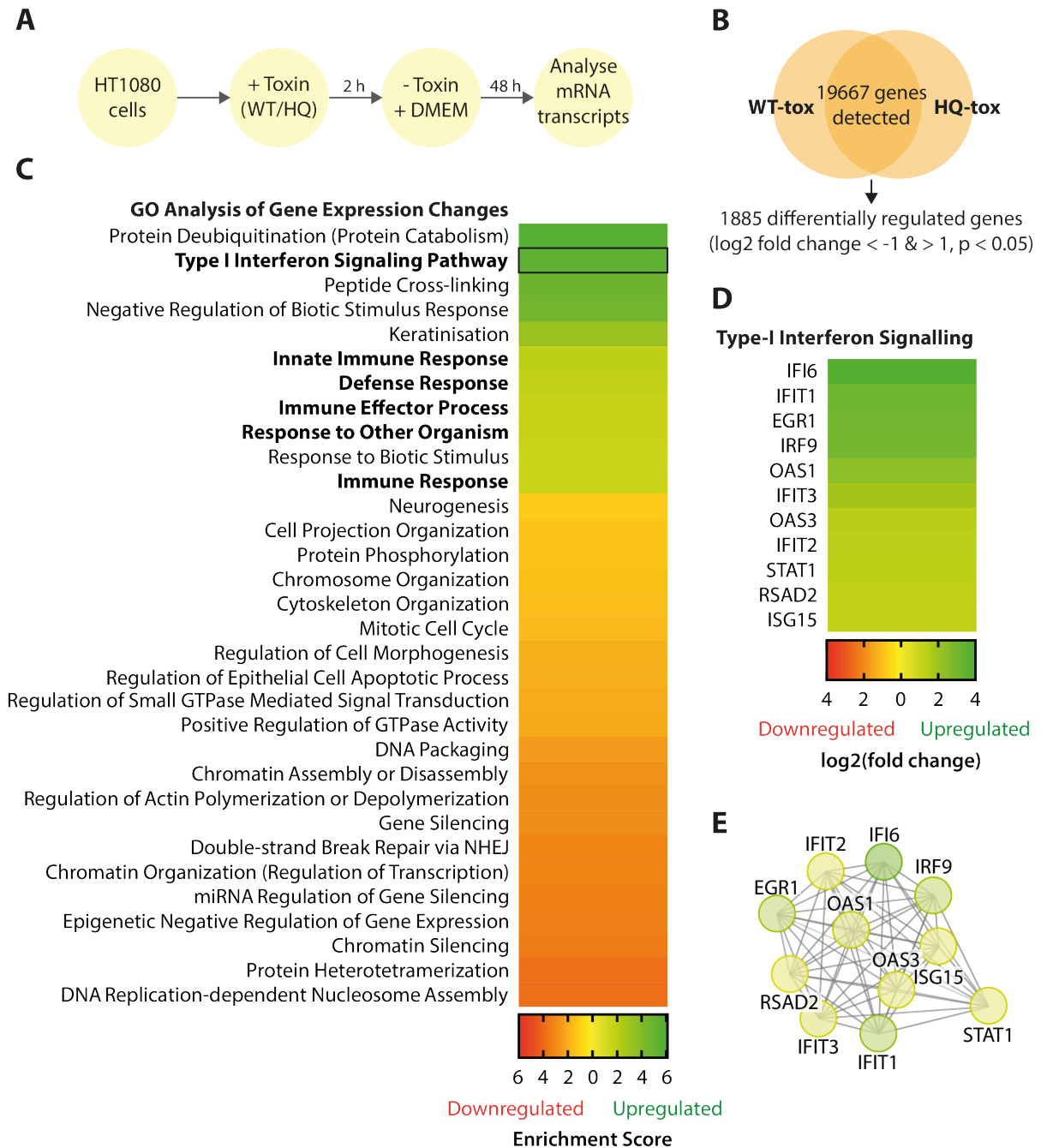


Fig. 4.4 The typhoid toxin induces a type-1 IFN signalling response

(A) Workflow for microarray analysing gene expression in HT1080 cells 48h post-intoxication by WT- and HQ-toxin. (B) Fold changes were calculated between treatments for 19460 genes. Of these, 1885 genes were significantly differentially regulated ($p < 0.05$) with a log₂ fold change >1 or <-1. Results from three independent replicates. (C) Heatmap shows significant enrichment of Gene Ontology (GO) terms detected by STRING in the set of 1885 genes indicated in (B). (D) Heatmap shows 11 genes related to the type-1 interferon signalling pathway, including ISGs upregulated in response to WT-toxin. (E) STRING network highlighting close functional and annotated relationships between the genes presented in (D), using same colour scale. Intoxication of HT1080 cells and RNA extraction were performed by Angela Ibler. I analysed the Affymetrix Gene Chip Microarray data, which was provided by the Sheffield Microarray and Next Generation Sequencing Core Facility.

4.2.4 The IFN response is not S/G2 dependent

To determine whether the type-I IFN response was triggered by toxin-induced replication stress, transcriptome changes were analysed following WT- and HQ-toxin treatment of HT1080s in the presence (10%) or absence (0%) of serum at 48h. Serum-starvation prevents entry into S phase, locking cells in G0/G1, which therefore inhibits toxin-induced replication stress (Ibler *et al.*, 2019). Toxin-induced DSBs are permissive in the presence and absence of serum while SSBs in S/G2 are only permissive in the presence of serum (WT-tox, 10% serum), which enabled identification of 1195 genes associated with DNA replication stress that were significantly differentially expressed ($p < 0.05$) with a log₂ fold change > 1 or < -1 (**Fig. 4.5A**). To identify genes associated with DSBs in G0/G1, the transcriptome of cells treated with WT-tox and HQ-tox in the absence of serum were analysed (**Fig. 4.5B**). Of these, 343 were significantly differentially expressed ($p < 0.05$) with a log₂ fold change > 1 or < -1 .

The type-I IFN response has been shown to be induced by replication stress, and to lead to senescence (Kreienkamp *et al.*, 2018). Thus, it was hypothesised that the type-I IFN response was caused by toxin-induced replication stress, possibly due to host DNA leakage into the cytosol. The transcriptome experiment in **Fig. 4.4** was also performed in the absence of serum to block entry into S phase and therefore replication stress (**Fig. 4.5**). Relative to HQ-toxin, WT-toxin induced a type-I IFN response in serum-starved cells showing that the IFN response occurred independently of S phase and was instead occurring in G0/G1 phase (**Fig. 4.5C-D**) where 53BP1-labelled DSBs were observed in **Fig. 4.3**). The major differences between the presence and absence of serum in intoxicated cells was in cell cycle and cell metabolic processes, most likely due to serum-starvation blocking replication and the supply of nutrients. When focussing on individual ISGs, the type-I IFN response in serum-starved cells was particularly evident for ISGs such as IFI6 and IFIT1 that were observed in G0/G1 but not for ISGs such as ISG15 and RSAD2, which were up-regulated in asynchronous replication-competent cells in the presence of serum (**Fig. 4.5D**). This suggests divergent mechanisms underlying ISG regulation.

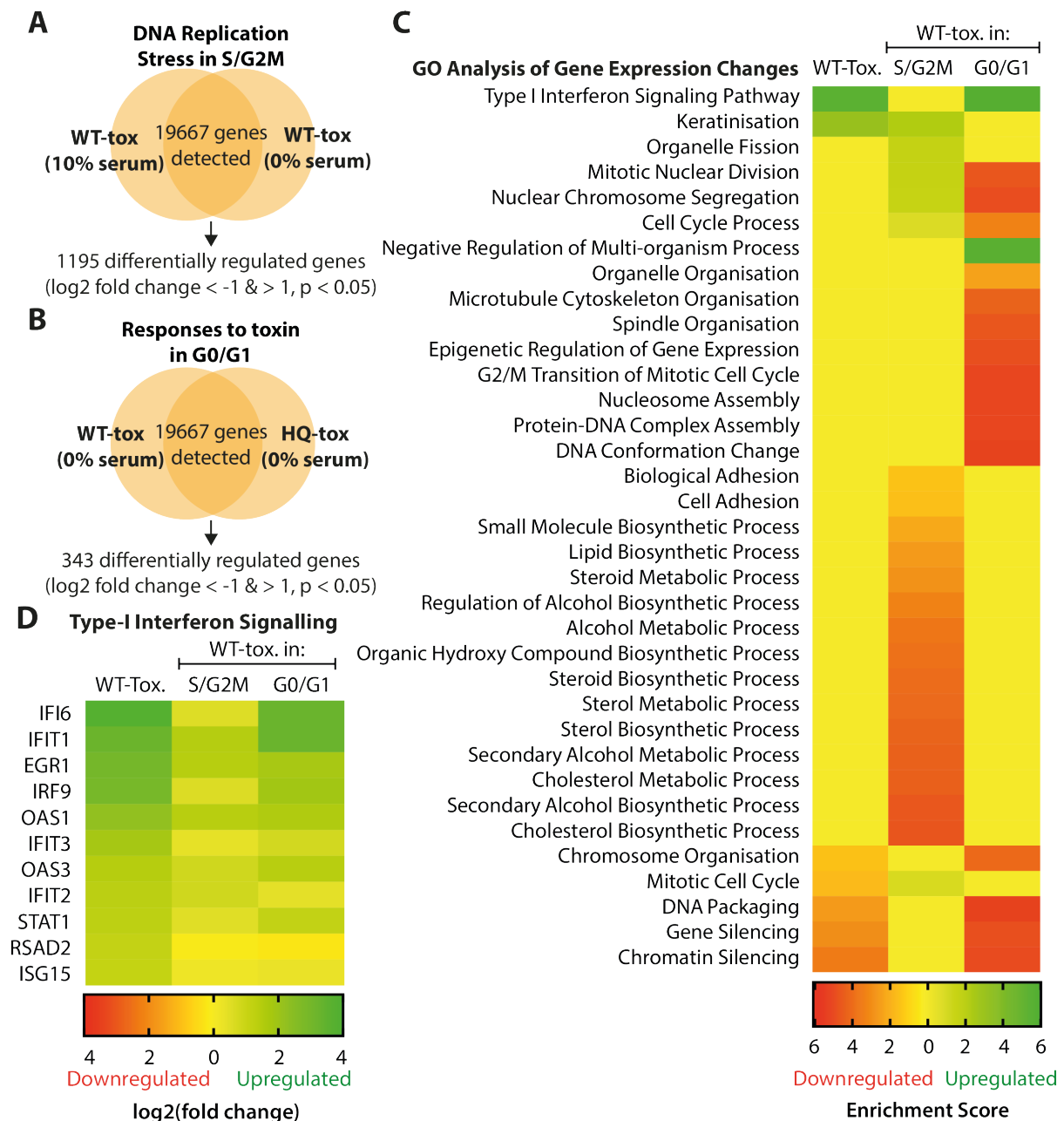


Fig. 4.5 The toxin-dependent type-I IFN-like response occurs in G0/G1

(A) Fold changes were calculated 48h post-intoxication between WT-toxin treated cells in normal (10% serum) and serum-starved (0% serum) conditions for all detected genes, in order to determine toxin responses due to replication stress in S/G2M phase. 1195 genes were significantly differentially regulated ($p < 0.05$) with a log₂ fold change > 1 or < -1 . Results from three independent replicates. (B) Fold changes were calculated between WT- and HQ-toxin treated cells in serum-starved (0% serum) conditions for all detected genes, in order to determine toxin responses in G0/G1 phase. 343 genes were significantly differentially regulated ($p < 0.05$) with a log₂ fold change > 1 or < -1 . Results from three independent replicates. (C) Heatmap shows significant enrichment of Gene Ontology (GO) terms detected by STRING in the 1195 genes indicated in (A) and the 343 genes indicated in (B). Enrichment of detected GO terms was also compared with asynchronous toxin-dependent responses in fig. 3.4C. Intoxication of HT1080 cells and RNA extraction were performed by Angela Ibler. I analysed the Affymetrix Gene Chip Microarray data, which was provided by the Sheffield Microarray and Next Generation Sequencing Core Facility. (D) Heatmap shows 11 genes related to the type-1 IFN signalling pathway upregulated in response to WT-toxin due to replication stress in S/G2M phase or damage in G0/G1 phase and compared to asynchronous responses from Fig. 4.4D.

4.2.5 Validation of the toxin-induced IFN response

As the type-I IFN response has been linked to both DDRs and senescence, the 11 type-I IFN related genes identified by the microarray were chosen for further analysis. To validate the microarray data, qRT-PCR was carried out in HT1080 cells on 9 of the IFN-related genes: IFI6, IFIT1, IFIT2, IFIT3, IRF9, ISG15, OAS1, OAS3 and STAT1. For 2 of the genes, RSAD2 and EGR1, efficient primers could not be designed. Untreated cells were used as a calibrator and cells were harvested 24 h following intoxication with WT- or HQ-toxin. 5 of the type-I IFN related genes were significantly upregulated in WT-toxin treated cells compared to untreated cells, compared to only 3 genes upregulated in HQ-toxin treated cells compared to untreated (**Fig. 4.6A-I**). Furthermore, 5 genes were significantly upregulated in WT-toxin compared to HQ-toxin (ISG transcription factor IRF-9 and ISGs IFIT1, IFIT2, IFIT3, and ISG15). Overall, this provided further evidence that some ISGs are upregulated in a toxin-dependent manner, although not all ISG expression changes found in the microarray could be validated.

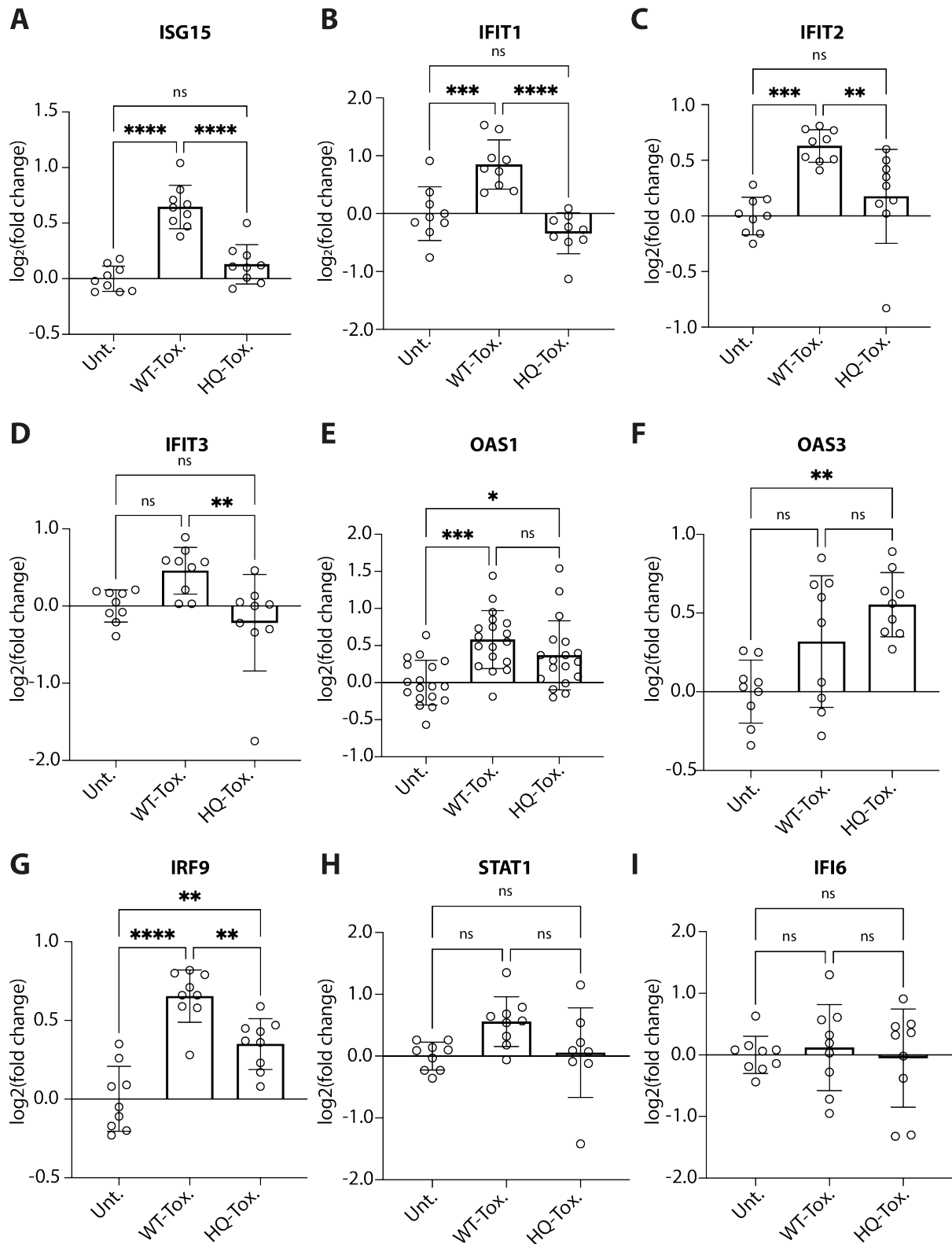


Fig. 4.6 Validation of the toxin-dependent type-I IFN-like response by qRT-PCR

(A-I) Quantification of mRNA levels in HT1080s of 9 type-1 IFN-related genes compared between untreated and 24h WT- and HQ-toxin treated samples. Bars represent mean and error bars indicate SD. Each circle is an individual technical replicate from minimum three independent replicates. One way ANOVA was used with Šidák's multiple comparison test. Asterisks indicate significance.

To further validate the IFN-like response, levels of ISG15 and IFIT1 were assayed by immunoblotting, as these showed the greatest significance in mRNA levels between WT- and HQ-toxin treatment. Levels of phosphorylated STAT1 (pSTAT1) were also assayed, as STAT phosphorylation is a key component of ISG regulation (**Fig. 4.7A**). In contrast to mRNA (**Fig. 4.6**), immunoblot analysis revealed that there was no difference in IFIT1, pSTAT1, STAT1 or ISG15 protein levels 24 h after intoxication with WT-toxin (**Fig. 4.7A**). However, ISG15 protein levels were significantly increased at the 72 h timepoint compared to both untreated and HQ-toxin treated cells (**Fig. 4.7A, B**). IFIT1 was significantly upregulated at 72 h in WT-intoxicated cells compared to untreated cells and showed a non-significant increase compared to HQ intoxication (**Fig. 4.7C**). Both STAT1 and pSTAT1 showed an increase in response to WT toxin at 48 – 72 h, but this increase was not significant to either untreated or HQ-intoxicated cells. As a positive control, sustained 72 h treatment with purified IFN α triggered both phosphorylation and upregulation of STAT1, as well as upregulation of IFIT1 and ISG15 (**Fig. 4.7A**). IFN α also induced a smear of high molecular weight ISG15-conjugated (ISGylated) proteins which was not visible following intoxication where only free ISG15 was observed. No toxin induced ISGylation was observed in over exposed blots (**data not shown**). ISG15 is a ubiquitin-like protein and has been shown to act as a covalent adduct to other proteins throughout the cell (Morales and Lenschow, 2013; Perng and Lenschow, 2018).

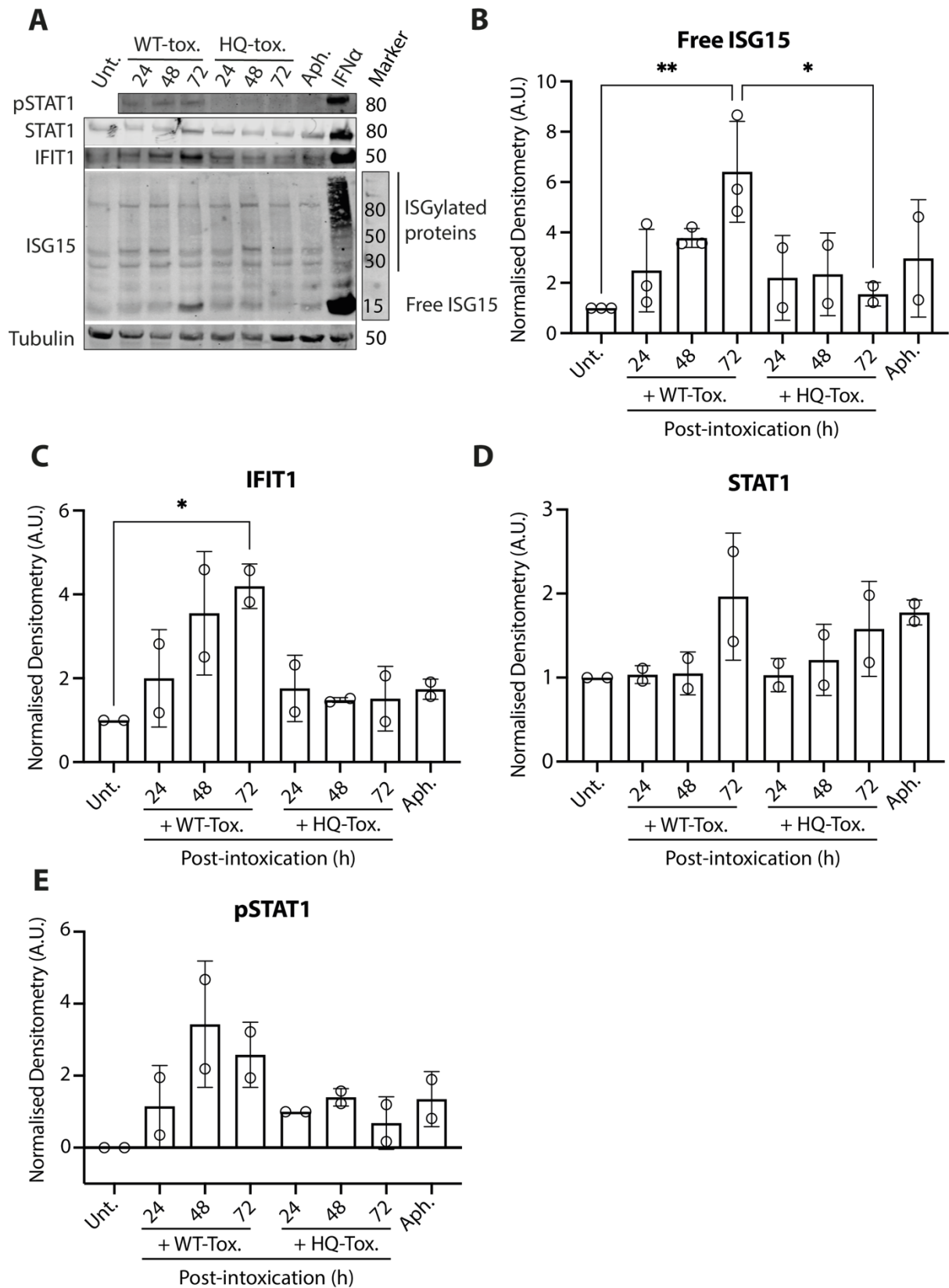


Fig. 4.7 ISG15 and IFIT1 are upregulated in response to typhoid toxin

(A) Immunoblots of protein levels in HT1080s of STAT1, phosphorylated STAT1 (pSTAT1), ISG15, and IFIT1 24 h, 48 h and 72 h after either treatment with WT-toxin, HQ-toxin or 100ng/ml purified IFN α . The pSTAT1 untreated band was not shown due to leakage from the lane containing the molecular weight marker. (B - E) Graph shows densitometry analysis (ImageStudio) of ISGs relative to tubulin and normalised to untreated (minimum 2 independent immunoblots). ISG15 densitometry is of the 15 kDa free ISG15 band. One way ANOVA was used with Šidák's multiple comparison test. Asterisks indicate significance.

Immunofluorescence was also used to determine localisation of ISG15 in response to the toxin. Interestingly, ISG15 predominantly localised to the nucleus, suggesting it could be modulating function of nuclear proteins (**Fig. 4.8A**). ISG15 was significantly upregulated in the nucleus in WT-toxin treated cells and IFN-treated cells compared to untreated and HQ-toxin treated cells (**Fig. 4.8B**). Approximately 60% of WT intoxicated and IFN α -treated nuclei were positive for ISG15 compared to 20% of untreated and HQ-intoxicated nuclei.

In **Fig. 4.5**, the IFN response occurred in G0/G1 phase, but this was less clear for ISG15, which was best observed in asynchronous cells suggesting upregulation in both G0/G1 and S/G2. When ISG15 was assayed in WT- and HQ-intoxicated cells in serum-free conditions by immunofluorescence (**Fig. 4.8C**), there was significant variation in the data for HQ-intoxication and IFN-treatment, which made it difficult to interpret the results. However, there was a significant increase in ISG15 in WT-intoxicated cells compared to untreated cells (**Fig. 4.8D**). However, compared to around 60% positive cells in 10% serum, only 40% of cells were positive for ISG15 in response to the WT toxin in 0% serum.

ISG15 was assayed in WT- and HQ-intoxicated cells in serum-free conditions using immunoblotting. Consistent with the immunofluorescence data, WT-intoxication induced an increase in ISG15 in 0% serum, but not to the same extent as in 10% serum conditions (**Fig. 4.8E**). Taken together, this suggested that toxin induced ISG15 is not solely a product of the G0/G1 DDR and further suggests divergent regulation of ISG15 relative to other ISGs, e.g., IFI6 in **Fig. 4.5D**. It therefore seems possible that ISG15 is upregulated in response to the 53BP1-labelled DSBs in G1 and RPA-labelled SSBs in S/G2 observed in in **Fig. 4.3**.

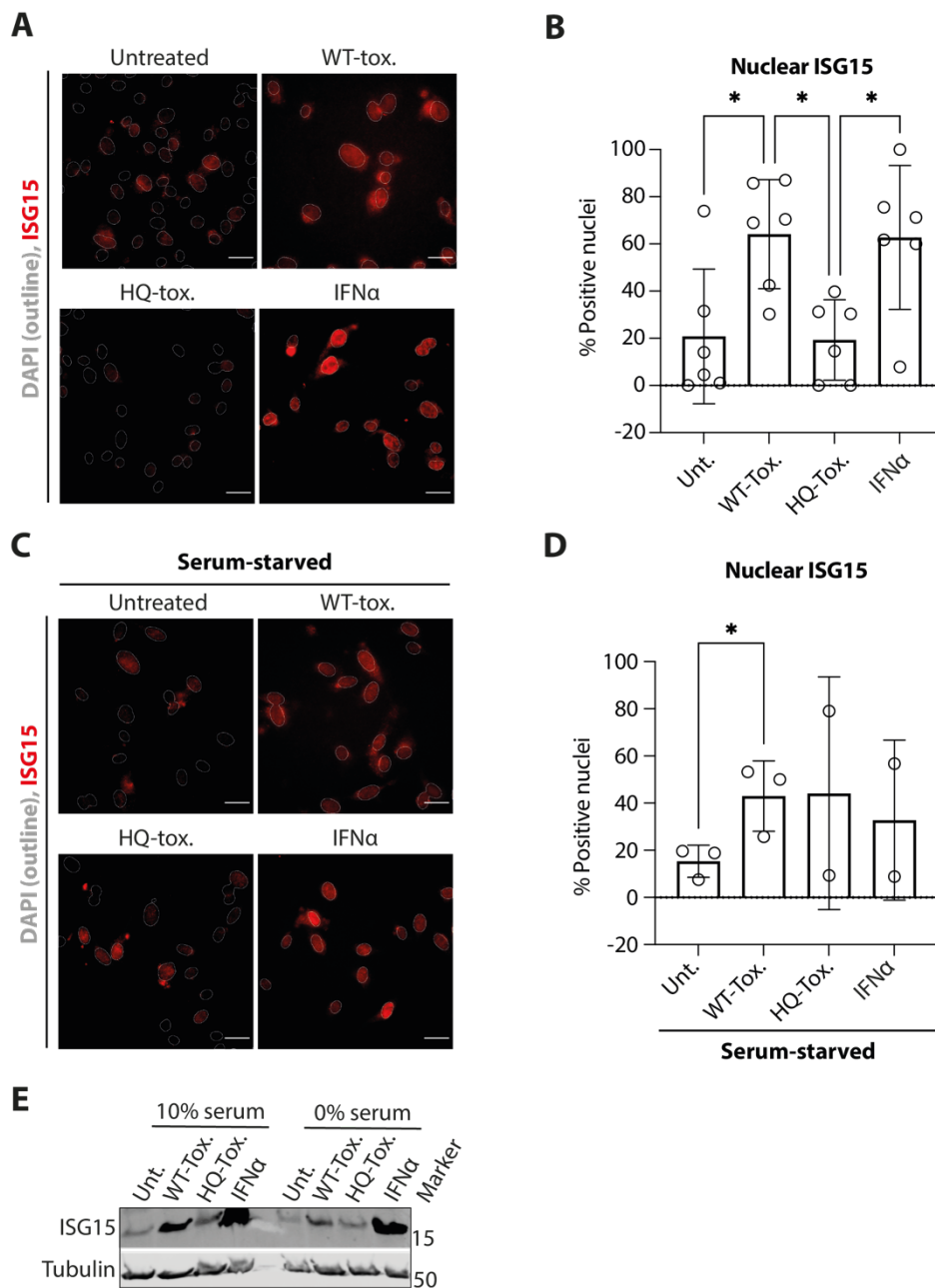


Fig. 4.8 Immunofluorescence analysis of ISG15

(A) Immunofluorescence of ISG15 (red) 72h after treatment with WT-toxin, HQ-toxin or 100ng/ml purified IFNα in HT1080 cells. (B) Quantification of ISG15-positive nuclei in (A). Each circle is a technical replicate from two independent replicates. One way ANOVA was used with Šidák's multiple comparison test. (C) Same as (A) in serum-starved (0% serum) conditions. (D) Quantification of ISG15-positive nuclei in (C). Each circle is a technical replicate from a single independent replicate. An unpaired t-test was used to compare Unt and WT-toxin conditions. (E) Immunoblot of protein levels in HT1080s of ISG15 72 h after treatment with WT-toxin, HQ-toxin or 100ng/ml purified IFNα in normal (10% serum) and serum-starved (0% serum) conditions. Nuclei were counted as positive if greater than the upper quartile of untreated ISG15 intensity. Asterisks indicate significance. Bars indicate mean and error bars indicate SD. Nuclei indicated by DAPI outline (grey). Scale bars indicate 20μm.

4.2.6 Determining the role of IFNs in the toxin ISG response

ISGs are canonically regulated by IFNs binding to cognate receptors and activating a downstream JAK/STAT signalling pathway, triggering formation of heteromeric signalling complexes that bind to ISREs in ISG promoter sequences (Boxx and Cheng, 2016). Despite seeing upregulation of ISGs in the microarray (**Fig. 4.4**), no IFN genes were significantly differentially regulated between WT and HQ treatment, suggesting that ISG upregulation was IFN-independent (**Fig. 4.9A**). To examine this in further detail, IFN α and IFN β mRNA levels were analysed by qRT-PCR. IFN α was significantly increased in both WT and HQ treatments compared to untreated but these were not significantly different to each other, suggesting that the increase was independent of toxin activity (**Fig. 4.9B**). IFN β mRNA levels showed no significant difference between any treatments (**Fig. 4.9C**). It is important to note that the CT values for these IFNs were very high (approximately 39) compared to, for example, GAPDH (approximately 20), showing that mRNA levels of IFNs were low even in response to either WT- or HQ-toxin.

ISG15 expression was also examined following type-I IFN inhibition by B18R, which is encoded by vaccinia virus and competitively binds to IFN, thus inhibiting downstream signalling of IFN (Radoshevich *et al.*, 2015). As expected, B18R abolished ISG15 upon addition of IFN α (**Fig. 4.9D-E**). However, whilst there was a reduction in ISG15, B18R did not abolish WT-toxin dependent ISG15 upregulation, suggesting that the toxin was upregulating ISG15 via both type-I IFN-dependent and -independent pathways.

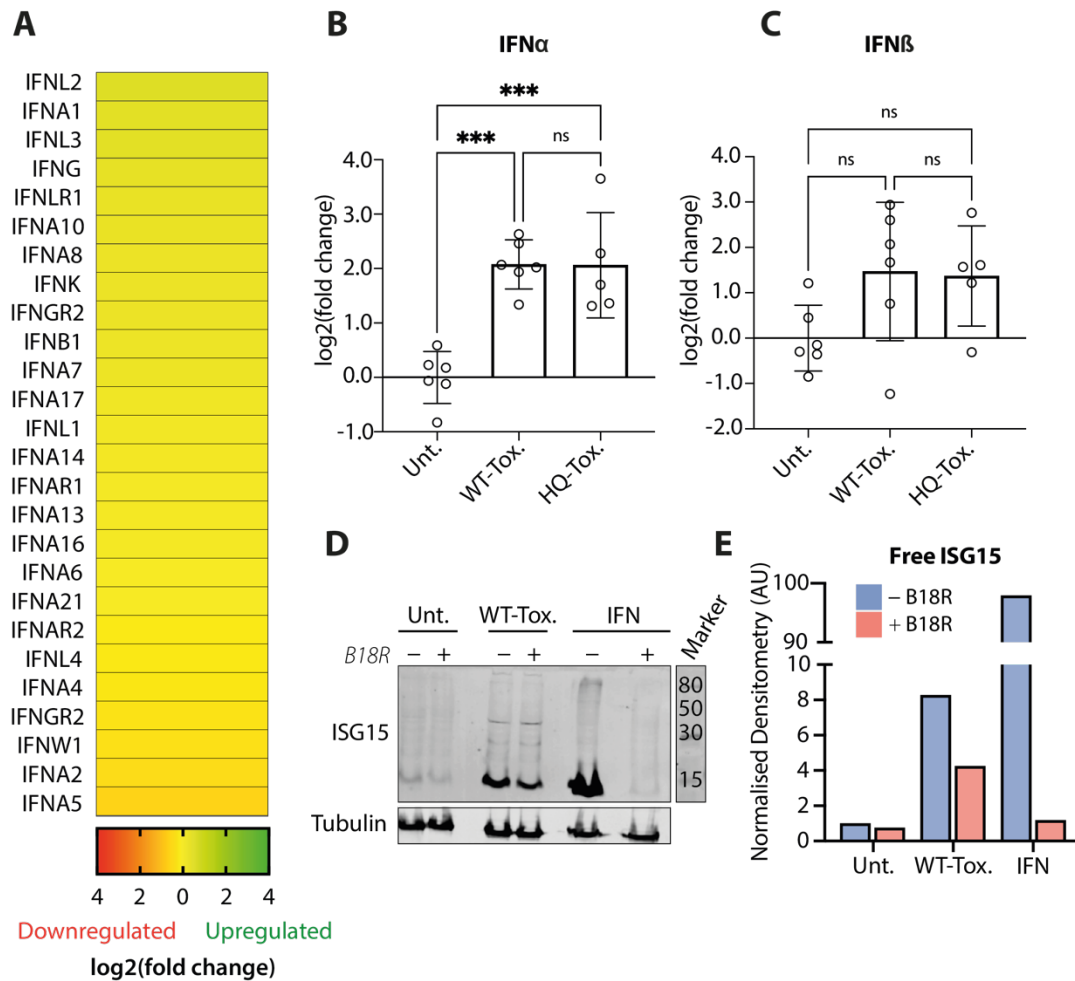


Fig. 4.9 **Examining the role of IFN in the toxin ISG response**

(A) Heatmap shows all IFN genes detected in the microarray presented in fig. 3.4 and represents fold change between WT- and HQ-toxin treated cells. (B-C) Quantification of mRNA levels in HT1080s of IFN α and β compared between untreated and 24h WT- and HQ-toxin treated samples. Bars represent mean fold change of three samples (three technical replicates run for each sample). Each circle is an individual technical replicate. One way ANOVA was used with Šidák's multiple comparison test. Asterisks indicate significance. Error bars indicate SD. (D) Immunoblot of protein levels in HT1080s of ISG15 72 h after treatment with WT-toxin or 100 ng/ml purified IFN α in the presence and absence of B18R. (E) Densitometry analysis (ImageStudio) of 15 kDa free ISG15 band in (D) relative to tubulin (one independent replicate).

4.3 Discussion

The host response to the typhoid toxin is key to understanding mechanistic links between the toxin and systemic *Salmonella* dissemination, chronic carriage, bacteraemia, and cancer. For *Salmonella* to establish chronic infection it must evade or manipulate host immune responses, and indeed data in this chapter has shown that the typhoid toxin induced upregulation of genes involved in the type-I IFN pathway.

Beyond responses to pathogen invasion, which were discussed in section 3.5, the type-I IFN response has been observed in response to inducers of replication stress, such as progerin or knockdown of RPA. Replication stress leads to DNA leakage into the cytosol, activation of cGAS and a type-I IFN response (Wolf *et al.*, 2016; Kreienkamp *et al.*, 2018). In these contexts, the IFN response regulates cell fate decisions, such as inducing senescence in order to prevent escalation of genomic instability into oncogenic phenotypes. It is possible that the toxin IFN response links toxin-induced replication stress to the senescence phenotype observed in Ibler *et al.* However, the IFN response was observed predominantly in G0/G1 phase rather than with replication stress in G2/S phase. Further work will be needed to determine whether the toxin IFN response is part of a distinct host response to damage in G0/G1, including further replicates of immunoblotting and immunofluorescence experiments to examine toxin induced ISG responses following serum starvation.

Of the ISGs identified from the microarray data, ISG15 showed the greatest significant upregulation in response to the toxin when using qRT-PCR, immunoblotting and immunofluorescence. Because of this, ISG15 was used as a marker for the toxin ISG response going forward. However, the myriad functions of ISG15 prompted interest in determining its specific role in the host response to the toxin, which I will discuss in the following chapters.

Although ISG15 upregulation was validated by other methods, this was not the case for other ISGs detected. For example, significant differences were not seen in OAS1, OAS3, STAT1 and IFI6 mRNA levels between WT- and HQ-toxin treated cells. It is possible that the 24h timepoint at which RNA samples were prepared post-intoxication was not optimal for seeing toxin-dependent changes in ISG mRNA levels. RNA samples for the microarray were taken 48h post-intoxication whereas qRT-PCR samples were prepared 24h post-intoxication. Furthermore, increases in ISG15 and IFIT1 protein levels were not seen until 48h post-intoxication and were strongest at 72h post-intoxication. It would be interesting to repeat the qRT-PCR experiments at different timepoints, including shorter timepoints (approx. 2h) and longer timepoints (48h-72h).

Initial data suggested that the toxin ISG response was partially independent of type-I IFNs. IFN upregulation was not seen in the microarray, and mRNA levels of IFN α and IFN β did not change in a toxin-dependent manner. It was interesting to observe that IFN α was significantly upregulated in response to both WT- and HQ-toxin compared to untreated. This could be because *E. coli* contaminants in the toxin preparations were acting as PAMPs and inducing IFN production in a canonical manner. However, based on the observed CT values, these levels of IFN mRNA were low, especially when compared to toxin dependent induction of ISGs.

The type-I IFN inhibitor B18R did not abolish toxin induced ISG15. It is possible that some of the ISGs seen to be upregulated in the microarray may be upregulated in an IFN-independent manner. For example, ISG15 has been shown to have a P53-response element and is induced in response to P53 activation following DNA damage (Park *et al.*, 2016). However, further information will be needed to confirm whether the toxin ISG response is IFN-independent. The experiment with B18R was a single immunoblot and should be repeated. Furthermore, as B18R is an inhibitor of type-I IFNs only, it would be interesting to use inhibitors of other types of IFN. Alternatively, toxin responses could be examined in genetically engineered cells lacking IFN receptors.

In order to better understand the toxin ISG response, an understanding of how the response was regulated, and how it was linked to the DDR induced by the toxin, was required. The next chapter presents efforts to elucidate the link between toxin-induced DNA damage and the ISG response.

5 Regulation of the toxin ISG response

5.1 Introduction

The toxin is thought to functionally mimic mammalian DNase-1 by introducing SSBs before their accumulation on complementary strands generate DSBs (Bezine, Vignard and Mirey, 2014). This causes replication stress which can lead to DNA leakage into the cytosol, which acts as a DAMP and triggers activation of DNA sensing PRRs (MacKenzie *et al.*, 2017; Bakhoun *et al.*, 2018). PRRs signal to downstream kinases that induce immune responses including the type-I IFN pathway. It was hypothesised that the toxin was inducing an ISG response by triggering cytosolic leakage of DNA.

5.2 Results

5.2.1 The toxin induces single strand breaks, micronuclei and cytosolic DNA leakage

Previous work in the Humphreys lab has established that the typhoid toxin creates SSBs in DNA, which can be shown by assaying RPA32 pT21 (Ibler *et al.*, 2019). In order to further confirm these findings, it was necessary to find a method to identify SSBs.

To detect SSBs a novel *in vitro* polymerase assay was used, whereby ssDNA within fixed nuclei acts as a template for a DNA polymerase reaction, which can incorporate complementary nucleotide analogues to these sites. Using antibodies targeting these nucleotide analogues, in this case CldU, sites of ssDNA were identified (**Fig. 5.1A**). 100% of nuclei treated with WT-toxin were positive for CldU foci when using the upper quartile of untreated cell intensity as a threshold (**Fig. 5.1B**). In comparison, only 25% of nuclei were positive for CldU in HQ-toxin treated cells. CldU in intoxicated nuclei was coincident with a DDR characterised by both RPA32 pT21 and gH2AX.

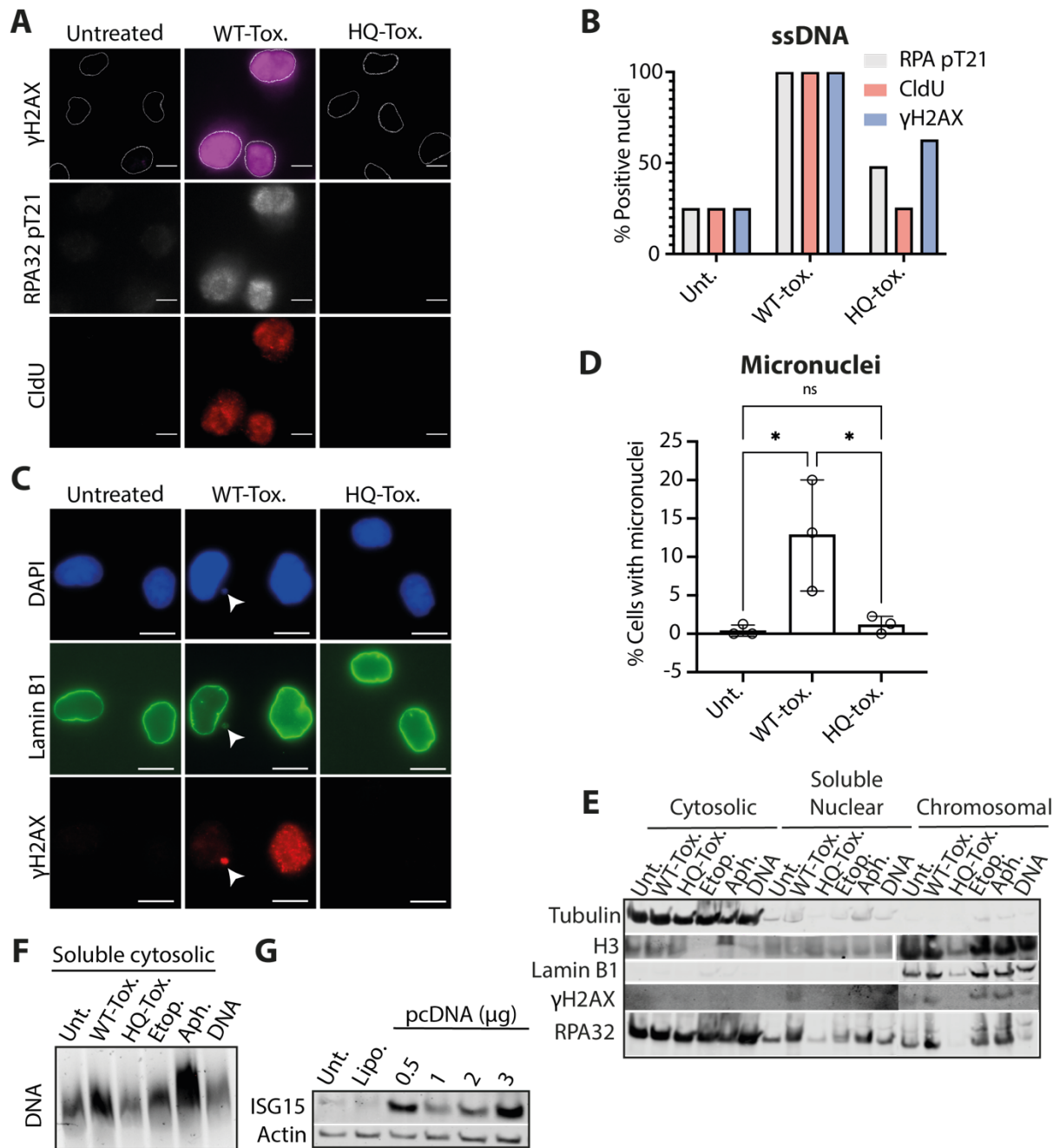


Fig. 5.1 Toxin activity results in ssDNA formation and DNA leakage into the cytosol

(A) Immunofluorescence of γ H2AX (magenta) and RPA32 pT21 (grey) 24h post-intoxication by WT- and HQ-toxin in HT1080 cells. Sites of exposed ssDNA are detected using the in vitro polymerase assay and are shown by CldU foci (red). Scale bars indicate 10 μ m. (B) Quantification of nuclei positive for the markers indicated in (A). Bars represent percentages of approximately 40-100 nuclei in one independent replicate. (C) Immunofluorescence of Lamin B1 (green) and γ H2AX (red) 24h post-intoxication by WT- and HQ-toxin in HT1080 cells. Micronucleus indicated with white arrow. Scale bars indicate 10 μ m. (D) Quantification of cells containing micronuclei. Each circle is a technical replicate from a single independent replicate. One way ANOVA was used with Tukey's multiple comparison test. Asterisks indicate significance. Bars indicate mean and error bars indicate SD. (E) Immunoblot of protein levels of tubulin, histone H3, Lamin B1, γ H2AX and RPA32 in HT1080s 24h after treatment with WT-toxin, HQ-toxin, etoposide, aphidicolin or transfection with 20 nM immunostimulatory DNA. Cells were fractionated into cytosolic, soluble nuclear and chromosomal fractions. (F) DNA gel of the soluble cytosolic fraction in (E), showing relative levels of DNA in the soluble cytosolic fractions from (E). (G) Immunoblot of protein levels in HT1080s of ISG15 48h after transfection with empty vector pcDNA. Lipo. is lipofectamine.

Micronuclei are small membrane-bound fragments of chromosomes which are associated with genomic instability and are indicative of cytosolic DNA leakage. To investigate whether the toxin was inducing micronuclei formation, micronuclei were visualised by immunofluorescence using a combination of DAPI and lamin B1.

Micronuclei marked by γ H2AX were observed (**Fig. 5.1C**, marked by white arrow). Only 10-15% of cells contained micronuclei following intoxication, however this was significantly greater than untreated or HQ-intoxicated cells where less than 1% of cells contained micronuclei (**Fig. 5.1D**).

Visualisation of unprotected cytosolic ssDNA was attempted by labelling DNA with EdU and measuring cytosolic foci. However, foci could not be identified, possibly because the signal was overwhelmed by nuclear EdU, and possibly because the image resolution was not sufficient to identify such small DNA fragments (**data not shown**). Instead, whole cell lysates were fractionated into soluble cytosolic, soluble nuclear and chromosomal fractions following a standard intoxication assay. As positive controls, cells were fractionated following treatment with the DNA damage inducers aphidicolin and etoposide, and cells transfected with 20 nM of immunostimulatory DNA which had been shown to mimic cytosolic DNA in other studies (Fu *et al.*, 2019; Lama *et al.*, 2019).

The reliability of the fractionation was confirmed by the presence of tubulin in the cytosolic fraction and histone H3 and lamin B1 in the chromosomal fraction using immunoblotting (**Fig. 5.1E**). A reliable marker for the soluble nuclear fraction could not be found. γ H2AX was also assayed, which as expected was predominantly found in the chromosomal fraction and was particularly evident in WT-intoxicated and aphidicolin- and etoposide -treated cells. Finally, RPA32 was assayed, which was found predominantly in the soluble cytosolic fraction. This makes sense as in RPA32 immunofluorescence protocols, cultured cells must be treated briefly with detergent prior to fixation that extracts cytosolic RPA whilst retaining nuclear RPA (Ibler *et al.*, 2019).

In order to compare levels of cytosolic DNA, the soluble cytosolic fraction was run on an agarose gel to visualise relative amounts of DNA. DNA was visible in each fraction but was more intense in WT-intoxicated and aphidicolin- and etoposide -

treated cells compared to untreated and HQ-intoxicated (**Fig. 5.1F**). The DNA-transfected cells did not show evidence of any increased DNA in the cytosolic fraction (**Fig. 5.1F**) despite confirming that transfection with empty pcDNA vector induced ISG15 expression (**Fig. 5.1G**). Taken together, this suggests that the toxin was inducing an ISG response by triggering leakage of damaged DNA into the cytosol, however further experiments would be needed for definitive evidence.

5.2.2 The role of ssDNA-binding proteins in regulation of the toxin ISG response

SsDNA binding proteins (SBPs) are essential for prevention of the accumulation of cytosolic self-DNA. For example, the SBP RPA was found to sequester fragments of damaged DNA at nuclear pores to prevent leakage (Wolf *et al.*, 2016). RPA knockdown was shown to amplify levels of cytosolic DNA, cGAS-STING activity and a type-I IFN response including upregulation of ISG15.

The Humphreys lab recently established that the RPA binds toxin induced SSBs in S/G2 (Ibler *et al.*, 2019). RPA plays an important role in the cellular response to the toxin. Toxin-induced DNA damage creates an excess of ssDNA substrate that overwhelms the pool of RPA, resulting in the build-up of unprotected ssDNA that ultimately results in DSBs (Ibler *et al.*, 2019). However, the phenomenon of RPA exhaustion was restricted to S/G2 of the cell cycle and whether the toxin induces SSBs in G1 is not known. As the RPA response was restricted to G2/S phase, and data presented in **Fig. 4.5D** suggested that the ISG response was occurring in G0/G1 phase, the possibility that different SBPs were detecting toxin induced SSBs in G0/G1 phase was explored.

Global changes in expression of genes labelled as ssDNA binding were examined on STRING v11 within the transcriptome of toxin-treated cells. Of particular interest were those SBPs that were co-incident with the ISG response in G1. Interestingly, most SBPs were downregulated in response to the toxin including all three components of the RPA complex (**Fig. 5.2A**). Identified hits were involved in DNA metabolism, the DDR or telomere function, with SSBP2, SSBP3 and SSBP4 being of unknown function (**Fig. 5.2B**). Of the SBPs analysed, HMGB2 and NABP1 were chosen for further analysis.

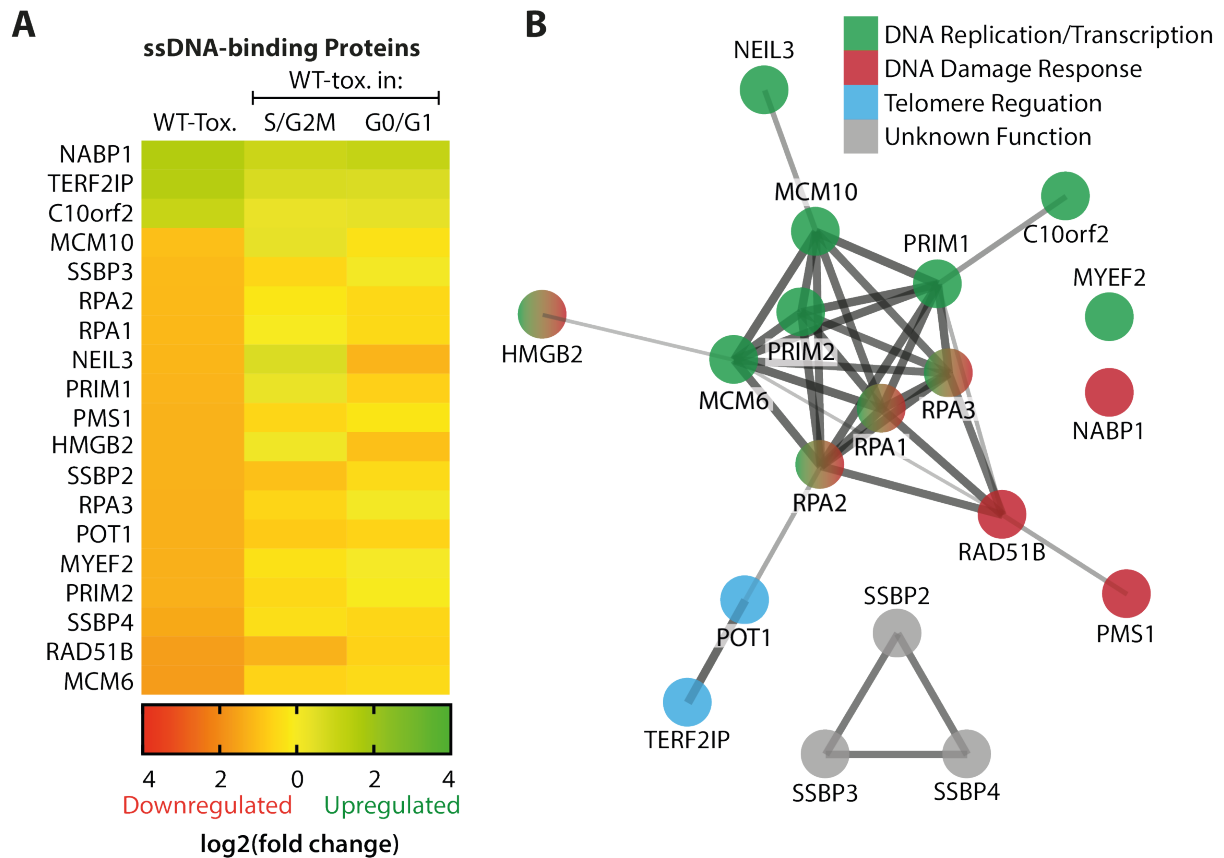


Fig. 5.2 Regulation of ssDNA-binding proteins in response to the toxin
(A) Heatmap shows 19 genes for ssDNA-binding proteins detected in the microarray presented in fig. 3.4 and represents fold change 24h post-intoxication in WT- and HQ-toxin treated cells due to replication stress in S/G2M phase or damage in G0/G1 phase and compared to asynchronous responses. **(B)** STRING network highlighting functional and annotated relationships between the genes presented in (A).

HMGB2 (high mobility group box 2) is a master regulator of senescence that regulates transcription of SASP and formation of senescence-associated heterochromatin foci (Aird *et al.*, 2016). HMGB2 is also a DNA sensor and a regulator of innate immune responses (Yanai *et al.*, 2009; Kawasaki, Kawai and Akira, 2011). HMGB2 is typically downregulated upon entry into senescence and its knockdown is sufficient to trigger the senescent program (Zirkel *et al.*, 2018). Indeed, HMGB2 was downregulated two-fold by the toxin compared to HQ (**Fig. 5.2A**). It was hypothesised that the toxin may be inducing downregulation of HMGB2 resulting in induction of the senescent program, which may include upregulation of the toxin induced ISG response.

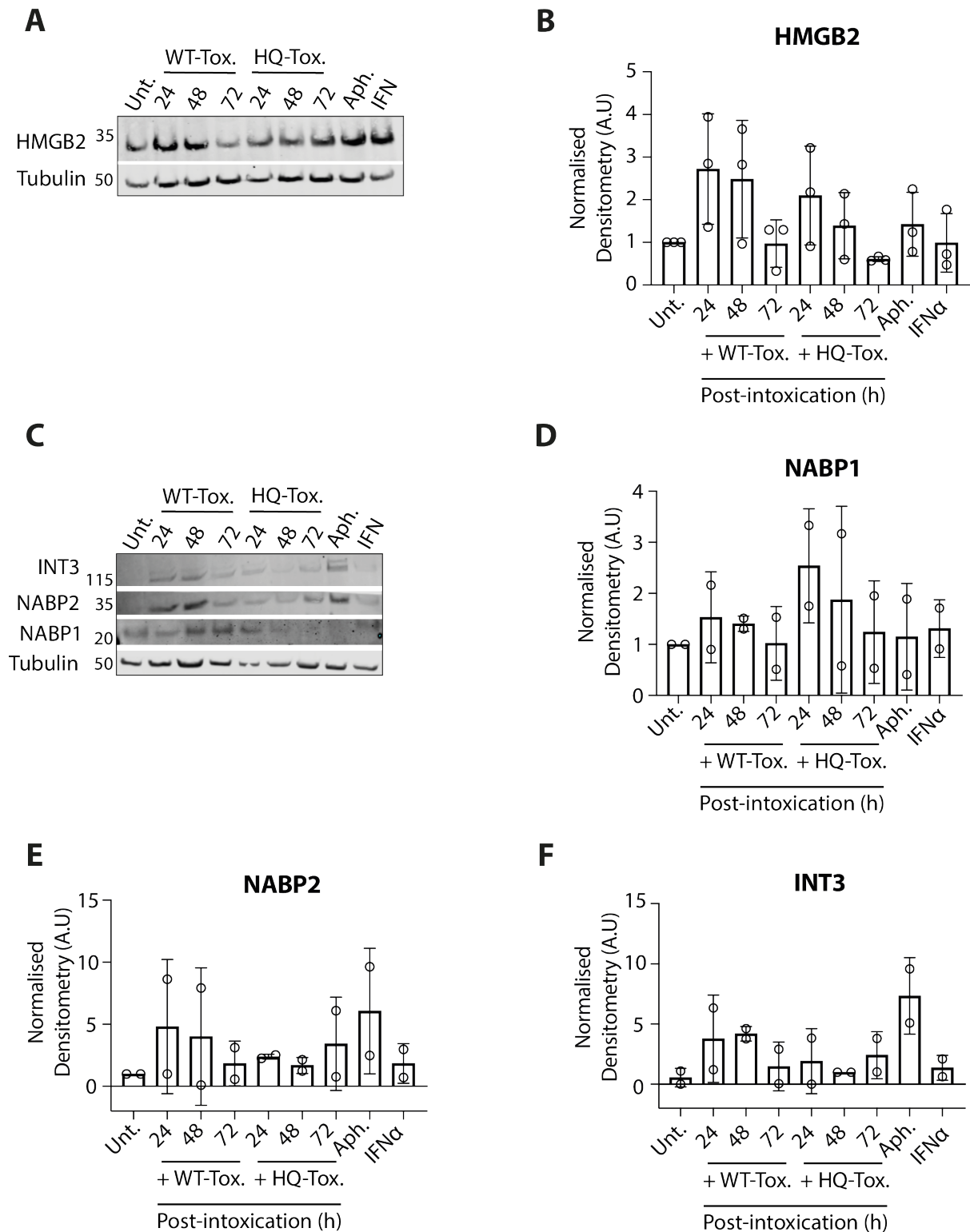


Fig. 5.3 Regulation of HMGB2 and the SOSS complex in response to the toxin

(A) Immunoblots of protein levels in HT1080s of HMGB2 24 h, 48 h and 72 h after treatment with either WT- or HQ-toxin, 24h after treatment with aphidicolin or after 72h of treatment with purified IFN α . (B) Graph shows densitometry analysis (ImageStudio) of HMGB2 relative to tubulin and normalised to untreated (3 independent immunoblots). (C) Immunoblots of protein levels in HT1080s of NABP1, NABP2 and INT3 24 h, 48 h and 72 h after treatment with either WT- or HQ-toxin, 24h after treatment with aphidicolin or after 72h of treatment with purified IFN α . (D - F) Graph shows densitometry analysis (ImageStudio) of NABP1, NABP2 and INT3 relative to tubulin and normalised to untreated (2 independent immunoblots).

Analysis of HMGB2 protein levels by immunoblotting revealed a downregulatory trend between 24-72h post-intoxication (**Fig. 5.3A**). HMGB2 was upregulated 3-fold by the toxin 24h after intoxication but by 72h had returned to untreated levels (**Fig. 5.3B**). However, this phenotype was also seen with HQ-toxin, suggesting that HMGB2 regulation was not toxin dependent though later timepoints may be required to assess any role in toxin-induced senescence.

NABP1, together with INT3 and C9Orf80, forms a heterotrimeric SBP known as the SOSS complex, with similar roles to RPA in DNA replication and repair (Huang *et al.*, 2009; Kar *et al.*, 2015). It was one of only three SBPs that were upregulated in a toxin-dependent manner including the mitochondrial helicase C10Orf2 and the telomere regulator TERF2IP. NABP1 was also upregulated two-fold in serum-starved conditions, showing it was possibly sensing SSBs in G0/G1 (**Fig. 5.2A**). A complementary SOSS complex can be formed with the NABP1 homologue NABP2, INT3 and C9Orf80, although interestingly neither NABP2 nor INT3 were significantly differentially regulated between any conditions in the microarray data (**data not shown**).

Protein levels of all three components of the SOSS complex were analysed 24-72 h post-intoxication. More intense protein bands were observed for NABP1, NABP2 and INT3 48h post-intoxication compared to HQ (**Fig. 5.3C**). INT3 and NABP2 were also upregulated by 24 h of continuous treatment with aphidicolin, but interestingly not NABP1. However, quantification revealed that these observable increases were not significant and that there was a high level of variation between replicates (**Fig. 5.3E-F**). In the case of NABP1, the antibody used was not specifically designed for immunoblotting and the data may be unreliable. NABP1, NABP2 and INT3 were assayed using immunofluorescence following a standard 24 h intoxication assay and with 24 h continuous treatment by aphidicolin as a positive control. Levels of all three proteins increased following treatment with either WT-toxin or aphidicolin compared to untreated and HQ-toxin (**Fig. 5.4A**). However, only NABP1 showed a significant increase in positive nuclei between untreated and WT-intoxication, and an increase between WT-toxin and HQ-toxin that was not significant (**Fig. 5.4B**).

There were no significant differences in NABP2 and INT3 levels between any treatments (**Fig. 5.4C-D**).

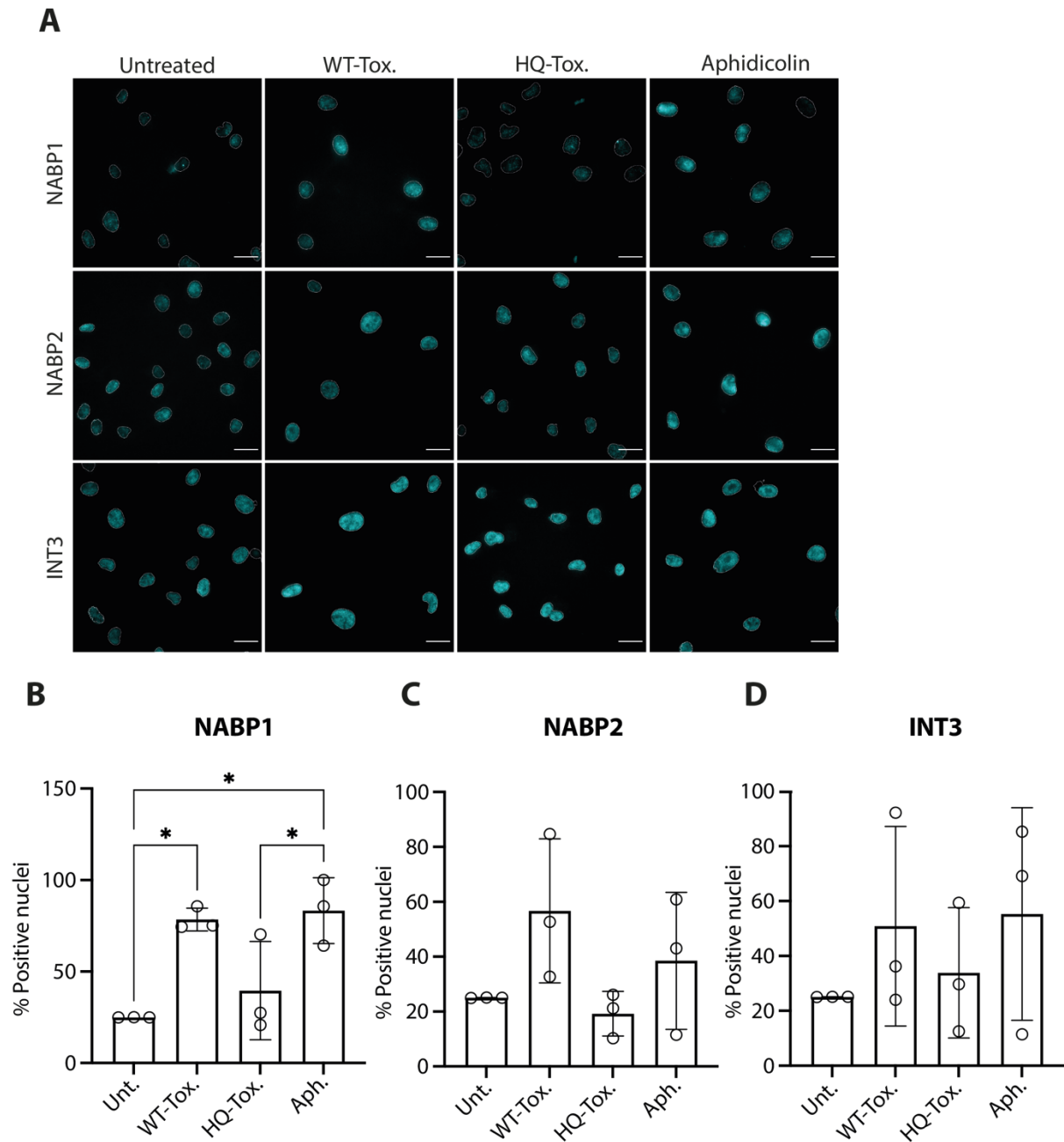


Fig. 5.4 NABP1 is upregulated in response to the toxin

(A) Immunofluorescence of NABP1, NABP2 and INT3 24h after treatment with WT-toxin, HQ-toxin and aphidicolin in HT1080 cells. Scale bars indicate 20 μ m. **(B - D)** Quantification of nuclei positive for the proteins in **(A)**. Each circle is the percentage of nuclei from three technical replicates of an independent replicate. One way ANOVA was used with Tukey's multiple comparison test. Nuclei were counted as positive if greater than the upper quartile of untreated intensity. Asterisks indicate significance. Bars indicate mean and error bars indicate SD. Nuclei indicated by DAPI outline (grey).

It was investigated whether the SOSS complex was performing a similar role to that of RPA in sequestering fragments of damaged DNA and preventing leakage, as

shown in Wolf *et al* 2016. Cells were transfected with siRNA for each component of the SOSS complex before performing a standard intoxication assay with a 72h chase. The combination of NABP1 or NABP2 siRNA transfection with WT-toxin increased ISG15 expression compared to toxin alone or toxin with control siRNA (**Fig. 5.5A**). Whereas the increase in ISG15 expression following WT-intoxication was approximately 5-fold with control siRNA, it was 8-fold for NABP1 siRNA and 6-fold for NABP2 siRNA (**Fig. 5.5B**). However, these differences were not found to be significant, although only WT-toxin with NABP1 siRNA was found to be significantly increased compared to untreated.

ISG15 was assayed following SOSS siRNA transfection using immunofluorescence. As seen with immunoblotting, transfection with siRNA for NABP1, NABP2 and INT3 followed by intoxication caused an observable increase in ISG15 levels compared to control siRNA (**Fig. 5.5C**). High levels of variability were seen between repeats, possibly because the transfection process was inducing ISG15 expression as seen in **Fig. 5.1G**. It was found that transfection with siRNA for SOSS components caused approximately 60% of nuclei to be positive for ISG15 when compared to the upper quartile of control siRNA intensity in the presence of WT-toxin (**Fig. 5.5D**). However, this increase was not significant. Together, the data show that SOSS complex components play no significant role in the toxin induced ISG response.

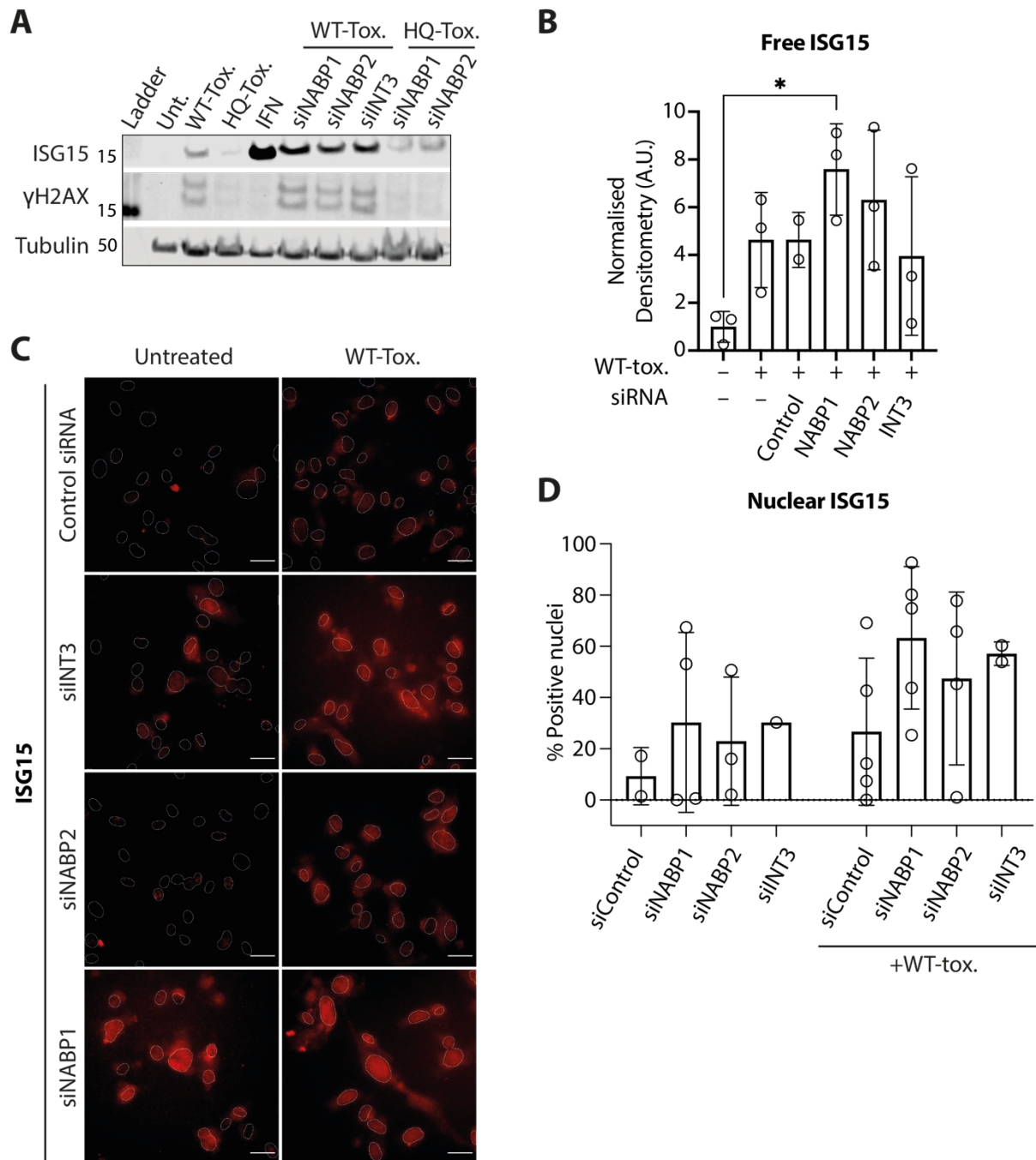


Fig. 5.5 NABP1 knockdown enhances the toxin dependent ISG15 response

(A) Immunoblots of protein levels in HT1080s of ISG15 and γ H2AX following 48h transfection with siRNA for NABP1, NABP2, INT3 or control, and 72h treatment with WT- or HQ-toxin. (B) Graph shows densitometry analysis (ImageStudio) of 15 kDa free ISG15 band relative to tubulin and normalised to untreated (minimum 2 independent immunoblots). (C) Immunofluorescence of ISG15 (red) 48h after transfection with siRNA for NABP1, NABP2, INT3 or control, and 72h treatment with WT- or HQ-toxin in HT1080 cells. (D) Quantification of ISG15-positive nuclei in (C). Nuclei were counted as positive if greater than the upper quartile of control siRNA-transfected and WT-toxin treated ISG15 intensity. Nuclei indicated by DAPI outline (grey). Scale bars indicate 20 μ m. Circles indicate technical replicates from two independent replicates.

One way ANOVA was used with Tukey's multiple comparison test. Asterisks indicate significance. Bars indicate mean and error bars indicate SD.

5.2.3 Toxin induced ISG15 is dependent on STING

It was investigated whether the toxin was activating cytosolic DNA sensing pathways. Further analysis of the microarray data, using a list of known DNA sensors summarised in the literature (Dempsey and Bowie, 2015), revealed that only two DNA sensors, IFIH1/MDA5 and PQBP1, were significantly upregulated in response to the toxin (**Fig. 5.6A**). Of particular interest was IFIH1 (IFN induced with helicase C domain 1) as it is a type-I ISG. However, there was no significant difference in IFIH1 mRNA levels in HT1080 cells between treatment for 24 h with WT- or HQ-toxin (**Fig. 5.6B**). qRT-PCR was also performed for cGAS, as it was seen to be responsible for detecting cytosolic DNA following RPA knockdown in Wolf *et al.* However, cGAS mRNA was not upregulated in a toxin-dependent manner and indeed HQ-toxin treatment was shown to significantly induce higher mRNA levels compared to WT-toxin or untreated (**Fig. 5.6C**). Furthermore, analysis of cGAS protein levels using immunoblotting following a standard intoxication assay revealed no difference between untreated, WT- and HQ-intoxicated cells (**Fig. 5.6D**).

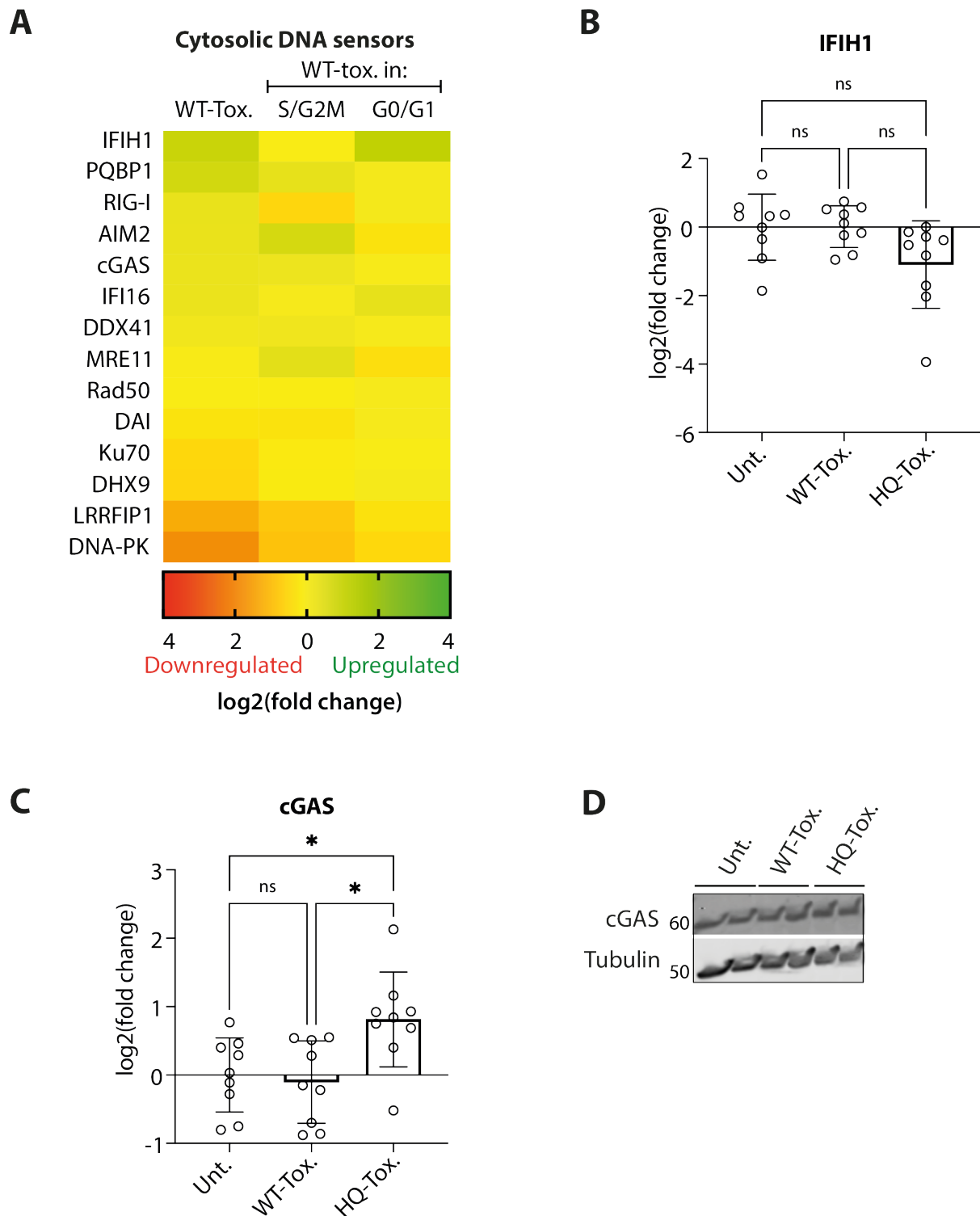


Fig. 5.6 The toxin does not directly regulate expression of cytosolic DNA sensors

(A) Heatmap shows all genes for cytosolic DNA sensing proteins detected in the microarray presented in fig. 3.4C and represents fold change 24h post-intoxication in WT- and HQ-toxin treated cells. (B - C) Quantification of mRNA levels in HT1080s of IFIH1 and cGAS compared between untreated and 24h WT- and HQ-toxin treated samples. Bars represent mean fold change of three samples (three technical replicates run for each sample). Each circle is an individual technical replicate. One way ANOVA was used with Šidák's multiple comparison test. Asterisks indicate significance. Error bars indicate SD. (D) Immunoblot of protein levels in HT1080s of cGAS 24 h after treatment with either WT- or HQ-toxin. 2 technical replicates per treatment.

However, DNA sensors would not necessarily be differentially expressed at the mRNA or protein level and could instead be constitutively expressed and post-translationally modified in response to stimulus. Therefore, activation of downstream effectors was investigated instead. STING, IRF3 and TBK1 were assayed, all of which are phosphorylated following activation of multiple DNA sensors including cGAS (**Fig. 5.7A**). Phosphorylated IRF3 could not be detected using immunoblotting and no difference was detected in levels of phosphorylated STING in response to the toxin (**Fig. 5.7B**). A slight increase of phosphorylated TBK1 (pTBK1) was observed 24, 48 and 72 h post-intoxication with WT-toxin compared to HQ-toxin, although this increase was not found to be significant at any timepoint (**Fig. 5.7C**).

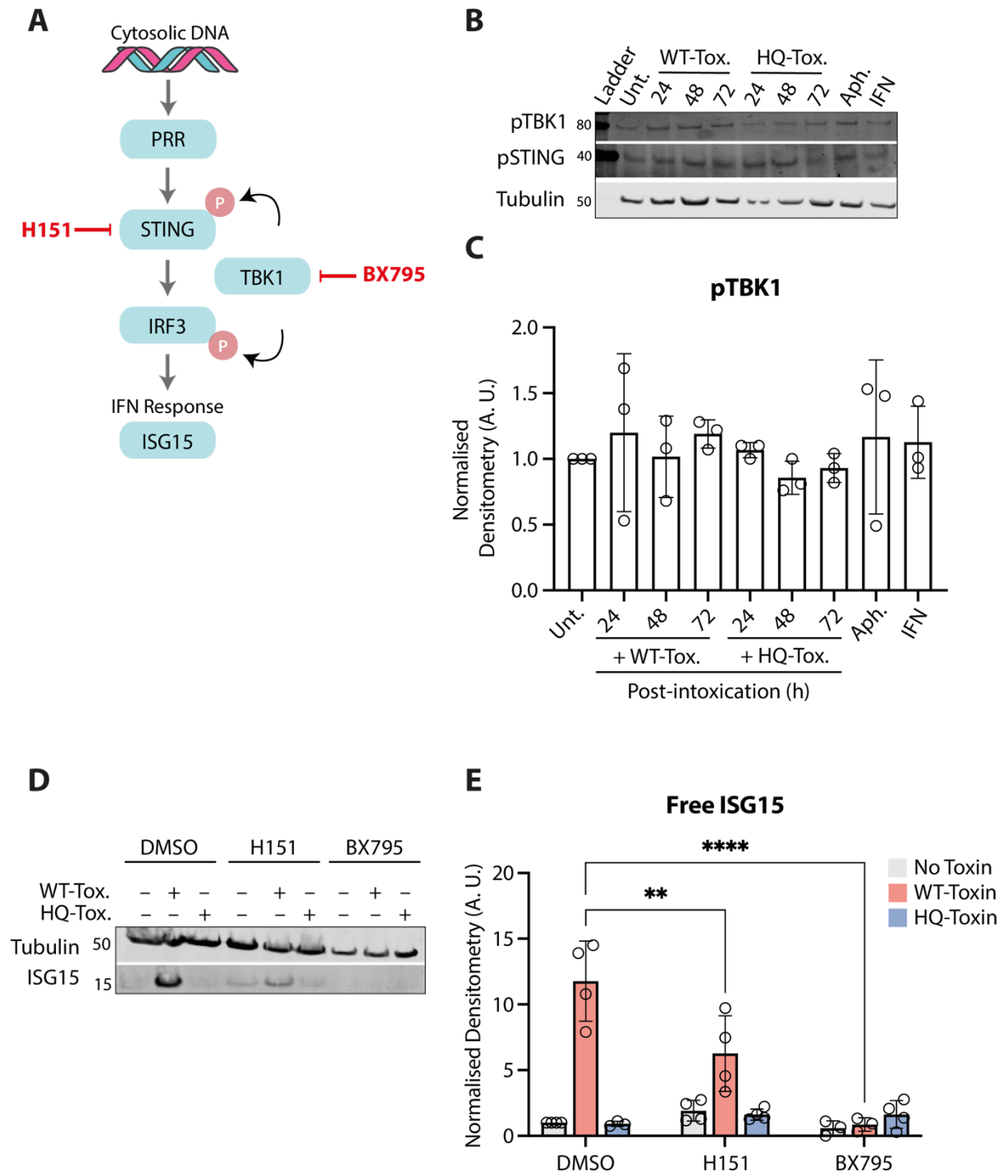


Fig. 5.7 The toxin dependent ISG15 response is dependent on STING and TBK1

(A) Schematic of the signalling pathway initiated by some PRRs following ligand binding and activation. STING is activated and phosphorylated by TBK1, resulting in phosphorylation and dimerisation of IRF3, which acts as a transcription factor for IFNs and ISGs. H151 is a STING inhibitor, and BX795 is a TBK1 inhibitor. (B) Immunoblot of protein levels in HT1080s of pTBK1 and pSTING 24 h, 48 h and 72 h after treatment with either WT- or HQ-toxin, 24h after treatment with aphidicolin or after 72h of treatment with purified IFN α . (C) Graph shows densitometry analysis (ImageStudio) of pTBK1 relative to tubulin and normalised to untreated (3 independent immunoblots). (D) Immunoblots of protein levels in HT1080s of ISG15 following 72h treatment with 4 μ g/ml H151 or 10 μ M BX795, and treatment with WT- or HQ-toxin. (E) Graph shows densitometry analysis (ImageStudio) of 15 kDa free ISG15 band relative to tubulin and normalised to untreated (4 independent immunoblots). One way ANOVA was used with Tukey's multiple comparison test. Asterisks indicate significance.

ISG15 was assayed following inhibition of STING and TBK1 by small molecule inhibitors H151 and BX795 respectively. Continual inhibition by both during a standard 72h intoxication assay reduced toxin induced ISG15 (**Fig. 5.7D**). This effect was significant in the case of both inhibitors, and indeed TBK1 inhibition by BX795 abrogated the toxin induced ISG15 response entirely (**Fig. 5.7E**). BX795-treated cells displayed stressed morphology characterised by extreme cellular elongation (**data not shown**), suggesting that the inhibitor may have been affecting other cell processes as well. Regardless, the effects of H151 STING inhibition showed that the toxin ISG response was dependent on STING.

5.3 Discussion

This chapter explored the mechanisms by which the toxin may induce an ISG response. It was hypothesised that the toxin was causing cytosolic leakage of DNA that was activating PRRs and stimulating ISG expression. Using a novel method, the *in vitro* polymerase assay, it was confirmed that the toxin was inducing SSBs in DNA. Furthermore, it was confirmed that there was a significant increase in micronuclei in intoxicated cells, indicative of genomic instability and cytosolic leakage. However, it proved too challenging to find a reliable and direct method of identifying cytosolic DNA. It was possible to show that more DNA was detected in the soluble cytosolic fraction of intoxicated cell lysates, however it is not possible to be certain that this was due to the toxin causing DNA leakage. For example, DNA damage may have weakened the integrity of the nuclear envelope, thus reducing the reliability of the fractionation process. DNA was labelled with EdU in an attempt to detect cytosolic foci, but fragments of cytosolic DNA were likely too small and

thus beyond the limits of detection, especially when the nuclear EdU signal was high enough to overwhelm less intense signals. In future, immuno-FISH using a telomere probe may be a good method to identify cytosolic DNA (Kreienkamp *et al.*, 2018).

The SBP NABP1 was found to be upregulated by the toxin. Most studies in the literature regarding NABP1 focus on its role in the heterotrimeric SOSS complex, formed of NABP1 or NABP2, INT3 and C90rf80 (Huang *et al.*, 2009). The NABP1/NABP2 complexes are complementary and the distinction between their functions remains uncertain. It has been suggested that the SOSS complex is a redundancy measure to RPA at the replication fork due to its ssDNA binding activity and ability to recruit and activate ATR (Kar *et al.*, 2015). Both NABP1 and NABP2 have been shown to cooperate to resolve replication stress, and loss of both was shown to activate P53 and IFN pathways in hematopoietic stem cells (Shi *et al.*, 2017). Interestingly, only NABP1 was seen to be significantly upregulated by the toxin in the microarray, suggesting that it had a distinct role rather than as a component of the SOSS complex. Whereas NABP2 has been shown to directly interact with the MRN complex at DSBs where it initiates homologous recombination, and to localise to stalled replication forks where it has roles in stabilisation and repair, NABP1 remains uncharacterised in comparison (Richard *et al.*, 2011; Bolderson *et al.*, 2014). Recent data has revealed a direct role for NABP1 in RPA recruitment to sites of UV-induced DNA damage (Boucher *et al.*, 2021), and it is possible that NABP1 is performing a similar cooperative role with RPA in response to the toxin.

Knockdown of components of the SOSS complex, especially NABP1, resulted in amplification of the toxin ISG15 response following intoxication. Studies have shown that RPA sequesters fragments of damaged DNA and prevents leakage into the cytosol where they act an IFN response (Wolf *et al.*, 2016). As SOSS has been suggested to have redundant functions to RPA, it is possible that SOSS, or NABP1 alone, may be preventing cytosolic DNA leakage in a similar manner. It is important to note that the increase in ISG15 was not found to be statistically significant following knockdown of NABP2 and INT3, nor was it found to be significant between WT-toxin and untreated in this experiment. Further replicates of both the

immunoblotting and immunofluorescence experiments will be needed to increase the statistical power of the analysis.

Inhibitors of STING and TBK1, which are key regulators of innate immunity, were found to abrogate the toxin ISG response. STING is both a cytosolic DNA sensor itself as well as an adaptor protein regulating signalling via other DNA sensors such as cGAS (Dempsey and Bowie, 2015). TBK1 has numerous roles beyond innate immunity, including in apoptosis, autophagy and cell proliferation (Louis, Burns and Wicks, 2018). Consistent with this, inhibition of TBK1 appeared to have other effects beyond abrogation of the toxin ISG response, as inhibited cells displayed a stressed and abnormal morphology. Furthermore, whereas inhibition of TBK1 abrogated the toxin ISG15 response, significant increases in pTBK1 were not seen between WT- and HQ-toxin treatment. The role of STING and TBK1 in response to the toxin will need further study, for example by examining toxin dependent ISG responses following siRNA mediated knockdown of STING, TBK1 or other components of DNA sensing pathways.

In summary, the toxin induces SSBs in DNA and triggers release of micronuclei. Furthermore, the toxin ISG response is dependent on STING, suggesting that cytosolic DNA sensing pathways are being activated by the toxin. Finally, the toxin ISG response can be amplified by interruption of SBP complexes which could be preventing cytosolic leakage of DNA. Having examined regulation of the toxin ISG response, the role it was playing in the wider host response was explored. As ISG15 was the most reliably and consistently expressed component of the toxin ISG response, the specific role of ISG15 was explored in greater detail.

6 The role of ISG15 in the host response to the typhoid toxin

6.1 Introduction

IFN-stimulated gene 15 (ISG15) was first identified in 1979 when researchers found that treating mouse Ehrlich ascites tumour cells with purified IFN stimulated production of mRNA for a 15 kDa protein, which they translated *in vitro* (Farrell, Broeze and Lengyel, 1979). It was not described again until five years later when the human and bovine forms were identified and correlated with a level of IFN α and IFN β stimulation sufficient to induce an antiviral state (Korant *et al.*, 1984). ISG15 expression was shown to be dose dependent on IFN concentration and to inversely correlate with vesicular stomatitis virus yield (Haas *et al.*, 1987).

Attempts to sequence the protein showed that cDNA clones for the protein could be prepared from IFN-treated human lymphoblastic cells but not untreated cells (Blomstrom *et al.*, 1986). Whilst the initial sequence was erroneous, the correct sequence was found the following year and showed that ISG15 was 168 amino acids long and had a molecular weight of 17,890 Da (Reich *et al.*, 1987). This full-length protein was found to be a precursor to the mature form of ISG15, which is formed by cleavage of 8 C-terminus amino acids to form a 17,145 Da protein (Knight *et al.*, 1988).

ISG15 was initially named ubiquitin cross-reactive protein (UCRP) as it was of sufficient sequence homology to ubiquitin to be detected by mono-ubiquitin antibodies at the time (Haas *et al.*, 1987). ISG15 is formed of two ubiquitin-like domains and has an identical C-terminus motif of LRLRGG to ubiquitin, leading to initial hypotheses that it was a ubiquitin isoform (**Fig. 6.1A-B**) (Knight *et al.*, 1988). Interestingly however, whereas ubiquitin is highly conserved between different species, ISG15 is only found in vertebrates, unlike ubiquitin which is found in most eukaryotic cells (Zhang and Zhang, 2011).

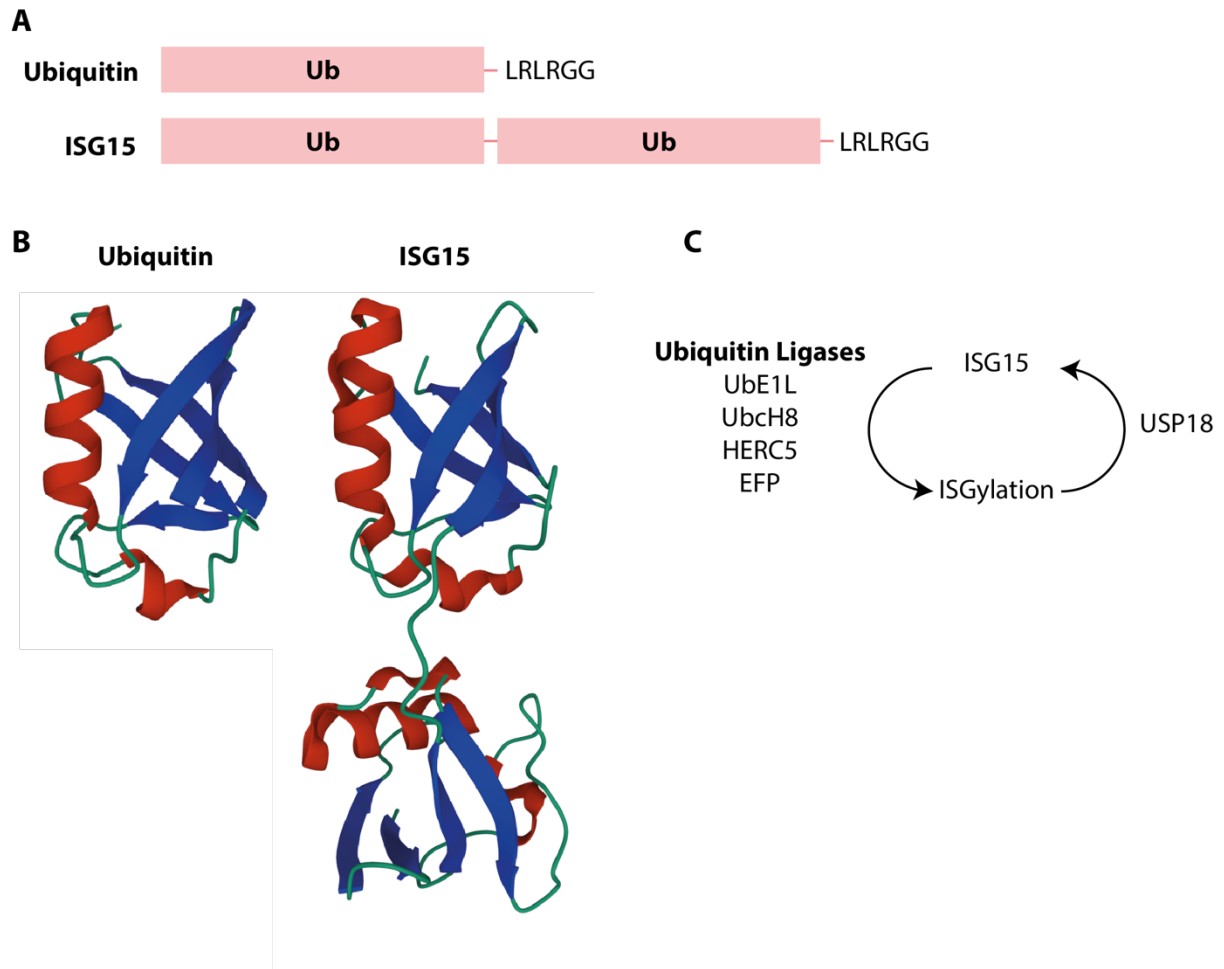


Fig. 6.1 ISG15 is a ubiquitin-like modifier that ISGylates other proteins

(A) Schematic comparing the domain structure of ISG15 to that of ubiquitin and highlighting the common LRLRGG motif. (B) The 3D structures of ubiquitin and ISG15 (Vijay-kumar, Bugg and Cook, 1987; Narasimhan *et al.*, 2005). (C) Illustration of the ISGylation pathway. Ubiquitin ligases catalyse the conjugation of ISG15 to other proteins, whereas USP18 is a specific protease that cleaves ISG15 from its target.

6.1.1 The ISGylation pathway

Much like ubiquitin, ISG15 was found to conjugate to other intracellular proteins in a process now known as ISGylation (**Fig. 6.1C**) (Loeb and Haas, 1992). Ubiquitination is a three-step process involving ubiquitin activation, conjugation and ligation using E1, E2 and E3 enzymes respectively (Pickart and Eddins, 2004). It was hypothesised by Loeb and Haas that ISGylation would be a ‘parallel pathway’ to ubiquitination, and a proteomics study in 2005 revealed that known E1, E2 and E3 ubiquitination enzymes were pulled down with ISG15 (Zhao *et al.*, 2005).

Ubiquitin E1-like protein 1 (UBE1L) is an E1 activating enzyme for ISG15 and was found to be inhibited by the NS1B protein of influenza B (Yuan and Krug, 2001).

UbcH8 and UbcH6 were identified as ISGylation E2 enzymes (Kim *et al.*, 2004; Zhao *et al.*, 2004; Takeuchi *et al.*, 2005). E3 ligases include HERC5 (HECT E3 ligase) (Dastur *et al.*, 2006; Takeuchi, Inoue and Yokosawa, 2006; Wong *et al.*, 2006) and EFP (oestrogen-responsive finger protein) (Zou and Zhang, 2006) in humans, as well as HERC6 in mice (Ketscher *et al.*, 2012; Oudshoorn *et al.*, 2012). Several of these studies found that the ISGylation machinery was also induced by IFN.

Surprisingly, it was not until 10 years after the process of ISGylation was discovered that the first ISGylated substrate was found. Serpin 2A was shown to be upregulated in macrophages following infection with *Mycobacterium bovis* bacillus Calmette-Guérin (BCG), *Salmonella* Typhimurium and *Listeria monocytogenes* and indeed ISGylated conjugates were found following incubation with bacterial products (Hamerman *et al.*, 2002). This was followed by the discovery of ISGylation of signal transducers such as C γ 1, JAK1, ERK1 and STAT1, in the context of which ISGylation appeared to have a regulatory role rather than marking proteins for proteasomal degradation like ubiquitin (Malakhov *et al.*, 2003). The use of high throughput proteomics massively increased the known pool of ISGylation substrates. Mass spectrometry of NiNTA purified His-tagged ISG15 revealed 158 target proteins with a wide range of functions including antiviral activity, chromatin remodelling, mRNA splicing, translation, cytoskeletal organisation and stress responses (Zhao *et al.*, 2005). More recent proteomic analysis revealed 930 ISGylated sites on 434 proteins in response to *L. monocytogenes* infection, including modification of factors involved in autophagy (Y. Zhang *et al.*, 2019).

The process of ISGylation is carefully regulated. Ubiquitin specific protease 18 (USP18) was shown to be an ISG15-specific protease and found to be IFN-inducible (Malakhov *et al.*, 2002). USP18 is specific to ISG15 based on a small hydrophobic patch within the interaction site (Basters *et al.*, 2017). Interestingly, USP18 does not solely act as a ISG15-protease but also directly binds to the IFN receptor and negatively regulates IFN signalling in a STAT2 dependent process (Malakhova *et al.*, 2006; Arimoto *et al.*, 2017). Furthermore, USP18-deficient mice die and are not rescued by excess ISG15, showing that USP18 has roles beyond ISG15 deconjugation (Knobeloch *et al.*, 2005).

ISG15 does not appear to mark proteins for degradation like ubiquitin, but it does competitively conjugate to ubiquitin-binding sites and in the process interfere with ubiquitin-dependent proteasomal degradation (Liu, Xiao-Ling and Hassel, 2003; Desai *et al.*, 2006). Furthermore, ISG15 can form mixed chains with ubiquitin, which also negatively regulates ubiquitin-dependent proteasomal degradation (Fan *et al.*, 2015).

6.1.2 Free ISG15

As well as functioning as an adduct for regulation of other proteins, ISG15 has also been shown to act freely and is secreted as a cytokine. ISG15 was detected in conditioned media from IFN β -treated monocytes and lymphocytes (Knight and Cordova, 1991), and detected in healthy human serum following IFN treatment (D’Cunha, Ramanujam, *et al.*, 1996). Free ISG15 was seen to induce IFN γ secretion in CD3⁺ cells (Recht, Borden and Knight, 1991) and has been linked to natural killer T cell proliferation (D’Cunha, Knight, *et al.*, 1996) dendritic cell maturation (Neves *et al.*, 2005) and as a chemotactic factor for neutrophils (Owhashi *et al.*, 2003). Regulation of the ratio of free ISG15 to ISGylated ISG15 is cell-type dependent (Tecalco Cruz and Mejía-Barreto, 2017).

6.1.3 Antiviral Functions of ISG15

The function of ISG15 as an antiviral molecule is well established in the literature and has been extensively reviewed (Morales and Lenschow, 2013; Hermann and Bogunovic, 2017; Perng and Lenschow, 2018). HERC5, the ISG15 E3 ligase, is associated with the polyribosome, meaning that it is primarily newly synthesised proteins that are targeted for ISGylation. In a virally infected cell the majority of newly synthesised proteins will be viral proteins, meaning that ISG15 is able to preferentially ISGylate viral proteins (Durfee *et al.*, 2010). ISGylation of viral proteins can disrupt interaction of viral proteins with host pathways or prevent formation of oligomeric viral protein structures, therefore interrupting viral replication (Perng and Lenschow, 2018). Examples of the antiviral effects of ISG15 include activity against

influenza, herpes and Sindbis virus (Lenschow *et al.*, 2005, 2007; Giannakopoulos *et al.*, 2009).

ISG15 can regulate host responses and induce an antiviral state in cells. For example, ISGylation has been shown to have a role in mitochondrial dysfunction and oxidative phosphorylation in macrophages infected with vaccinia virus, reducing viral titre (Baldanta *et al.*, 2017). ISG15 enhances viral antigen processing and MHC class I antigen presentation (Held *et al.*, 2021). ISG15 can also inhibit translation of viral proteins. ISGylation was shown to activate the ds-RNA dependent protein kinase (PKR), which inhibits translation by phosphorylation of eIF2 α in response to viral infection (Okumura *et al.*, 2013). ISGylation of mRNA-binding 4EHP allows it outcompete the translation initiation factor eIF4E when binding 5' mRNA caps, thus inhibiting translation (Okumura, Zou and Zhang, 2007).

Many of the antiviral roles of ISG15 are dependent on its role ISGylating other proteins, and indeed mice lacking the conjugating UBE1L enzyme showed increased susceptibility to influenza B infection (Lai *et al.*, 2009). However, conjugation is not essential for viral protection in some contexts, as ISG15 was found to be essential to the control of Chikungunya virus infection in both the presence and absence of UBE1L (Werneke *et al.*, 2011). Interestingly, clinical studies of patients with ISG15 deficiency revealed that ISG15 plays a redundant role in antiviral immunity in humans (Bogunovic *et al.*, 2012).

6.1.4 Role of ISG15 in non-viral infections

Upregulation of ISG15 by bacterial PAMPs was found several decades ago (Li *et al.*, 2001), but until recently the role of ISG15 in response to non-viral pathogens was not clear. Recent studies have shed light on the roles of ISG15 in response to bacterial pathogens including *S. Typhimurium*, *L. monocytogenes*, *M. tuberculosis* and fungal pathogens including *Candida albicans* (Perng and Lenschow, 2018).

Mice with a loss of function mutation in the deconjugating enzyme USP18 showed increased susceptibility to *S. Typhimurium* infection. However, this found to be due to the role of USP18 as an inhibitor of IFN regulation, rather than its role as a

deISGylase, as ISG15 knockout had no effect on survival or bacterial burden either *in vivo* or *in vitro* (Dauphinee *et al.*, 2014; Radoshevich *et al.*, 2015).

Data on the role of ISG15 in *M. tuberculosis* infection is conflicted. One study reported that ISG15-deficient mice were susceptible to infection, suffering from increased lethality after 150 days (Bogunovic *et al.*, 2012). The study went on to show clinical data revealing that ISG15 deficient patients are susceptible to mycobacterial infection. However, a separate study found no difference in lethality in mice and showed that ISG15 knockout mice had reduced bacterial burden in their spleens and lungs at acute (7 day) and chronic (77 day) phases of infection, suggesting that ISG15 was having a detrimental effect (Kimmey *et al.*, 2017).

ISG15 was shown to have a host defensive role against *L. monocytogenes* infection *in vivo* and *in vitro*, with ISG15 deficiency resulting in increased bacterial burden. The role of ISG15 was protective in a conjugation-dependent manner that required activation of cytosolic DNA sensing processes involving STING, TBK1 and IRF-3 and -7, but was type-I IFN independent. The study further revealed that infection triggered ISGylation of components of secretory pathways and modulation of cytokine release (Radoshevich *et al.*, 2015).

ISG15 was found to be upregulated, along with the ISGylation machinery, by *C. albicans* infection. Knockdown of ISG15 increased the severity of keratitis in mice, suggesting that ISG15 again had a defensive role (Dong *et al.*, 2017).

6.1.5 ISG15 in the DDR

ISG15 has been shown to be induced in response to different genotoxic agents such as camptothecin, doxorubicin and UV radiation. Recent studies have shown that ISG15 plays a role in response to genotoxic stress by ISGylating transcription factors controlling cell fate such as P53 and the P53-related p63 isotype $\Delta Np63\alpha$, as well as key components of the replisome such as PCNA (Jeon, Park and Chung, 2017).

ISGylation of PCNA was found to prevent translesion DNA synthesis (TLS) and hence reduce mutagenesis. Polymerase- η is recruited by ubiquitinated PCNA

following DNA damage, which can continue DNA synthesis despite the presence of breaks. ISGylation of PCNA stimulated the release Polymerase- η , terminating TLS and thus preventing error-prone DNA replication (Park *et al.*, 2014).

Another study indicated that non-covalent localisation of ISG15 at replication forks in complex with PCNA leads to conjugation-independent interaction with the helicase RECQ1, promoting replication fork restart after stalling and causing replication stress and chromosomal breakage. This led to sensitisation of cells treated with chemotherapeutic drugs (Raso *et al.*, 2020).

ISGylation of $\Delta Np63\alpha$, which inhibits P53 transcription, triggers its cleavage by caspase-2 and hence prevents tumorigenesis (Jeon *et al.*, 2012). ISG15 and indeed the ISGylation machinery components UBE1L, UBCH8 and EFP were shown to have P53-response elements and to be activated in a DNA damage dependent manner by P53. Furthermore, ISG15 was shown to ISGylate P53 itself and enhance P53 binding to its target promoters, including its own promoter. This positive feedback loop was necessary for prevention of excessive cell growth and tumorigenesis (Park *et al.*, 2016). A further role of ISG15 in tumorigenesis was shown by ISGylation of the tumour suppressor PTEN, and that regulation and stability of PTEN was dependent upon USP18 activity (Mustachio *et al.*, 2017). ISG15 and USP18 have been shown to induce apoptosis in cancer cells by suppression of the NF- κ B pathway (Mao *et al.*, 2016).

6.2 Results

The toxin has been shown to promote *Salmonella* infection (Ibler *et al.*, 2019), and *S. Typhi* infection has also been shown to increase the likelihood of gallbladder cancer (Scanu *et al.*, 2015). ISG15 has been shown to have roles in response to bacterial infection and regulation of oncogenesis. Therefore, potential roles for ISG15 in response to the toxin were investigated in the context of both *Salmonella* infection and development of oncogenic phenotypes.

6.2.1 ISG15 is upregulated by *Salmonella* Javiana infection

It was first investigated whether ISG15 was upregulated by infection with *Salmonella*. For this, four strains of *Salmonella* were used including the NTS serovar *S. Typhimurium* 19 (ST19), iNTS serovar *S. Typhimurium* 313 (ST313), toxigenic wild-type *S. Javiana* (*S. J.*^{WT}) and mutant non-toxigenic *S. Javiana* (*S. J.*^{ΔCdtB}). *S. Javiana* encodes the Javiana toxin with an identical CdtB subunit to the typhoid toxin, and thus was used as a hazard group 2 (HG2) model for *S. Typhi*, which is HG3 and requires level 3 containment. Javiana toxin has been shown to cause a similar DNA damage phenotype to the typhoid toxin of *S. Typhi* (R. A. Miller and Wiedmann, 2016). As ISG15 was strongly upregulated 72 h post-intoxication with purified toxin, ISG15 was assayed using immunofluorescence in HT1080s 72 h after infection with an MOI of 10. The intracellular presence of all four serovars of *Salmonella* was confirmed (**Fig. 6.2A**). ISG15 was not significantly upregulated by infection with any of the four serovars after 72 h, although it was slightly elevated by *Javiana*^{WT}, *Javiana*^{ΔCdtB} and ST19 compared to untreated (**Fig. 6.2B**). However, *Javiana*^{WT} infection did cause a significant reduction in EdU positive cells compared to untreated (**Fig. 6.2C**). None of the other serovars caused a significant reduction in EdU, showing that *Javiana*^{WT} was likely causing cell cycle arrest through the action of the toxin.

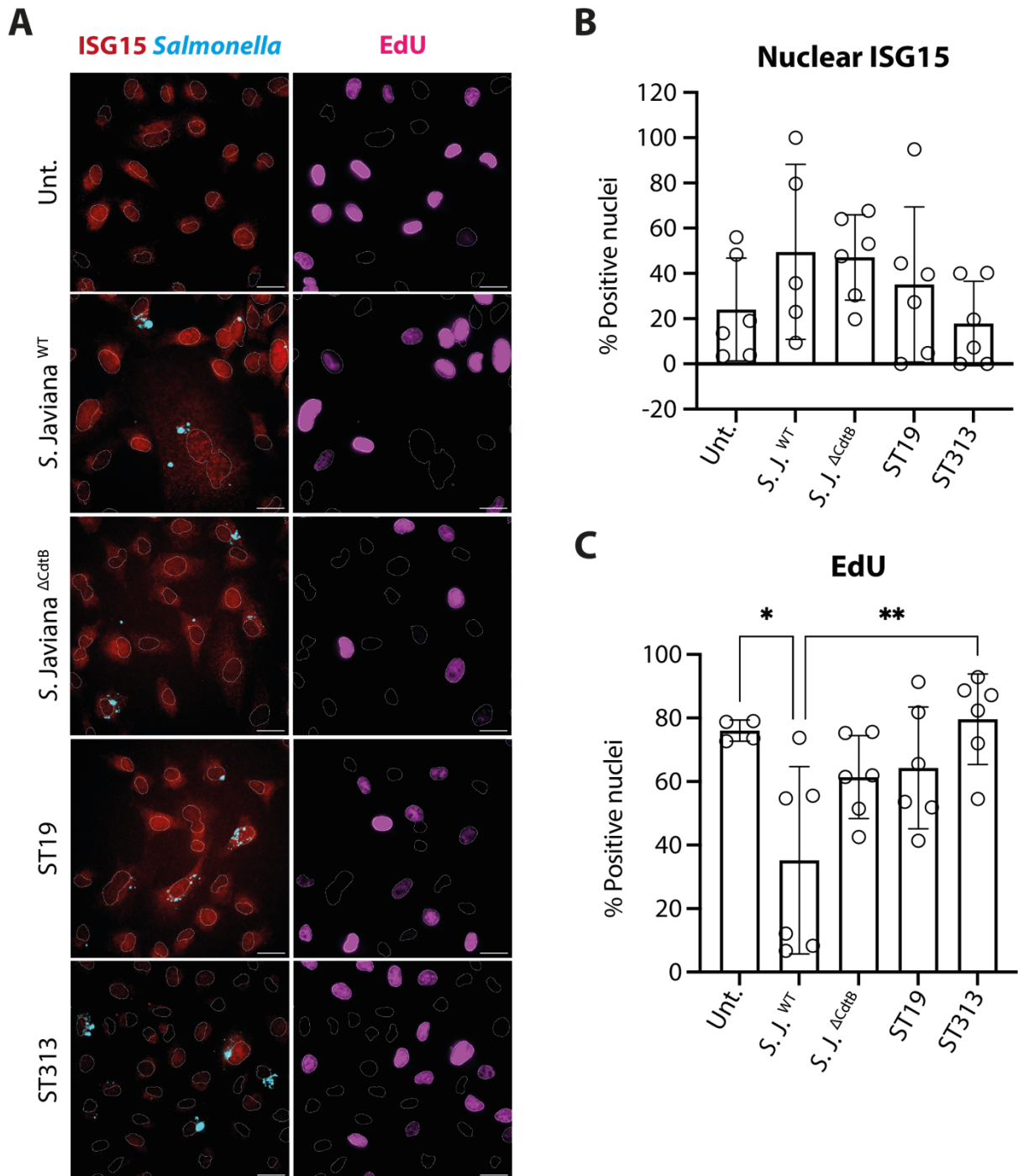


Fig. 6.2 **Salmonella Javiana** infection causes cell cycle arrest

(A) Immunofluorescence of ISG15 (red), Salmonella (cyan) and EdU (magenta) in HT1080 cells 72h after infection with ST19, ST313, *S. Javiana*^{WT} or *S. Javiana*^{ΔCdtB}. Nuclei indicated by DAPI outline (grey). Scale bars indicate 10 μ m. (B) Quantification of nuclei positive for ISG15 in (A). (C) Quantification of nuclei positive for EdU in (A).

Each circle is a technical replicate from two independent replicates. One way ANOVA was used with Tukey's multiple comparison test. Bars indicate mean and error bars indicate SD.

To confirm that *Javiana*^{WT} was secreting the toxin and inducing a DDR, γ H2AX was assayed using immunoblotting 24h post-infection. Infection with *Javiana*^{WT} caused a strong observable increase in γ H2AX protein levels unlike ST19, ST313 and

Javiana^{ΔCdtB}, showing that the response was toxin dependent (**Fig. 6.3A**). This increase was ~12-fold compared to untreated, although this was not found to be significant to the ~5-fold increase observed with purified toxin or the ~4-fold increase with Javiana^{ΔCdtB} (**Fig. 6.3B**). However, only Javiana^{WT} was significant to untreated, unlike Javiana^{ΔCdtB}.

ISG15 was assayed at 48h and 72h post-infection and saw faint bands for ISG15 following Javiana^{WT} infection at both timepoints, however this was not comparable to the ISG15 levels observed following intoxication with purified toxin (**Fig. 6.3C-D**). Javiana^{WT} infection did appear to induce slightly more ISG15 expression compared to ST19, ST313 and Javiana^{ΔCdtB}. It was investigated whether higher MOIs or longer timepoints would affect the ISG15 response. ISG15 was assayed 6 days (144 h) post-infection with Javiana^{WT} and Javiana^{ΔCdtB} with MOIs of 10, 20 and 50. A strong ISG15 upregulation was observed with Javiana^{WT} at an MOI of 10 (**Fig. 6.3E**). This was significantly higher than the response to Javiana^{ΔCdtB} which was not significant to untreated, showing that the response was toxin dependent (**Fig. 6.3F**).

Interestingly the Javiana^{WT} ISG15 response was reduced at MOIs of 20 and 50, where it was not significant to untreated. This was possibly due to higher MOIs causing cell death, which can be seen in the reduction in intensity of the tubulin bands at higher MOIs of Javiana^{WT} but not with Javiana^{ΔCdtB}. Consistent with earlier findings with WT-Tox (**Fig. 4.7A**), ISGylation was observed with IFN but not Javiana^{WT} (**Fig. 6.3E**).

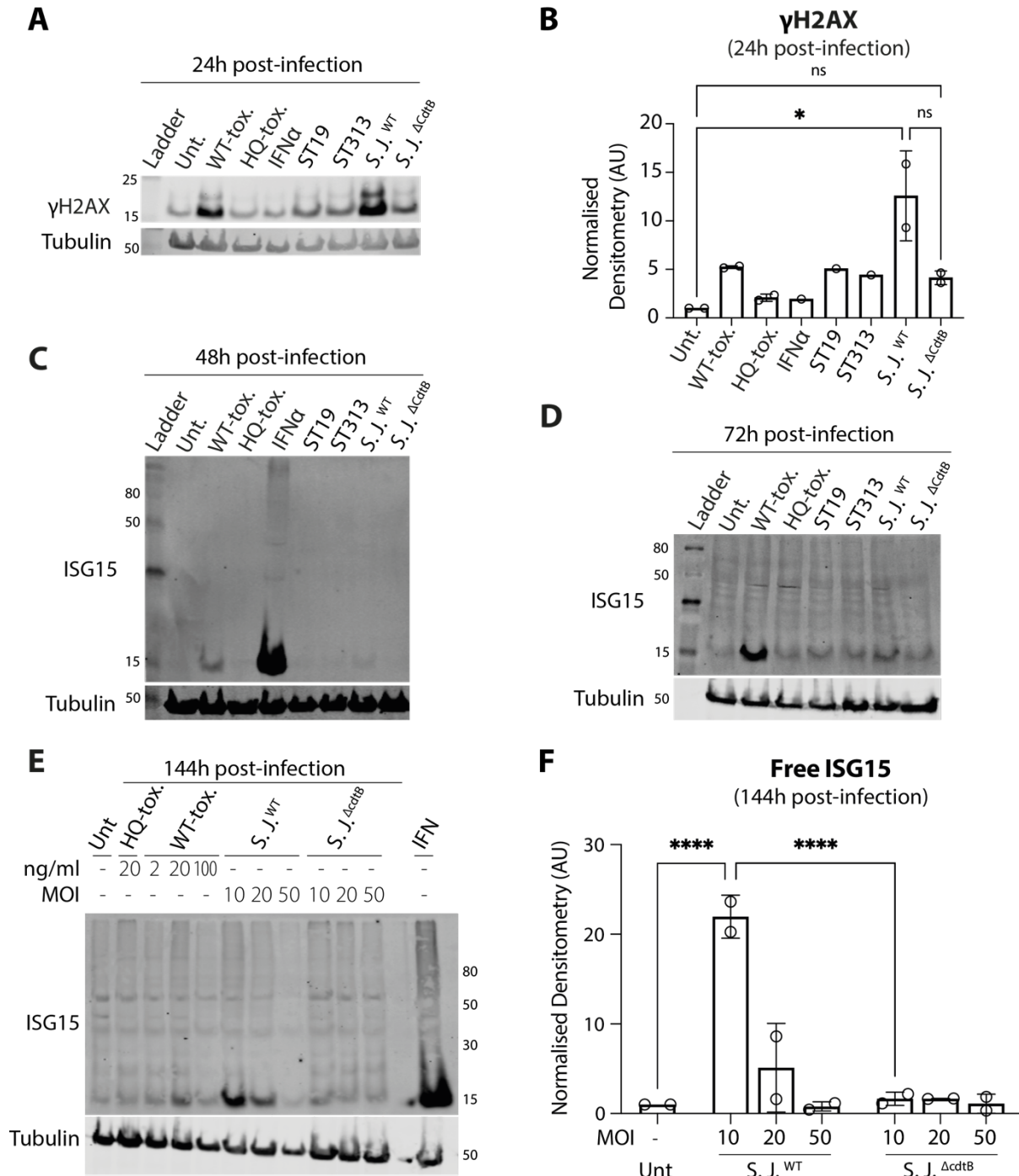


Fig. 6.3 *Salmonella* Javiana infection induces a DNA damage response and upregulates ISG15

(A) Immunoblot of protein levels of γ H2AX in HT1080s 24 h after treatment with either WT- or HQ-toxin, after 24 h continuous treatment with purified IFN α , or 24 h after infection with ST19, ST313, *S. Javiana*^{WT} or *S. Javiana* ^{Δ CdtB}. (B) Densitometry analysis (ImageStudio) of γ H2AX relative to tubulin from (A) and normalised to untreated (circles represent independent immunoblots). One way ANOVA with Tukey's multiple comparisons test. (C) Immunoblot of protein levels in HT1080s of ISG15 48 h after treatment with either WT- or HQ-toxin, after 48 h continuous treatment with purified IFN α , or 48 h after infection with ST19, ST313, *S. Javiana*^{WT} or *S. Javiana* ^{Δ CdtB}. (D) as (C) but 72 h after treatment or infection. (E) Immunoblot of protein levels in HT1080s of ISG15 144 h after treatment with 2, 20 and 100 ng/ml WT-toxin, 20 ng/ml HQ-toxin, 144 h continuous treatment with purified IFN α or 144 h after infection with MOI 10, 20 or 50 of *S. Javiana*^{WT} or *S. Javiana* ^{Δ CdtB}. (F) Densitometry analysis (ImageStudio) of 15 kDa free ISG15 band relative to tubulin from (E) and normalised to untreated (circles represent independent immunoblots). One way ANOVA with Šidák's multiple comparisons test.

Asterisks indicate significance. Bars indicate mean and error bars indicate SD.

6.2.2 ISG15 overexpression reduces *Salmonella* CFUs

Having established that ISG15 was upregulated by *Salmonella* infection in a toxin-dependent manner, role that it was playing in the host response was explored.

HT1080s were pre-treated with 72 h of continuous IFN α treatment to strongly upregulate ISG15. Both pre-treated and untreated cells were infected with *Javiana*^{WT} and *Javiana* ^{Δ CdtB} and *Salmonella* invasion assayed 24 h post-infection by culturing whole cell lysates on LB agar. At 24h, intracellular *Javiana*^{WT} had approximately doubled from 2 h post-infection, but interestingly there was no significant difference between CFUs from pre-treated and untreated cells (**Fig. 6.4A**). Intracellular *Javiana* ^{Δ CdtB} however approximately quadrupled in untreated cells, a significant increase compared to IFN α pre-treated cells where they only doubled (**Fig. 6.4B**). At 48 h post-infection, there was significantly more *Javiana*^{WT} CFUs in IFN pre-treated cells compared to untreated cells, but there was no significant difference in *Javiana* ^{Δ CdtB} CFUs between treatments.

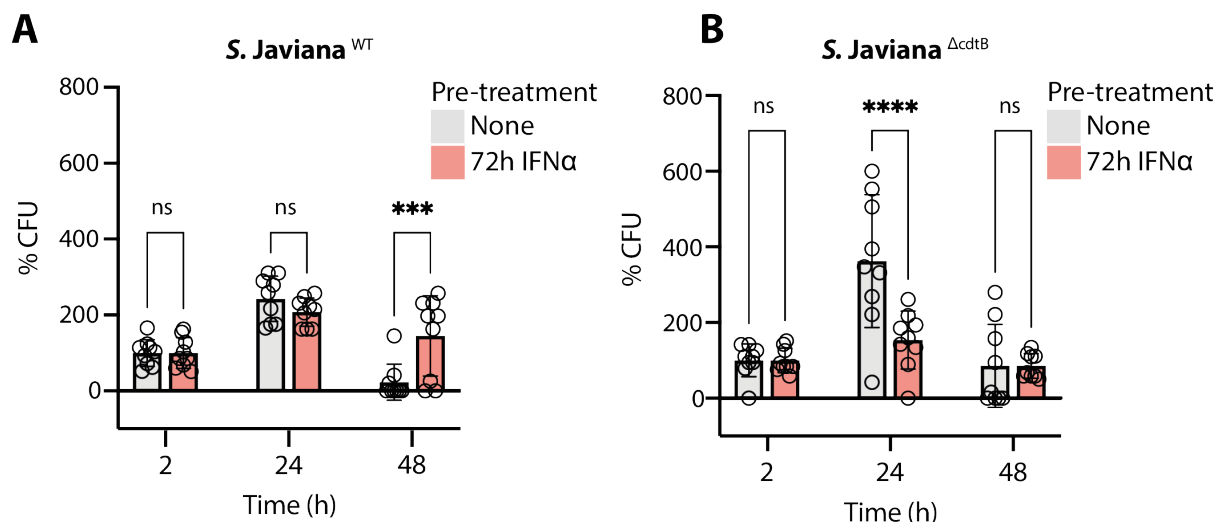


Fig. 6.4 IFN pre-treatment reduces *Salmonella* burden 24 h post-infection

(A) *S. Javiana*^{WT} CFUs 2, 24 and 48 h after infection in HT1080s with and without 72 h continuous pre-treatment with purified IFN α . CFUs are a percentage of CFUs at 2h. **(B)** as (A) but for *S. Javiana*^{ΔcdtB}.

Circles indicate individual CFU counts from one independent replicate. One way ANOVA with Šidák's multiple comparisons test. Asterisks indicate significance. Bars indicate mean and error bars indicate SD.

IFN upregulates a large array of different ISGs, meaning that the differences seen in **Fig. 6.4** cannot be attributed to ISG15 alone. To uncouple the role of ISG15 from other ISGs, HT1080s were transfected with a mammalian expression vector encoding a 5HA-tagged mouse ISG15 (pCAGGs-5HA-mISG15). It was first confirmed that the transfection did induce increased expression of 5HA-ISG15 by detecting a 20 kDa band using both ISG15 and HA antibodies (**Fig. 6.5A**). It was determined that the optimal transfection reagent was FuGENE as opposed to lipofectamine, which caused ISG15 expression. A pcDNA empty vector was transfected into cells as a control and did not lead to ISG15 induction. However, a non-specific band from the HA antibody was visible at approximately 20-25 kDa.

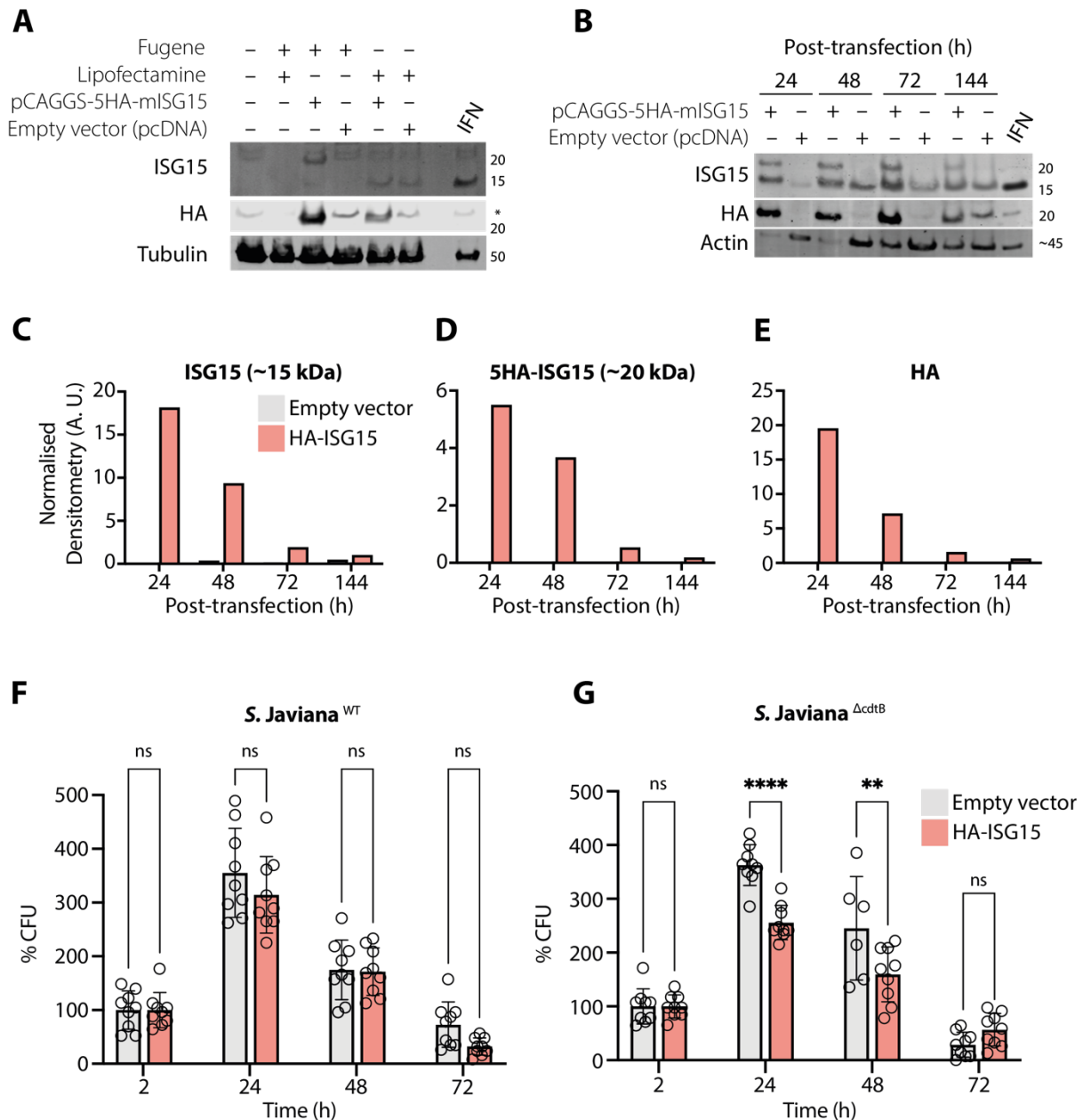


Fig. 6.5 ISG15 over-expression reduces *Salmonella* burden 24 h post-infection

(A) Immunoblot of protein levels of ISG15 and HA in HT1080s 24 h after transfection with either pCAGGS-5HA-mISG15 or empty vector pcDNA using lipofectamine or FuGENE as a transfection reagent. Non-specific band indicated by asterisk. (B) Immunoblot of protein levels of ISG15 and HA in HT1080s 24, 48, 72 and 144 h after transfection with either pCAGGS-5HA-mISG15 or empty vector pcDNA using FuGENE as a transfection reagent. (C - E) Densitometry analysis (ImageStudio) of one immunoblot showing free ISG15 (15 kDa), free 5HA-ISG15 (20 kDa) and HA (20 kDa) relative to tubulin from (B). (F) *S. Javiana*^{WT} CFUs 2, 24, 48 and 72 h after infection in HT1080s with and without 24 h transfection with pCAGGS-5HA-mISG15 or empty vector pcDNA. CFUs are a percentage of CFUs at 2h. Circles indicate individual CFU counts from one independent replicate. (G) as (F) but for *S. Javiana*^{ΔcdtB}. One way ANOVA with Šidák's multiple comparisons test. Asterisks indicate significance. Bars indicate mean and error bars indicate SD.

ISG15 and HA were assayed using immunoblotting every 24 h over a 6-day time course to determine the timepoint at which ISG15 was best expressed (Fig. 6.5B).

Endogenous ISG15 (15 kDa) and 5HA-ISG15 (20 kDa) were most strongly detected at 24 h and decreased steadily to low levels at 6-days post-transfection (**Fig. 6.5C-E**). Interestingly, it was also apparent that transfection with the pcDNA empty vector at later timepoints (48 h onwards) induced endogenous ISG15 expression, with bands visible at 15 kDa in the control lanes. Approximately 60% of ISG15 induced by the HA-ISG15 transfection was not HA-tagged, suggesting that the HA tags were being cleaved or not expressed.

Cells were transfected with 5HA-ISG15 and empty vector before infection with *Javiana*^{WT} 24 h post-transfection, when ISG15 was highest expressed. Invasion was assayed by culturing whole cell lysates on LB agar 24 h post-infection. Like previous results, there was no significant difference between 5HA-ISG15 and empty vector transfection in *Javiana*^{WT} CFU counts at any timepoint (**Fig. 6.5F**), presumably because ISG15 is present in all conditions due to the toxin. Thus, to avoid ISG15-induction by the toxin, the experiment was repeated with *Javiana*^{ΔCdtB}. ISG15 overexpression resulted in significantly less CFUs of *Javiana*^{ΔCdtB} 24h and 48h post-infection (**Fig. 6.5G**). Taken together, ISG15 overexpression caused a decrease in *Salmonella* CFUs suggesting ISG15 counteracts infection.

6.2.3 ISG15 knockout promotes oncogenic phenotypes

In order to further examine the role of ISG15 in the host response to the toxin, responses to the toxin in wild-type mouse embryonic fibroblasts (MEF^{WT}), ISG15 knockout MEFs (MEF^{ISG15^{-/-}}) and USP18 C61A MEFs (MEF^{USP18^{CA}}) were investigated, all of which were kindly donated by Lilliana Radoshevich (University of Iowa). USP18 C61A is a constitutive inactive mutant of USP18, meaning that ISGylated proteins cannot be deISGylated and build up within the cell (**Fig. 6.6A**).

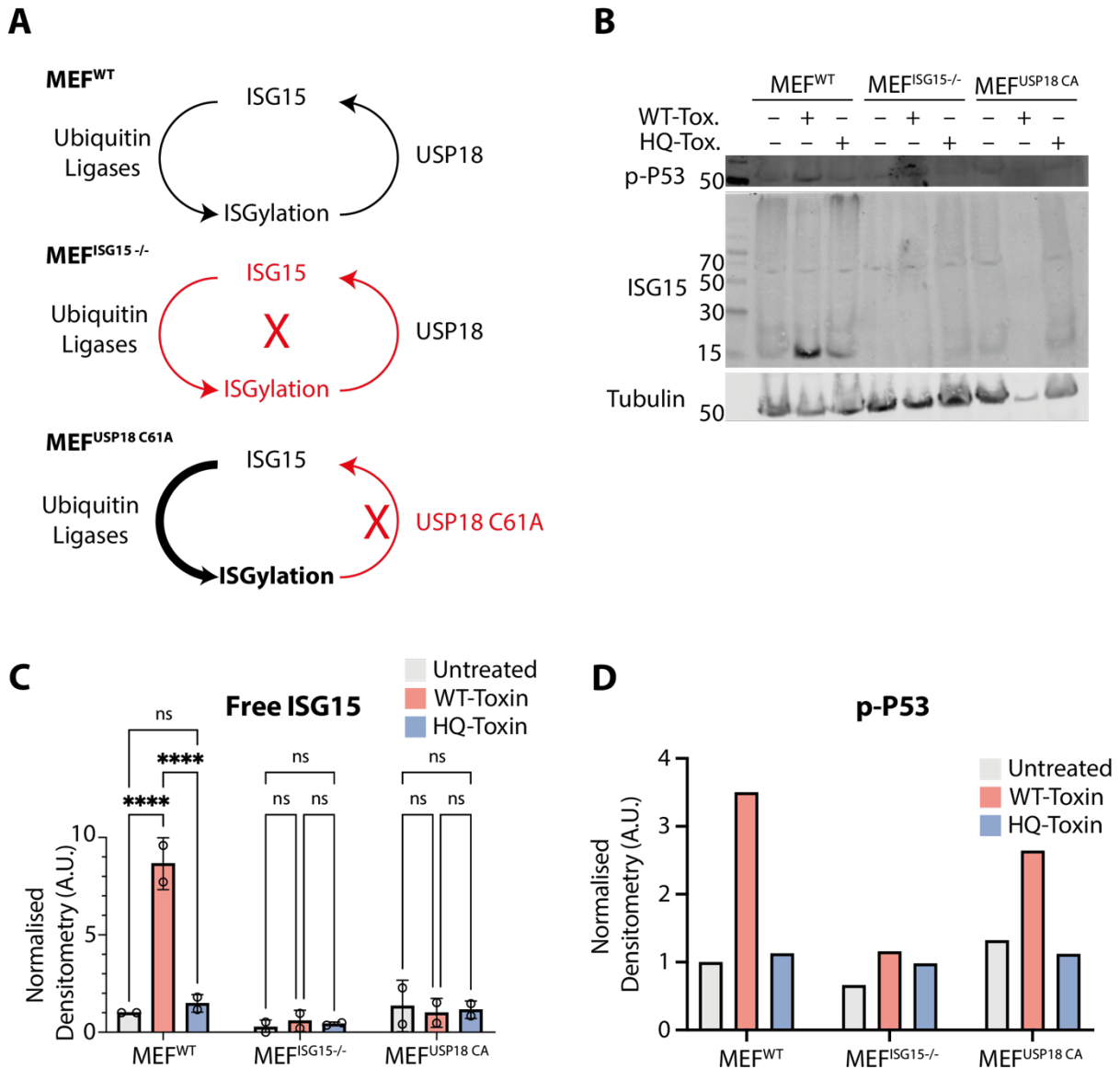


Fig. 6.6 Validation of MEF^{ISG15}^{-/-} and MEF^{USP18 C61A} cell lines

(A) Schematic of the ISGylation process and how it is modified in MEF^{WT}, MEF^{ISG15}^{-/-} and MEF^{USP18 C61A} cell lines. (B) Immunoblot of protein levels of ISG15 and phospho-P53 in MEF^{WT}, MEF^{ISG15}^{-/-} and MEF^{USP18 C61A} cells 72 h after treatment with either WT- or HQ-toxin. (C) Densitometry analysis (ImageStudio) of 15 kDa free ISG15 band relative to tubulin from (B) and normalised to untreated (circles represent independent immunoblots). One way ANOVA with Tukey's multiple comparisons test. Asterisks indicate significance. Bars indicate mean and error bars indicate SD. (D) Densitometry analysis (ImageStudio) of phospho-P53 relative to tubulin from (B) and normalised to untreated (one immunoblot).

ISG15 levels were tested within these cell lines in response to a standard intoxication assay with WT- and HQ-toxin. WT-toxin significantly induced ISG15 72 h post-intoxication compared to untreated and HQ (Fig. 6.6B-C). ISG15 was not detectable in MEF^{ISG15}^{-/-} cells aside from a faint background signal. Only low levels of ISG15 were visible in MEF^{USP18CA} cells. Interestingly, WT-toxin caused high levels of

cell death in MEF^{USP18CA} cells, which is reflected by the fainter tubulin signal in the WT-toxin lane.

As ISG15 has been shown to be induced by P53, and to promote activation of P53, levels of phosphorylated P53 (p-P53) were assayed in the MEF lines. There was no observable difference in p-P53 levels in untreated or HQ-intoxicated cells of any of the three cell lines (**Fig. 6.6B**). However, there was approximately three-fold more p-P53 in WT-intoxicated MEF^{WT} cells compared to MEF^{ISG15-/-} (**Fig. 6.6D**). P-P53 also increased approximately two-fold in WT-intoxicated MEF^{USP18CA} cells, although the reliability of this figure is uncertain due to the high levels of cell death and comparatively low sample amount. This experiment will need to be repeated before P53 activation can be reliably determined, however it does provide an initial indicator that ISG15 is involved in P53-activation in response to the toxin.

EdU was assayed using immunofluorescence to determine cell fate responses in the MEF lines 72 h after intoxication. EdU was added for 2 h pre-fixation. Untreated and HQ-intoxicated cells of all three lines appeared to be replicating normally (**Fig. 6.7A**). However, WT-toxin caused high levels of cell death in both MEF^{WT} and MEF^{USP18CA} cells, with only approximately 5% cells per field of view (FOV) compared to untreated (**Fig. 6.7B**). Of the MEF^{WT} and MEF^{USP18CA} cells that remained, there was a significant reduction in EdU positive nuclei, with approximately 20% of nuclei EdU positive following WT-intoxication compared to 40-50% in untreated and HQ-intoxicated cells (**Fig. 6.7C**). This showed that in MEF^{WT} and MEF^{USP18CA} cells the toxin was causing both cell death and cell cycle arrest.

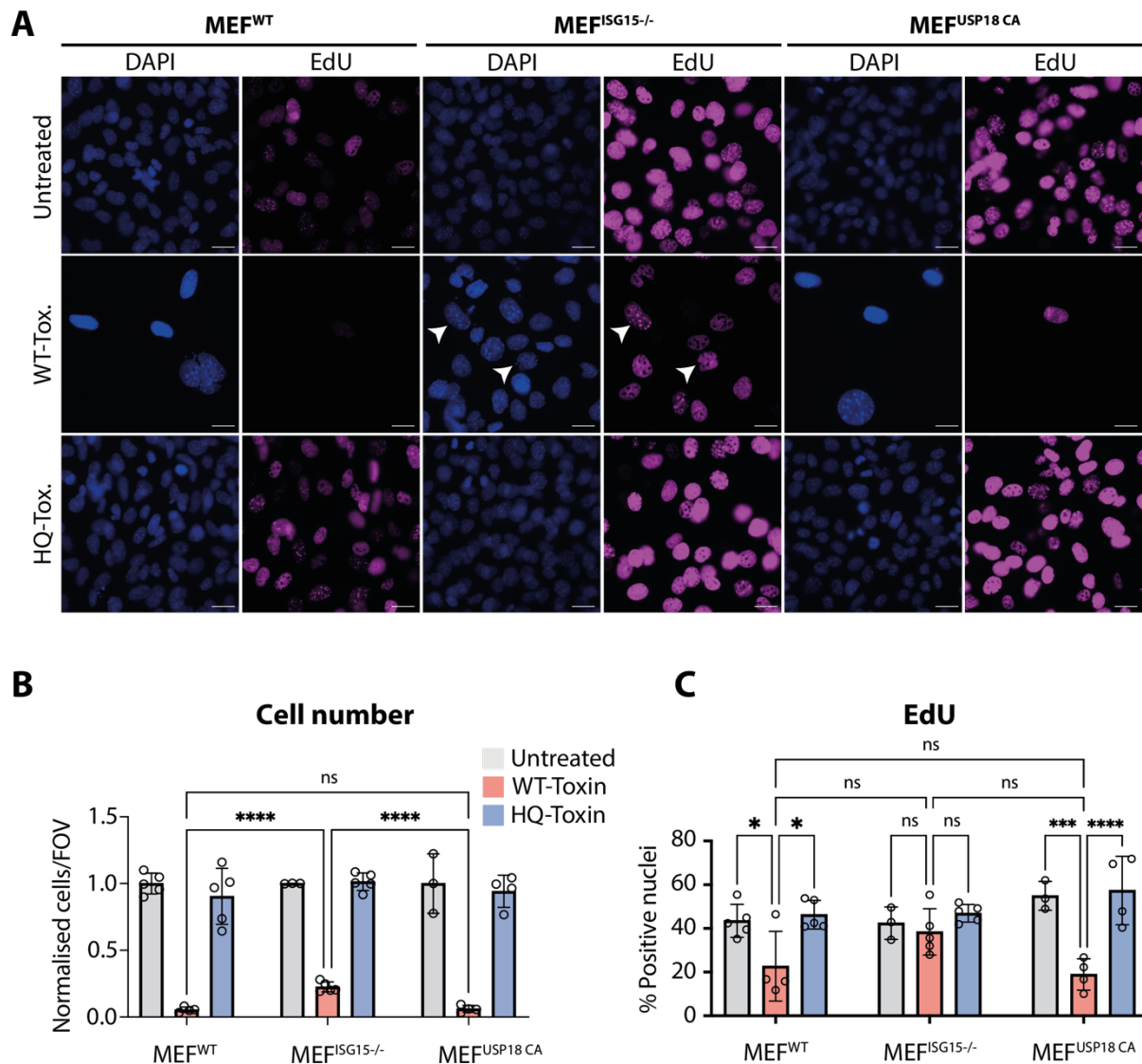


Fig. 6.7 ISG15 knockout promotes tumorigenic phenotypes in response to the toxin
(A) Immunofluorescence of DAPI (blue) and EdU (magenta) in response to WT- and HQ-toxin in MEF^{WT}, MEF^{ISG15^{-/-}} and MEF^{USP18 C61A} cells 72 h post-intoxication. Scale bars indicate 10 μ m. Micronuclei indicated with white arrows. **(B)** Quantification of cells per field of view (FOV) in (A). Cell count is normalised to untreated in each cell line. **(C)** Quantification of nuclei positive for EdU in (A). Each circle is a technical replicate from two independent replicates. One way ANOVA was used with Tukey's multiple comparison test. Bars indicate mean and error bars indicate SD.

However, in MEF^{ISG15^{-/-}} cells, less cell death and less cell cycle arrest were observed in response to the toxin. There were approximately 3-fold more cells observed per FOV in WT-intoxicated MEF^{ISG15^{-/-}} cells compared to MEF^{WT} and MEF^{USP18CA} cells (**Fig. 6.7B**). Furthermore, WT-intoxicated MEF^{ISG15^{-/-}} cells showed no significant difference in EdU-labelling compared to untreated and HQ-intoxicated cells (**Fig. 6.7C**). This showed that cell death and cell-cycle arrest by the toxin was impaired in MEF^{ISG15^{-/-}} cells relative to MEF^{WT}. Notably, several of the nuclei positive for EdU in WT-intoxicated MEF^{ISG15^{-/-}} cells contained micronuclei (**Fig. 6.7A**, indicated with

white arrows), hallmarks of genomic instability. Thus, WT-intoxicated MEF^{ISG15-/-} cells appear to replicate despite DNA damage. It was hypothesised that ISG15 was protecting against development of oncogenic phenotypes by causing cell death in damaged MEF^{WT} cells, and ISG15 knockout was allowing survival of these potentially cancerous cells.

In order to examine this further, a clonogenic assay was used to determine the ability of each cell line to replicate and form colonies in the presence of the toxin. None of the three MEF lines were able to form colonies in response to 20 ng/ml of WT-toxin (**data not shown**), so the toxin concentration was reduced to 0.2 ng/ml. WT-toxin caused a 30% reduction in MEF^{WT} and MEF^{USP18CA} colonies, but only a 15% reduction in MEF^{ISG15-/-} colonies, again showing that ISG15 knockout enabled increased survival and replication in the presence of the toxin (**Fig. 6.8A-B**).

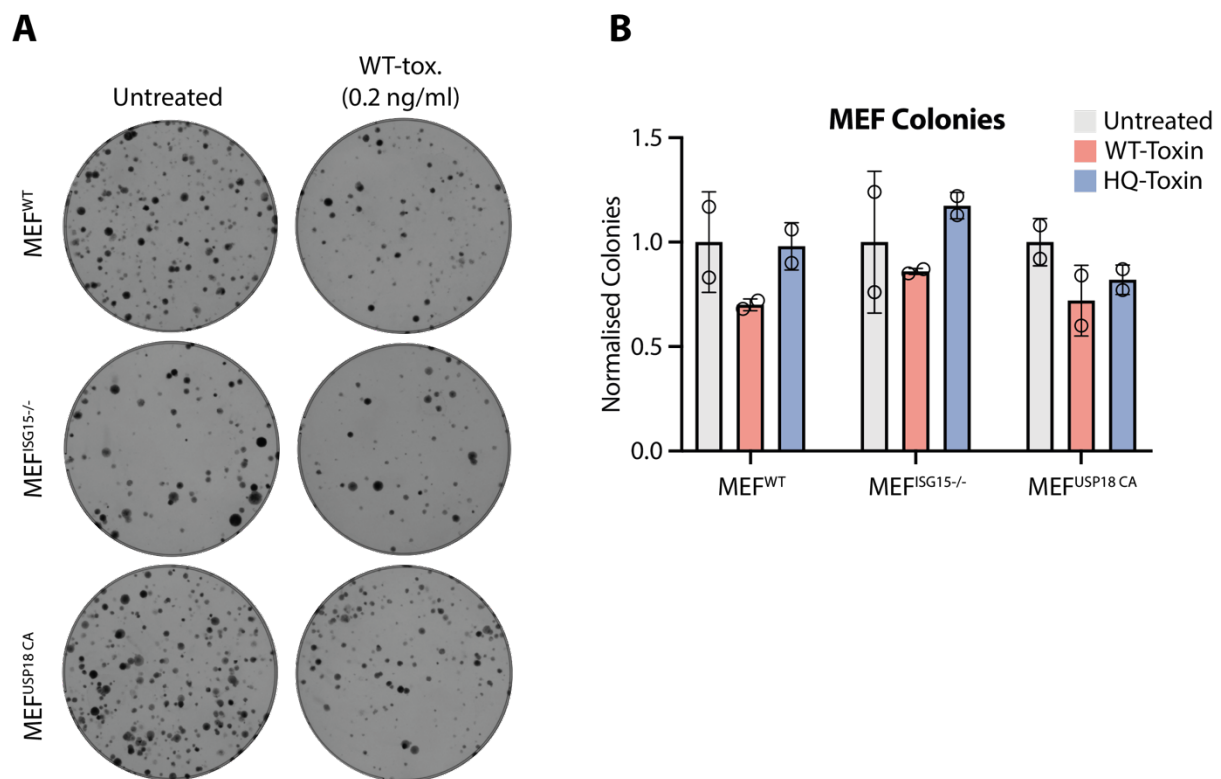


Fig. 6.8 ISG15 knockout permits greater MEF colony formation in the presence of the toxin (A) Images of all MEF^{WT}, MEF^{ISG15-/-} and MEF^{USP18 C61A} colonies in 10cm dishes 8 days after treatment with 0.2 ng/ml of WT-toxin. (B) Quantification of colony count in (A) 8 d after treatment with 0.2 ng/ml of WT-toxin or HQ-toxin. Colony counts are normalised to untreated of each cell line. Circles are technical replicates from one independent replicate.

6.3 Discussion

Both intoxication with purified toxin and infection with toxigenic *S. Javiana* was found to induce ISG15 expression. *Salmonella* infection in the absence of toxin (*S. Javiana*^{ΔCdtB}) did not induce ISG15, indicating that other PAMPs such as LPS are not responsible for the response. Whereas the concentration of purified toxin was controlled (20 ng/ml), the concentration of toxin secreted during infection was unknown. However, the ISG15 response at 144 h post-infection was comparable to the responses seen at earlier timepoints with purified toxin. The difference in time could be attributed to the time taken for *Salmonella* to replicate intracellularly and to express and secrete the toxin. However, higher γ H2AX expression was observed 24h post infection compared to 24h following intoxication, indicative of higher toxin activity even at this early timepoint. However, significant γ H2AX responses to the toxin have been seen with as low as 0.05 ng/ml of toxin (Ibler *et al.*, 2019). It is possible that *S. Javiana* infection was able to induce a higher γ H2AX response than purified toxin alone in combination of other PAMPs such as LPS. To conclusively determine the regulation of ISG15 following *S. Javiana* infection, experiments examining the ISG15 response at 24h, 48h and 72h will need to be repeated. Furthermore, it would be interesting to perform similar infection time courses with *S. Typhi*.

The timeline of ISG15 expression differs greatly from that observed in other studies, where ISGs including ISG15 are not seen until 55 days after intoxication with *E. coli* CDT (Pons *et al.*, 2021). However, Pons *et al* used a considerably lower concentration of CDT (0.25 ng/ml) than this study (20 ng/ml) and chronically exposed cells to the toxin as opposed to a 2 h pulse followed by fresh media chase. It would be interesting to replicate their experiments using the typhoid toxin, as this would possibly be a more suitable method of analysing chronic exposure to *Salmonella* and the toxin.

Interestingly, ISG15 was the strongest expressed when infecting cells with lower MOIs (10 compared to 20 or 50). It is possible that at higher MOIs, ISG15-expressing cells were killed by higher bacterial loads. Indeed, higher amounts of cell death were observed at higher MOIs.

Overexpression of ISG15 reduced *Salmonella* burden 24 h after infection, whether overexpression was caused by pre-treatment with purified IFN or transfection with a mammalian expression vector encoding ISG15. ISG15 has previously been shown to have no effect on *Salmonella* Typhimurium invasion (Radoshevich *et al.*, 2015), with no significant difference observed in *Salmonella* invasion between ISG15^{-/-} MEFs and WT MEFs. However, it is important to note that CFU measurements were taken at 4 h post-infection in Radoshevich *et al.*, as opposed to 24 h in this study. It may take a longer period of time for ISG15 to exert its role.

Interestingly, a decrease in *Salmonella* burden was only seen in Δ CdtB *Salmonella*. This could be because wild-type Javiana encodes the toxin, which would have been inducing ISG15 even in the absence of purified IFN or ISG15 transfection, albeit at lower levels. At later timepoints (48 h and 72 h), *Salmonella* burden reduced to almost zero, probably because intracellular *Salmonella* replication caused infected cells to lyse and spill *Salmonella* into media containing gentamicin where they were killed.

Beyond a function of ISG15 in protecting against infection, ISG15 knockout promotes survival of intoxicated cells with signs of genomic instability, suggesting that ISG15 could be protecting the host against tumorigenic effects of the toxin. Initial data also showed that ISG15 knockout was concomitant with a reduction in phosphorylated P53. However, further experiments will be needed to confirm these findings regarding suppression of P53-activation in ISG15^{-/-} cells and thus determine if ISG15 is indeed acting as a tumour suppressor.

Part 3: Discussion

7 Discussion

My thesis explored the host responses to the toxin with an aim of understanding the role of the toxin in *Salmonella* infection and potential links to cancer. I found that the toxin upregulates genes linked to the type-I IFN pathway, which has links to infection, senescence and cancer. One of these genes, ISG15, plays a role in the response to the toxin by both reducing the burden of *Salmonella* infection and potentially acting as a suppressor of genomic instability.

7.1 The effect of the toxin ISG response on *Salmonella* infection

The typhoid toxin facilitates chronic carriage and systemic *Salmonella* infection in mice (Del Bel Belluz *et al.*, 2016; Miller *et al.*, 2018). In a human infection challenge study, the toxin was shown to have no effect on initiating typhoid, in fact, toxin-negative *S. Typhi* increased pathology and significantly prolonged bacteraemia (Gibani *et al.*, 2019). This is consistent with mouse infection models where toxigenic *Salmonella* reduced inflammation (Miller *et al.*, 2018) and promoted host survival relative to the lethal effects of the toxin-negative strain (Del Bel Belluz *et al.*, 2016). How does this correlate with findings in this study that the toxin induces an innate immune response characterised by expression of ISGs, which typically are associated with anti-infective roles?

It is possible that the toxin ISG response is anti-inflammatory and thus protects *Salmonella*. Type-I IFN responses have been shown to have anti-inflammatory roles (Benveniste and Qin, 2007). For example, ISG15 protects hosts from excessive inflammation by negatively regulating IFN signalling (Zhang *et al.*, 2015). A recent *in vivo* study in mice showed that the typhoid toxin induced an anti-inflammatory senescent state characterised by NF κ B and P16 activation following DNA damage (Martin *et al.*, 2021). Furthermore, senescent cells are more susceptible to

Salmonella infection (Ibler *et al.*, 2019). It is interesting to speculate whether the toxin ISG response is involved in establishing an anti-inflammatory state.

7.2 What regulates the toxin ISG response?

In **chapter 4**, it was shown that the toxin led to upregulation of ISGs but not IFNs themselves. Canonically, ISG expression is triggered by expression and secretion of IFNs. However, no significant differential IFN expression was seen between WT and HQ-intoxicated cells, and qRT-PCR revealed that IFN α was significantly upregulated by both WT- and HQ-toxin compared to untreated cells. It is possible that other PAMPs in the toxin preparations such as *E.coli* LPS were inducing IFN expression. Further information will be needed to confirm the role of IFNs in response to the toxin.

In **chapter 6**, initial data suggested that the toxin was also causing P53 activation in MEFs. ISG15 and the ISGylation machinery contain P53 response elements (Park *et al.*, 2016), and thus it is possible that ISG15 is being directly induced by P53 in an IFN independent manner. ISG15 has also been shown to ISGylate and stabilise P53, creating a positive feedback loop whereby it can be phosphorylated and induce expression of more ISG15. Other ISGs detected in the microarray, such as IRF9, have also been found to be direct P53 target genes (Rivas, Aaronson and Munoz-Fontela, 2010).

It was found that STING inhibition reduced toxin dependent ISG15 induction. This is consistent with findings with other CDTs, which showed activation of a type-I IFN response in a cGAS-STING dependent manner (Pons *et al.*, 2021). As STING inhibition did not completely abrogate ISG15, it was hypothesised that the toxin was inducing ISG15 in both STING dependent and independent ways. Activation of STING canonically leads to upregulation of type-I IFNs via phosphorylation of TBK1 and IRF3, so the role of STING in the IFN independent toxin ISG response is uncertain. However, studies have shown that STING can be non-canonically activated by a signalling process involving ATM, P53 and IFI16, leading to NF κ B signalling in DNA damage conditions (Dunphy *et al.*, 2018). STING has been shown to have IFN independent roles in restricting viral infection, tumour immune evasion

and adaptive immunity (Wu *et al.*, 2020; Yamashiro *et al.*, 2020). These findings merit further investigation, including examining ISG15 levels in intoxicated cells following siRNA mediated STING depletion.

7.3 Is toxin induced ISG15 in free or conjugated form?

When assaying ISG15 using immunoblotting in both HT1080s and MEFs, the toxin was observed to induce ISG15 but did not appear to be ISGylating other proteins. Whereas IFN-treatment resulted in an intense smear of ISGylated proteins in HT1080 lysates, the same was not seen in intoxicated cells. Furthermore, intoxication did not induce ISGylation in MEFs, unlike what has been shown following IFN treatment or *Listeria* infection (Radoshevich *et al.*, 2015). ISGylation machinery (UBE1L, UbcH6/8 and HERC5) was not upregulated in a toxin dependent manner in the microarray data (**Chapter 4**). This suggests that toxin induced ISG15 is free and performing a role that does not involve conjugation to other proteins, although validation of the microarray data regarding the ISGylation machinery in response to the toxin will be necessary to confirm this.

It was hypothesised in **Chapter 6** that ISG15 promotes P53 activation by conjugation, but how does this correlate with the fact that ISGylation was not observed? It is possible that in response to the toxin, ISG15 is only targeted to a small number of specific proteins including P53. However, there is little evidence of such targeted ISGylation in the literature, and indeed studies have suggested that ISGylation is a broad process targeting all newly synthesised proteins (Durfee *et al.*, 2010). This question will need to be explored further and could be addressed by immunoprecipitation of either ISG15 or P53 following intoxication.

Free ISG15 can act as an extracellular cytokine and can be secreted from both fibroblasts and certain immune cells including neutrophils, monocytes and lymphocytes. Secreted ISG15 binds to leukocyte function-associated antigen 1 (LFA-1) and triggers IFN γ expression in NK cells and T lymphocytes (Dzimianski *et al.*, 2019). Interestingly, ISG15 was a hit in a mass spectrometry analysis within the Humphreys lab that analysed the secretome of cells treated with typhoid toxin

(ElGhazaly, unpublished). Further analysis will be needed to confirm whether ISG15 is acting as an extracellular cytokine in response to the toxin.

Free intracellular ISG15 was also shown to stabilise USP18 and prevent its degradation by S-phase kinase-associated protein 2 (SKP2) (Zhang *et al.*, 2015). This allows for accumulation of USP18 that prevents over-amplification of immune responses and autoinflammation. Human patients deficient in ISG15 display symptoms similar to interferonopathies including Aicardi-Goutières syndrome and spondyloenchondrodysplasia, characterised by autoinflammation and higher steady states of other ISG transcripts in blood samples (Zhang *et al.*, 2015). ISG15 may be activated by the host as a countermeasure to dampen inflammatory responses to the toxin.

ISG15 and USP18 have been shown to exist in a dynamic equilibrium with SKP2, with deregulation of either resulting in cell cycle arrest (Vuillier *et al.*, 2019). It is therefore possible that increased expression of ISG15 is inducing toxin dependent cell cycle arrest.

Free ISG15 has also been shown to interact non-covalently with DNA replication machinery. ISG15 forms a complex with PCNA and DNA at the replication fork, where it accelerates fork progression and induces chromosomal breakage (Raso *et al.*, 2020). The authors suggested that this process is controlled by the dynamic ratio of free to conjugated ISG15. The pool of intracellular ISG15 is limited by its constant conjugation by the ISGylation machinery, and it is only when this process is uncoupled, for example by infection, that such detrimental effects occur. It is possible that increased levels of ISG15 triggered by toxin activity exacerbate the replication stress response initiated by the toxin, leading to increased genomic instability and senescence. This could explain how the typhoid toxin can trigger a potent DDR despite having attenuated nuclease activity compared to bovine DNase I (Elwell *et al.*, 2001).

7.4 The role of ISG15 in *Salmonella* infection

Overexpression of ISG15 reduced *Salmonella* CFUs 24h post-infection, suggesting that ISG15 is performing a host defensive role. However, the exact mechanism by which ISG15 is protecting the host against *Salmonella* infection is uncertain. In response to viral infection, ISG15 directly ISGylates viral proteins to interrupt the viral life cycle (Perng and Lenschow, 2018). However, a recent review of proteomic studies that have identified ISGylation targets in innate immune responses did not find evidence of direct ISGylation of bacterial effectors (Thery, Eggermont and Impens, 2021). Nonetheless, it remains possible that ISG15 is modulating the functions of *Salmonella* effectors in a similar manner to ubiquitin. For example, the *Salmonella* Type III effector SopB has been shown to be ubiquitinated by the host, thus modulating its enzymatic function (Knodler *et al.*, 2009). It would be interesting to pull down ISG15 and analyse, by specific immunoblotting or a more non-biased approach such as mass spectrometry, whether there was evidence of ISGylation of *Salmonella* effectors.

ISG15 may be ISGylating other host proteins and promoting expression of antibacterial effectors. For example, in the case of *Listeria* infection, increased ISGylation of Golgi and ER proteins promotes secretion of cytokines that counteract infection (Radoshevich *et al.*, 2015; Y. Zhang *et al.*, 2019). However as previously discussed, there is little evidence of toxin induced ISGylation. Alternatively, ISG15 could be being secreted as a cytokine, which has been shown to trigger IFN γ release and counteract *Mycobacterium* infection (Bogunovic *et al.*, 2012). However, IFN γ is predominantly secreted by NK cells and T lymphocytes, so it unlikely an antibacterial effect via IFN γ secretion would be seen in the context of HT1080 fibrosarcoma cells (Schoenborn and Wilson, 2007). Finally, it is possible that ISG15 may be preventing bacterial growth via modulation of P53. Data in **chapter 6** showed that levels of P53 were increased in WT MEFs compared to ISG15^{-/-} MEFs. P53 has been shown to suppress cell metabolism and thus inhibit growth of *Chlamydia*, another intracellular bacteria (Siegl *et al.*, 2014). It is possible that ISG15 is increasing P53 levels and thus preventing *Salmonella* replication in a similar

manner. However, further work will be needed to determine how ISG15 is exerting an antibacterial role in response to *Salmonella* infection.

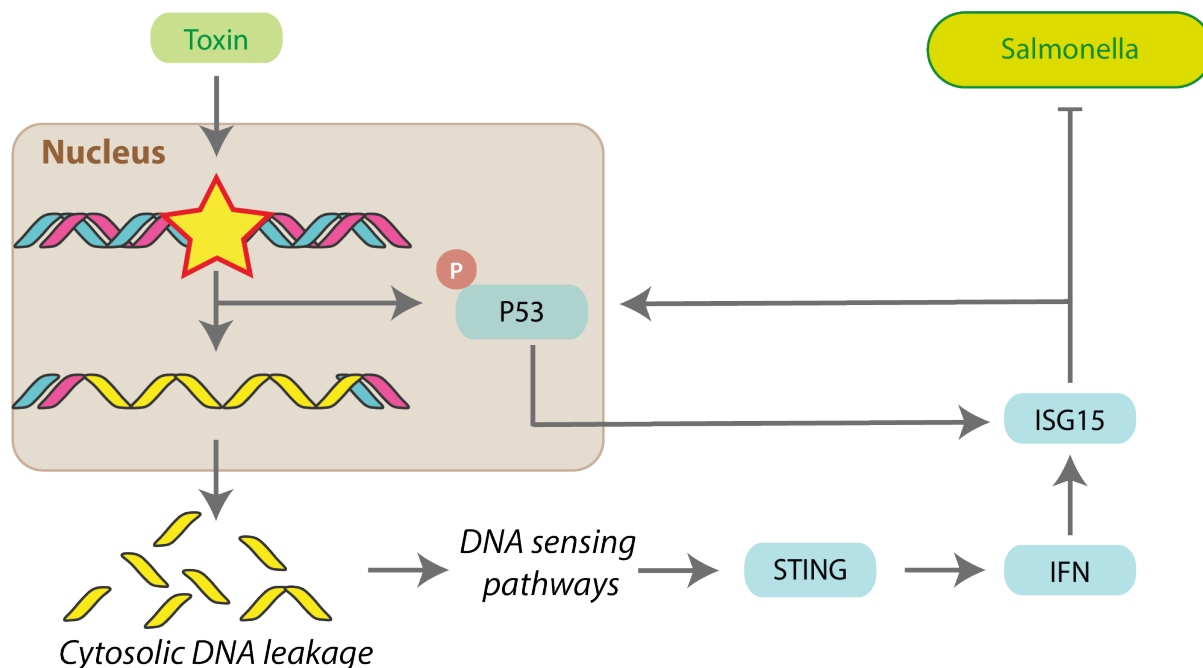


Fig. 7.1 **Proposed model for the role of ISG15 in response to the toxin.**

The toxin-induced DDR results in cytosolic leakage of DNA and activation of an ISG response in a STING-dependent manner. Toxin-induced damage also activates P53, which may upregulate ISG15 directly. ISG15 inhibits *Salmonella* infection and may stabilise P53, thus influencing cell fate decisions.

7.5 The role of ISG15 in cancer

S. Typhi infection has been shown to positively correlate with incidence of gallbladder cancer. As the typhoid toxin causes DNA damage, which is commonly associated with cancer, it was hypothesised that toxin activity may be linked to this cancerous phenotype. The finding that ISG15 was induced by the toxin was interesting, as ISG15 expression has been shown to be elevated in many types of cancer, including bladder, breast and colon (Andersen *et al.*, 2006; Talvinen *et al.*, 2006; Bektas *et al.*, 2008). Indeed, several studies suggest that ISG15 is a tumour promoter (Desai *et al.*, 2012; Burks, Reed and Desai, 2014; Forsys *et al.*, 2014). Interestingly in these studies, malignant transformation appeared to be dependent on conjugated but not free ISG15. However, addition of extracellular free ISG15 to tumours was seen to inhibit growth, and intracellular free ISG15 triggered expression of MHC complexes which are critical for activation of adaptive

immunity (Burks, Reed and Desai, 2014, 2015). This suggests that ISG15 broadly has pro-tumour effects when conjugated and anti-tumour effects when free.

Data in **chapter 6** showed that ISG15 had a tumour suppressive role in response to the toxin. It was found that wild-type MEFs treated with the typhoid toxin died, but ISG15^{-/-} MEFs survived and continued to proliferate, even with evidence of genomic instability. These ISG15^{-/-} MEFs also showed reduced levels of P53, and indeed one of the determining factors for oncogenic transformation of MEFs in response to *S. Typhi* was found to be mutated P53 (Scanu *et al.*, 2015). ISGylation of P53 in response to DNA damage was shown to promote its activation and binding to enhancer regions of pro-apoptotic target genes including CDKN1 and BAX (Park *et al.*, 2016). It is possible that ISG15 is performing a similar tumour suppressor function in response to the DNA damaging activity of the toxin. However, the role of ISG15 in tumorigenesis remains uncertain and further work will be needed to determine its role in response to the toxin.

7.6 Conclusion

This thesis provided an unbiased analysis of the host response to the typhoid toxin by identifying the toxin-dependent transcriptome. By doing this, it was found that a type-I IFN like response is induced in a toxin dependent manner. Through validation of the microarray data, ISG15 was identified as a regulator of *Salmonella* infection and a potential suppressor of bacterial induced genomic instability. Recent studies have determined that other CDTs trigger a type-I IFN response, and therefore it possible that the findings of this thesis will be of relevance to other CDT-secreting bacterial pathogens. This thesis contributes to elucidating the functional role of the toxin and opens new avenues of research into links between the toxin, chronic carriage and cancer.

Part 4: Materials & Methods

8 Biochemical assays

8.1 Bacterial transformation

8.1.1 Creation of chemically competent cells

E. coli (i.e., DH5 α , C41 Rosetta) was cultured in 500 ml sterile LB broth in a shaking incubator at 37°C and 200 rpm to an OD of 0.5. Cultures were centrifuged at 3000 rpm for 10 mins, supernatant discarded, and pellets resuspended in 40 ml of sterile 0.1M CaCl₂. Centrifugation was repeated, pellets resuspended in 2-3 ml of sterile CaCl₂ with glycerol and stored at -80°C in 50 μ l aliquots.

8.1.2 Transformation in chemically competent cells

Frozen plasmid and bacterial stocks were thawed on ice. Approximately 200 ng of plasmid DNA was added to 50 μ l of chemically competent *E. coli* and incubated on ice for 30 mins. Bacteria were heat shocked at 42°C for 30 seconds and immediately placed on ice for 5 mins, before incubation in 900 μ l of SOC broth (BioBasic, SD7009) at 37°C for 1h. Cultures were centrifuged at 13000 rpm for 1 min and resuspended in 200 μ l of SOC broth. Bacteria were spread onto LB-agar with relevant antibiotic(s) and incubated overnight at 37°C.

8.1.3 Purification of plasmid DNA by midiprep

A single colony of freshly transformed bacteria was added to 100 ml of LB broth supplemented with appropriate antibiotic(s) and grown overnight in a shaking incubator at 37 °C and 180 rpm. Midipreps were carried out using the NucleoBond Xtra Midi (Macherey-Nagel, 740410) kit according to manufacturer's instructions. Concentration was determined using a Nanodrop Lite spectrophotometer (Thermo Fisher) and plasmid preparations were stored at -20 °C.

8.2 Purification of recombinant typhoid toxin

The T7 expression vector encoding pETDuet1-*pltB*-HIS/*pltA*-MYC/*cdtB*-FLAG was transformed into chemically competent C41 Rosetta *E. coli*. Transformed colonies were used to inoculate 3x 10 ml starter cultures, which were incubated overnight at 37°C and 200 rpm and used to seed 3x 1000 ml cultures the following day. Day cultures were incubated at 37°C and 200 rpm to an OD of 0.8-1.0. Toxin expression was induced by addition of 0.1 mM Isopropyl β -D-1-thiogalactopyranoside (IPTG) and incubation at 30°C overnight. Cultures were pelleted for 10 mins at 6000 \times g and supernatant discarded. All pellets were resuspended, combined and homogenised in 50 ml TBS (tris-buffered saline, 20 mM tris, 150 mM NaCl, pH 7.4) with two tablets of cOmplete™ protease inhibitor cocktail (Roche). Bacteria were lysed using a French press at 40 ksi and lysate centrifuged at 70000 \times g for 40 mins at 4°C. Supernatant was added to 1 ml of NiNTA agarose beads (Jena Bioscience, AC-501-25), with 5 mM imidazole and incubated overnight at 4°C. Beads were immobilised on a column and washed with wash buffer (20 mM tris, 500 mM NaCl, pH 7.4) before bound protein was eluted in elution buffer (20 mM tris, 50 mM NaCl, 250 mM imidazole, pH 7.4). The elution was dialysed in TBS at 4°C overnight using cellulose dialysis tubing (Spectrum Labs™ 128058). Toxin concentration was estimated by relative densitometry to an ~80% pure preparation of GST-CdtB. Toxin preparations were kept at -80°C with 20% glycerol.

8.3 Cell fractionation

Cells were trypsinised and spun down at 1000 rpm for 5 mins. Supernatant was removed and pellets resuspended in buffer A (10 mM HEPES pH 7.9, 10 mM KCl, 1.5 mM MgCl₂, 0.34 M sucrose, 10% glycerol, 1 mM DTT, 0.1 mM PMSF, one tablet Roche cOmplete™ protease inhibitor cocktail). A 0.1% final volume of 10% Triton X-100 stock was added to the suspension and mixed by inversion. The suspension was incubated on ice for 5 mins and spun down at 1300 \times g for 5 mins at 4°C, leaving the supernatant (S1) and pellet (P1). Residual debris in S1 was removed by centrifugation at 20,000 \times g for 15 mins at 4°C and supernatant retrieved (soluble

cytosolic fraction). P1 was resuspended in Buffer A, incubated on ice for 5 mins and centrifuged at 1300g for 5 mins at 4°C. Supernatant was discarded and remaining pellet resuspended in buffer B (3 mM EDTA, 0.1 mM EGTA, 1 mM DTT, one tablet Roche cOmplete™ protease inhibitor cocktail). The suspension was incubated on ice for 30 mins to lyse, before spinning at 1700g for 5 mins at 4°C. The supernatant was retrieved (soluble nuclear fraction). Buffer B was added to the pellet and incubated on ice for 5 mins, before centrifugation again at 1700xg for 5 mins at 4°C. The supernatant was discarded, and remaining pellet retrieved (insoluble nuclear fraction).

8.4 Protein gels

8.4.1 Cell lysate preparation

Cells were either seeded in 10 cm dishes or 6-well plates. Generally, for 24 h experiments, cells were seeded at 1×10^6 cells/well or 2×10^5 cells/well respectively, with these values halved for every additional 24 h.

At the end of the experiment, cells were washed up to 3 times with PBS, and 1 ml of PBS added. Cells were scraped across the whole plate using a cell scraper and their OD_{600} measured using a spectrophotometer. The cell suspension was then centrifuged at 2000 rpm for 5 mins and supernatant discarded. The pellet was resuspended in sample buffer (50 mM Tris pH 6.8, 8 M Urea, 2% SDS, 0.3% Bromo blue, 1% β -mercaptoethanol). Volume of sample buffer in μ l was determined by multiplying the OD_{600} value by 250. Samples were stored at -20°C.

8.4.2 SDS-PAGE protein gel preparation

SDS-PAGE was performed using 9% Bis-tris acrylamide gels cast in BioRad Mini PROTEAN Tetra Cell Casting Stand Clamps (1658050). Resolving gel was formed of 9% 37.5:1 acrylamide/bis solution (1610148), 356 mM Bis-Tris (pH 6.5), 0.1% SDS and MQ water. Stacking gel was formed of 29:1 acrylamide/bis solution (1610156), 356 mM Bis-Tris (pH 6.5), 0.1% SDS and MQ water.

In both cases, 0.1% Ammonium Persulfate (APS, Melford, A1512), and 0.1% TEMED (Sigma Aldrich, T9281) were added for polymerisation. Gels were run at 40 mA/gel in Mini-PROTEAN Tetra System (Bio-Rad) in MES buffer (Life Technologies, NP0001). PageRuler Plus Prestained Protein Ladder (Thermo Scientific, #26619) was used as a protein size standard. Gels were analysed with either Coomassie staining or immunoblotting.

8.4.3 Coomassie staining

Gels were incubated in a petri dish containing Coomassie (50% methanol, 10% acetic acid, 2.5 g/L Blue R250) until protein bands appear. The stain was then discarded, and gels washed with destain (40% methanol, 10% acetic acid, MQ water) overnight with agitation. Gels were imaged using a Gel Doc EZ Imaging System.

8.4.4 Immunoblotting

Prior to transfer, PVDF membrane (Thermo Scientific, 88518) was cut to size and activated by 100% methanol (Sigma, 900658) for 10 seconds. Transfer was performed using either wet or semi-dry methods.

Wet Transfer: Activated PVDF membranes were submerged into fresh transfer buffer (20mM Tris-base, 150 mM Glycine, 20% methanol v/v). Membrane and gel were sandwiched in filter paper and sponge and immersed fully in the transfer tank. Transfer was performed at 400 mA for 80 min on ice or 20 mV at room temperature overnight.

Semi-dry transfer: The Trans-Blot Turbo Transfer System (Bio-Rad, 1704150), or iBlot 2 (ThermoFisher Scientific, IB21001) were used according to manufacturer's instructions using the default programs.

Membranes were blocked with 5% non-fat dried milk in TBS for 1 h at room temperature with agitation. Membranes were then washed 3 times in TBS with 0.1% Tween for 5 mins each before incubation with primary antibody (**Table 8-1**). Primary antibody diluted in TBS with 0.1% Tween was added overnight at 4°C with

agitation. The following day, membranes were washed 3 times in TBS with 0.1% Tween for 5 mins each before addition of secondary antibody. IRDye 800CW anti-mouse (926-32212, Li-Corr) and IRDye 680CW anti-rabbit (926-68073, Li-Corr) were diluted in TBS with 0.1% Tween at 1:10000 for 1 hour at room temperature with agitation. Membranes were imaged at 200 μ m resolution using an OdysseySa Li-Cor scanner and images processed using ImageStudioLite v5.2.5.

Antibody	Species	Product code	Dilution
FLAG	mouse monoclonal	Sigma-Aldrich 5F3165	1:1000
c-Myc	rabbit monoclonal	Abcam 32072	1:500
pSTAT1	rabbit monoclonal	Cell Signalling 9167	1:1000
STAT1	rabbit polyclonal	Cell Signalling 9172	1:1000
IFIT1	rabbit polyclonal	Thermo Fisher PA3-848	1:1000
ISG15	mouse monoclonal	Santa Cruz sc-166755	1:100
Tubulin	mouse monoclonal	Abcam ab7291 Invitrogen 62204	1:1000-1:5000
Actin	rabbit polyclonal	Sigma A2066	1:1000
Lamin B1	rabbit polyclonal	Abcam ab16048	1:1000
H3	rabbit monoclonal	Abcam ab176916	1:1000
γH2AX	rabbit monoclonal mouse monoclonal	Cell Signalling #9718 Merck/Sigma 05-636	1:1000
RPA32	mouse monoclonal	Abcam ab16850	1:1000
HMGB2	rabbit monoclonal	Abcam ab124670	1:1000
NABP1	rabbit polyclonal	Genetex GTX12092	1:1000
NABP2	rabbit polyclonal	Bethyl A301-938A-M	1:1000
INT3	rabbit polyclonal	Bethyl A302-050A-M	1:1000
cGAS	rabbit monoclonal	Cell Signalling 15102T	1:1000

pTBK1	rabbit monoclonal	Cell Signalling 5483	1:1000
pSTING	rabbit monoclonal	Cell Signalling 19781	1:1000
HA	rabbit	Gift from Andrew Peden	1:400
p-P53	rabbit polyclonal	R&D Systems AF1043	1:20

Table 8-1 **Primary antibodies used for immunoblotting**

8.5 Flow cytometry

Flow cytometry was used to measure DNA content and thus cell cycle phase using propidium iodide (PI). A standard intoxication assay was performed with samples prepared every 2h after intoxication over the 24h media chase. Cells were detached using trypsin and fixed with 1 ml ice-cold 70% ethanol in PBS. Cell pellets were resuspended in 300 μ l PBS containing 100 μ g/ml RNase and 40 μ g/ml PI, incubated at 37 °C for 30 min and analysed using a FACSCalibur Flow Cytometer (Beckman Coulter). At least 10,000 cells were counted per sample.

Analysis was performed with FlowJo. The percentage of cells in G1 phase was determined by calculating the integral of the lowest PI value of the G1 curve to the peak of G1, whereas the percentage of cells in G2 phase was determined by calculating the integral of the highest PI value of the G2 curve to the peak of G2. S phase percentage was calculated as the remainder after G1 and G2 values were subtracted from 100.

8.6 Microarray

Microarray samples were prepared by Angela Ibler, who performed a standard intoxication assay with 5 ng/ml of WT- and HQ-toxin and a 48h chase and isolated RNA. Samples were analysed in the Paul Heath lab at SITraN, University of Sheffield, using a human ClariomTMS assay (ThermoFisher Scientific, 902927). Analysis was performed with Transcriptome Analysis Console 4.0 software (Applied Biosystems, Thermo Fisher Scientific), which uses the LIMMA statistical analysis framework (Ritchie *et al.*, 2015). The microarray data comparing WT- and HQ-toxin

treated HT1080s used in Fig. 4.4 was uploaded to the EBI ArrayExpress database under accession number [E-MTAB-12333](#).

The gene list was analysed by me using the ‘proteins with values/ranks’ function of the online tool STRING v11.0 (<https://string-db.org/>) (Szklarczyk *et al.*, 2019). The gene list was clustered using gene ontology terms for biological processes. STRING v11.0 was also used to visualise protein interactions in the clusters found.

8.7 qRT-PCR

Standard intoxication assays were performed in HT1080s with a 24 h media chase. Cells were washed in PBS, scraped in 5ml PBS, aliquoted and spun down. Cell pellets were stored at -80°C.

RNA was isolated using the illustra RNAspin Mini kit (GE healthcare) according to manufacturer’s instructions with 1 unit (0.5 µl) of DNase 1 (M0303S, New England BioLabs). RNA concentration was measured using a Nanodrop Lite spectrophotometer (ND-LITE-PR, Thermo Fisher Scientific) and RNA integrity tested by running the sample on a TAE agarose gel.

cDNA synthesis was performed using the RevertAid H Minus First Strand cDNA synthesis kit (Thermo scientific). qRT-PCR was performed using Maxima SYBR Green/ROX qPCR Master mix (Thermo Scientific) on the CFX96 Real-Time System. 10 µl of master mix were used per sample, and primers were added at a concentration of 0.25 µM (**Table 8-2**). Analysis was performed using the comparative C_T Method ($\Delta\Delta$ C_T Method) according to guidelines by Thermo Fisher (Applied Biosystems, 2008).

Gene	Forward	Reverse	Source
ISG15	CTCTGAGCATCCTGGTGAGGAA	AAGGTCAGCCAGAACAG GTCGT	OriGene NM_005101
IFIT1	GCCTTGCTGAAGTGTGGAGGAA	ATCCAGGCGATAGGCAG AGATC	OriGene NM_001548

IFIT2	ATTCTATCACCAAGCCCGTGG	TGGAGTCTGGAAGCCTCA TCC	(Brzostek-Racine <i>et al.</i> , 2011)
IFIT3	AGCTCCTCTCTAACTCAGAGCA AC	CCACTGCAGGCTTCTGAT G	(Calonge <i>et al.</i> , 2017)
IFI6	GGTCTGCGATCCTGAATGGG	TCACTATCGAGATACTTG TGGGT	(Zhao and Liu, 2021)
IRF9	TTCTGTCCCTGGTGTAGAGCCT	TTTCAGGACACGATTATC ACGG	(Haseley <i>et al.</i> , 2012)
OAS1	TGGCCTTCTATGCCCTCTATCC	TCCCATCAGGTGCACAGA AGA	(Haseley <i>et al.</i> , 2012)
OAS3	CCTGATTCTGCTGGTGAAGCAC	TCCAGGCAAAGATGGT GAGGA	OriGene NM_006187
STAT1	GGAACCTTGATGGCCCTAAAGGA	ACAGAGCCCACTATCCGA GACA	(Haseley <i>et al.</i> , 2012)
IFNA	CACACAGGCTTCCAGGCATTC	TCTTCAGCACAAAGGACT CATCTG	(Brzostek-Racine <i>et al.</i> , 2011)
IFNB	TGCTCTCCTGTTGTGCTTCTCCA C	ATAGATGGTCAATGCGGC GTCC	(Brzostek-Racine <i>et al.</i> , 2011)
IFIH1	GCTGAAGTAGGAGTCAAAGCCC	CCACTGTGGTAGCGATAA GCAG	OriGene NM_022168
cGAS	GGAGCCCTGCTGTAACACTT	TTTCCTTCCTTTGCATGCT T	(Calonge <i>et al.</i> , 2017)

Table 8-2 Primers used for qRT-PCR

9 Cell biology

9.1 Mammalian cell culture

This thesis used both HT1080 human fibrosarcoma cells and mouse embryonic fibroblasts (MEFs, kindly donated by Lilliana Radoshevich, University of Iowa), both of which were maintained in high glucose Dulbecco's Modified Eagle's Medium (DMEM; Sigma Aldrich, D6546) with 10% foetal bovine serum (FBS) (Sigma Aldrich, F7524), 10 U/ml Penicillin/Streptomycin (Gibco, 11548876), 50 µg/ml Kanamycin sulphate (BioBasic, KB0286) and 2 mM L-glutamine (ThermoFisher Scientific, #25030024).

Cells were kept frozen in 10% sterile DMSO (dimethyl sulfoxide, Sigma-Aldrich, D2438) and 90% complete media at -80°C. Cells were thawed at 37°C, diluted 1:10 with complete growth media and transferred to flasks. Cells were maintained in a humidified incubator (Panasonic) at 37°C and 5% CO₂. Cells were passaged when 80% confluent (approximately every 2 days).

For seeding cells for experiments, media was aspirated, and cells washed with sterile PBS (Sigma Aldrich, D8537). Cells were detached using sterile trypsin at 37°C for 5 mins (Sigma Aldrich, T4049). Trypsin was neutralised using a 1:1 volume of complete growth media. Cells were counted in a glass haemocytometer.

9.2 Mammalian cell treatment

9.2.1 Standard intoxication assay

Culture media was replaced with media containing 20 ng/ml (unless otherwise stated) WT- or HQ-toxin for 2h. Cells were then washed with sterile PBS and chased with fresh complete growth media.

9.2.2 Cell cycle arrest by serum-starvation

Cells were serum-starved in media containing all components apart from 10% FBS for the full duration of one replication cycle (24 h in HT1080s).

9.2.3 Drug and recombinant protein treatment

Cells were treated with drugs and recombinant proteins listed in **Table 9-1** with the indicated incubation times.

Drug	Summary	Working concentration	Incubation time	Product code
Aphidicolin	DNA polymerase α inhibitor	20 μ M	24 h	Sigma-Aldrich (A0781)
Etoposide	Topoisomerase inhibitor	10 μ M	24 h	Cayman Chemicals (12092)
BX795	TBK1 inhibitor	10 μ M	Duration of experiment	Invivogen tlr1-bx7
H151	STING inhibitor	4 μ g/ml	Duration of experiment	Invivogen inh-h151
B18R	Type-I IFN inhibitor	0.1 μ g/ml	Duration of experiment	Invitrogen 14-8185-62
IFN α	Recombinant interferon α	0.1 μ g/ml	Duration of experiment	Novus Biologicals NBP2-34971

Table 9-1 **Drugs and recombinant proteins used to treat mammalian cells**

9.2.4 Transfection of mammalian cells

For siRNA transfection, cells were transfected in 6 well plates by addition of 3 μ l/well Lipofectamine RNAiMax (Invitrogen, 13778-150) and 20 nM siRNA (**Table 9-2**) in 100 μ l of serum-free, antibiotic-free DMEM. Cells were incubated for 48h before any further treatments.

siRNA	Product code
Non-targeting Control	Horizon D-001810-01-20
GAPDH	Ambion AM4605
NABP1	Horizon L-014224-01-0005
NABP2	Horizon L-014288-01-0005
INT3	Horizon L-018360-01-0005

Table 9-2 **siRNAs used for transfection of mammalian cells**
Horizon siRNAs are ON-TARGETplus SMARTpool.

For transfection with immunostimulatory DNA, cells were transfected by addition of 3 μ l/well Lipofectamine RNAiMax (Invitrogen, 13778-150) and 5 μ l each of two 100 μ M oligonucleotide stocks (TACAGATCTACTAGTGATCTATGACTGATCTGTACA-TGATCTACA, TGTAGATCATGTACAGATCAGTCATAGATCACTAGTAGATCTGTA) (Fu *et al.*, 2019; Lama *et al.*, 2019) in 100 μ l of serum-free, antibiotic-free DMEM.

For transfection with mammalian expression vectors, 3 μ l/well Lipofectamine RNAiMax (Invitrogen, 13778-150) or 6 μ l/well FuGENE transfection reagent (Promega) was used. pCAGGS-5HA-mISG15 was a gift from Dong-Er Zhang (Addgene plasmid # 12444) (Kim *et al.*, 2004). As a control, an empty pcDNATM3.1⁽⁺⁾ mammalian expression vector (Thermo Fisher, V79020) was used.

9.3 Clonogenic Assay

2000 cells were seeded into a 10 cm dish, treated, and incubated in fresh media for 8 days. Media was aspirated and cells were washed with PBS. Next, 80% ethanol was applied to cells for 15 minutes, then removed and cells were left to air-dry. 1% methylene blue was added until colonies were visible, washed off with distilled water and then air-dried before imaging with a ChemiDoc XRS+ imager (BioRad). Images were thresholded and colonies counted using Fiji v2.3.

9.4 Cell staining

9.4.1 Immunofluorescence

Cells were seeded in 24 well plates on glass coverslips. At the end of the experiment, media was aspirated, and cells washed three times with PBS. For staining of RPA32 pT21 and components of the SOSS complex, cells were pre-permeabilised with PBS + 0.1% Tween for 1 minute on ice. Cells were fixed with 4% paraformaldehyde (PFA) in PBS for 10-15 mins at room temperature. PFA was removed and cells washed twice more with PBS before being stored in PBS at 4°C until staining.

Cells were blocked using 3% BSA (Sigma-Aldrich, 1073508600) and 0.2% Triton X-100 (VWR, 28817.295) in PBS at room temperature for 1h. Coverslips were washed by dipping in PBS and 0.2% Triton X-100. Primary and secondary antibody dilutions were prepared in PBS 0.2% Triton X-100. Primary antibodies were diluted as appropriate (**Table 9-3**) and added for an hour at room temperature.

Secondary antibodies (**Table 9-4**) were added at a 1:500 dilution in PBS with 0.2% Triton X-100 for 30 mins at room temperature. Coverslips were then mounted on 6 µl of VectaShield mounting agent including DAPI (Vector Lab, H1200), sealed and left to dry before being imaged.

Antibody	Species	Product code	Dilution
BrdU	rat monoclonal	Abcam ab6326	1:400
ISG15	mouse monoclonal	Santa Cruz sc-166755	1:100
Lamin B1	rabbit polyclonal	Abcam ab16048	1:1000
γ H2AX	mouse monoclonal	Merck/Sigma 05-636	1:1000
RPA32 pT21	rabbit polyclonal	Abcam ab61065	1:1000
NABP1	rabbit polyclonal	Genetex GTX12092	1:1000
NABP2	rabbit polyclonal	Bethyl A301-938A-M	1:1000
INT3	rabbit polyclonal	Bethyl A302-050A-M	1:1000
53BP1	mouse monoclonal	Merck MAB3802	1:500
<i>Salmonella</i>	rabbit polyclonal	Abcam ab35156	1:1000

Table 9-3 **Primary antibodies used for immunofluorescence**

Antibody	Product code
Anti-mouse 488	Alexa-Fluor A21202
Anti-rabbit 488	Alexa-Fluor A110008
Anti-rat 555	Alexa-Fluor A21434
Anti-rabbit 568	Alexa-Fluor A11036
Anti-rabbit 568	Alexa-Fluor A11036
Anti-mouse 594	Alexa-Fluor A21203

Table 9-4 **Secondary antibodies used for immunofluorescence**

9.4.2 EdU staining

Cells were incubated for 2h with 10 μ M EdU prior to fixation. Cells were stained for EdU using a Click-iT™ EdU Cell Proliferation kit with Alexa Fluor™ 647 dye (ThermoFisher, C10340) as per the manufacturer's instruction. Cells were then blocked for 20 mins using 3% BSA (Sigma-Aldrich, 1073508600) and 0.2% Triton X-100 (VWR, 28817.295) in PBS before proceeding with primary and secondary antibodies as detailed in **section 9.4.1**.

9.4.3 *In vitro* polymerase assay

A standard intoxication assay was performed in HT1080s in 24 well plate format with a 24 h media chase. The *in vitro* polymerase mixture (0.4 mM CldU, 0.1 mM dNTP mix, Dream Taq buffer to final concentration 1x, 1 μ l/ml Dream Taq polymerase, MQ water) was added to a fresh 24-well plate on ice. The glass cover slips with samples were placed top down onto the *in vitro* polymerase reaction mixture. The plate was placed in a pre-heated water bath at 72°C for 5 min to allow the polymerase reaction. The reaction was interrupted by placing the plate on ice and washing coverslips with PBS three times. A standard immunofluorescence assay was performed using anti-BrdU (which also recognises CldU) and anti-RPA32pT21 (**Table 9-3**).

9.5 Infection assay

9.5.1 Preparation of cells and bacterial culture

Cells were seeded in a 24-well plate at an appropriate density to reach approximately 80% confluency by the end of the experiment.

A *Salmonella* colony was cultured in 5 ml LB broth with the relevant antibiotic overnight at 37°C in a shaking incubator. Next day, a 1:100 dilution of the overnight culture was performed into 10 ml of fresh LB broth with the relevant antibiotic and incubated at 37°C in a shaking incubator until OD₆₀₀ was approximately 1.0. The number of *Salmonella* at an OD⁶⁰⁰ of 1.0 was estimated to be 8×10⁸ bacteria/ml. Unless otherwise stated, infections were performed with an MOI of 10.

Bacteria were spun down at 13,000 rpm for 1 minute and supernatant discarded. The pellet was resuspended in 1 ml of sterile PBS before adding to cells. The plate was centrifuged for 1 min at $1000 \times g$ and incubated for 30 min at 37°C 5% CO_2 . Infection media was removed, cells were washed with PBS, and fresh media added containing 50 $\mu\text{g}/\text{ml}$ gentamicin (Chem Cruz, sc203334) for 90 mins. This media was then replaced with fresh media containing 10 $\mu\text{g}/\text{ml}$ gentamicin for the duration of the experiment.

9.5.2 CFU assay

HT1080s were seeded at 2×10^4 cells per well in a 24-well plate before infection with *Salmonella* as described previously. Cells were lysed 2h, 24h, 48h and 72h cells post-infection. Cells were washed 3 \times with PBS, lysed with 1% Triton X-100 in deionised sterile water for 10 mins, and pipetted vigorously. The supernatant was transferred to a 96-well plate, and serially diluted 10-fold using a multichannel pipette. 5 μl of each *Salmonella* dilution was then cultured on agar overnight in a dry incubator at 37°C . Colonies at the highest countable dilution were counted manually and % CFU calculated as a percentage of *Salmonella* colony forming units (CFUs) at the 2h timepoint.

9.6 Microscopy

Immunostained cells were imaged using a Nikon Widefield microscope equipped with an sCMOS Andor Zyla camera. NIS elements software was used for imaging. Images were processed using Fiji v2.3. For chosen representative images, brightness and contrast were normalised, scalebar added and images cropped if necessary. The DAPI channel was converted into a binary image to obtain DAPI outlines, which were overlaid with other channels.

Quantitative analysis of image intensity was generally carried out using the RING-tracking MATLAB code published in Ibler et al., 2019. For images of MEFs (**Fig. 6.7**), images were analysed using Fiji v.2.3. Briefly, nuclei were identified by manual thresholding of the DAPI channel. EdU was auto-thresholded using default settings and the percentage of positive pixels within nuclei measured.

Adobe Illustrator was used to prepare illustrations and assemble all results figures.

9.7 Statistical analysis

Graphs and statistical analysis were carried out using GraphPad Prism 9. Generally, one-way ANOVAs were used with Šidák's or Tukey's multiple comparisons tests as appropriate. Significance is denoted by asterisks where * $p < 0.05$, ** $p < 0.01$, *** $p < 0.001$ and **** $p < 0.0001$.

Bibliography

- Ablasser, A. *et al.* (2009) 'RIG-I-dependent sensing of poly(dA:dT) through the induction of an RNA polymerase III-transcribed RNA intermediate', *Nature Immunology*, 10(10), pp. 1065–1072. doi:10.1038/ni.1779.
- Ablasser, A. and Chen, Z.J. (2019) 'CGAS in action: Expanding roles in immunity and inflammation', *Science*, 363(6431). doi:10.1126/science.aat8657.
- Agarwal, M.L. *et al.* (1995) 'p53 controls both the G2/M and the G1 cell cycle checkpoints and mediates reversible growth arrest in human fibroblasts', *Proceedings of the National Academy of Sciences of the United States of America*, 92(18), pp. 8493–8497. doi:10.1073/pnas.92.18.8493.
- Agarwal, M.L. *et al.* (1998) 'A p53-dependent S-phase checkpoint helps to protect cells from DNA damage in response to starvation for pyrimidine nucleotides', *Proceedings of the National Academy of Sciences of the United States of America*, 95(25), pp. 14775–14780. doi:10.1073/pnas.95.25.14775.
- Aird, K.M. *et al.* (2016) 'HMGB2 orchestrates the chromatin landscape of senescence-associated secretory phenotype gene loci', *Journal of Cell Biology*, 215(3), pp. 325–334. doi:10.1083/jcb.201608026.
- Akira, S., Uematsu, S. and Takeuchi, O. (2006) 'Pathogen recognition and innate immunity', *Cell*, 124(4), pp. 783–801. doi:10.1016/j.cell.2006.02.015.
- Alaoui-El-Azher, M. *et al.* (2010) 'Role of the ATM-checkpoint kinase 2 pathway in CDT-mediated apoptosis of gingival epithelial cells', *PLoS ONE*, 5(7), pp. 1–10. doi:10.1371/journal.pone.0011714.
- Alphonse, N. *et al.* (2022) 'A family of conserved bacterial virulence factors dampens interferon responses by blocking calcium signaling', *Cell*, 185(13), pp. 2354–2369.e17. doi:10.1016/j.cell.2022.04.028.
- Alphonse, N., Dickenson, R.E. and Odendall, C. (2021) 'Interferons: Tug of War Between Bacteria and Their Host', *Frontiers in Cellular and Infection Microbiology*. Available at: <https://www.frontiersin.org/article/10.3389/fcimb.2021.624094>.
- Als, D. *et al.* (2018) 'Global trends in typhoidal salmonellosis: A systematic review', *American Journal of Tropical Medicine and Hygiene*, 99(3), pp. 10–19. doi:10.4269/ajtmh.18-0034.
- Andersen, J.B. *et al.* (2006) 'Stage-associated overexpression of the ubiquitin-like protein, ISG15, in bladder cancer', *British Journal of Cancer*, 94(10), pp. 1465–1471. doi:10.1038/sj.bjc.6603099.

Andrews, J.R. and Ryan, E.T. (2015) 'Diagnostics for invasive Salmonella infections: Current challenges and future directions', *Vaccine*. *Vaccine*, pp. C8–C15. doi:10.1016/j.vaccine.2015.02.030.

Applied Biosystems (2008) *Guide to Performing Relative Quantitation of Gene Expression Using Real-Time Quantitative PCR*. Available at: https://assets.thermofisher.com/TFS-Assets/LSG/manuals/cms_042380.pdf (Accessed: 18 July 2022).

Arimoto, K.I. *et al.* (2017) 'STAT2 is an essential adaptor in USP18-mediated suppression of type I interferon signaling', *Nature Structural and Molecular Biology*, 24(3), pp. 279–289. doi:10.1038/nsmb.3378.

Bai, J. and Liu, F. (2019) 'The cGAS-cGAMP-STING pathway: A molecular link between immunity and metabolism', *Diabetes*, 68(6), pp. 1099–1108. doi:10.2337/dbi18-0052.

Bakhom, S.F. *et al.* (2018) 'Chromosomal instability drives metastasis through a cytosolic DNA response', *Nature*, 553(7689), pp. 467–472. doi:10.1038/nature25432.

Bakkenist, C.J. and Kastan, M.B. (2003) 'DNA damage activates ATM through intermolecular autophosphorylation and dimer dissociation', *Nature*, 421(6922), pp. 499–506. doi:10.1038/nature01368.

den Bakker, H.C. *et al.* (2011) 'Genome sequencing reveals diversification of virulence factor content and possible host adaptation in distinct subpopulations of *Salmonella enterica*', *BMC Genomics*, 12(1), pp. 1–11. doi:10.1186/1471-2164-12-425.

Baldanta, S. *et al.* (2017) 'ISG15 governs mitochondrial function in macrophages following vaccinia virus infection', *PLoS Pathogens*, 13(10). doi:10.1371/journal.ppat.1006651.

Baranovskiy, A.G. *et al.* (2014) 'Structural basis for inhibition of DNA replication by aphidicolin', *Nucleic Acids Research*, 42(22), pp. 14013–14021. doi:10.1093/nar/gku1209.

Barnett, K.C. *et al.* (2019) 'Phosphoinositide Interactions Position cGAS at the Plasma Membrane to Ensure Efficient Distinction between Self- and Viral DNA', *Cell*, 176(6), pp. 1432–1446.e11. doi:10.1016/j.cell.2019.01.049.

Barrat, F.J. *et al.* (2005) 'Nucleic acids of mammalian origin can act as endogenous ligands for Toll-like receptors and may promote systemic lupus erythematosus', *Journal of Experimental Medicine*, 202(8), pp. 1131–1139. doi:10.1084/jem.20050914.

- Bass, T.E. *et al.* (2016) 'ETAA1 acts at stalled replication forks to maintain genome integrity', *Nature Cell Biology*, 18(11), pp. 1185–1195. doi:10.1038/ncb3415.
- Basters, A. *et al.* (2017) 'Structural basis of the specificity of USP18 toward ISG15', *Nature Structural and Molecular Biology*, 24(3), pp. 270–278. doi:10.1038/nsmb.3371.
- Bäumler, A.J., Tsois, R.M. and Heffron, F. (1996) 'Contribution of fimbrial operons to attachment to and invasion of epithelial cell lines by *Salmonella typhimurium*', *Infection and Immunity*, 64(5), pp. 1862–1865. doi:10.1128/iai.64.5.1862-1865.1996.
- Bekker-Jensen, S. *et al.* (2006) 'Spatial organization of the mammalian genome surveillance machinery in response to DNA strand breaks', *Journal of Cell Biology*, 173(2), pp. 195–206. doi:10.1083/jcb.200510130.
- Bektas, N. *et al.* (2008) 'The ubiquitin-like molecule interferon-stimulated gene 15 (ISG15) is a potential prognostic marker in human breast cancer', *Breast Cancer Research*, 10(4). doi:10.1186/bcr2117.
- Del Bel Belluz, L. *et al.* (2016) 'The Typhoid Toxin Promotes Host Survival and the Establishment of a Persistent Asymptomatic Infection', *PLoS Pathogens*, 12(4), pp. 1–25. doi:10.1371/journal.ppat.1005528.
- Benveniste, E.N. and Qin, H. (2007) 'Type I interferons as anti-inflammatory mediators.', *Science's STKE: signal transduction knowledge environment*, 2007(416). doi:10.1126/stke.4162007pe70.
- Bermudez, V.P. *et al.* (2003) 'Loading of the human 9-1-1 checkpoint complex onto DNA by the checkpoint clamp loader hRad17-replication factor C complex in vitro', *Proceedings of the National Academy of Sciences of the United States of America*, 100(4), pp. 1633–1638. doi:10.1073/pnas.0437927100.
- Bétermier, M., Bertrand, P. and Lopez, B.S. (2014) 'Is Non-Homologous End-Joining Really an Inherently Error-Prone Process?', *PLoS Genetics*, 10(1), p. e1004086. doi:10.1371/journal.pgen.1004086.
- Beucher, A. *et al.* (2009) 'ATM and Artemis promote homologous recombination of radiation-induced DNA double-strand breaks in G2', *EMBO Journal*, 28(21), pp. 3413–3427. doi:10.1038/emboj.2009.276.
- Bewersdorf, J., Bennett, B.T. and Knight, K.L. (2006) 'H2AX chromatin structures and their response to DNA damage revealed by 4Pi microscopy', *Proceedings of the National Academy of Sciences of the United States of America*, 103(48), pp. 18137–18142. doi:10.1073/pnas.0608709103.
- Bezine, E., Vignard, J. and Mirey, G. (2014) 'The Cytolethal Distending Toxin Effects on Mammalian Cells: A DNA Damage Perspective', *Cells*, 3(2), pp. 592–615.

doi:10.3390/cells3020592.

Bhat, N. and Fitzgerald, K.A. (2014) 'Recognition of cytosolic DNA by cGAS and other STING-dependent sensors', *European Journal of Immunology*, 44(3), pp. 634–640. doi:10.1002/eji.201344127.

Bi, D. *et al.* (2017) 'NOD1 is the innate immune receptor for iE-DAP and can activate NF- κ B pathway in teleost fish', *Developmental and Comparative Immunology*, 76, pp. 238–246. doi:10.1016/j.dci.2017.06.012.

Bishop, A. *et al.* (2008) 'Interaction of *Salmonella enterica* serovar Typhi with cultured epithelial cells: Roles of surface structures in adhesion and invasion', *Microbiology*, 154(7), pp. 1914–1926. doi:10.1099/mic.0.2008/016998-0.

Blackford, A.N. and Jackson, S.P. (2017) 'ATM, ATR, and DNA-PK: The Trinity at the Heart of the DNA Damage Response', *Molecular Cell*, 66(6), pp. 801–817. doi:10.1016/j.molcel.2017.05.015.

Blohmke, C.J. *et al.* (2019) 'Diagnostic host gene signature for distinguishing enteric fever from other febrile diseases', *EMBO Molecular Medicine*, 11(10). doi:10.15252/emmm.201910431.

Blomstrom, D.C. *et al.* (1986) 'Molecular characterization of the interferon-induced 15-kDa protein. Molecular cloning and nucleotide and amino acid sequence', *Journal of Biological Chemistry*, 261(19), pp. 8811–8816. doi:10.1016/s0021-9258(19)84453-8.

Bogunovic, D. *et al.* (2012) 'Mycobacterial disease and impaired IFN- γ immunity in humans with inherited ISG15 deficiency', *Science*, 337(6102), pp. 1684–1688. doi:10.1126/science.1224026.

Bolderson, E. *et al.* (2014) 'Human single-stranded DNA binding protein 1 (hSSB1/NABP2) is required for the stability and repair of stalled replication forks', *Nucleic Acids Research*, 42(10), pp. 6326–6336. doi:10.1093/nar/gku276.

Boucher, D. *et al.* (2021) 'hSSB2 (NABP1) is required for the recruitment of RPA during the cellular response to DNA UV damage', *Scientific Reports 2021 11:1*, 11(1), pp. 1–12. doi:10.1038/s41598-021-99355-0.

Boxx, G.M. and Cheng, G. (2016) 'The Roles of Type I Interferon in Bacterial Infection', *Cell Host and Microbe*. Cell Press, pp. 760–769. doi:10.1016/j.chom.2016.05.016.

Brenner, F.W. *et al.* (2000) 'Salmonella nomenclature', *Journal of Clinical Microbiology*, 38(7), pp. 2465–2467. doi:10.1128/jcm.38.7.2465-2467.2000.

Brzostek-Racine, S. *et al.* (2011) 'The DNA Damage Response Induces IFN', *The*

Journal of Immunology, 187(10), pp. 5336–5345. doi:10.4049/jimmunol.1100040.

Bürckstümmer, T. *et al.* (2009) 'An orthogonal proteomic-genomic screen identifies AIM2 as a cytoplasmic DNA sensor for the inflammasome', *Nature Immunology*, 10(3), pp. 266–272. doi:10.1038/ni.1702.

Burks, J., Reed, R.E. and Desai, S.D. (2014) 'ISGylation governs the oncogenic function of Ki-Ras in breast cancer', *Oncogene*, 33(6), pp. 794–803. doi:10.1038/onc.2012.633.

Burks, J., Reed, R.E. and Desai, S.D. (2015) 'Free ISG15 triggers an antitumor immune response against breast cancer: A new perspective', *Oncotarget*, 6(9), pp. 7221–7231. doi:10.18632/oncotarget.3372.

Calonge, E. *et al.* (2017) 'Different Expression of Interferon-Stimulated Genes in Response to HIV-1 Infection in Dendritic Cells Based on Their Maturation State', *Journal of Virology*, 91(8), pp. 1–22. doi:10.1128/jvi.01379-16.

Caron, P. *et al.* (2015) 'Non-redundant Functions of ATM and DNA-PKcs in Response to DNA Double-Strand Breaks', *Cell Reports*, 13(8), pp. 1598–1609. doi:10.1016/j.celrep.2015.10.024.

Casper, A.M. *et al.* (2002) 'ATR regulates fragile site stability', *Cell*, 111(6), pp. 779–789. doi:10.1016/S0092-8674(02)01113-3.

Castiglia, V. *et al.* (2016) 'Type I Interferon Signaling Prevents IL-1 β -Driven Lethal Systemic Hyperinflammation during Invasive Bacterial Infection of Soft Tissue', *Cell Host and Microbe*, 19(3), pp. 375–387. doi:10.1016/j.chom.2016.02.003.

Celeste, A. *et al.* (2003) 'Histone H2AX phosphorylation is dispensable for the initial recognition of DNA breaks', *Nature Cell Biology*, 5(7), pp. 675–679. doi:10.1038/ncb1004.

Celhar, T., Magalhães, R. and Fairhurst, A.M. (2012) 'TLR7 and TLR9 in SLE: When sensing self goes wrong', *Immunologic Research*, 53(1–3), pp. 58–77. doi:10.1007/s12026-012-8270-1.

Chan, K. *et al.* (2003) 'Genomic comparison of *Salmonella enterica* serovars and *Salmonella bongori* by use of an *S. enterica* serovar Typhimurium DNA microarray', *Journal of Bacteriology*, 185(2), pp. 553–563. doi:10.1128/JB.185.2.553-563.2003.

Chang, S.J. *et al.* (2019) 'Unique features in the intracellular transport of typhoid toxin revealed by a genome-wide screen', *PLoS Pathogens*, 15(4). doi:10.1371/journal.ppat.1007704.

Cheon, H. *et al.* (2013) 'IFN β -dependent increases in STAT1, STAT2, and IRF9 mediate resistance to viruses and DNA damage', *EMBO Journal*, 32(20), pp. 2751–

2763. doi:10.1038/emboj.2013.203.

Chiu, Y.H., MacMillan, J.B. and Chen, Z.J. (2009) 'RNA Polymerase III Detects Cytosolic DNA and Induces Type I Interferons through the RIG-I Pathway', *Cell*, 138(3), pp. 576–591. doi:10.1016/j.cell.2009.06.015.

Cho, H.Y. *et al.* (2008) 'Interferon-sensitive response element (ISRE) is mainly responsible for IFN- α -induced upregulation of programmed death-1 (PD-1) in macrophages', *Biochimica et Biophysica Acta - Gene Regulatory Mechanisms*, 1779(12), pp. 811–819. doi:10.1016/j.bbagr.2008.08.003.

Chumduri, C. *et al.* (2016) 'Subversion of host genome integrity by bacterial pathogens', *Nature Reviews Molecular Cell Biology*, 17(10), pp. 659–673. doi:10.1038/nrm.2016.100.

Collier-Hyams, L.S. *et al.* (2002) 'Cutting edge: Salmonella AvrA effector inhibits the key proinflammatory, anti-apoptotic NF-kappa B pathway', *Journal of immunology (Baltimore, Md. : 1950)*, 169(6), pp. 2846–2850. doi:10.4049/JIMMUNOL.169.6.2846.

Collins, A. and Oates, D.J. (1987) 'Hydroxyurea: effects on deoxyribonucleotide pool sizes correlated with effects on DNA repair in mammalian cells', *European Journal of Biochemistry*, 169(2), pp. 299–305. doi:10.1111/j.1432-1033.1987.tb13612.x.

Cope, L.D. *et al.* (1997) 'A diffusible cytotoxin of *Haemophilus ducreyi*', *Proceedings of the National Academy of Sciences of the United States of America*, 94(8), pp. 4056–4061. doi:10.1073/pnas.94.8.4056.

Coppé, J.P. *et al.* (2010) 'The senescence-associated secretory phenotype: The dark side of tumor suppression', *Annual Review of Pathology: Mechanisms of Disease*. Annu Rev Pathol, pp. 99–118. doi:10.1146/annurev-pathol-121808-102144.

Cortes-Bratti, X. *et al.* (2001) 'The *Haemophilus ducreyi* Cytotoxic Distending Toxin Induces Cell Cycle Arrest and Apoptosis via the DNA Damage Checkpoint Pathways', *Journal of Biological Chemistry*, 276(7), pp. 5296–5302. doi:10.1074/jbc.M008527200.

Cortez, D. *et al.* (2001) 'ATR and ATRIP: Partners in checkpoint signaling', *Science*, 294(5547), pp. 1713–1716. doi:10.1126/science.1065521.

Cougnoux, A. *et al.* (2014) 'Bacterial genotoxin colibactin promotes colon tumour growth by inducing a senescence-associated secretory phenotype', *Gut*, 63(12), pp. 1932–1942. doi:10.1136/gutjnl-2013-305257.

Crawford, R.W. *et al.* (2010) 'Gallstones play a significant role in *Salmonella* spp. gallbladder colonization and carriage', *Proceedings of the National Academy of*

Sciences of the United States of America, 107(9), pp. 4353–4358.

doi:10.1073/pnas.1000862107.

Crouse, J., Kalinke, U. and Oxenius, A. (2015) 'Regulation of antiviral T cell responses by type I interferons', *Nature Reviews Immunology*. Nature Publishing Group, pp. 231–242. doi:10.1038/nri3806.

Crump, J.A. *et al.* (2015) 'Epidemiology, clinical presentation, laboratory diagnosis, antimicrobial resistance, and antimicrobial management of invasive *Salmonella* infections', *Clinical Microbiology Reviews*, 28(4), pp. 901–937.

doi:10.1128/CMR.00002-15.

Crump, J.A. and Mintz, E.D. (2010) 'Global trends in typhoid and paratyphoid fever', *Clinical Infectious Diseases*, 50(2), pp. 241–246. doi:10.1086/649541.

Cuella-Martin, R. *et al.* (2016) '53BP1 Integrates DNA Repair and p53-Dependent Cell Fate Decisions via Distinct Mechanisms', *Molecular Cell*, 64(1), pp. 51–64.

doi:10.1016/j.molcel.2016.08.002.

D'Costa, V.M. *et al.* (2015) 'Salmonella Disrupts Host Endocytic Trafficking by SopD2-Mediated Inhibition of Rab7', *Cell Reports*, 12(9), pp. 1508–1518.

doi:10.1016/J.CELREP.2015.07.063.

D'Cunha, J., Knight, E., *et al.* (1996) 'Immunoregulatory properties of ISG15, an interferon-induced cytokine', *Proceedings of the National Academy of Sciences of the United States of America*, 93(1), pp. 211–215. doi:10.1073/pnas.93.1.211.

D'Cunha, J., Ramanujam, S., *et al.* (1996) 'In vitro and in vivo secretion of human ISG15, an IFN-induced immunomodulatory cytokine.', *Journal of immunology (Baltimore, Md. : 1950)*, 157(9), pp. 4100–8. Available at:

<http://www.jimmunol.org/content/157/9/4100> (Accessed: 6 April 2022).

Dastur, A. *et al.* (2006) 'Herc5, an interferon-induced HECT E3 enzyme, is required for conjugation of ISG15 in human cells', *Journal of Biological Chemistry*, 281(7), pp. 4334–4338. doi:10.1074/jbc.M512830200.

Dauphinee, S.M. *et al.* (2014) 'Contribution of increased ISG15, ISGylation and deregulated type I IFN signaling in Usp18 mutant mice during the course of bacterial infections', *Genes and Immunity*, 15(5), pp. 282–292.

doi:10.1038/gene.2014.17.

Deans, A.J. and West, S.C. (2011) 'DNA interstrand crosslink repair and cancer', *Nature Reviews Cancer*, 11(7), pp. 467–480. doi:10.1038/nrc3088.

Dellaire, G., Kepkay, R. and Bazett-Jones, D.P. (2009) 'High resolution imaging of changes in the structure and spatial organization of chromatin, γ -H2A.X and the MRN complex within etoposide-induced DNA repair foci', *Cell Cycle*, 8(22), pp.

3750–3769. doi:10.4161/cc.8.22.10065.

Dempsey, A. and Bowie, A.G. (2015) 'Innate immune recognition of DNA: A recent history', *Virology*, 479–480, pp. 146–152. doi:10.1016/j.virol.2015.03.013.

Deng, L. *et al.* (2014) 'Host adaptation of a bacterial toxin from the human pathogen salmonella typhi', *Cell*, 159(6), pp. 1290–1299. doi:10.1016/j.cell.2014.10.057.

Desai, S.D. *et al.* (2006) 'Elevated Expression of ISG15 in Tumor Cells Interferes with the Ubiquitin/26S Proteasome Pathway', *Cancer Research*, 66(2), pp. 921–928. doi:10.1158/0008-5472.CAN-05-1123.

Desai, S.D. *et al.* (2012) 'ISG15 disrupts cytoskeletal architecture and promotes motility in human breast cancer cells', *Experimental Biology and Medicine*, 237(1), pp. 38–49. doi:10.1258/ebm.2011.011236.

Deshpande, A., Sicinski, P. and Hinds, P.W. (2005) 'Cyclins and cdks in development and cancer: A perspective', *Oncogene*. Nature Publishing Group, pp. 2909–2915. doi:10.1038/sj.onc.1208618.

Di Domenico, E.G. *et al.* (2017) 'Biofilm producing Salmonella typhi: Chronic colonization and development of gallbladder cancer', *International Journal of Molecular Sciences*, 18(9). doi:10.3390/ijms18091887.

Dong, C. *et al.* (2017) 'ISG15 in host defense against Candida albicans infection in a mouse model of fungal keratitis', *Investigative Ophthalmology and Visual Science*, 58(7), pp. 2948–2958. doi:10.1167/iovs.17-21476.

Dougan, G. and Baker, S. (2014) 'Salmonella enterica serovar typhi and the pathogenesis of typhoid fever', *Annual Review of Microbiology*, 68(1), pp. 317–336. doi:10.1146/annurev-micro-091313-103739.

Dumble, M. *et al.* (2007) 'The impact of altered p53 dosage on hematopoietic stem cell dynamics during aging', *Blood*, 109(4), pp. 1736–1742. doi:10.1182/blood-2006-03-010413.

Dunphy, G. *et al.* (2018) 'Non-canonical Activation of the DNA Sensing Adaptor STING by ATM and IFI16 Mediates NF-κB Signaling after Nuclear DNA Damage', *Molecular Cell*, 71(5), pp. 745–760.e5. doi:10.1016/j.molcel.2018.07.034.

Durfee, L.A. *et al.* (2010) 'The ISG15 Conjugation System Broadly Targets Newly Synthesized Proteins: Implications for the Antiviral Function of ISG15', *Molecular Cell*, 38(5), pp. 722–732. doi:10.1016/j.molcel.2010.05.002.

Dutta, U. *et al.* (2000) 'Typhoid carriers among patients with gallstones are at increased risk for carcinoma of the gallbladder', *The American Journal of Gastroenterology*, 95(3), pp. 784–787. doi:10.1111/j.1572-0241.2000.01860.x.

- Dzimianski, J. V. *et al.* (2019) 'ISG15: It's Complicated', *Journal of Molecular Biology*. Academic Press, pp. 4203–4216. doi:10.1016/j.jmb.2019.03.013.
- Edsall, G. *et al.* (1960) 'Studies on infection and immunity in experimental typhoid fever. I. Typhoid fever in chimpanzees orally infected with *Salmonella typhosa*', *The Journal of experimental medicine*, 112(1), pp. 143–166. doi:10.1084/jem.112.1.143.
- Eigenbrod, T. *et al.* (2015) 'TLR8 Senses Bacterial RNA in Human Monocytes and Plays a Nonredundant Role for Recognition of *Streptococcus pyogenes*', *The Journal of Immunology*, 195(3), pp. 1092–1099. doi:10.4049/jimmunol.1403173.
- El-Deiry, W.S. *et al.* (1993) 'WAF1, a potential mediator of p53 tumor suppression', *Cell*, 75(4), pp. 817–825. doi:10.1016/0092-8674(93)90500-P.
- Elwell, C. *et al.* (2001) 'Escherichia coli CdtB mediates cytolethal distending toxin cell cycle arrest', *Infection and Immunity*, 69(5), pp. 3418–3422. doi:10.1128/IAI.69.5.3418-3422.2001.
- Elwell, C.A. and Dreyfus, L.A. (2000) 'DNase I homologous residues in CdtB are critical for cytolethal distending toxin-mediated cell cycle arrest', *Molecular Microbiology*, 37(4), pp. 952–963. doi:10.1046/j.1365-2958.2000.02070.x.
- Fàbrega, A. and Vila, J. (2013) 'Salmonella enterica serovar Typhimurium skills to succeed in the host: Virulence and regulation', *Clinical Microbiology Reviews*, 26(2), pp. 308–341. doi:10.1128/CMR.00066-12.
- Fahrer, J. *et al.* (2014) 'Cytolethal distending toxin (CDT) is a radiomimetic agent and induces persistent levels of DNA double-strand breaks in human fibroblasts', *DNA Repair*, 18(1), pp. 31–43. doi:10.1016/j.dnarep.2014.03.002.
- Falck, J., Coates, J. and Jackson, S.P. (2005) 'Conserved modes of recruitment of ATM, ATR and DNA-PKcs to sites of DNA damage', *Nature*, 434(7033), pp. 605–611. doi:10.1038/nature03442.
- Fan, J.B. *et al.* (2015) 'Identification and characterization of a novel ISG15-ubiquitin mixed chain and its role in regulating protein homeostasis', *Scientific Reports 2015 5:1*, 5(1), pp. 1–11. doi:10.1038/srep12704.
- Fanning, E., Klimovich, V. and Nager, A.R. (2006) 'A dynamic model for replication protein A (RPA) function in DNA processing pathways', *Nucleic Acids Research*, 34(15), pp. 4126–4137. doi:10.1093/nar/gkl550.
- Farrell, P.J., Broeze, R.J. and Lengyel, P. (1979) 'Accumulation of an mRNA and protein in interferon-treated Ehrlich ascites tumour cells', *Nature*. Nature Publishing Group, pp. 523–525. doi:10.1038/279523a0.
- Feasey, N.A. *et al.* (2015) 'Rapid Emergence of Multidrug Resistant, H58-Lineage

Salmonella Typhi in Blantyre, Malawi', *PLoS Neglected Tropical Diseases*, 9(4). doi:10.1371/journal.pntd.0003748.

Fedor, Y. *et al.* (2013) 'From single-strand breaks to double-strand breaks during S-phase: A new mode of action of the Escherichia coli Cytotoxic Distending Toxin', *Cellular Microbiology*, 15(1), pp. 1–15. doi:10.1111/cmi.12028.

Feng, S. *et al.* (2016) 'Ewing tumor-associated antigen 1 interacts with replication protein A to promote restart of stalled replication forks', *Journal of Biological Chemistry*, 291(42), pp. 21956–21962. doi:10.1074/jbc.C116.747758.

Feng, W. *et al.* (2011) 'Replication stress-induced chromosome breakage is correlated with replication fork progression and is preceded by single-stranded DNA formation', *G3: Genes, Genomes, Genetics*, 1(5), pp. 327–335. doi:10.1534/g3.111.000554.

Feringa, F.M. *et al.* (2018) 'Persistent repair intermediates induce senescence', *Nature Communications*, 9(1). doi:10.1038/s41467-018-06308-9.

Fernandes-Alnemri, T. *et al.* (2009) 'AIM2 activates the inflammasome and cell death in response to cytoplasmic DNA', *Nature*, 458(7237), pp. 509–513. doi:10.1038/nature07710.

Fitzgerald, K.A. *et al.* (2003) 'IKKε and TBK1 are essential components of the IRF3 signalling pathway', *Nature Immunology*, 4(5), pp. 491–496. doi:10.1038/ni921.

Forest, C.G. *et al.* (2010) 'Intracellular survival of Salmonella enterica serovar Typhi in human macrophages is independent of Salmonella pathogenicity island (SPI)-2', *Microbiology (Reading, England)*, 156(Pt 12), pp. 3689–3698. doi:10.1099/MIC.0.041624-0.

Forys, J.T. *et al.* (2014) 'ARF and p53 Coordinate Tumor Suppression of an Oncogenic IFN-β-STAT1-ISG15 Signaling Axis', *Cell Reports*, 7(2), pp. 514–526. doi:10.1016/j.celrep.2014.03.026.

Fowler, C.C. and Galán, J.E. (2018) 'Decoding a Salmonella Typhi Regulatory Network that Controls Typhoid Toxin Expression within Human Cells', *Cell Host and Microbe*, 23(1), pp. 65–76.e6. doi:10.1016/j.chom.2017.12.001.

Frisan, T. *et al.* (2003) 'The Haemophilus ducreyi cytolethal distending toxin induces DNA double-strand breaks and promotes ATM-dependent activation of RhoA', *Cellular Microbiology*, 5(10), pp. 695–707. doi:10.1046/j.1462-5822.2003.00311.x.

Frisan, T. (2016) 'Bacterial genotoxins: The long journey to the nucleus of mammalian cells', *Biochimica et Biophysica Acta - Biomembranes*, 1858(3), pp. 567–575. doi:10.1016/j.bbamem.2015.08.016.

- Fu, Y.Z. *et al.* (2019) 'Human cytomegalovirus protein UL42 antagonizes cGAS/MITA-mediated innate antiviral response', *PLoS Pathogens*, 15(5), p. e1007691. doi:10.1371/journal.ppat.1007691.
- Furnari, B., Rhind, N. and Russell, P. (1997) 'Cdc25 mitotic inducer targeted by Chk1 DNA damage checkpoint kinase', *Science*, 277(5331), pp. 1495–1497. doi:10.1126/science.277.5331.1495.
- Gaines, S., Tully, J.G. and Tigertt, W.D. (1968) 'Studies on infection and immunity in experimental typhoid fever', *Journal of Infectious Diseases*, 118(4), pp. 393–401. doi:10.1093/infdis/118.4.393.
- Gal-Mor, O. (2019) 'Persistent infection and long-term carriage of typhoidal and nontyphoidal salmonellae', *Clinical Microbiology Reviews*, 32(1). doi:10.1128/CMR.00088-18.
- Gal-Mor, O., Boyle, E.C. and Grassl, G.A. (2014) 'Same species, different diseases: How and why typhoidal and non-typhoidal *Salmonella enterica* serovars differ', *Frontiers in Microbiology*, 5(AUG), pp. 1–10. doi:10.3389/fmicb.2014.00391.
- Galán, J.E. (2016) 'Typhoid toxin provides a window into typhoid fever and the biology of salmonella typhi', *Proceedings of the National Academy of Sciences of the United States of America*, 113(23), pp. 6338–6344. doi:10.1073/pnas.1606335113.
- Geiger, T. *et al.* (2018) 'Peptidoglycan editing by a specific Id-transpeptidase controls the muramidase-dependent secretion of typhoid toxin', *Nature Microbiology*, 3(11), pp. 1243–1254. doi:10.1038/s41564-018-0248-x.
- Gelfanova, V., Hansen, E.J. and Spinola, S.M. (1999) 'Cytotoxic distending toxin of *Haemophilus ducreyi* induces apoptotic death of Jurkat T cells', *Infection and Immunity*, 67(12), pp. 6394–6402. doi:10.1128/iai.67.12.6394-6402.1999.
- Giannakopoulos, N. V. *et al.* (2009) 'ISG15 Arg151 and the ISG15-Conjugating Enzyme UbE1L Are Important for Innate Immune Control of Sindbis Virus', *Journal of Virology*, 83(4), pp. 1602–1610. doi:10.1128/jvi.01590-08.
- Gibani, M.M. *et al.* (2019) 'Investigation of the role of typhoid toxin in acute typhoid fever in a human challenge model', *Nature Medicine*, 25(7), pp. 1082–1088. doi:10.1038/s41591-019-0505-4.
- Gilman, R.H. *et al.* (1975) 'Relative efficacy of blood, urine, rectal swab, bone marrow, and rose-spot cultures for recovery of *Salmonella Typhi* in typhoid fever', *The Lancet*, 305(7918), pp. 1211–1213. doi:10.1016/S0140-6736(75)92194-7.
- Grandvaux, N. *et al.* (2002) 'Transcriptional Profiling of Interferon Regulatory Factor 3 Target Genes: Direct Involvement in the Regulation of Interferon-Stimulated

Genes', *Journal of Virology*, 76(11), pp. 5532–5539. doi:10.1128/jvi.76.11.5532-5539.2002.

Grasso, F. and Frisan, T. (2015) 'Bacterial genotoxins: Merging the DNA damage response into infection biology', *Biomolecules*, 5(3), pp. 1762–1782. doi:10.3390/biom5031762.

Grazioli, S. and Pugin, J. (2018) 'Mitochondrial damage-associated molecular patterns: From inflammatory signaling to human diseases', *Frontiers in Immunology*. Frontiers Media SA, p. 1. doi:10.3389/fimmu.2018.00832.

Gross, A. *et al.* (1998) 'Enforced dimerization of BAX results in its translocation, mitochondrial dysfunction and apoptosis', *EMBO Journal*, 17(14), pp. 3878–3885. doi:10.1093/emboj/17.14.3878.

Guerra, L. *et al.* (2005) 'Cellular internalization of cytolethal distending toxin: A new end to a known pathway', *Cellular Microbiology*, 7(7), pp. 921–934. doi:10.1111/j.1462-5822.2005.00520.x.

Guerra, L. *et al.* (2009) 'A novel mode of translocation for cytolethal distending toxin', *Biochimica et Biophysica Acta - Molecular Cell Research*, 1793(3), pp. 489–495. doi:10.1016/j.bbamcr.2008.11.017.

Guerra, L. *et al.* (2011) 'The biology of the cytolethal distending toxins', *Toxins*, 3(3), pp. 172–190. doi:10.3390/toxins3030172.

Gui, X. *et al.* (2019) 'Autophagy induction via STING trafficking is a primordial function of the cGAS pathway', *Nature*, 567(7747), pp. 262–266. doi:10.1038/s41586-019-1006-9.

Guidi, R., Guerra, L., *et al.* (2013) 'Chronic exposure to the cytolethal distending toxins of Gram-negative bacteria promotes genomic instability and altered DNA damage response', *Cellular Microbiology*, 15(1), pp. 98–113. doi:10.1111/cmi.12034.

Guidi, R., Levi, L., *et al.* (2013) 'Salmonella enterica delivers its genotoxin through outer membrane vesicles secreted from infected cells', *Cellular Microbiology*, 15(12), pp. 2034–2050. doi:10.1111/cmi.12172.

Gunn, J.S. *et al.* (2014) 'Salmonella chronic carriage: Epidemiology, diagnosis, and gallbladder persistence', *Trends in Microbiology*, 22(11), pp. 648–655. doi:10.1016/j.tim.2014.06.007.

Günster, R.A. *et al.* (2017) 'SseK1 and SseK3 T3SS effectors inhibit NF- κ B signalling and necroptotic cell death in Salmonella-infected macrophages', *Infection and Immunity*, 85(6). Available at: <http://iai.asm.org/> (Accessed: 15 November 2022).

Guo, Z. *et al.* (2010) 'ATM activation by oxidative stress', *Science*, 330(6003), pp. 517–521. doi:10.1126/science.1192912.

Haahr, P. *et al.* (2016) 'Activation of the ATR kinase by the RPA-binding protein ETAA1', *Nature Cell Biology*, 18(11), pp. 1196–1207. doi:10.1038/ncb3422.

Haas, A.L. *et al.* (1987) 'Interferon induced a 15-kilodalton protein exhibiting marked homology to ubiquitin', *Journal of Biological Chemistry*, 262(23), pp. 11315–11323. doi:10.1016/s0021-9258(18)60961-5.

Haghjoo, E. and Galán, J.E. (2004) 'Salmonella typhi encodes a functional cytolethal distending toxin that is delivered into host cells by a bacterial-internalization pathway', *Proceedings of the National Academy of Sciences of the United States of America*, 101(13), pp. 4614–4619. doi:10.1073/pnas.0400932101.

Haghjoo, E. and Galán, J.E. (2007) 'Identification of a transcriptional regulator that controls intracellular gene expression in Salmonella Typhi', *Molecular Microbiology*, 64(6), pp. 1549–1561. doi:10.1111/j.1365-2958.2007.05754.x.

Haller, O., Kochs, G. and Weber, F. (2007) 'Interferon, Mx, and viral countermeasures', *Cytokine and Growth Factor Reviews*, 18(5–6), pp. 425–433. doi:10.1016/j.cytogfr.2007.06.001.

Hamerman, J.A. *et al.* (2002) 'Serpine 2a Is Induced in Activated Macrophages and Conjugates to a Ubiquitin Homolog', *The Journal of Immunology*, 168(5), pp. 2415–2423. doi:10.4049/jimmunol.168.5.2415.

Hannemann, S. and Galán, J.E. (2017) 'Salmonella enterica serovar-specific transcriptional reprogramming of infected cells', *PLoS Pathogens*. Edited by A.J. Baumler, 13(7), p. e1006532. doi:10.1371/journal.ppat.1006532.

Hardt, W.D. *et al.* (1998) 'S. typhimurium Encodes an activator of Rho GTPases that induces membrane ruffling and nuclear responses in host cells', *Cell*, 93(5), pp. 815–826. doi:10.1016/S0092-8674(00)81442-7.

Haseley, A. *et al.* (2012) 'Extracellular matrix protein CCN1 limits oncolytic efficacy in glioma', *Cancer Research*, 72(6), pp. 1353–1362. doi:10.1158/0008-5472.CAN-11-2526.

Hassane, D.C. *et al.* (2001) 'Cytolethal distending toxin demonstrates genotoxic activity in a yeast model', *Infection and Immunity*, 69(9), pp. 5752–5759. doi:10.1128/IAI.69.9.5752-5759.2001.

Hassane, D.C., Lee, R.B. and Pickett, C.L. (2003) 'Campylobacter jejuni cytolethal distending toxin promotes DNA repair responses in normal human cells', *Infection and Immunity*, 71(1), pp. 541–545. doi:10.1128/IAI.71.1.541-545.2003.

- Haupt, Y. *et al.* (1997) 'Mdm2 promotes the rapid degradation of p53', *Nature*, 387(6630), pp. 296–299. doi:10.1038/387296a0.
- Helbig, K.J. *et al.* (2019) 'The interferon stimulated gene viperin, restricts *Shigella flexneri* in vitro', *Scientific Reports*, 9(1), p. 15598. doi:10.1038/s41598-019-52130-8.
- Helbig, K.J. and Beard, M.R. (2014) 'The role of viperin in the innate antiviral response', *Journal of Molecular Biology*, 426(6), pp. 1210–1219. doi:10.1016/j.jmb.2013.10.019.
- Held, T. *et al.* (2021) 'Evidence for an involvement of the ubiquitin-like modifier ISG15 in MHC class I antigen presentation', *European Journal of Immunology*, 51(1), pp. 138–150. doi:10.1002/eji.202048646.
- Henry, T. *et al.* (2010) 'Type I IFN Signaling Constrains IL-17A/F Secretion by $\gamma\delta$ T Cells during Bacterial Infections', *The Journal of Immunology*, 184(7), pp. 3755 LP – 3767. doi:10.4049/jimmunol.0902065.
- Hensel, M. *et al.* (1998) 'Genes encoding putative effector proteins of the type III secretion system of *Salmonella* pathogenicity island 2 are required for bacterial virulence and proliferation in macrophages', *Molecular microbiology*, 30(1), pp. 163–174. doi:10.1046/J.1365-2958.1998.01047.X.
- Hermann, M. and Bogunovic, D. (2017) *ISG15: In Sickness and in Health*, *Trends in Immunology*. Elsevier Ltd. doi:10.1016/j.it.2016.11.001.
- Hernandez-Segura, A., Nehme, J. and Demaria, M. (2018) 'Hallmarks of Cellular Senescence', *Trends in Cell Biology*, 28(6), pp. 436–453. doi:10.1016/j.tcb.2018.02.001.
- Hernandez, L.D. *et al.* (2004) 'Salmonella Modulates Vesicular Traffic by Altering Phosphoinositide Metabolism', *Science*, 304(5678), pp. 1805–1807. doi:10.1126/science.1098188.
- Hodak, H. and Galán, J.E. (2013) 'A *Salmonella Typhi* homologue of bacteriophage muramidases controls typhoid toxin secretion', *EMBO Reports*, 14(1), pp. 95–102. doi:10.1038/embor.2012.186.
- Honda, K., Takaoka, A. and Taniguchi, T. (2006) 'Type I Interferon Gene Induction by the Interferon Regulatory Factor Family of Transcription Factors', *Immunity*. Cell Press, pp. 349–360. doi:10.1016/j.immuni.2006.08.009.
- Hornung, V. *et al.* (2009) 'AIM2 recognizes cytosolic dsDNA and forms a caspase-1-activating inflammasome with ASC', *Nature*, 458(7237), pp. 514–518. doi:10.1038/nature07725.

- Hsiang, Y.H. *et al.* (1985) 'Camptothecin induces protein-linked DNA breaks via mammalian DNA topoisomerase I', *Journal of Biological Chemistry*, 260(27), pp. 14873–14878. doi:10.1016/s0021-9258(17)38654-4.
- Huang, J. *et al.* (2009) 'SOSS Complexes Participate in the Maintenance of Genomic Stability', *Molecular Cell*, 35(3), pp. 384–393. doi:10.1016/j.molcel.2009.06.011.
- Humphreys, D. *et al.* (2012) 'Salmonella virulence effector SopE and host GEF ARNO cooperate to recruit and activate WAVE to trigger bacterial invasion', *Cell Host and Microbe*, 11(2), pp. 129–139. doi:10.1016/j.chom.2012.01.006.
- Hussein Gasem, M. *et al.* (1995) 'Culture of Salmonella typhi and Salmonella paratyphi from blood and bone marrow in suspected typhoid fever', *Tropical and Geographical Medicine*, 47(4), pp. 164–167. Available at: <https://pubmed.ncbi.nlm.nih.gov/8560588/> (Accessed: 12 May 2022).
- Ibler, A.E.M. *et al.* (2019) 'Typhoid toxin exhausts the RPA response to DNA replication stress driving senescence and Salmonella infection', *Nature Communications*, 10(1), pp. 1–14. doi:10.1038/s41467-019-12064-1.
- Innocente, S.A. *et al.* (1999) 'p53 regulates a G2 checkpoint through cyclin B1', *Proceedings of the National Academy of Sciences of the United States of America*, 96(5), pp. 2147–2152. doi:10.1073/pnas.96.5.2147.
- Isaacs, A. and Lindenmann, J. (1988) 'Virus Interference: I. The Interferon', *CA: A Cancer Journal for Clinicians*, 38(5), pp. 280–290. doi:10.3322/canjclin.38.5.280.
- Ishii, K.J. *et al.* (2008) 'Host Innate Immune Receptors and Beyond: Making Sense of Microbial Infections', *Cell Host and Microbe*. Cell Press, pp. 352–363. doi:10.1016/j.chom.2008.05.003.
- Ishikawa, H. and Barber, G.N. (2008) 'STING is an endoplasmic reticulum adaptor that facilitates innate immune signalling', *Nature*, 456(7219), p. 274. doi:10.1038/nature07432.
- Jackson, S.P. and Bartek, J. (2009) 'The DNA-damage response in human biology and disease', *Nature*, 461(7267), pp. 1071–1078. doi:10.1038/nature08467.
- Jalal, S., Earley, J.N. and Turchi, J.J. (2011) 'DNA repair: From genome maintenance to biomarker and therapeutic target', *Clinical Cancer Research*, 17(22), pp. 6973–6984. doi:10.1158/1078-0432.CCR-11-0761.
- Jansen, A.M. *et al.* (2011) 'A salmonella typhimurium-typhi genomic chimera: A model to study vi polysaccharide capsule function in vivo', *PLoS Pathogens*, 7(7). doi:10.1371/journal.ppat.1002131.

- Jennings, E., Thurston, T.L.M. and Holden, D.W. (2017) 'Salmonella SPI-2 Type III Secretion System Effectors: Molecular Mechanisms And Physiological Consequences', *Cell host & microbe*, 22(2), pp. 217–231. doi:10.1016/J.CHOM.2017.07.009.
- Jeon, Y.J. *et al.* (2012) 'Chemosensitivity is controlled by p63 modification with ubiquitin-like protein ISG15', *Journal of Clinical Investigation*, 122(7), pp. 2622–2636. doi:10.1172/JCI61762.
- Jeon, Y.J., Park, J.H. and Chung, C.H. (2017) *Interferon-stimulated gene 15 in the control of cellular responses to genotoxic stress*, *Molecules and Cells*. Korean Society for Molecular and Cellular Biology. doi:10.14348/molcells.2017.0027.
- Jette, N. and Lees-Miller, S.P. (2015) 'The DNA-dependent protein kinase: A multifunctional protein kinase with roles in DNA double strand break repair and mitosis', *Progress in Biophysics and Molecular Biology*. Elsevier Ltd, pp. 194–205. doi:10.1016/j.pbiomolbio.2014.12.003.
- Jin, C. *et al.* (2017) 'Efficacy and immunogenicity of a Vi-tetanus toxoid conjugate vaccine in the prevention of typhoid fever using a controlled human infection model of Salmonella Typhi: a randomised controlled, phase 2b trial', *The Lancet*, 390(10111), pp. 2472–2480. doi:10.1016/S0140-6736(17)32149-9.
- Johnson, R. *et al.* (2017) 'The Type III Secretion System Effector SptP of Salmonella enterica Serovar Typhi', *Journal of bacteriology*, 199(4). doi:10.1128/JB.00647-16.
- Kagan, J.C. *et al.* (2008) 'TRAM couples endocytosis of Toll-like receptor 4 to the induction of interferon- β ', *Nature Immunology*, 9(4), pp. 361–368. doi:10.1038/ni1569.
- Kanteh, A. *et al.* (2021) 'Invasive atypical non-typhoidal Salmonella serovars in The Gambia', *Microbial Genomics*, 7(11). doi:10.1099/mgen.0.000677.
- Kar, A. *et al.* (2015) 'RPA70 depletion induces hSSB1/2-INTS3 complex to initiate ATR signaling', *Nucleic Acids Research*, 43(10), pp. 4962–4974. doi:10.1093/nar/gkv369.
- Kawasaki, T., Kawai, T. and Akira, S. (2011) 'Recognition of nucleic acids by pattern-recognition receptors and its relevance in autoimmunity', *Immunological Reviews*, 243(1), pp. 61–73. doi:10.1111/j.1600-065X.2011.01048.x.
- Kerr, J.F.R., Wyllie, A.H. and Currie, A.R. (1972) 'Apoptosis: A basic biological phenomenon with wide-ranging implications in tissue kinetics', *British Journal of Cancer*, 26(4), pp. 239–257. doi:10.1038/bjc.1972.33.
- Ketscher, L. *et al.* (2012) 'MHERC6 is the essential ISG15 E3 ligase in the murine system', *Biochemical and Biophysical Research Communications*, 417(1), pp. 135–

140. doi:10.1016/j.bbrc.2011.11.071.

Kim, K. Il *et al.* (2004) 'Interferon-Inducible Ubiquitin E2, Ubc8, Is a Conjugating Enzyme for Protein ISGylation', *Molecular and Cellular Biology*, 24(21), pp. 9592–9600. doi:10.1128/mcb.24.21.9592-9600.2004.

Kim, Y.C. *et al.* (2009) 'Activation of ATM depends on chromatin interactions occurring before induction of DNA damage', *Nature Cell Biology*, 11(1), pp. 92–96. doi:10.1038/ncb1817.

Kimmey, J.M. *et al.* (2017) 'The impact of ISGylation during Mycobacterium tuberculosis infection in mice', *Microbes and Infection*, 19(4–5), pp. 249–258. doi:10.1016/j.micinf.2016.12.006.

Kinner, A. *et al.* (2008) 'Gamma-H2AX in recognition and signaling of DNA double-strand breaks in the context of chromatin.', *Nucleic acids research*. Nucleic Acids Res, pp. 5678–5694. doi:10.1093/nar/gkn550.

Kisiela, D.I. *et al.* (2012) 'Evolution of Salmonella enterica Virulence via point mutations in the fimbrial adhesin', *PLoS Pathogens*, 8(6). doi:10.1371/journal.ppat.1002733.

Klemm, E.J. *et al.* (2018) 'Emergence of an extensively drug-resistant Salmonella enterica serovar typhi clone harboring a promiscuous plasmid encoding resistance to fluoroquinolones and third-generation cephalosporins', *mBio*, 9(1). doi:10.1128/mBio.00105-18.

Knight, E. *et al.* (1988) 'A 15-kDa interferon-induced protein is derived by COOH-terminal processing of a 17-kDa precursor', *Journal of Biological Chemistry*, 263(10), pp. 4520–4522. doi:10.1016/s0021-9258(18)68812-x.

Knight, E. and Cordova, B. (1991) 'IFN-induced 15-kDa protein is released from human lymphocytes and monocytes.', *Journal of immunology (Baltimore, Md. : 1950)*, 146(7), pp. 2280–4. Available at: <http://www.jimmunol.org/> (Accessed: 6 April 2022).

Knobeloch, K.-P. *et al.* (2005) 'Reexamination of the Role of Ubiquitin-Like Modifier ISG15 in the Phenotype of UBP43-Deficient Mice', *Molecular and Cellular Biology*, 25(24), pp. 11030–11034. Available at: <https://journals.asm.org/doi/full/10.1128/MCB.25.24.11030-11034.2005> (Accessed: 6 April 2022).

Knodler, L.A. *et al.* (2009) 'Ubiquitination of the bacterial inositol phosphatase, SopB, regulates its biological activity at the plasma membrane.', *Cellular microbiology*, 11(11), pp. 1652–1670. doi:10.1111/j.1462-5822.2009.01356.x.

Knodler, L.A. *et al.* (2014) 'Noncanonical inflammasome activation of caspase-

4/caspase-11 mediates epithelial defenses against enteric bacterial pathogens', *Cell Host and Microbe*, 16(2), pp. 249–256. doi:10.1016/j.chom.2014.07.002.

Knodler, L.A., Finlay, B. and Steele-Mortimer, O. (2005) 'The Salmonella effector protein SopB protects epithelial cells from apoptosis by sustained activation of Akt', *Journal of Biological Chemistry*, 280(10), pp. 9058–9064. doi:10.1074/jbc.M412588200.

Knuff, K. and Finlay, B.B. (2017) 'What the SIF Is happening—The role of intracellular Salmonella-induced filaments', *Frontiers in Cellular and Infection Microbiology*, 7(JUL), p. 335. doi:10.3389/fcimb.2017.00335.

Kondo, T. *et al.* (2013) 'DNA damage sensor MRE11 recognizes cytosolic double-stranded DNA and induces type I interferon by regulating STING trafficking', *Proceedings of the National Academy of Sciences of the United States of America*, 110(8), pp. 2969–2974. doi:10.1073/pnas.1222694110.

Konno, H. *et al.* (2018) 'Suppression of STING signaling through epigenetic silencing and missense mutation impedes DNA damage mediated cytokine production', *Oncogene*, 37(15), pp. 2037–2051. doi:10.1038/s41388-017-0120-0.

Korant, B.D. *et al.* (1984) 'Interferon-induced proteins. Purification and characterization of a 15,000-dalton protein from human and bovine cells induced by interferon', *Journal of Biological Chemistry*, 259(23), pp. 14835–14839. doi:10.1016/s0021-9258(17)42679-2.

Koshiol, J. *et al.* (2016) 'Salmonella enterica serovar Typhi and gallbladder cancer: a case-control study and meta-analysis', *Cancer Medicine*, 5(11), pp. 3235–3310. doi:10.1002/cam4.915.

Kozlov, S. V. *et al.* (2011) 'Autophosphorylation and ATM activation: Additional sites add to the complexity', *Journal of Biological Chemistry*, 286(11), pp. 9107–9119. doi:10.1074/jbc.M110.204065.

Kreienkamp, R. *et al.* (2018) 'A Cell-Intrinsic Interferon-like Response Links Replication Stress to Cellular Aging Caused by Progerin', *Cell Reports*, 22(8), pp. 2006–2015. doi:10.1016/j.celrep.2018.01.090.

Kumagai, A. *et al.* (2006) 'TopBP1 activates the ATR-ATRIP complex', *Cell*, 124(5), pp. 943–955. doi:10.1016/j.cell.2005.12.041.

Kumagai, A. and Dunphy, W.G. (2000) 'Claspin, a novel protein required for the activation of Chk1 during a DNA replication checkpoint response in *Xenopus* egg extracts', *Molecular Cell*, 6(4), pp. 839–849. doi:10.1016/S1097-2765(05)00092-4.

Kunkel, T.A. and Loeb, L.A. (1981) 'Fidelity of mammalian DNA polymerases', *Science*, 213(4509), pp. 765–767. doi:10.1126/science.6454965.

- Lai, C. *et al.* (2009) 'Mice Lacking the ISG15 E1 Enzyme UbE1L Demonstrate Increased Susceptibility to both Mouse-Adapted and Non-Mouse-Adapted Influenza B Virus Infection', *Journal of Virology*, 83(2), pp. 1147–1151. doi:10.1128/jvi.00105-08.
- Lama, L. *et al.* (2019) 'Development of human cGAS-specific small-molecule inhibitors for repression of dsDNA-triggered interferon expression', *Nature Communications*, 10(1), p. 2261. doi:10.1038/s41467-019-08620-4.
- Lara-Tejero, M. and Galán, J.E. (2000) 'A bacterial toxin that controls cell cycle progression as a deoxyribonuclease I-like protein', *Science*, 290(5490), pp. 354–357. doi:10.1126/science.290.5490.354.
- Lara-Tejero, M. and Galán, J.E. (2001) 'CdtA, CdtB, and CdtC form a tripartite complex that is required for cytolethal distending toxin activity', *Infection and Immunity*, 69(7), pp. 4358–4365. doi:10.1128/IAI.69.7.4358-4365.2001.
- Lara-Tejero, M. and Galán, J.E. (2002) 'Cytolethal distending toxin: Limited damage as a strategy to modulate cellular functions', *Trends in Microbiology*, 10(3), pp. 147–152. doi:10.1016/S0966-842X(02)02316-8.
- Lazebnik, Y.A. *et al.* (1994) 'Cleavage of poly(ADP-ribose) polymerase by a proteinase with properties like ICE', *Nature*, 371(6495), pp. 346–347. doi:10.1038/371346a0.
- Lazebnik, Y.A. *et al.* (1995) 'Studies of the lamin proteinase reveal multiple parallel biochemical pathways during apoptotic execution', *Proceedings of the National Academy of Sciences of the United States of America*, 92(20), pp. 9042–9046. doi:10.1073/pnas.92.20.9042.
- Lee, J., Kumagai, A. and Dunphy, W.G. (2007) 'The Rad9-Hus1-Rad1 checkpoint clamp regulates interaction of TopBP1 with ATR', *Journal of Biological Chemistry*, 282(38), pp. 28036–28044. doi:10.1074/jbc.M704635200.
- Lee, J.J. *et al.* (2019) 'HMGB1 modulates the balance between senescence and apoptosis in response to genotoxic stress', *FASEB Journal*, 33(10), pp. 10942–10953. doi:10.1096/fj.201900288R.
- Lee, S. *et al.* (2020) 'Salmonella Typhoid Toxin PltB Subunit and Its Non-typhoidal Salmonella Ortholog Confer Differential Host Adaptation and Virulence', *Cell host & microbe*, 27(6), pp. 937-949.e6. doi:10.1016/J.CHOM.2020.04.005.
- Lee, Y.C. *et al.* (2016) 'RPA-Binding Protein ETAA1 Is an ATR Activator Involved in DNA Replication Stress Response', *Current Biology*, 26(24), pp. 3257–3268. doi:10.1016/j.cub.2016.10.030.
- Leisching, G. *et al.* (2019) 'OAS1, OAS2 and OAS3 restrict intracellular M. tb

- replication and enhance cytokine secretion.’, *International journal of infectious diseases: IJID: official publication of the International Society for Infectious Diseases*, 80S, pp. S77–S84. doi:10.1016/j.ijid.2019.02.029.
- LeMessurier, K.S. *et al.* (2013) ‘Type I Interferon Protects against Pneumococcal Invasive Disease by Inhibiting Bacterial Transmigration across the Lung’, *PLOS Pathogens*, 9(11), p. e1003727. Available at: <https://doi.org/10.1371/journal.ppat.1003727>.
- Lenschow, D.J. *et al.* (2005) ‘Identification of Interferon-Stimulated Gene 15 as an Antiviral Molecule during Sindbis Virus Infection In Vivo’, *Journal of Virology*, 79(22), pp. 13974–13983. doi:10.1128/jvi.79.22.13974-13983.2005.
- Lenschow, D.J. *et al.* (2007) ‘IFN-stimulated gene 15 functions as a critical antiviral molecule against influenza, herpes, and Sindbis viruses’, *Proceedings of the National Academy of Sciences of the United States of America*, 104(4), pp. 1371–1376. doi:10.1073/pnas.0607038104.
- Levy, D.E. *et al.* (1989) ‘Cytoplasmic activation of ISGF3, the positive regulator of interferon-alpha-stimulated transcription, reconstituted in vitro.’, *Genes & development*, 3(9), pp. 1362–1371. doi:10.1101/gad.3.9.1362.
- Li, D. and Wu, M. (2021) ‘Pattern recognition receptors in health and diseases’, *Signal Transduction and Targeted Therapy*. doi:10.1038/s41392-021-00687-0.
- Li, J. *et al.* (2001) ‘Novel NEMO/I κ B Kinase and NF- κ B Target Genes at the Pre-B to Immature B Cell Transition’, *Journal of Biological Chemistry*, 276(21), pp. 18579–18590. doi:10.1074/jbc.M100846200.
- Li, L.Q. *et al.* (2002) ‘The Haemophilus ducreyi cytolethal distending toxin activates sensors of DNA damage and repair complexes in proliferating and non-proliferating cells’, *Cellular Microbiology*, 4(2), pp. 87–99. doi:10.1046/j.1462-5822.2002.00174.x.
- Liang, S.L., Quirk, D. and Zhou, A. (2006) ‘RNase L: Its biological roles and regulation’, *IUBMB Life*, 58(9), pp. 508–514. doi:10.1080/15216540600838232.
- Lin, S.L., Le, T.X. and Cowen, D.S. (2003) ‘SptP, a Salmonella typhimurium type III-secreted protein, inhibits the mitogen-activated protein kinase pathway by inhibiting Raf activation’, *Cellular microbiology*, 5(4), pp. 267–275. doi:10.1046/J.1462-5822.2003.T01-1-00274.X.
- Lindahl, T. and Barnes, D.E. (2000) ‘Repair of endogenous DNA damage’, *Cold Spring Harbor Symposia on Quantitative Biology*, 65, pp. 127–133. doi:10.1101/sqb.2000.65.127.
- Liss, V. *et al.* (2017) ‘Salmonella enterica Remodels the Host Cell Endosomal

- System for Efficient Intravacuolar Nutrition', *Cell Host and Microbe*, 21(3), pp. 390–402. doi:10.1016/j.chom.2017.02.005.
- Liu, M., Xiao-Ling and Hassel, B.A. (2003) 'Proteasomes Modulate Conjugation to the Ubiquitin-like Protein, ISG15', *Journal of Biological Chemistry*, 278(3), pp. 1594–1602. doi:10.1074/JBC.M208123200.
- Liu, Q. *et al.* (2000) 'Chk1 is an essential kinase that is regulated by Atr and required for the G2/M DNA damage checkpoint', *Genes and Development*, 14(12), pp. 1448–1459. doi:10.1101/gad.14.12.1448.
- Liu, S. *et al.* (2012) 'Distinct roles for DNA-PK, ATM and ATR in RPA phosphorylation and checkpoint activation in response to replication stress', *Nucleic Acids Research*, 40(21), pp. 10780–10794. doi:10.1093/nar/gks849.
- Loeb, K.R. and Haas, A.L. (1992) 'The interferon-inducible 15-kDa ubiquitin homolog conjugates to intracellular proteins', *Journal of Biological Chemistry*, 267(11), pp. 7806–7813. doi:10.1016/s0021-9258(18)42585-9.
- Lorkowski, M. *et al.* (2014) 'Salmonella enterica invasion of polarized epithelial cells is a highly cooperative effort', *Infection and Immunity*, 82(6), pp. 2657–2667. doi:10.1128/IAI.00023-14.
- Louis, C., Burns, C. and Wicks, I. (2018) 'TANK-binding kinase 1-dependent responses in health and autoimmunity', *Frontiers in Immunology*. Frontiers Media SA, p. 434. doi:10.3389/fimmu.2018.00434.
- Luu, K. *et al.* (2014) 'STAT1 plays a role in TLR signal transduction and inflammatory responses', *Immunology and Cell Biology*, 92(9), pp. 761–769. doi:10.1038/icb.2014.51.
- Ma, Y. *et al.* (2002) 'Hairpin opening and overhang processing by an Artemis/DNA-dependent protein kinase complex in nonhomologous end joining and V(D)J recombination', *Cell*, 108(6), pp. 781–794. doi:10.1016/S0092-8674(02)00671-2.
- MacKenzie, K.J. *et al.* (2017) 'CGAS surveillance of micronuclei links genome instability to innate immunity', *Nature*, 548(7668), pp. 461–465. doi:10.1038/nature23449.
- Malakhov, M.P. *et al.* (2002) 'UBP43 (USP18) specifically removes ISG15 from conjugated proteins', *Journal of Biological Chemistry*, 277(12), pp. 9976–9981. doi:10.1074/jbc.M109078200.
- Malakhov, M.P. *et al.* (2003) 'High-throughput immunoblotting: Ubiquitin-like protein ISG15 modifies key regulators of signal transduction', *Journal of Biological Chemistry*, 278(19), pp. 16608–16613. doi:10.1074/jbc.M208435200.

- Malakhova, O.A. *et al.* (2006) 'UBP43 is a novel regulator of interferon signaling independent of its ISG15 isopeptidase activity', *EMBO Journal*, 25(11), pp. 2358–2367. doi:10.1038/sj.emboj.7601149.
- Mancuso, G. *et al.* (2009) 'Bacterial recognition by TLR7 in the lysosomes of conventional dendritic cells', *Nature Immunology*, 10(6), pp. 587–594. doi:10.1038/ni.1733.
- Mao, H. *et al.* (2016) 'Interferon-stimulated gene 15 induces cancer cell death by suppressing the NF- κ B signaling pathway', *Oncotarget*, 7(43), pp. 70143–70151. doi:10.18632/oncotarget.12160.
- Martin, O.C.B. *et al.* (2021) 'Influence of the microenvironment on modulation of the host response by typhoid toxin', *Cell Reports*, 35(1), p. 108931. doi:10.1016/j.celrep.2021.108931.
- Martínez-Campos, C., Burguete-García, A.I. and Madrid-Marina, V. (2017) 'Role of TLR9 in Oncogenic Virus-Produced Cancer', *Viral Immunology*, 30(2), pp. 98–105. doi:10.1089/vim.2016.0103.
- Matsuoka, S. *et al.* (2000) 'Ataxia telangiectasia-mutated phosphorylates Chk2 in vivo and in vitro', *Proceedings of the National Academy of Sciences of the United States of America*, 97(19), pp. 10389–10394. doi:10.1073/pnas.190030497.
- Mattiroli, F. *et al.* (2012) 'RNF168 ubiquitinates K13-15 on H2A/H2AX to drive DNA damage signaling', *Cell*, 150(6), pp. 1182–1195. doi:10.1016/j.cell.2012.08.005.
- Mavragani, I. V. *et al.* (2019) 'Ionizing radiation and complex DNA damage: From prediction to detection challenges and biological significance', *Cancers*. Multidisciplinary Digital Publishing Institute (MDPI). doi:10.3390/cancers11111789.
- Maya-Mendoza, A. *et al.* (2007) 'Chk1 regulates the density of active replication origins during the vertebrate S phase', *EMBO Journal*, 26(11), pp. 2719–2731. doi:10.1038/sj.emboj.7601714.
- Mazurkiewicz, P. *et al.* (2008) 'SpvC is a Salmonella effector with phosphothreonine lyase activity on host mitogen-activated protein kinases', *Molecular Microbiology*, 67(6), pp. 1371–1383. doi:10.1111/J.1365-2958.2008.06134.X.
- McGhie, E.J. *et al.* (2009) 'Salmonella takes control: effector-driven manipulation of the host', *Current Opinion in Microbiology*, 12(1), pp. 117–124. doi:10.1016/j.mib.2008.12.001.
- McGhie, E.J., Hayward, R.D. and Koronakis, V. (2001) 'Cooperation between actin-binding proteins of invasive Salmonella: SipA potentiates SipC nucleation and bundling of actin', *EMBO Journal*, 20(9), pp. 2131–2139. doi:10.1093/emboj/20.9.2131.

McGhie, E.J., Hayward, R.D. and Koronakis, V. (2004) 'Control of actin turnover by a Salmonella invasion protein', *Molecular Cell*, 13(4), pp. 497–510. doi:10.1016/S1097-2765(04)00053-X.

Medzhitov, R. (2007) 'Recognition of microorganisms and activation of the immune response', *Nature*, pp. 819–826. doi:10.1038/nature06246.

Meyer, K. *et al.* (2015) 'Interferon- α inducible protein 6 impairs EGFR activation by CD81 and inhibits hepatitis C virus infection', *Scientific Reports*, 5, pp. 1–10. doi:10.1038/srep09012.

Michalska, A. *et al.* (2018) 'A positive feedback amplifier circuit that regulates interferon (IFN)-stimulated gene expression and controls type I and type II IFN responses', *Frontiers in Immunology*, 9(MAY), pp. 1–17. doi:10.3389/fimmu.2018.01135.

Miller, R. and Wiedmann, M. (2016) 'Dynamic duo—The salmonella cytolethal distending toxin combines ADP-ribosyltransferase and nuclease activities in a novel form of the cytolethal distending toxin', *Toxins*. Toxins (Basel). doi:10.3390/toxins8050121.

Miller, R.A. *et al.* (2018) 'The typhoid toxin produced by the Nontyphoidal Salmonella enterica Serotype javiana is required for induction of a DNA damage response in Vitro and systemic spread in Vivo', *mBio*, 9(2), pp. 1–16. doi:10.1128/mBio.00467-18.

Miller, R.A. and Wiedmann, M. (2016) 'The cytolethal distending toxin produced by nontyphoidal Salmonella serotypes javiana, montevideo, oranienburg, and mississippi induces DNA damage in a manner similar to that of serotype Typhi', *mBio*, 7(6). doi:10.1128/mBio.02109-16.

Milligan, R. *et al.* (2018) 'Vaccines for preventing typhoid fever', *Cochrane Database of Systematic Reviews*, 2018(5). doi:10.1002/14651858.CD001261.pub4.

Morales, D.J. and Lenschow, D.J. (2013) 'The antiviral activities of ISG15', *Journal of Molecular Biology*. J Mol Biol, pp. 4995–5008. doi:10.1016/j.jmb.2013.09.041.

Mukherjee, B. *et al.* (2006) 'DNA-PK phosphorylates histone H2AX during apoptotic DNA fragmentation in mammalian cells', *DNA Repair*, 5(5), pp. 575–590. doi:10.1016/j.dnarep.2006.01.011.

Muñoz-Fontela, C. *et al.* (2008) 'Transcriptional role of p53 in interferon-mediated antiviral immunity', *Journal of Experimental Medicine*, 205(8), pp. 1929–1938. doi:10.1084/jem.20080383.

Murai, J. *et al.* (2018) 'SLFN11 Blocks Stressed Replication Forks Independently of ATR', *Molecular Cell*, 69(3), pp. 371–384.e6. doi:10.1016/j.molcel.2018.01.012.

- Mustachio, L.M. *et al.* (2017) 'The ISG15-specific protease USP18 regulates stability of PTEN', *Oncotarget*, 8(1), pp. 3–14. doi:10.18632/oncotarget.13914.
- Nakad, R. and Schumacher, B. (2016) 'DNA damage response and immune defense: Links and mechanisms', *Frontiers in Genetics*, 7(AUG), p. 147. doi:10.3389/FGENE.2016.00147/BIBTEX.
- Narasimhan, J. *et al.* (2005) 'Crystal structure of the interferon-induced ubiquitin-like protein ISG15', *Journal of Biological Chemistry*, 280(29), pp. 27356–27365. doi:10.1074/jbc.M502814200.
- Näsström, E. *et al.* (2018) 'Diagnostic metabolite biomarkers of chronic typhoid carriage', *PLoS Neglected Tropical Diseases*. Edited by E.T. Ryan, 12(1), p. e0006215. doi:10.1371/journal.pntd.0006215.
- Nath, G. *et al.* (2008) 'Association of carcinoma of the gallbladder with typhoid carriage in a typhoid endemic area using nested PCR.', *Journal of infection in developing countries*, 2(4), pp. 302–307. doi:10.3855/jidc.226.
- Nešić, D., Hsu, Y. and Stebbins, C.E. (2004) 'Assembly and function of a bacterial genotoxin', *Nature*, 429(6990), pp. 429–433. doi:10.1038/nature02532.
- Neves, A.R. *et al.* (2005) 'Dendritic cells derived from metastatic cancer patients vaccinated with allogeneic dendritic cell-autologous tumor cell hybrids express more CD86 and induce higher levels of interferon-gamma in mixed lymphocyte reactions', *Cancer Immunology, Immunotherapy*, 54(1), pp. 61–66. doi:10.1007/s00262-004-0550-8.
- Nishikubo, S. *et al.* (2003) 'An N-terminal Segment of the Active Component of the Bacterial Genotoxin Cytolethal Distending Toxin B (CDTB) Directs CDTB into the Nucleus', *Journal of Biological Chemistry*, 278(50), pp. 50671–50681. doi:10.1074/jbc.M305062200.
- Odendall, C., Voak, A.A. and Kagan, J.C. (2017) 'Type III IFNs Are Commonly Induced by Bacteria-Sensing TLRs and Reinforce Epithelial Barriers during Infection', *The Journal of Immunology*, 199(9), pp. 3270 LP – 3279. doi:10.4049/jimmunol.1700250.
- Ohl, M.E. and Miller, S.I. (2001) 'Salmonella: A model for bacterial pathogenesis', *Annual Review of Medicine*, 52, pp. 259–274. doi:10.1146/annurev.med.52.1.259.
- Ohtani, N. *et al.* (2004) 'The p16INK4a-RB pathway: Molecular link between cellular senescence and tumor suppression', *Journal of Medical Investigation*. J Med Invest, pp. 146–153. doi:10.2152/jmi.51.146.
- Okuda, J., Kurazono, H. and Takeda, Y. (1995) 'Distribution of the cytolethal distending toxin A gene (*cdtA*) among species of *Shigella* and *Vibrio*, and cloning

and sequencing of the *cdt* gene from *Shigella dysenteriae*', *Microbial Pathogenesis*, 18(3), pp. 167–172. doi:10.1016/S0882-4010(95)90022-5.

Okumura, F. *et al.* (2013) 'Activation of double-stranded rna-activated protein kinase (PKR) by interferon-stimulated gene 15 (ISG15) modification down-regulates protein translation', *Journal of Biological Chemistry*, 288(4), pp. 2839–2847. doi:10.1074/jbc.M112.401851.

Okumura, F., Zou, W. and Zhang, D.E. (2007) 'ISG15 modification of the eIF4E cognate 4EHP enhances cap structure-binding activity of 4EHP', *Genes and Development*, 21(3), pp. 255–260. doi:10.1101/gad.1521607.

Orzalli, M.H. *et al.* (2015) 'CGAS-mediated stabilization of IFI16 promotes innate signaling during herpes simplex virus infection', *Proceedings of the National Academy of Sciences of the United States of America*, 112(14), pp. E1773–E1781. doi:10.1073/pnas.1424637112.

Oudshoorn, D. *et al.* (2012) 'HERC6 is the main E3 ligase for global ISG15 conjugation in mouse cells', *PLoS ONE*, 7(1), p. e29870. doi:10.1371/journal.pone.0029870.

Owen, K.A., Anderson, C.J. and Casanova, J.E. (2016) 'Salmonella suppresses the TRIF-dependent type I interferon response in macrophages', *mBio*, 7(1). doi:10.1128/mBio.02051-15.

Owhashi, M. *et al.* (2003) 'Identification of a ubiquitin family protein as a novel neutrophil chemotactic factor', *Biochemical and Biophysical Research Communications*, 309(3), pp. 533–539. doi:10.1016/j.bbrc.2003.08.038.

Paludan, S.R. and Bowie, A.G. (2013) 'Immune Sensing of DNA', *Immunity*, 38(5), pp. 870–880. doi:10.1016/j.immuni.2013.05.004.

Paludan, S.R., Reinert, L.S. and Hornung, V. (2019) 'DNA-stimulated cell death: implications for host defence, inflammatory diseases and cancer', *Nature Reviews Immunology*, pp. 141–153. doi:10.1038/s41577-018-0117-0.

Pandey, A.K. *et al.* (2009) 'Nod2, Rip2 and Irf5 play a critical role in the type I interferon response to *Mycobacterium tuberculosis*', *PLoS Pathogens*, 5(7), p. e1000500. doi:10.1371/journal.ppat.1000500.

Papagrigorakis, M.J. *et al.* (2006) 'DNA examination of ancient dental pulp incriminates typhoid fever as a probable cause of the Plague of Athens', *International Journal of Infectious Diseases*, 10(3), pp. 206–214. doi:10.1016/j.ijid.2005.09.001.

Pardo, B., Gómez-González, B. and Aguilera, A. (2009) 'DNA double-strand break repair: How to fix a broken relationship', *Cellular and Molecular Life Sciences*. Cell

Mol Life Sci, pp. 1039–1056. doi:10.1007/s00018-009-8740-3.

Park, J.H. *et al.* (2016) 'Positive feedback regulation of p53 transactivity by DNA damage-induced ISG15 modification', *Nature Communications*, 7(1), pp. 1–13. doi:10.1038/ncomms12513.

Park, J.M. *et al.* (2014) 'Modification of PCNA by ISG15 Plays a Crucial Role in Termination of Error-Prone Translesion DNA Synthesis', *Molecular Cell*, 54(4), pp. 626–638. doi:10.1016/j.molcel.2014.03.031.

Parkhill, J. *et al.* (2001) 'Complete genome sequence of a multiple drug resistant *Salmonella enterica* serovar Typhi CT18', *Nature*, 413(6858), pp. 848–852. doi:10.1038/35101607.

Parry, C.M. *et al.* (2002) 'Typhoid Fever', *The New England Journal of Medicine*, 347(22), pp. 1770–1782. doi:10.4269/ajtmh.2010.09-0233.

Parry, C.M. *et al.* (2011) 'The utility of diagnostic tests for enteric fever in endemic locations', *Expert Review of Anti-Infective Therapy*, 9(6), pp. 711–725. doi:10.1586/eri.11.47.

Parvatiyar, K. *et al.* (2012) 'The helicase DDX41 recognizes the bacterial secondary messengers cyclic di-GMP and cyclic di-AMP to activate a type I interferon immune response', *Nature Immunology*, 13(12), pp. 1155–1161. doi:10.1038/ni.2460.

Pavlova, B. *et al.* (2011) 'SPI-1-encoded type III secretion system of *Salmonella enterica* is required for the suppression of porcine alveolar macrophage cytokine expression', *Veterinary Research*, 42(1), pp. 1–7. doi:10.1186/1297-9716-42-16/FIGURES/3.

Peng, C.Y. *et al.* (1997) 'Mitotic and G2 checkpoint control: Regulation of 14-3-3 protein binding by phosphorylation of Cdc25c on serine-216', *Science*, 277(5331), pp. 1501–1505. doi:10.1126/science.277.5331.1501.

Péré-Védrenne, C. *et al.* (2017) 'The cytolethal distending toxin subunit CdtB of *Helicobacter hepaticus* promotes senescence and endoreplication in xenograft mouse models of hepatic and intestinal cell lines', *Frontiers in Cellular and Infection Microbiology*, 7(JUN). doi:10.3389/fcimb.2017.00268.

Pérès, S.Y. *et al.* (1997) 'A new cytolethal distending toxin (CDT) from *Escherichia coli* producing CNF2 blocks HeLa cell division in G2/M phase', *Molecular Microbiology*, 24(5), pp. 1095–1107. doi:10.1046/j.1365-2958.1997.4181785.x.

Perkins, D.J. *et al.* (2015) '*Salmonella* Typhimurium Co-opts the Host Type I IFN System To Restrict Macrophage Innate Immune Transcriptional Responses Selectively', *The Journal of Immunology*, 195(5), pp. 2461 LP – 2471. doi:10.4049/jimmunol.1500105.

Perng, Y.C. and Lenschow, D.J. (2018) 'ISG15 in antiviral immunity and beyond', *Nature Reviews Microbiology*. Nature Publishing Group, pp. 423–439. doi:10.1038/s41579-018-0020-5.

Pervolaraki, K. *et al.* (2018) *Differential induction of interferon stimulated genes between type I and type III interferons is independent of interferon receptor abundance*, *PLoS Pathogens*. doi:10.1371/journal.ppat.1007420.

Pickard, D. *et al.* (2003) 'Composition, acquisition, and distribution of the Vi exopolysaccharide-encoding *Salmonella enterica* pathogenicity island SPI-7', *Journal of Bacteriology*, 185(17), pp. 5055–5065. doi:10.1128/JB.185.17.5055-5065.2003.

Pickart, C.M. and Eddins, M.J. (2004) 'Ubiquitin: Structures, functions, mechanisms', *Biochimica et Biophysica Acta - Molecular Cell Research*, pp. 55–72. doi:10.1016/j.bbamcr.2004.09.019.

Pilar, A.V.C. *et al.* (2012) 'GogB Is an Anti-Inflammatory Effector that Limits Tissue Damage during *Salmonella* Infection through Interaction with Human FBXO22 and Skp1', *PLOS Pathogens*, 8(6), p. e1002773. doi:10.1371/JOURNAL.PPAT.1002773.

Pitzer, V.E. *et al.* (2014) 'Predicting the Impact of Vaccination on the Transmission Dynamics of Typhoid in South Asia: A Mathematical Modeling Study', *PLoS Neglected Tropical Diseases*, 8(1), p. 40. doi:10.1371/journal.pntd.0002642.

Pommier, Y. *et al.* (1998) 'Mechanism of action of eukaryotic DNA topoisomerase I and drugs targeted to the enzyme', *Biochimica et biophysica acta*, 1400(1–3), pp. 83–106. doi:10.1016/S0167-4781(98)00129-8.

Pons, B.J. *et al.* (2021) 'Chronic exposure to Cytolethal Distending Toxin (CDT) promotes a cGAS-dependent type I interferon response', *Cellular and Molecular Life Sciences*, 78(17–18), pp. 6319–6335. doi:10.1007/s00018-021-03902-x.

Pribluda, A. *et al.* (2013) 'A Senescence-inflammatory switch from cancer-inhibitory to cancer-promoting mechanism', *Cancer Cell*, 24(2), pp. 242–256. doi:10.1016/j.ccr.2013.06.005.

Prouty, A.M., Schwesinger, W.H. and Gunn, J.S. (2002) 'Biofilm formation and interaction with the surfaces of gallstones by *Salmonella* spp.', *Infection and Immunity*, 70(5), pp. 2640–2649. doi:10.1128/IAI.70.5.2640-2649.2002.

Qi, Y. *et al.* (2015) 'IFI6 inhibits apoptosis via mitochondrial-dependent pathway in dengue virus 2 infected vascular endothelial cells', *PLoS ONE*, 10(8), pp. 1–14. doi:10.1371/journal.pone.0132743.

Radoshevich, L. *et al.* (2015) 'ISG15 counteracts *Listeria monocytogenes* infection', *eLife*, 4(AUGUST2015). doi:10.7554/eLife.06848.

- Raffatellu, M. *et al.* (2008) 'Clinical pathogenesis of typhoid fever.', *Journal of infection in developing countries*, 2(4), pp. 260–266. doi:10.3855/jidc.219.
- Rajashekar, R. *et al.* (2008) 'Dynamic remodeling of the endosomal system during formation of Salmonella-induced filaments by intracellular salmonella enterica', *Traffic*, 9(12), pp. 2100–2116. doi:10.1111/j.1600-0854.2008.00821.x.
- Ramachandran, G. *et al.* (2015) 'Invasive Salmonella Typhimurium ST313 with Naturally Attenuated Flagellin Elicits Reduced Inflammation and Replicates within Macrophages', *PLoS Neglected Tropical Diseases*, 9(1), p. e3394. doi:10.1371/journal.pntd.0003394.
- Raso, M.C. *et al.* (2020) 'Interferon-stimulated gene 15 accelerates replication fork progression inducing chromosomal breakage', *Journal of Cell Biology*, 219(8 August). doi:10.1083/JCB.202002175.
- Rastogi, R.P. *et al.* (2010) 'Molecular mechanisms of ultraviolet radiation-induced DNA damage and repair', *Journal of Nucleic Acids*. Hindawi Limited, p. 32. doi:10.4061/2010/592980.
- Recht, M., Borden, E.C. and Knight, E. (1991) 'A human 15-kDa IFN-induced protein induces the secretion of IFN-gamma.', *Journal of immunology (Baltimore, Md. : 1950)*, 147(8), pp. 2617–23. Available at: <http://www.jimmunol.org/content/147/8/2617> (Accessed: 6 April 2022).
- Redon, C.E. *et al.* (2009) 'γ-H2AX as a biomarker of DNA damage induced by ionizing radiation in human peripheral blood lymphocytes and artificial skin', *Advances in Space Research*, 43(8), pp. 1171–1178. doi:10.1016/j.asr.2008.10.011.
- Reich, N. *et al.* (1987) 'Interferon-induced transcription of a gene encoding a 15-kDa protein depends on an upstream enhancer element', *Proceedings of the National Academy of Sciences of the United States of America*, 84(18), pp. 6394–6398. doi:10.1073/pnas.84.18.6394.
- Riballo, E. *et al.* (2004) 'A pathway of double-strand break rejoining dependent upon ATM, Artemis, and proteins locating to γ-H2AX foci', *Molecular Cell*, 16(5), pp. 715–724. doi:10.1016/j.molcel.2004.10.029.
- Richard, D.J. *et al.* (2011) 'HSSB1 rapidly binds at the sites of DNA double-strand breaks and is required for the efficient recruitment of the MRN complex', *Nucleic Acids Research*, 39(5), pp. 1692–1702. doi:10.1093/nar/gkq1098.
- Richardson, R.B. *et al.* (2018) 'A CRISPR screen identifies IFI6 as an ER-resident interferon effector that blocks flavivirus replication', *Nature Microbiology*, 3(11), pp. 1214–1223. doi:10.1038/s41564-018-0244-1.
- Ritchie, M.E. *et al.* (2015) 'limma powers differential expression analyses for RNA-

sequencing and microarray studies', *Nucleic Acids Research*, 43(7), pp. e47–e47. doi:10.1093/NAR/GKV007.

Rivas, C., Aaronson, S.A. and Munoz-Fontela, C. (2010) 'Dual Role of p53 in Innate Antiviral Immunity.', *Viruses*, 2(1), pp. 298–313. doi:10.3390/v2010298.

Roberts, T.L. *et al.* (2009) 'HIN-200 proteins regulate caspase activation in response to foreign cytoplasmic DNA', *Science*, 323(5917), pp. 1057–1060. doi:10.1126/science.1169841.

Robinson, N. *et al.* (2012) 'Type I interferon induces necroptosis in macrophages during infection with *Salmonella enterica* serovar Typhimurium', *Nature Immunology*, 13(10), pp. 954–962. doi:10.1038/ni.2397.

Rodriguez-Rivera, L.D. *et al.* (2015) 'Characterization of the cytolethal distending toxin (typhoid toxin) in non-typhoidal *Salmonella* serovars', *Gut Pathogens*, 7(1). doi:10.1186/s13099-015-0065-1.

Rogakou, E.P. *et al.* (1999) 'Megabase chromatin domains involved in DNA double-strand breaks in vivo', *Journal of Cell Biology*, 146(5), pp. 905–915. doi:10.1083/jcb.146.5.905.

Rolhion, N. *et al.* (2016) 'Inhibition of Nuclear Transport of NF- κ B p65 by the *Salmonella* Type III Secretion System Effector SpvD', *PLOS Pathogens*, 12(5), p. e1005653. doi:10.1371/JOURNAL.PPAT.1005653.

Roth, S. *et al.* (2014) 'Rad50-CARD9 interactions link cytosolic DNA sensing to IL-1 β production', *Nature Immunology*, 15(6), pp. 538–545. doi:10.1038/ni.2888.

Saldivar, J.C. *et al.* (2018) 'An intrinsic S/G2 checkpoint enforced by ATR', *Science*, 361(6404), pp. 806–810. doi:10.1126/science.aap9346.

Sanchez, Y. *et al.* (1997) 'Conservation of the Chk1 checkpoint pathway in mammals: Linkage of DNA damage to Cdk regulation through Cdc25', *Science*, 277(5331), pp. 1497–1501. doi:10.1126/science.277.5331.1497.

Scanu, T. *et al.* (2015) 'Salmonella Manipulation of Host Signaling Pathways Provokes Cellular Transformation Associated with Gallbladder Carcinoma', *Cell Host and Microbe*, 17(6), pp. 763–774. doi:10.1016/j.chom.2015.05.002.

Schmolke, M. *et al.* (2014) 'RIG-I detects mRNA of intracellular *Salmonella enterica* serovar typhimurium during bacterial infection', *mBio*, 5(2). doi:10.1128/MBIO.01006-14/SUPPL_FILE/MBO002141788SF03.TIF.

Schoenborn, J.R. and Wilson, C.B. (2007) 'Regulation of Interferon- γ During Innate and Adaptive Immune Responses', *Advances in Immunology*. Adv Immunol, pp. 41–101. doi:10.1016/S0065-2776(07)96002-2.

- Secher, T. *et al.* (2013) 'Escherichia coli Producing Colibactin Triggers Premature and Transmissible Senescence in Mammalian Cells', *PLoS ONE*, 8(10), p. e77157. doi:10.1371/journal.pone.0077157.
- Sekirov, I. *et al.* (2010) 'Salmonella SPI-1-mediated neutrophil recruitment during enteric colitis is associated with reduction and alteration in intestinal microbiota', *Gut microbes*, 1(1), pp. 30–41. doi:10.4161/GMIC.1.1.10950.
- Shang, G. *et al.* (2019) 'Cryo-EM structures of STING reveal its mechanism of activation by cyclic GMP–AMP', *Nature*, 567(7748), pp. 389–393. doi:10.1038/s41586-019-0998-5.
- Sharma, S. *et al.* (2003) 'Triggering the interferon antiviral response through an IKK-related pathway', *Science*, 300(5622), pp. 1148–1151. doi:10.1126/science.1081315.
- Shastri, N. *et al.* (2018) 'Genome-wide Identification of Structure-Forming Repeats as Principal Sites of Fork Collapse upon ATR Inhibition', *Molecular Cell*, 72(2), pp. 222–238.e11. doi:10.1016/j.molcel.2018.08.047.
- Shechter, D., Costanzo, V. and Gautier, J. (2004) 'ATR and ATM regulate the timing of DNA replication origin firing', *Nature Cell Biology*, 6(7), pp. 648–655. doi:10.1038/ncb1145.
- Shi, W. *et al.* (2017) 'Ssb1 and Ssb2 cooperate to regulate mouse hematopoietic stem and progenitor cells by resolving replicative stress', *Blood*, 129(18), pp. 2471–2478. doi:10.1182/blood-2016-06-725093.
- Shieh, S.Y. *et al.* (1997) 'DNA damage-induced phosphorylation of p53 alleviates inhibition by MDM2', *Cell*, 91(3), pp. 325–334. doi:10.1016/S0092-8674(00)80416-X.
- Shotland, Y., Krämer, H. and Groisman, E.A. (2003) 'The Salmonella SpiC protein targets the mammalian Hook3 protein function to alter cellular trafficking', *Molecular Microbiology*, 49(6), pp. 1565–1576. doi:10.1046/j.1365-2958.2003.03668.x.
- Shu, K.X., Li, B. and Wu, L.X. (2007) 'The p53 network: p53 and its downstream genes', *Colloids and Surfaces B: Biointerfaces*. *Colloids Surf B Biointerfaces*, pp. 10–18. doi:10.1016/j.colsurfb.2006.11.003.
- Sibanda, B.L. *et al.* (2001) 'Crystal structure of an Xrcc4-DNA ligase IV complex', *Nature Structural Biology*, 8(12), pp. 1015–1019. doi:10.1038/nsb725.
- Siegl, C. *et al.* (2014) 'Tumor Suppressor p53 Alters Host Cell Metabolism to Limit Chlamydia trachomatis Infection', *Cell Reports*, 9(3), pp. 918–929. doi:10.1016/J.CELREP.2014.10.004.
- Solier, S. *et al.* (2009) 'Death Receptor-Induced Activation of the Chk2- and Histone

H2AX-Associated DNA Damage Response Pathways', *Molecular and Cellular Biology*, 29(1), pp. 68–82. doi:10.1128/mcb.00581-08.

Solier, S. and Pommier, Y. (2014) 'The nuclear γ -H2AX apoptotic ring: Implications for cancers and autoimmune diseases', *Cellular and Molecular Life Sciences*. *Cell Mol Life Sci*, pp. 2289–2297. doi:10.1007/s00018-013-1555-2.

Song, J., Gao, X. and Galan, J.E. (2013) 'Conferring virulence: structure and function of the chimeric A2B5 Typhoid Toxin', *Nature*, 499(7458), pp. 350–354. doi:10.1038/nature12377.Conferring.

Sørensen, B.S. *et al.* (1994) 'Antagonistic effect of aclarubicin on camptothecin induced cytotoxicity: Role of topoisomerase I', *Biochemical Pharmacology*, 47(11), pp. 2105–2110. doi:10.1016/0006-2952(94)90087-6.

Spanò, S. *et al.* (2016) 'A Bacterial Pathogen Targets a Host Rab-Family GTPase Defense Pathway with a GAP', *Cell Host & Microbe*, 19(2), pp. 216–226. doi:10.1016/J.CHOM.2016.01.004.

Spanò, S., Ugalde, J.E. and Galán, J.E. (2008) 'Delivery of a Salmonella Typhi Exotoxin from a Host Intracellular Compartment', *Cell Host and Microbe*, 3(1), pp. 30–38. doi:10.1016/j.chom.2007.11.001.

Stanaway, J.D. *et al.* (2019) 'The global burden of non-typhoidal salmonella invasive disease: a systematic analysis for the Global Burden of Disease Study 2017', *The Lancet Infectious Diseases*, 19(12), pp. 1312–1324. doi:10.1016/S1473-3099(19)30418-9.

Stein, M.A. *et al.* (1996) 'Identification of a Salmonella virulence gene required for formation of filamentous structures containing lysosomal membrane glycoproteins within epithelial cells', *Molecular Microbiology*, 20(1), pp. 151–164. doi:10.1111/j.1365-2958.1996.tb02497.x.

Stucki, M. *et al.* (2005) 'MDC1 directly binds phosphorylated histone H2AX to regulate cellular responses to DNA double-strand breaks', *Cell*, 123(7), pp. 1213–1226. doi:10.1016/j.cell.2005.09.038.

Sugai, M. *et al.* (1998) 'The cell cycle-specific growth-inhibitory factor produced by *Actinobacillus actinomycetemcomitans* is a cytolethal distending toxin', *Infection and Immunity*, 66(10), pp. 5008–5019. doi:10.1128/iai.66.10.5008-5019.1998.

Sun, H. *et al.* (2016) 'A Family of Salmonella Type III Secretion Effector Proteins Selectively Targets the NF- κ B Signaling Pathway to Preserve Host Homeostasis', *PLOS Pathogens*, 12(3), p. e1005484. doi:10.1371/JOURNAL.PPAT.1005484.

Sun, L. *et al.* (2013) 'Cyclic GMP-AMP Synthase is a Cytosolic DNA Sensor that Activates the Type-I Interferon Pathway', *Science*, 339(6121), pp. 220–231.

doi:10.1093/biostatistics/kxs032.

Szklarczyk, D. *et al.* (2019) 'STRING v11: protein-protein association networks with increased coverage, supporting functional discovery in genome-wide experimental datasets', *Nucleic acids research*, 47(D1), pp. D607–D613.

doi:10.1093/NAR/GKY1131.

Tait, S.W.G. and Green, D.R. (2010) 'Mitochondria and cell death: Outer membrane permeabilization and beyond', *Nature Reviews Molecular Cell Biology*. Nature Publishing Group, pp. 621–632. doi:10.1038/nrm2952.

Takaoka, A. *et al.* (2007) 'DAI (DLM-1/ZBP1) is a cytosolic DNA sensor and an activator of innate immune response', *Nature*, 448(7152), pp. 501–505.

doi:10.1038/nature06013.

Takeuchi, T. *et al.* (2005) 'Link between the ubiquitin conjugation system and the ISG15 conjugation system: ISG15 conjugation to the UbcH6 ubiquitin E2 enzyme', *Journal of Biochemistry*, 138(6), pp. 711–719. doi:10.1093/jb/mvi172.

Takeuchi, T., Inoue, S. and Yokosawa, H. (2006) 'Identification and Herc5-mediated ISGylation of novel target proteins', *Biochemical and Biophysical Research Communications*, 348(2), pp. 473–477. doi:10.1016/j.bbrc.2006.07.076.

Talvinen, K. *et al.* (2006) 'Biochemical and clinical approaches in evaluating the prognosis of colon cancer', *Anticancer Research*, 26(6 C), pp. 4745–4751.

Taylor, R.C., Cullen, S.P. and Martin, S.J. (2008) 'Apoptosis: Controlled demolition at the cellular level', *Nature Reviews Molecular Cell Biology*. Nature Publishing Group, pp. 231–241. doi:10.1038/nrm2312.

Tecalco Cruz, A.C. and Mejía-Barreto, K. (2017) 'Cell type-dependent regulation of free ISG15 levels and ISGylation', *Journal of Cell Communication and Signaling*, 11(2), pp. 127–135. doi:10.1007/s12079-017-0385-7.

Thanh, D.P. *et al.* (2016) 'A novel ciprofloxacin-resistant subclade of h58. *Salmonella typhi* is associated with fluoroquinolone treatment failure', *eLife*, 5(MARCH2016), pp. 1–13. doi:10.7554/eLife.14003.

They, F., Eggermont, D. and Impens, F. (2021) 'Proteomics Mapping of the ISGylation Landscape in Innate Immunity', *Frontiers in Immunology*. Available at: <https://www.frontiersin.org/article/10.3389/fimmu.2021.720765>.

Thomas, A., Giesler, T. and White, E. (2000) 'p53 mediates Bcl-2 phosphorylation and apoptosis via activation of the Cdc42/JNK1 pathway', *Oncogene*, 19(46), pp. 5259–5269. doi:10.1038/sj.onc.1203895.

Tibbetts, R.S. *et al.* (1999) 'A role for ATR in the DNA damage-induced

phosphorylation of p53', *Genes and Development*, 13(2), pp. 152–157.

doi:10.1101/gad.13.2.152.

Toledo, L., Neelsen, K.J. and Lukas, J. (2017) 'Replication Catastrophe: When a Checkpoint Fails because of Exhaustion', *Molecular Cell*, 66(6), pp. 735–749.

doi:10.1016/j.molcel.2017.05.001.

Toledo, L.I. *et al.* (2008) 'ATR signaling can drive cells into senescence in the absence of DNA breaks', *Genes and Development*, 22(3), pp. 297–302.

doi:10.1101/gad.452308.

Toledo, L.I. *et al.* (2014) 'ATR prohibits replication catastrophe by preventing global exhaustion of RPA', *Cell*, 156(1–2), p. 374. doi:10.1016/j.cell.2014.01.001.

Toshiyuki, M. and Reed, J.C. (1995) 'Tumor suppressor p53 is a direct transcriptional activator of the human bax gene', *Cell*, 80(2), pp. 293–299.

doi:10.1016/0092-8674(95)90412-3.

Townsend, S.M. *et al.* (2001) 'Salmonella enterica serovar Typhi possesses a unique repertoire of fimbrial gene sequences', *Infection and Immunity*, 69(5), pp. 2894–2901. doi:10.1128/IAI.69.5.2894-2901.2001.

Tsui, I.S.M. *et al.* (2003) 'The type IVB pili of Salmonella enterica serovar Typhi bind to the cystic fibrosis transmembrane conductance regulator', *Infection and Immunity*, 71(10), pp. 6049–6050. doi:10.1128/IAI.71.10.6049-6050.2003.

Tyner, S.D. *et al.* (2002) 'P53 mutant mice that display early ageing-associated phenotypes', *Nature*, 415(6867), pp. 45–53. doi:10.1038/415045a.

Uchiya, K.I. *et al.* (1999) 'A Salmonella virulence protein that inhibits cellular trafficking', *EMBO Journal*. doi:10.1093/emboj/18.14.3924.

Unterholzner, L. *et al.* (2010) 'IFI16 is an innate immune sensor for intracellular DNA', *Nature Immunology*, 11(11), pp. 997–1004. doi:10.1038/ni.1932.

Varki, N.M. *et al.* (2011) 'Biomedical differences between human and nonhuman hominids: Potential roles for uniquely human aspects of sialic acid biology', *Annual Review of Pathology: Mechanisms of Disease*, 6(1), pp. 365–393.

doi:10.1146/annurev-pathol-011110-130315.

van Velkinburgh, J.C. and Gunn, J.S. (1999) 'PhoP-PhoQ-Regulated Loci Are Required for Enhanced Bile Resistance in Salmonella spp', *Infection and Immunity*, 67(4), pp. 1614–1622. doi:10.1128/iai.67.4.1614-1622.1999.

Vermeulen, K., Van Bockstaele, D.R. and Berneman, Z.N. (2003) 'The cell cycle: A review of regulation, deregulation and therapeutic targets in cancer', *Cell Proliferation*. *Cell Prolif*, pp. 131–149. doi:10.1046/j.1365-2184.2003.00266.x.

- Vijay-kumar, S., Bugg, C.E. and Cook, W.J. (1987) 'Structure of ubiquitin refined at 1.8 Å resolution', *Journal of molecular biology*, 194(3), pp. 531–544. doi:10.1016/0022-2836(87)90679-6.
- Vuillier, F. *et al.* (2019) 'USP18 and ISG15 coordinately impact on SKP2 and cell cycle progression', *Scientific Reports*, 9(1). doi:10.1038/s41598-019-39343-7.
- Wain, J. *et al.* (2001) 'Quantitation of bacteria in bone marrow from patients with typhoid fever: Relationship between counts and clinical features', *Journal of Clinical Microbiology*, 39(4), pp. 1571–1576. doi:10.1128/JCM.39.4.1571-1576.2001.
- Walker, J.R., Corpina, R.A. and Goldberg, J. (2001) 'Structure of the Ku heterodimer bound to dna and its implications for double-strand break repair', *Nature*, 412(6847), pp. 607–614. doi:10.1038/35088000.
- Wanford, J.J., Hachani, A. and Odendall, C. (2022) 'Reprogramming of Cell Death Pathways by Bacterial Effectors as a Widespread Virulence Strategy', *Infection and Immunity*. American Society for Microbiology. doi:10.1128/iai.00614-21.
- Wang, J.C. (1985) 'DNA topoisomerases', *Annual Review of Biochemistry*, VOL. 54, pp. 665–697. doi:10.1146/annurev.bi.54.070185.003313.
- Wang, Wenshi *et al.* (2017) 'Unphosphorylated ISGF3 drives constitutive expression of interferon-stimulated genes to protect against viral infections', *Science Signaling*, 10(476), pp. 1–13. doi:10.1126/scisignal.aah4248.
- Wangdi, T. *et al.* (2014) 'The Vi Capsular Polysaccharide Enables Salmonella enterica Serovar Typhi to Evade Microbe-Guided Neutrophil Chemotaxis', *PLoS Pathogens*, 10(8). doi:10.1371/journal.ppat.1004306.
- Ward, I.M. and Chen, J. (2001) 'Histone H2AX Is Phosphorylated in an ATR-dependent Manner in Response to Replicational Stress', *Journal of Biological Chemistry*, 276(51), pp. 47759–47762. doi:10.1074/jbc.C100569200.
- Wassermann, K. *et al.* (1990) 'Effects of morpholinyl doxorubicins, doxorubicin, and Actinomycin D on mammalian DNA topoisomerases I and II', *Molecular Pharmacology*, 38(1), pp. 38–45.
- Watanabe, T. *et al.* (2010) 'NOD1 contributes to mouse host defense against Helicobacter pylori via induction of type I IFN and activation of the ISGF3 signaling pathway', *Journal of Clinical Investigation*, 120(5), pp. 1645–1662. doi:10.1172/JCI39481.
- Watson, K.G. and Holden, D.W. (2010) 'Dynamics of growth and dissemination of Salmonella in vivo', *Cellular Microbiology*, 12(10), pp. 1389–1397. doi:10.1111/j.1462-5822.2010.01511.x.

- Weitzman, M.D. and Weitzman, J.B. (2014) 'What's the damage? The impact of pathogens on pathways that maintain host genome integrity', *Cell Host and Microbe*, 15(3), pp. 283–294. doi:10.1016/j.chom.2014.02.010.
- Welton, J.C., Marr, J.S. and Friedman, S.M. (1979) 'ASSOCIATION BETWEEN HEPATOBILIARY CANCER AND TYPHOID CARRIER STATE', *The Lancet*, 313(8120), pp. 791–794. doi:10.1016/S0140-6736(79)91315-1.
- Werneke, S.W. *et al.* (2011) 'ISG15 is critical in the control of chikungunya virus infection independent of UbE1 mediated conjugation', *PLoS Pathogens*, 7(10). doi:10.1371/journal.ppat.1002322.
- West, M.H.P. and Bonner, W.M. (1980) 'Histone 2A, a Heteromorphous Family of Eight Protein Species', *Biochemistry*, 19(14), pp. 3238–3245. doi:10.1021/bi00555a022.
- Wilson, R.P. *et al.* (2008) 'The Vi-capsule prevents Toll-like receptor 4 recognition of Salmonella', *Cellular Microbiology*, 10(4), pp. 876–890. doi:10.1111/j.1462-5822.2007.01090.x.
- Winter, S.E. *et al.* (2008) 'The Salmonella enterica serotype Typhi regulator TviA reduces interleukin-8 production in intestinal epithelial cells by repressing flagellin secretion', *Cellular Microbiology*, 10(1), pp. 247–261. doi:10.1111/j.1462-5822.2007.01037.x.
- Winter, S.E. *et al.* (2015) 'The flagellar regulator TviA reduces pyroptosis by Salmonella enterica serovar Typhi', *Infection and Immunity*, 83(4), pp. 1546–1555. doi:10.1128/IAI.02803-14.
- Wold, M.S. (1997) 'Replication protein A: A heterotrimeric, single-stranded DNA-binding protein required for eukaryotic DNA metabolism', *Annual Review of Biochemistry*, 66(1), pp. 61–92. doi:10.1146/annurev.biochem.66.1.61.
- Wolf, C. *et al.* (2016) 'RPA and Rad51 constitute a cell intrinsic mechanism to protect the cytosol from self DNA', *Nature Communications*, 7(May). doi:10.1038/ncomms11752.
- Wong, J.J.Y. *et al.* (2006) 'HERC5 is an IFN-induced HECT-type E3 protein ligase that mediates type I IFN-induced ISGylation of protein targets', *Proceedings of the National Academy of Sciences of the United States of America*, 103(28), pp. 10735–10740. doi:10.1073/pnas.0600397103.
- Wood, M.W. *et al.* (2000) 'The secreted effector protein of Salmonella dublin, SopA, is translocated into eukaryotic cells and influences the induction of enteritis', *Cellular microbiology*, 2(4), pp. 293–303. doi:10.1046/J.1462-5822.2000.00054.X.
- World Health Organization (2018) *Typhoid vaccines: WHO position paper – March*

2018, *Weekly epidemiological record*. doi:10.1186/1750-9378-2-15.Voir.

Wu, H., Jones, R.M. and Neish, A.S. (2012) 'The Salmonella effector AvrA mediates bacterial intracellular survival during infection in vivo', *Cellular microbiology*, 14(1), pp. 28–39. doi:10.1111/J.1462-5822.2011.01694.X.

Wu, J. *et al.* (2013) 'Cyclic GMP-AMP is an endogenous second messenger in innate immune signaling by cytosolic DNA', *Science*, 339(6121), pp. 826–830. doi:10.1126/science.1229963.

Wu, J. *et al.* (2020) 'Interferon-Independent Activities of Mammalian STING Mediate Antiviral Response and Tumor Immune Evasion', *Immunity*, 53(1), pp. 115-126.e5. doi:10.1016/j.immuni.2020.06.009.

Xu, B. *et al.* (2011) 'Replication stress induces micronuclei comprising of aggregated DNA double-strand breaks', *PLoS ONE*, 6(4). doi:10.1371/journal.pone.0018618.

Yamano, R. *et al.* (2003) 'Prevalence of cytolethal distending toxin production in periodontopathogenic bacteria', *Journal of Clinical Microbiology*, 41(4), pp. 1391–1398. doi:10.1128/JCM.41.4.1391-1398.2003.

Yamashiro, L.H. *et al.* (2020) 'Interferon-independent STING signaling promotes resistance to HSV-1 in vivo', *Nature Communications*, 11(1), pp. 1–11. doi:10.1038/s41467-020-17156-x.

Yanai, H. *et al.* (2009) 'HMGB proteins function as universal sentinels for nucleic-acid-mediated innate immune responses', *Nature*, 462(7269), pp. 99–103. doi:10.1038/nature08512.

Yang, H. *et al.* (2017) 'CGAS is essential for cellular senescence', *Proceedings of the National Academy of Sciences of the United States of America*, 114(23), pp. E4612–E4620. doi:10.1073/pnas.1705499114.

Yang, P. *et al.* (2010) 'The cytosolic nucleic acid sensor LRRFIP1 mediates the production of type I interferon via a B-catenin-dependent pathway', *Nature Immunology*, 11(6), pp. 487–494. doi:10.1038/ni.1876.

Yang, Y.A., Chong, A. and Song, J. (2018) 'Why is eradicating typhoid fever so challenging: Implications for vaccine and therapeutic design', *Vaccines*, 6(3), p. 45. doi:10.3390/vaccines6030045.

Yang, Z. *et al.* (2015) 'SseK3 Is a Salmonella Effector That Binds TRIM32 and Modulates the Host's NF- κ B Signalling Activity', *PLOS ONE*, 10(9), p. e0138529. doi:10.1371/JOURNAL.PONE.0138529.

Young, V.B., Knox, K.A. and Schauer, D.B. (2000) 'Cytolethal distending toxin

sequence and activity in the enterohepatic pathogen *Helicobacter hepaticus*', *Infection and Immunity*, 68(1), pp. 184–191. doi:10.1128/IAI.68.1.184-191.2000.

Yu, Q. *et al.* (2015) 'DNA-Damage-Induced Type I Interferon Promotes Senescence and Inhibits Stem Cell Function', *Cell Reports*, 11(5), pp. 785–797. doi:10.1016/j.celrep.2015.03.069.

Yuan, W. and Krug, R.M. (2001) 'Influenza B virus NS1 protein inhibits conjugation of the interferon (IFN)-induced ubiquitin-like ISG15 protein', 20(3), pp. 362–371. doi:10.1093/EMBOJ/20.3.362.

Zhang, C. *et al.* (2019) 'Structural basis of STING binding with and phosphorylation by TBK1', *Nature*, 567(7748), pp. 394–398. doi:10.1038/s41586-019-1000-2.

Zhang, D. and Zhang, D.E. (2011) 'Interferon-stimulated gene 15 and the protein ISGylation system', *Journal of Interferon and Cytokine Research*, 31(1), pp. 119–130. doi:10.1089/jir.2010.0110.

Zhang, X. *et al.* (2011) 'Cutting Edge: Ku70 Is a Novel Cytosolic DNA Sensor That Induces Type III Rather Than Type I IFN', *The Journal of Immunology*, 186(8), pp. 4541–4545. doi:10.4049/jimmunol.1003389.

Zhang, X. *et al.* (2015) 'Human intracellular ISG15 prevents interferon- α/β over-amplification and auto-inflammation', *Nature*, 517(7532), pp. 89–93. doi:10.1038/nature13801.

Zhang, Y. *et al.* (2006) 'The inflammation-associated *Salmonella* SopA is a HECT-like E3 ubiquitin ligase', *Molecular microbiology*, 62(3), pp. 786–793. doi:10.1111/J.1365-2958.2006.05407.X.

Zhang, Y. *et al.* (2019) 'The in vivo ISGylome links ISG15 to metabolic pathways and autophagy upon *Listeria monocytogenes* infection', *Nature Communications*, 10(1), pp. 1–15. doi:10.1038/s41467-019-13393-x.

Zhang, Z. *et al.* (2011) 'The helicase DDX41 senses intracellular DNA mediated by the adaptor STING in dendritic cells', *Nature Immunology*, 12(10), pp. 959–965. doi:10.1038/ni.2091.

Zhao, C. *et al.* (2004) 'The UbchH8 ubiquitin E2 enzyme is also the E2 enzyme for ISG15, an IFN- α/β -induced ubiquitin-like protein', *Proceedings of the National Academy of Sciences of the United States of America*, 101(20), pp. 7578–7582. doi:10.1073/pnas.0402528101.

Zhao, C. *et al.* (2005) 'Human ISG15 conjugation targets both IFN-induced and constitutively expressed proteins functioning in diverse cellular pathways', *Proceedings of the National Academy of Sciences of the United States of America*, 102(29), pp. 10200–10205. doi:10.1073/pnas.0504754102.

Zhao, Y. and Liu, D. (2021) 'Expressions of interferon-stimulated genes in peripheral blood mononuclear cells from patients with secondary syphilis', *Infection, Genetics and Evolution*, 96, p. 105137. doi:10.1016/j.meegid.2021.105137.

Zhong, B. *et al.* (2008) 'The Adaptor Protein MITA Links Virus-Sensing Receptors to IRF3 Transcription Factor Activation', *Immunity*, 29(4), pp. 538–550. doi:10.1016/j.immuni.2008.09.003.

Zhu, Z. *et al.* (2018) 'Early Growth Response Gene-1 Suppresses Foot-and-Mouth Disease Virus Replication by Enhancing Type I Interferon Pathway Signal Transduction', *Frontiers in Microbiology*, 9(September), pp. 1–12. doi:10.3389/fmicb.2018.02326.

Zirkel, A. *et al.* (2018) 'HMGB2 Loss upon Senescence Entry Disrupts Genomic Organization and Induces CTCF Clustering across Cell Types', *Molecular Cell*, 70(4), pp. 730-744.e6. doi:10.1016/j.molcel.2018.03.030.

Zou, L. and Elledge, S.J. (2003) 'Sensing DNA damage through ATRIP recognition of RPA-ssDNA complexes', *Science*, 300(5625), pp. 1542–1548. doi:10.1126/science.1083430.

Zou, L., Liu, D. and Elledge, S.J. (2003) 'Replication protein A-mediated recruitment and activation of Rad17 complexes', *Proceedings of the National Academy of Sciences of the United States of America*, 100(SUPPL. 2), pp. 13827–13832. doi:10.1073/pnas.2336100100.

Zou, W. and Zhang, D.E. (2006) 'The interferon-inducible ubiquitin-protein isopeptidase ligase (E3) EFP also functions as an ISG15 E3 ligase', *Journal of Biological Chemistry*, 281(7), pp. 3989–3994. doi:10.1074/jbc.M510787200.